Master Thesis

Renewable Energy Storage in Energy Modules for RPA Vessels in the Port of Rotterdam; the Logistical Challenges and Optimisation

Bas Zwaal

Delft University of Technology / Port of Rotterdam

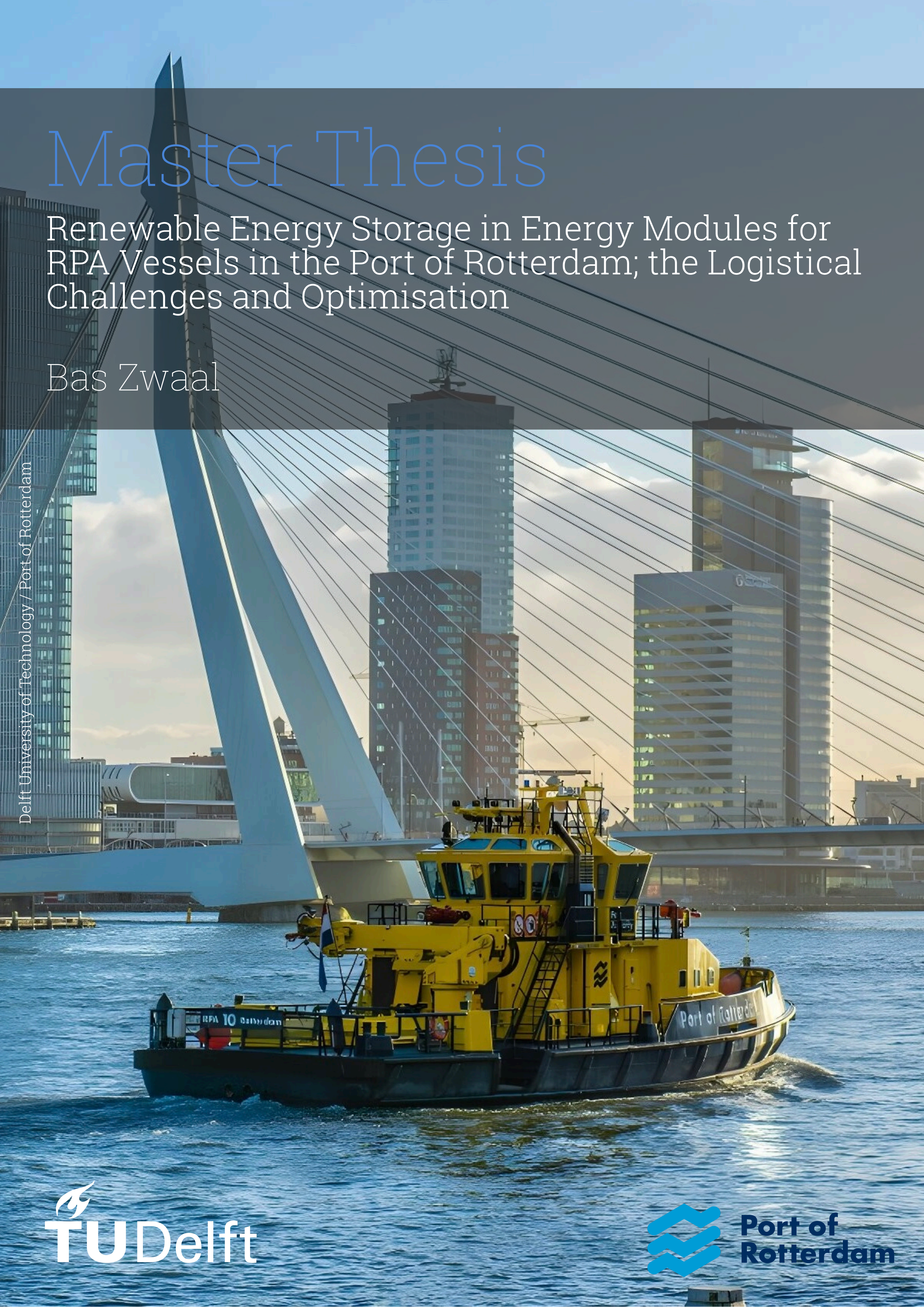

TU Delft

Port of Rotterdam

Master Thesis

Thesis for the degree of MSc in Marine Technology in the specialisation of Maritime Operations and Management (MOM):

Renewable Energy Storage in Energy Modules for RPA Vessels in the Port of Rotterdam; the Logistical Challenges and Optimisation

By

Bas Zwaal

Performed at:

Port of Rotterdam

This thesis (MT.24/25.024.M) is classified as confidential in accordance with the general conditions for projects performed by the TU Delft.

Date Exam: 20-01-2025

Company supervisor

Responsible supervisor:	G.J. (Bob) Madlener

Thesis Exam Committee:

Chair/Responsible Professor:	Prof. Dr. Ir. E. B. H. J. (Edwin) van Hassel
Chair:	Dr. Ir. J. F. J. (Jeroen) Pruyn
Chair/Company Supervisor:	G.J. (Bob) Madlener

Author details:

Student:	Bas Zwaal
Cover:	Bas Geerlings (Modified)

Preface

This thesis explores the implementation of a battery swapping method in the maritime industry. This subject aligned perfectly with my interest in sustainable energy solutions for modern transportation. During my academic journey of the master Marine Technology, I took some optimisation courses where one of which was 'Quantitative Methods for Logistics' which introduced me to the operational research field.

My passion for advancing sustainable energy technologies has been a driving force throughout my academic journey, and this thesis represents a significant step towards contributing to this field, especially with the application of a Battery Swapping Method for the RPA vessels in the Port of Rotterdam. When the Port of Rotterdam reached out with the opportunity to perform a master's thesis, I directly knew that this operational research field could be applied to the important question of making their vessels more sustainable for the future.

I am deeply grateful to Professor Edwin van Hassel for his valuable guidance, insightful feedback, and unwavering encouragement throughout this master thesis. I also extend my gratitude to Delft University of Technology for providing the resources and support necessary to conduct this research. Furthermore, I want to thank Associate Professor Bilge Atasoy for helping with detailed questions for the operational research challenges I ran into while writing thesis.

Furthermore, I want to thank the Port of Rotterdam for their support in performing this thesis. It was an honour to take part in the Fleet Renewal programme, because I strongly believe that this programme marks an important step toward creating a better world with more sustainable options for the RPA vessels. I am grateful for your guidance during this thesis from my company supervisor Bob Madlener, and to Anne Langerak who helped me with the data of the Port of Rotterdam.

Finally, I want to thank my family and friends for supporting me during this master's thesis, and through my academic journey. Especially to those who read my thesis and gave me valuable tips to make this thesis even better.

Bas Zwaal
Delft, January 2025

Summary

The maritime industry is under increasing pressure to reduce its greenhouse gas (GHG) emissions. European ports, including the Port of Rotterdam, are transitioning to sustainable solutions to reduce their environmental impact [1]. Since the Port of Rotterdam is large, patrol and incident-response (RPA) vessels are needed to ensure a safe port. However, the existing fleet is reaching its operational end of life. These vessels currently rely on conventional propulsion systems, which are not in line with the sustainability goals of the Port of Rotterdam. The Port of Rotterdam performed research with several companies to see what type of renewable energy solutions could be applied to the new RPA vessels. Given the 24/7 operational profile and energy demands of (relatively small) RPA vessels, a battery or hydrogen propulsion system installed onboard the vessels was not an option. Therefore, another possibility was proposed: the (rapid) swapping of energy modules to and from the vessel at swapping stations.

This research addresses the challenge of designing an optimal configuration for such a swapping method based on the operational sailing profiles of RPA vessels. A systematic methodology was applied, starting with a literature review for the technical and operational issues. The findings highlighted the feasibility of implementing a Battery Energy Storage System (BESS) powered by lithium-ion batteries, supported by decentralised swapping and charging stations structure. Different concepts for the Battery Swapping Method (BSM) were considered from which the Shfitr concept was the most promising application for this thesis. The Shiftr concept uses cranes to automatically swap energy modules to and from vessels. Different optimisation methods were investigated to see which one best supports finding an optimal configuration (energy modules, swapping/charging stations and vehicle related). It was concluded that a Mixed Integer Linear Programming method could be best applied, with the objective to minimise downtime of the swapping process for different configurations.

A mathematical model for the optimisation model was developed to minimise downtime during swapping, incorporating historical AIS data to simulate the vessels' operational profiles. This optimisation model can track both the vessel r and the modules m for each time t. This mathematical model is made in Gurobi (Python) and can, for different configurations, minimise the total swapping time for a given period of data. The configurations are used as input data, including the number of energy modules and the number/placement of swapping and charging stations based on the energy consumption of vessels and their sailing path defined during the pre-processing. Verification and validation confirmed the optimisation model was working, although computational challenges were observed when validating each individual vessel.

After verification and validation, two case studies were performed, which included multiple vessels. Due to the rapid increase in computational time, only two case studies were performed with two and three vessels, respectively. Except for the number of vessels, the configuration from the pre-processing was the same for both the case studies. For both cases, the number of swaps was in line with the expectations of each case and confirmed the working of the optimisation model. As the vessels only lost minutes on swapping while sailing for hours before the modules were depleted, a low swapping frequency was observed in the optimisation model. At the same time, there are too many swapping stations in the configuration, leading to a lot of unused energy modules.

In conclusion, the optimisation model can successfully optimise the sailing path to minimise swapping time, for a specific configuration. However, the research question of finding the optimal configuration could not be answered fully. Therefore, further research is needed to address computational limitations and to optimise module utilisation. This thesis provides a foundation for swapping renewable energy sources in modules, for relatively small vessels, which are operational 24/7.

Contents

Preface ii

Summary iii

Nomenclature xi

1 Introduction 1

2 Literature Review 4
2.1 Energy Storage System . . . 5
2.1.1 Hydrogen Energy Storage . . . 5
2.1.2 Battery Energy Storage System (BES) . . . 6
2.1.3 Conclusion . . . 6
2.2 Swapping Station . . . 7
2.2.1 Electric Vehicles . . . 7
2.2.2 Shipping industry . . . 8
2.2.3 Conclusion . . . 9
2.3 Energy Modules . . . 10
2.3.1 Lead-Acid Batteries . . . 10
2.3.2 Nickel-Cadmium Batteries . . . 10
2.3.3 Lithium-ion Batteries . . . 11
2.3.4 Conclusion . . . 11
2.4 Charging Station . . . 12
2.4.1 Charging strategies . . . 12
2.4.2 Battery degradation . . . 13
2.4.3 (De)Centralised charging infrastructure . . . 13
2.4.4 Impact on electricity grid . . . 14
2.4.5 Safety . . . 14
2.4.6 Conclusion . . . 14
2.5 Swapping Concepts . . . 15
2.5.1 ZES-pack containers (Zero Emission Services) . . . 15
2.5.2 Pontoon concept (with ZES-containers) (Port of Rotterdam) . . . 15
2.5.3 Cranes (SHIFTR) . . . 16
2.5.4 Conclusion . . . 16
2.6 Operational Research Methodology . . . 17
2.6.1 Linear Programming . . . 17
2.6.2 Mixed Integer (Linear) Programming . . . 17
2.6.3 Markov decision process . . . 18
2.6.4 Robust optimization . . . 18
2.6.5 Generic Algorithms . . . 18
2.6.6 Relevant literature . . . 18
2.6.7 Conclusion . . . 19
2.7 Literature Gap . . . 20

3 Methods 21
3.1 Scope . . . 22
3.2 Conceptual process . . . 23
3.3 Mathematical model . . . 24
3.3.1 Sets and indices . . . 24
3.3.2 (Decision) Variables . . . 24
3.3.3 Parameters . . . 25

3.3.4 Objective function . . . 26
3.3.5 (Functional) Constraints . . . 27
3.4 Conclusion . . . 37

4 Pre-Processing 38
4.1 RPA vessels . . . 39
4.2 Location data RPA vessels . . . 40
4.3 Zones . . . 41
4.4 Power estimation of the RPA vessels . . . 42
4.4.1 Original path . . . 42
4.4.2 Sailing to and from the swapping station . . . 44
4.5 Swapping duration . . . 45
4.6 Swapping method . . . 46
4.7 Possible Swap . . . 47
4.7.1 Data gaps . . . 47
4.7.2 RPAs doing tasks . . . 47
4.8 Time-intervals . . . 47
4.9 Conclusion . . . 48

5 Verification & Validation 49
5.1 Verification . . . 50
5.1.1 Test Base Case . . . 51
5.1.2 Test cases . . . 53
5.2 Validation . . . 56
5.3 Conclusion . . . 57

6 Case study 58
6.1 Caste study 1: two RPA vessels . . . 59
6.2 Case study 2: Three RPA vessels . . . 61
6.3 Conclusion . . . 63

7 Conclusion & Discussion 64
7.1 Conclusion . . . 64
7.2 Discussion . . . 65
7.3 Future Research . . . 67
7.3.1 Vessels . . . 67
7.3.2 Swapping Stations . . . 67
7.3.3 Charging Stations . . . 67
7.3.4 Inventory area . . . 68
7.3.5 Optimisation model . . . 68

References 69

A Appendix 79

B Appendix 86
B.1 Verification Test Case 1 . . . 87
B.2 Test Case 2 . . . 89
B.3 Test Case 3 . . . 91
B.4 Test Case 4 . . . 93
B.5 Test Case 5 . . . 94
B.6 Test Case 6 . . . 96
B.7 Test Case 7 . . . 97
B.8 Test Case 8 . . . 98
B.9 Test case 9 . . . 99
B.10 Test Case 10 . . . 100
B.11 Test Case 11 . . . 101

C Appendix D 102
C.1 Validation RPA6 . . . 103

C.1.1 Input 103
C.1.2 Results 104
C.2 Validation RPA7 107
C.2.1 Input 107
C.2.2 Results 108
C.3 Validation RPA10 111
C.3.1 Input 111
C.3.2 Results 112
C.4 Validation RPA13 115
C.4.1 Input 115
C.4.2 Results 116
C.5 Validation RPA15 119
C.5.1 Input 119
C.5.2 Results 120
C.6 Validation RPA16 123
C.6.1 Input 123
C.6.2 Results 124

List of Figures

1.1 Patrol vessel (RPA 8) [13] 2
1.2 Response-incident vessel (RPA 12) [14] 2

2.1 Hydrogen Energy Storage Topology [25]. 5
2.2 Battery Energy Storage System schematic diagram [25]. 6
2.3 The operation framework of BSS [39]. 7
2.4 Current Direct EcoSystem [56] 8
2.5 The battery-swapping process in the battery swapping station (BSS) [20] 9
2.6 The battery-swapping process in the battery swapping station (BSS) [20] 9
2.7 Charging Battery [57] 10
2.8 Discharging Battery [57] 10
2.9 Structure of EVs power supply through BSS [92]. 12
2.10 Battery Allocation strategy [101]. 13
2.11 Zero Emission Services (ZES) [21] 15
2.12 Port of Rotterdam concept (internal source) 15
2.13 SHIFTR concept for interchangeable batteries (1) [22] 16
2.14 SHIFTR concept for interchangeable batteries (2) [22] 16

3.1 Operational area RPA vessels Port of Rotterdam [Internal source/own work] 23
3.2 Swapping concept 23
3.3 Summary of the mathematical model 26
3.4 Module level 27

4.1 Used operational areas for RPA vessels (Pistoolhaven/Madroelhaven) [Internal source/own work] 39
4.2 Sailing distance for each RPA vessel validation test case 40
4.3 Zones for the RPA vessels 41
4.4 Engine load for RPA 10 42
4.5 Engine load for RPA 13 42
4.6 Engine load for RPA 16 42
4.7 Combined engine load 42
4.8 Combined power output 43
4.9 Energy consumption for one kilometre 44
4.10 Time synchronization for the vessel 45
4.11 Engine load for RPA 10 46
4.12 The initial power consumption with the 46

6.1 RPA15 and RPA16 locations (timestep = 6) 59
6.2 Cumulative distance for RPA15 and RPA16 59
6.3 Cumulative energy consumption for RPA15 and RPA16 59
6.4 Swapping state RPA vessels for case study 1 60
6.5 Power level RPA vessels Case Study 1 60
6.6 Charging area Case Study 1 60
6.7 Inventory area Case Study 1 60
6.8 Percentage of modules for each location in different swapping stations s for RPA10 . . . 60
6.9 RPA locations for Case Study 1 (timestep = 6) 61
6.10 Cumulative distance for Case Study 2 61
6.11 Cumulative power consumption for Case Study 2 61
6.12 Vessel state RPA vessels Case Study 2 62

6.13 Power level RPA vessels Case Study 2 . . . 62
6.14 Charging area Case Study 2 . . . 62
6.15 Inventory area Case Study 2 . . . 62
6.16 Percentage of modules for each location in different swapping stations s for RPA10 . . . 62

B.1 Verification TC_3 - Optimal usage . . . 91
B.2 Verification TC_{BC} - Optimal usage . . . 91

C.1 RPA6 locations (timestep = 6) . . . 103
C.2 Cumulative sailed distance for RPA6 . . . 103
C.3 Cumulative initial power for the RPA6 . . . 104
C.4 Power consumption RPA6 . . . 104
C.5 Swapping states RPA6 . . . 105
C.6 Charging area for validation RPA6 . . . 105
C.7 Inventory area validation RPA6 . . . 106
C.8 Percentage of modules for each location in different swapping stations s, validation RPA6 106
C.9 RPA7 locations (timestep = 6) . . . 107
C.10 Cumulative sailed distance for RPA7 . . . 107
C.11 Cumulative initial power for the RPA7 . . . 108
C.12 Power consumption RPA7 . . . 108
C.13 Power consumption RPA7 . . . 109
C.14 Charging area for validation RPA7 . . . 109
C.15 Inventory area validation RPA7 . . . 110
C.16 Percentage of modules for each location in different swapping stations s, validation RPA7 110
C.17 RPA10 locations (timestep = 6) . . . 111
C.18 Power consumption RPA10 . . . 111
C.19 Cumulative initial power for the RPA10 . . . 112
C.20 Power consumption RPA10 . . . 112
C.21 Swapping states RPA10 . . . 113
C.22 Charging area for validation RPA10 . . . 113
C.23 Inventory area validation RPA10 . . . 114
C.24 Percentage of modules for each location in different swapping stations s for RPA10 . . . 114
C.25 RPA13 locations (timestep = 6) . . . 115
C.26 Cumulative sailed distance for RPA13 . . . 115
C.27 Cumulative initial power for the RPA13 . . . 116
C.28 Power consumption RPA13 . . . 116
C.29 Swapping states RPA13 . . . 117
C.30 Charging area for validation RPA13 . . . 117
C.31 Inventory area validation RPA13 . . . 118
C.32 Percentage of modules for each location in different swapping stations s for RPA13 . . . 118
C.33 RPA15 locations (timestep = 6) . . . 119
C.34 Cumulative sailed distance for RPA15 . . . 119
C.35 Cumulative initial power for the RPA15 . . . 120
C.36 Power consumption RPA15 . . . 120
C.37 Swapping states RPA15 . . . 121
C.38 Charging area for validation RPA15 . . . 121
C.39 Inventory area validation RPA15 . . . 122
C.40 Percentage of modules for each location in different swapping stations s for RPA10 . . . 122
C.41 RPA6 locations (timestep = 6) . . . 123
C.42 Cumulative sailed distance for RPA16 . . . 123
C.43 Cumulative initial power for the RPA16 . . . 124
C.44 Power consumption RPA16 . . . 124
C.45 Swapping states RPA16 . . . 125
C.46 Charging area for validation RPA16 . . . 125
C.47 Inventory area validation RPA16 . . . 126
C.48 Percentage of modules for each location in different swapping stations s for RPA16 . . . 126

List of Tables

2.1 Comparison of available batteries to store renewable energy 11
2.2 Different optimisation studies from the literature 19

3.1 Sets and indices for the optimisation model 24
3.2 (Decision) Variables for the optimisation model 24
3.3 Parameters 25
3.4 The indication of different states of modules with a certain energy level $l_{t,m}$ 28

4.1 Chose of RPA vessels, and time frame for those vessels 39
4.2 Zones 1-7 for the optimisation model 41
4.3 Zones 8-14 for the optimisation model 41

5.1 Verification checks based on the mathematical model 50
5.2 Verification TCB 51
5.3 Verification TC_B for $R1$ 52
5.4 Verification TC_B for $R2$ 52
5.5 Overall verification test cases 53
5.6 Input for validation cases 56
5.7 Results for validation cases 56
5.8 Summary verification 57
5.9 Summary Validation 57

B.1 Verification TC_1 87
B.2 Verification TC_1 for $R1$ - objective 88
B.3 Verification TC_1 for $R2$ - objective 88
B.4 Verification $TC_{2,1}$ 89
B.5 Verification $TC_{2,1}$ for $R1$ - objective 89
B.6 Verification $TC_{2,1}$ for $R2$ - objective 89
B.7 Verification $TC_{2,2}$ 90
B.8 Verification $TC_{2,1}$ for $R1$ - objective 90
B.9 Verification $TC_{2,1}$ for $R2$ - objective 90
B.10 Verification TC_3 91
B.11 Verification TC_3 for $R1$ - Objective 92
B.12 Verification TC_3 for $R2$ - Objective 92
B.13 Verification TC_4 93
B.14 Verification TC_4 for $R1$ - Objective 93
B.15 Verification TC_4 for $R2$ - Objective 93
B.16 Verification TC_5 94
B.17 Verification TC_5 for $R1$ - Objective 95
B.18 Verification TC_5 for $R2$ - Objective 95
B.19 Verification TC_6 96
B.20 Verification TC_6 for $R1$ - Objective 96
B.21 Verification TC_6 for $R2$ - Objective 96
B.22 Verification TC_7 - energy consumption 97
B.23 Verification TC_7 97
B.24 Verification TC_7 for $R1$ - Objective 97
B.25 Verification TC_7 for $R2$ - Objective 97
B.26 Verification TC_8 98
B.27 Verification TC_8 for $R1$ - Objective 98

B.28 Verification TC_8 for $R2$ - Objective . . . 98
B.29 Verification TC_9 . . . 99
B.30 Verification TC_9 for $R1$ - Objective . . . 99
B.31 Verification TC_9 for $R2$ - Objective . . . 99
B.32 Verification TC_{10} . . . 100
B.33 Verification TC_{10} for $R1$ - Objective . . . 100
B.34 Verification TC_{10} for $R2$ - Objective . . . 100
B.35 Verification TC_{11} . . . 101
B.36 Verification TC_{11} for $R1$ - Objective . . . 101
B.37 Verification TC_{11} for $R2$ - Objective . . . 101

Nomenclature

Abbreviations

Abbreviation	Definition
AGV	Automated Guided Vehicles
BES	Battery Energy Storage System
BSS	Battery Swapping Station
DB	Depleted Batteries
EEA	European Environment Agency
ESS	Energy Storage System
EU	European Union
EV	Electric Vehicle
GA	Generic Algorithm
GHG	Greenhouse Gases
HES	Hydrogen Energy Storage
LP	Linear Programming
MILP	Mixed Integer Linear Programming
MIP	Mixed Integer Programming
MDP	Markov Decision Process
obj	Objective
RO	Robust Optimisation
RPA	Rotterdam Port Authority
UNFCCC	United Nations Framework Convention on Climate Change
VRP	Vehicle Routing Problem
ZES	Zero Emission Services

1 Introduction

The European Union (EU) has set targets for Greenhouse Gas (GHG) emissions. According to the European Climate Law, net GHG emissions should be reduced by, at least, 55% compared to the (overall) levels of 1990 by 2030 to reach net zero GHG emissions by 2050 eventually [2]. To quantify this goal, the European Environment Agency (EEA) has published a data viewer [3] (with data until 2021) where the (total) GHG emissions for each EU member state for each year can be seen compared to the levels of 1990. According to this data viewer, the EU achieved a total reduction (all member states) of net emissions (UNFCCC) of 30.41% in 2021, where an overall trend in the reduction of GHG emissions can be seen. The transport sector has a substantial negative effect on the environment in the EU, where 25% of the total GHG emissions are related to transport [4]. This percentage is mainly because of the current advanced modern society, where production and consumption depend on transport [5].

In the transport sector, maritime transport contributes to many cumulative pressures on Europe's regional seas [5]. It is estimated that maritime transport represented 3 to 4% of the total GHG in 2021 [6]. The EEA has provided a factual analysis of environmental pressure exerted by the maritime transport sector, the *'European Maritime Transport Environmental Report 2021'* [7]. This report researches the challenges and opportunities for the shipping sector. The EEA has concluded that the maritime industry has a significant environmental pressure on the atmosphere of the marine environment. To reduce GHG emissions, renewable energy is used to achieve the reduction goal. Transitioning to renewable energy sources, such as solar, wind and hydropower, is essential to reduce climate change and significantly reducing carbon dioxide and other harmful emissions associated with conventional energy production [8].

Ports in Europe have identified the necessity for implementing more sustainable alternatives for products and/or services and using renewable energy sources. The Port of Amsterdam, for instance, has set the objective of becoming one of Europe's most sustainable ports by 2030 [9]. Additionally, the Port of Antwerp has established objectives for a more sustainable port in the future, including an increase in freight transported by rail, inland navigation, and pipelines [10]. Furthermore, the Port of Rotterdam is improving the sustainability of marine transport by facilitating the use of clean bunkering fuels and new innovative developments (green hydrogen, biofuels and recycling activities). They also stimulate users to be sustainable through discounts if the companies comply with environmental performances in order to be net-positive [11]. As GHGs become increasingly important for clients and regulation, it is in the interest of the ports to consider sustainable solutions and make business cases of those. With this growing emphasis on sustainability, the ports are competing at the level of applying 'green' solutions since environmental issues are and will be more important in the future.

Among the ports in Europe, the Port of Rotterdam is the largest port [1]. In 2018, the Port of Rotterdam handled 441 million tonnes of freight, more than double compared to the second largest European port, the Port of Antwerp (212 million tonnes of freight) [12]. Besides the large numbers of freight, the Port of Rotterdam also has a large surface area of 12,600 hectares [1]. To ensure a safe port, the Port of Rotterdam has a fleet of patrol- (Figure 1.1) and incident-response (Figure 1.2) vessels, also known as RPA (Rotterdam Port Authority) vessels. Their task within the Port of Rotterdam is to patrol and respond to incidents. Both vessel types are operating 24/7. However, these vessels have conventional propulsion systems, which are not sustainable and are not in line with the goals of the Port of Rotterdam.

Figure 1.1: Patrol vessel (RPA 8) [13]

Figure 1.2: Response-incident vessel (RPA 12) [14]

In the coming years, the majority of those vessels will reach their end of life. As a result, the RPA vessels must either be refitted or renewed. Since the vessels will be refitted or renewed in the near future, the Port of Rotterdam wants to do this in line with their sustainability goals, where zero-emission operation of the vessel is their primary goal. The Port of Rotterdam has collaborated with several companies to research the possibility of applying renewable energy for RPA vessels, including batteries and hydrogen. According to these internal sources, the required energy demand for the given operational profile (maximum speeds, range, and duration of shifts) exceeds the available space in those vessels. It was therefore concluded that either the operational profile should be reconsidered or alternative solutions should be proposed.

Since the operational profile is not likely to be changed, an alternative possible concept is proposed: swapping energy modules with renewable energy. A swapping concept is where a vehicle (vessel) can access swapping- and charging locations, enabling the swapping of depleted energy modules for fully charged energy modules where the empty energy modules will be charged outside the vehicle (vessel). The range of vehicles to which this method is applied varies from electric vehicles (EVs) [15], electric taxis [16], [17], electric scooters [18], automated guided vehicles (AGVs) [19] and specific application in the maritime sector [20]–[22]. For all those (commercial) transportation methods, the main reason is minimising downtime while maintaining operational efficiency.

For example, Zero Emission Services (ZES) has already implemented this strategy with a similar concept of swapping battery containers for container barges in the Netherlands, parts of Germany and Belgium [21]. Existing infrastructure is used for container terminals to swap the depleted battery containers for fully charged battery containers. Furthermore, the container barges have pre-defined sailing paths where swapping stations are stationed alongside the route. Besides ZES, the company Shiftr plans to use the swapping concept for ferries in Norway with a pre-defined sailing path [22].

Nonetheless, the swapping concept has already been applied for container vessels (and will be for ferries) in the maritime sector but it is not yet applied to RPA vessels. Compared to ferries and container barges, the design of an RPA vessel is significantly different (e.g. smaller), and thus the method of ZES can probably not be applied. Furthermore, the infrastructure to facilitate the swapping concept within the port of Rotterdam is not yet available.

There are two problems with applying this method to these vessels. The first problem is the technical issue, so what is needed to use a swapping mechanism with those relatively small vessels? Since the RPA vessels will be refitted or renewed in the future, research is required to apply such a system for these vessels. This will be researched on a high level, where the concept of a swapping method for this vessel type is discussed. The other issue is the question of how often these vessels need a swap, and due to the 24/7 response task of those vessels, what is the most optimal configuration? To answer the second question, the first part should be known. Since the swapping concept has not yet been applied to patrol and incident-response vessels (RPAs), research will be done whether this concept can be used. This thesis focuses on the second problem, which is to optimize different configurations of the swapping method. In this way, the Port of Rotterdam can use this optimisation model to also consider other configurations. Therefore, the main research question of this thesis is as follows:

What is the optimal configuration (number of energy modules, swapping stations and charging stations) for the swapping concept for patrol and incident-response vessels (RPAs) in the Port of Rotterdam?

The thesis is divided into different chapters, in which the thesis outlines to answer the main research question. Every chapter has its own sub-question, which are answered in the specific chapter. The thesis will start with a literature review, where the first part of the literature review is used to research the necessary parts of the swapping concept. This first part discusses the type of energy storage that can be used, the storage medium, the swapping method, the charging methods, and the actual concept. Together, they will define what is needed to apply this to RPA vessels and when this method can be applied in the future. This first part is based on the technical application and what is required to have such a system. The second part of the literature review is what method can be used to optimise such a system. Based on this optimisation model, other configurations can also be used, which can be beneficial for the Port of Rotterdam when more details are known about the replacement of the RPA vessels.

Based on the literature review, the methods chapter (CH3) is discussed. This chapter begins with the scope (CH3.1) of this research based on a literature review. After the scope, the conceptual process (CH3.2) is discussed. This is for the current situation and the “improved” situation. Then, the model description and the Mathematical Model are described. The mathematical model includes everything to model the situation for this research.

After defining the mathematical model as discussed in CH3.2, the pre-processing chapter (CH4) is specified. This chapter consists of everything needed to optimise based on the mathematical model. The main objective of pre-processing is to reduce the calculations for the optimisation model, which can be done upfront. Also, pre-processing is necessary so that the optimisation model does not have to calculate each distance, time, and power consumption, which would make the optimisation model slower in computational time. This ranges from the choice of which data is used (vessels and swapping method) to the estimations of the power consumption of the RPA vessels. The data for the vessel, the (historical) AIS location data specific zones, data handling (when there are data gaps), the power estimation and the actual parameters for the used swapping method are discussed.

After specifying the mathematical model, verification and validation (CH5) are performed. This chapter ensures the optimisation model is correctly implemented and feasible for this research. For the validation, each RPA vessel is validated if this specific RPA vessel can use the swapping method based on the pre-processing. The actual choice of the vessels should be valid; when a vessel cannot be swapped as an individual vessel, applying those vessels in combination has no purpose. After this validation, different case studies (CH6) are performed. These case studies focus on applying multiple RPA vessels, which is used to answer the main question of whether a swapping method can be used and what the optimal configuration is. Based on these chapters, a conclusion, discussion and future research are discussed in CH7.

2
Literature Review

Renewable energy adoption is a fundamental driver in the transition of global energy systems away from fossil fuels. This shift is needed to achieve carbon neutrality and is critical in promoting sustainability in various industrial sectors, including the maritime sector. Central to this transition is optimising energy storage solutions, which are needed for managing renewable energy sources.

The Port of Rotterdam has performed internal research (with multiple companies) to apply (installed) batteries and hydrogen in the RPA vessels. According to these internal researches, both options were considered unfeasible since the required energy demand for the operational profile of the RPA vessels was higher than the space available. Therefore the swapping of energy was suggested. Because the swapping concept has not yet been applied to RPA vessels, it is important to study the relevant literature for this method. Given that the Port of Rotterdam is still in the early stages of the renewal and refitting of the RPA vessels, there is great uncertainty. Consequently, it is necessary to ascertain what can be found in the literature.

The primary purpose of the literature is to research both the technical and the operational aspects of a swapping method for RPA vessels in the Port of Rotterdam with random sailing paths. The literature review is divided into seven sections, each with its sub-questions. The first five sections are used to research the technical issue, so what is needed to apply a swapping method within the Port of Rotterdam for RPA vessels? Chapter 2.1 describes the different energy storage systems (ESS) used to store renewable energy. In the next Chapter 2.2, the application of this ESS for a swapping method is described. Chapter 2.3 discusses the various types of batteries available in the market. Chapter 2.4 describes what battery charging stations are and which configuration best suits for this research. Chapter 2.5 describes different (applied) swapping methods in the maritime sector. Chapter 2.6 describes the operational issue and what optimisation can be used to research the optimal configuration of the swapping method in the Port of Rotterdam, and the research methodology that can best be applied to this thesis. Finally, chapter 2.7 provides the literature gap for the thesis. The sub-questions used in each chapter are listed below:

1. *What is an Energy Storage System (ESS) and which system can be best applied for this thesis? (CH2.1)*
2. *What is a Battery Swapping Method (BSM)? (CH2.2)*
3. *Which battery types are used for Energy Storage Systems? (CH2.3)*
4. *What is the best charging strategy for charging stations? (CH2.4)*
5. *What are the different swapping concepts in the market? (CH2.5)*
6. *What is the research methodology for the thesis? (CH2.6)*
7. *What is the literature gap? (CH2.7)*

2.1. Energy Storage System

The increasing global adoption of renewable energy sources has increased the amount of generated energy [23]. Since renewable energy output fluctuates because of weather conditions and time of day, energy storage is important if the renewable electricity cannot be used instantly. Therefore, Energy Storage Systems (ESS) have been introduced. An ESS refers to converting energy, in different forms, to a storage medium. These systems enable excess energy, produced during optimal conditions, to be stored and utilised during periods of low generation or high demand which increases the reliability and efficiency [24]. Eventually, this energy is converted back to electrical energy when needed. It can be used for different purposes, such as [25]:

1. *Peak shaving electrical load demands*
2. *Offering dynamic energy management*
3. *Mitigating the variability of power generation from renewable sources*
4. *Improving power quality/reliability*
5. *Electric Vehicle Charging Stations*
6. *Helping with the management of distributed/standby power generation*
7. *Reducing electrical energy import during peak demand periods*

These systems come in various forms, each suitable for different scales and applications. Common types of energy storage include Pumped Hydro Storage (PHES), Thermal Energy Storage (TES), Flywheel Energy Storage (FES), Compressed Air Energy Storage (CAES), Hydrogen Energy Storage (HES) and Battery Energy Storage (BES). Each ESS plays a crucial role in smoothing out the supply variability, ensuring that the energy generated from renewable can replace conventional power sources effectively. Based on the initial research performed by the Port of Rotterdam and the application of ESS for vessels, the BES (Chapter 2.1.2) and HES (Chapter 2.1.1) systems will be discussed in this chapter. Both will be compared with the direct and indirect use of the ESS for the application of the RPA vessels.

2.1.1. Hydrogen Energy Storage

Hydrogen is considered a promising secondary energy source (energy carrier) for future applications [26], [27], and is the most abundant and simple substance in the universe [28]. Hydrogen is a carbon-free fuel (if the used electricity is renewable electricity [29]), and its oxidation process results in zero carbon dioxide emissions [27]. Moreover, it can be converted to electricity, and compared to fossil fuels, it is quieter, produces less pollution (the only byproduct is water), and can be more efficient [25], [30], [31]. The hydrogen can be stored and used as a clean fuel for various applications, including electricity generation, transportation, and industrial processes [26]. It uses two separate processes for storing energy and generating electricity [25]. Firstly, HES converts (surplus) renewable electricity into hydrogen through electrolysis [26]. Electrolysis is the process where electricity is used to split water H_2O into hydrogen H_2 and oxygen O_2 where the overall reaction is $2H_2O \rightarrow 2H_2 + O_2$ [28], [31]. The hydrogen is then stored or fed into a fuel cell, which converts chemical energy in hydrogen and oxygen into electricity [32]. Figure 2.1 illustrates the process schematically.

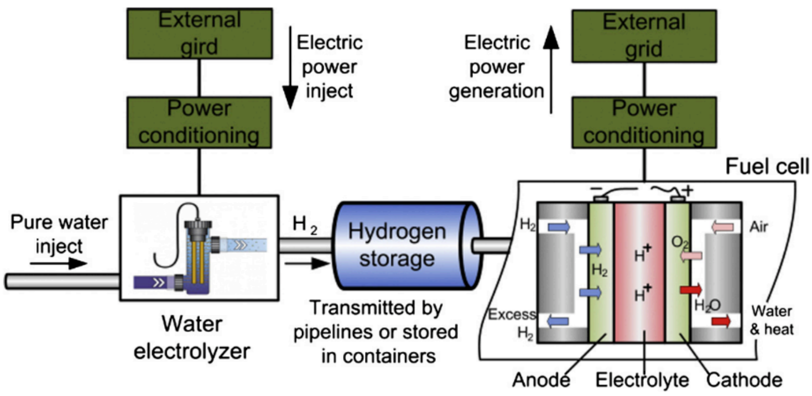

Figure 2.1: Hydrogen Energy Storage Topology [25].

The HES system can be split into hydrogen production (with renewable energy sources for powering this system) and electricity generation with fuel cells. The produced hydrogen can be stored in the vessel, where these tanks are connected to the fuel cells, which convert the hydrogen into electricity to directly propel the vessel. The production of hydrogen can either be centralised or decentralised, where the first has transportation issues (e.g. carbon emissions due to the transport), and the second could potentially have safety issues when producing this in the port. It is crucial that, if a HES system is used, the hydrogen is produced with 100% renewable energy to ensure the produced hydrogen is renewable as well. This method was also researched by the Port of Rotterdam, but due to the lack of available space this was no option. If this method is applied to interchangeable modules, it will take time to refuel the energy modules. Even more, it is most likely that the use of interchangeable modules with hydrogen will have technical issues.

2.1.2. Battery Energy Storage System (BES)

A Battery Energy Storage System (BESS) system uses batteries as a storage medium. A battery converts chemical energy into electrical energy and uses the electrochemical reactions to store and release energy efficiently (varies with battery types and technology) [33]. The BESS systems consist of interconnected arrays of rechargeable batteries (in series or parallel) for later electricity use [25]. Bu et al. [34] researched the BESS for external power supply, which contains all the necessary parts such as fans, air conditioning, battery modules, safety modules and fire measurement features. Electrochemical energy storage in batteries is attractive because it is compact (compared to the other ESSs), easy to deploy, economical and provides virtually instant response to the input from the battery and output from the network to the battery [23]. The schematic diagram of a BESS can be seen in Figure 2.2.

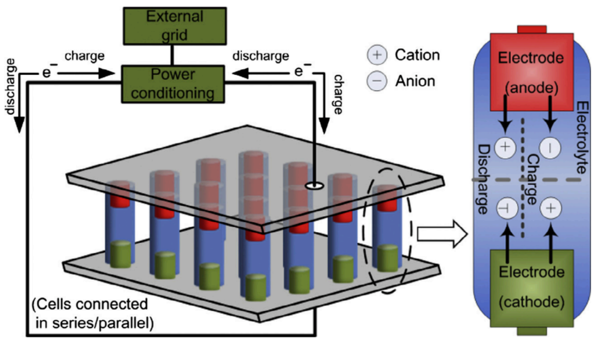

Figure 2.2: Battery Energy Storage System schematic diagram [25].

For the BES system, renewable energy can be used to power the vessel with batteries via cables directly. The vessel should then need enough batteries to power the vessels for the sailing profile, which is also a disadvantage because the energy density of batteries is lower compared to that of internal combustion engines (ICE). Another disadvantage is that charging the vessels takes significantly more time than fuelling conventional fuels, which decreases the operational time of the vessels. This was also the conclusion of the Port of Rotterdam, so installing batteries to directly power the vessel is no option. On the other hand, if batteries can be swapped in and from the vessel this could be an option. Therefore, this could be an interesting swapping method.

2.1.3. Conclusion

In this section, the BES and HES were discussed. The application to RPA vessels in the Port of Rotterdam is specific, and due to the 24/7 response task it is essential to swap the energy as fast as possible. The BES system could potentially be applied when batteries are interchangeable. For the HES, it is more complicated to apply this method with interchangeable energy modules. Therefore, the BES will be used in this thesis for further research. However, it is essential to keep track of the progress of ESSs, especially when ESSs will be available with more energy-dense structures and other storage mediums, which could be interesting for the application to RPA vessels in the future.

2.2. Swapping Station

Conventional plug-in EVs (PHEV), which are charged on site, have experienced several problems in the past such as high purchase costs [35]–[39], long charging times [35], [40], [41], battery degradation [35], [42], travelling distance per charge [35], [39], [43], [44] and inconvenient charging facilities [35], [45] have been restricted the promotion of EVs. Therefore, Battery Charging Stations (BCS) have been introduced [35], [39] to optimise the charging problem. However, due to the material properties of the batteries and the charging technologies, queuing and range anxiety were still a problem [35], [46].

One of the mentioned problems is range anxiety. According to the Cambridge Dictionary [47], range anxiety is: *"The fear that an electric vehicle will not have enough battery charge to take you where you want to go"*. This problem is addressed in the literature and is one of the prominent substantial barriers to the eventual adoption of EVs [48]. Noel et al. [48] raised the question whether range anxiety was a technical, mental problem, or even both and whether the range anxiety decreased the experience or not. They argued that those questions could not be answered and introduced a rhetorical construction of range anxiety. This was based on rhetoric reaction, where conservative forces and actors often resisted social changes and innovations. They concluded that range anxiety is neither purely technical nor psychological.

Based on the disadvantages of EVs, an alternative method was researched and introduced: the Battery Swapping Method (BSM). A BSM is the swapping of depleted batteries (DB) for fully charged batteries (FD) at a Battery Swapping Station (BSS) [49], where the depleted batteries are charged at a BCS [50]. This method is applied to reduce the downtime due to charging. The BSM was initially introduced in 2011 by the company Better Place [51]. They experimented with this method in Denmark and later promoted it in Australia, Japan and China. However, the company went bankrupt in 2013 because the market was not ready, the customer acceptance was low due to not owing the battery [52], it was premature, and there was a lack of understanding of battery characteristics, swapping costs, charging time and maintenance [51], [53]. However, in recent years, the BSM has been applied in several cases. The BSM is shown in Figure 2.3.

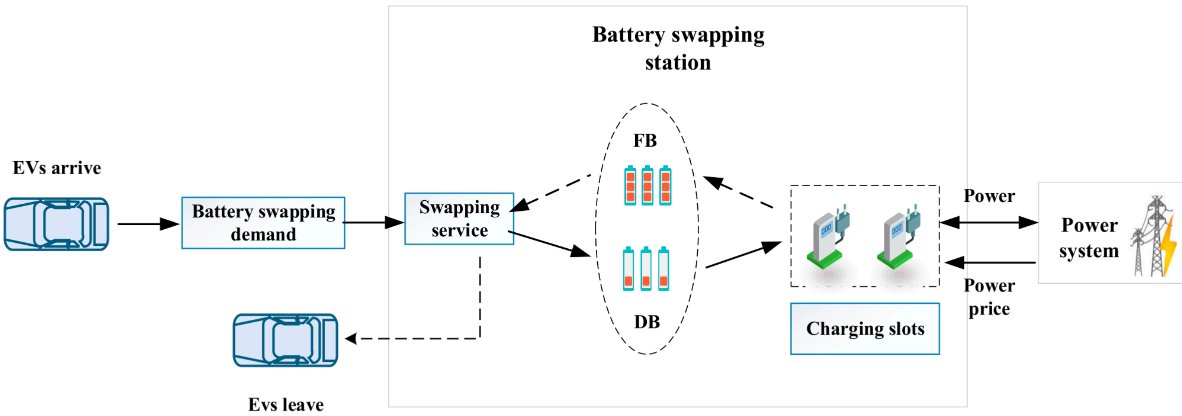

Figure 2.3: The operation framework of BSS [39].

2.2.1. Electric Vehicles

Due to the continuous growth of the EV market and technological advances, many companies have accelerated the adoption of the BSM. The range of vehicles in which the BSM is applied varies from Electric Vehicles (EVs) [15], electric taxis [16], [17], electric scooters [18], electric Busses [54] and Automated Guided Vehicles (AGVs) [19]. Also, For all these (commercial) transport methods, the main reason is to minimise downtime while maintaining operational efficiency.

Despite the increased adoption of the BSM, the BSM also has challenges. Schmidt [51] has researched this for the BSM in the car industry. He discussed the acceptance of battery-swapping technology and the lack of support from (car) manufacturers for implementing the BSM. Schmidt mentioned that for success, disadvantages needed to be eliminated. Both Adegbohun et al. [52] and Schmidt [51] mentioned the low customer acceptance for BSS operators, the swapping of healthier batteries for older batteries (range uncertainty and degradation), the low support of (car) manufacturers, standardisation of battery packs, disproportional high infrastructure and logistical costs (compared to conventional/fast-charging stations) and concerns about data protection due to the need of tracking of the battery packs.

Adegbohun et al. [52] researched the methodology for increasing EV adoption based on the Battery Sharing Stations (BShS), Battery Sharing Networks (BShN), which are a variant of the BSS. In their research, they mentioned that one of the disadvantages is the high costs of ownership because the price of the battery of an EV is 25% - 50% of the vehicle [49], [52], [55]. The high ownership costs can be solved by a third party, leasing/pay-as-you-go model, which owns the batteries and is responsible for the health, decommissioning and battery recycling. This leasing/pay-as-you-go construction can be a possible solution to this high initial investment cost [45].

2.2.2. Shipping industry

The BSM is significantly less applied in the shipping industry compared to other transportation sectors, as mentioned in the previous sections. Therefore, the European Commission has performed an innovation research named Current Direct, funded by the European Commission's Horizon 2020 program, to research the (battery) swapping concept [56]. They researched an innovative energy-as-a-service platform to accelerate the shift to clean energy. This study researched the relevant stakeholders, the operational and business requirements, the certification/ regulatory framework for waterborne transport batteries, the battery charging infrastructure and the recycling method. Figure 2.4 shows the layout of the Current Direct EcoSystem.

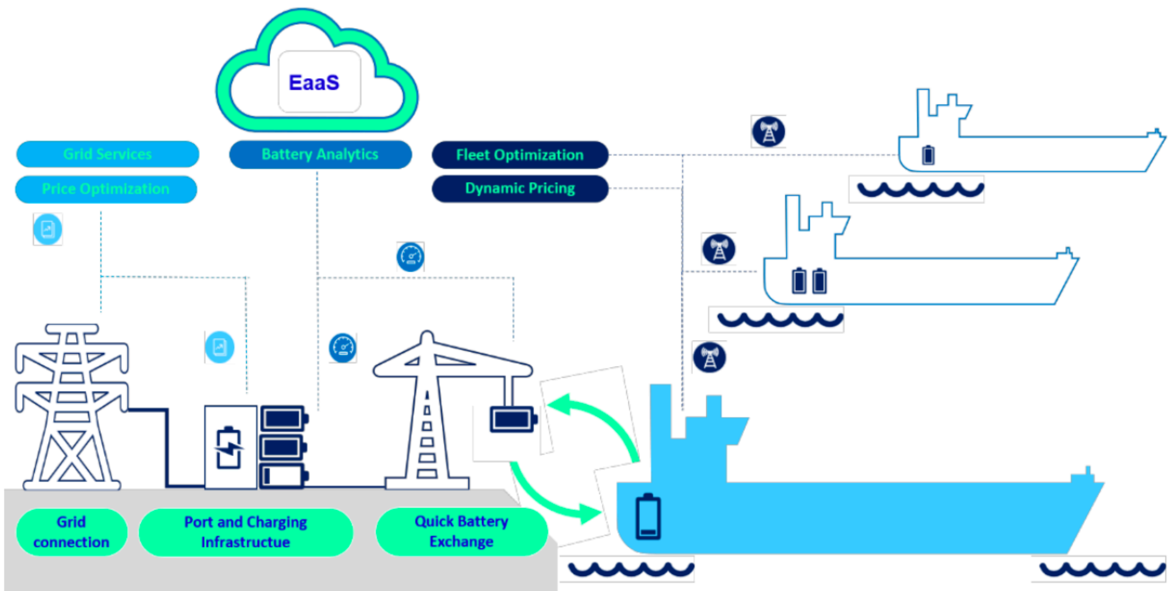

Figure 2.4: Current Direct EcoSystem [56]

Despite the pushing of the European Commission, problems still occurred. One of the problems is the amount of energy needed to propel a ship, which is based on the vessel's shape. Therefore, larger ships need significantly more energy to propel them compared to other transportation sectors (e.g. cars and buses). Moreover, the weight of the batteries is a problem since vessels are limited in the weight they can carry because of their buoyancy. Also, an increase in weight, and therefore draft, will increase the power needed to propel the ship since the resistance is higher (squared to the needed power). Also, infrastructure is a problem where vessels are floating; therefore, swapping energy is more difficult than BSM on land.

However, there is research on the application of the BSM in the Maritime industry. Zhang et al. [20] stated that the increased needed power for all-electric battery-powered ships resulted in increased charging times, longer routes and more batteries that could not be placed in the vessels. Therefore, Zhang et al. proposed the application of the BSM for an All Eclectic Ship (AES) in the Yangtze River in China. They proposed a BSM for cargo vessels, with a sailing path between Port A and Port B. Intermediate BSSs were added, and for each swapping station, the batteries were charged on the spot. Zhang et al. have researched the siting, sizing, optimal scheduling and cost-benefit analysis of battery swapping stations [53]. The primary purpose of the research of Zhang et al. [20] was to determine the optimal speed for AES where battery-swapping was used to minimise the operational costs between Port A and Port B. This can be seen in Figure 2.5 and Figure 2.6.

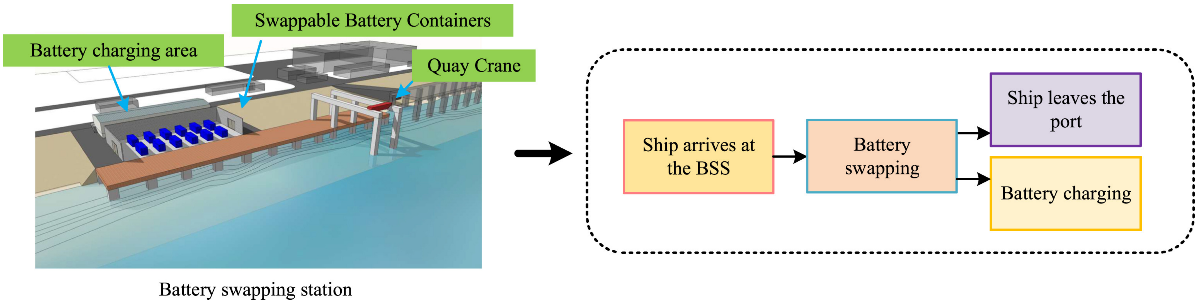

Figure 2.5: The battery-swapping process in the battery swapping station (BSS) [20]

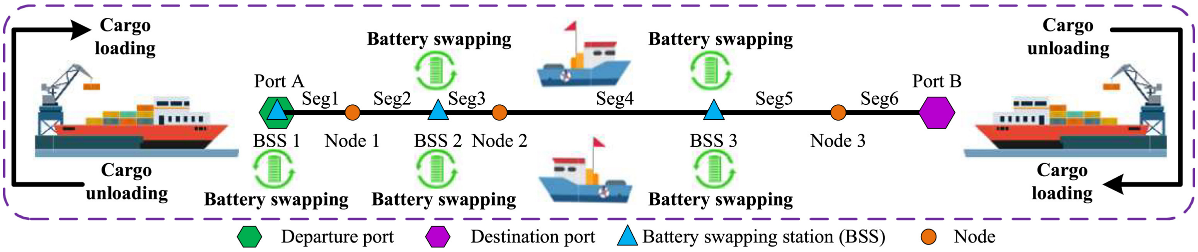

Figure 2.6: The battery-swapping process in the battery swapping station (BSS) [20]

Zhang et al. [20] are not discussing the layout of the BSS since those BSS are using the infrastructure of the container transhipment. For a BSS on land, the accessibility of swapping stations is more straightforward compared to swapping stations where ships are involved. Compared to land transportation, the vessel has to connect to the swapping station or have systems to load the batteries into the vessel. Therefore, most of the literature is not directly applied to the maritime sector, but the main working principle is (discussed in the previous section).

2.2.3. Conclusion

It can be concluded that there is a potential for adopting the battery swapping method in the maritime industry compared to the battery swapping stations used for land infrastructure-based EVs. However, the maritime industry faces obstacles to the energy requirements of ships, the significant weight constraints due to buoyancy, and the complexity of swapping batteries in a floating environment, especially when applied to RPA vessels. While the BSM offers a potential reduction in downtime for recharging and could theoretically improve operational efficiency, the practical application within the maritime industry requires innovative approaches to overcome the physical and logistical problems, which include adapting the infrastructure for effective battery swapping and swapping mechanisms specifically made for maritime conditions for specific types of vessels.

2.3. Energy Modules

Based on the ESS discussed in Chapter 2.1 and the BSM in Chapter 2.2, the storage medium will be batteries. A battery is a device which stores electrical energy. In a battery, chemical energy is converted into electrical energy [57]. There are two types of batteries [58]; disposable and rechargeable batteries (Redox, reduction-oxidation, a process when the battery is charged and discharged) [59]. This process involves electrochemical reactions where electrons are transferred from one material to another (depending on the type of battery), creating an electrical current. Specifically, a battery consists of two electrodes (an anode and a cathode) and an electrolyte [33]. The anode undergoes oxidation (loses electrons), and the cathode undergoes reduction (gains electrons). The electrolyte facilitates the movement of ions between the electrodes, which helps maintain charge balance throughout the cell. The flow of electrons from the anode to the cathode through an external circuit provides the electrical energy to power devices. A battery has two stages: charging (Figure 2.7) and discharging (Figure 2.8).

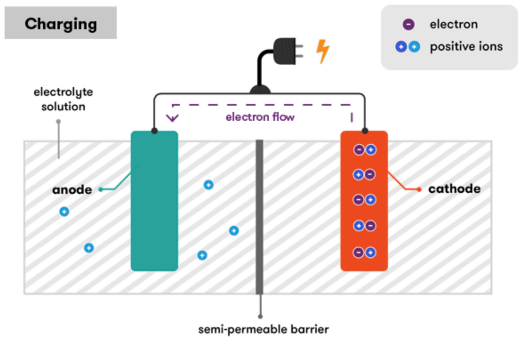

Figure 2.7: Charging Battery [57]

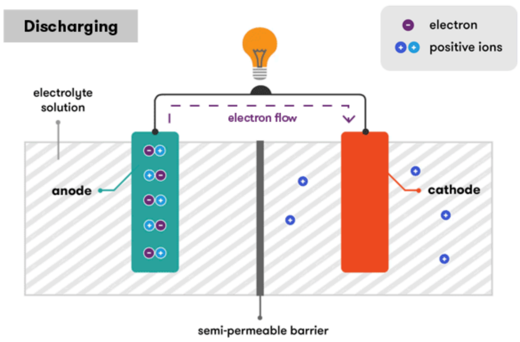

Figure 2.8: Discharging Battery [57]

In the following subsections, three different battery types are discussed: Lead-Acid (Chapter 2.3.1), Nickel-Cadmium (Chapter 2.3.2) and Lithium-Ion batteries (Chapter 2.3.3) for the potential application for a swapping method (Chapter 4.6). The utilisation of EVs remains limited compared to ICEs because of their low energy densities [60]. Especially when looking at the application of batteries in vessels with limited space, the energy/power density and specific energy/power are essential. Furthermore, the round trip efficiency and service life will impact the choice of battery type. Also the environmental impact is important. At last, the batteries are compared on energy and power costs. All these specifications will be compared for the considered battery types.

2.3.1. Lead-Acid Batteries

Gaston & Plante invented the Lead-Acid battery (Pb-Acid) type (LABs) in 1859 [61], [62], one of the oldest battery types in the world. The main component of LABs is lead (Pb) and can be divided into two categories: Flooded and sealed/valve-regulated LABs [62]. LABs have the advantages of mature technology, stable performance, good safety, low price and reliability [61]. For example, this battery type is used in the automobile and electric bike market [61]. Disadvantages for LABs are short cycle life (500 - 1000 cycles [33]), low energy density, low cycle life when deeply discharged, and low-temperature performance of LABs [61], [63]. Also, 85% of the worldwide production of lead is used for those battery types [64] where lead is very toxic and is found in the earth's crust, which is harmful [64] and has a high impact on the environment (mining, processing and recycling). Another disadvantage is battery degradation. The temperature sensitivity of LABs degrades significantly above 25°C. Also, the typical state of charge (SOC) window is 50%, and above this percentage, the efficiency significantly drops.

2.3.2. Nickel-Cadmium Batteries

Nickel-based batteries were invented in 1899 by Waldemar Jungner [65]. The positive electrode has nickel oxyhydroxide as the active material and metallic cadmium as the negative electrode [63]. Cadmium is highly toxic, but NiCd batteries can be recycled or disposed safely when the proper precautionary actions are taken [59]. Nickel-cadmium batteries have high charge/discharge cycle life [58], can function at extreme temperatures, have high internal resistance [58] and charge quickly. However, those batteries also have rapid self-discharge, low cell voltage, low energy density, and hazardous

Cadmium [59]. Nickel-Cadmium batteries can withstand high temperatures but perform poorly and are generally avoided for ESS [63]. Nickel-cadmium batteries are affected by the memory effect, which defines battery degradation when it is partially charged and discharged [58].

2.3.3. Lithium-ion Batteries

The concept of Lithium-Ion (Li-Ion) batteries (LIBs) dates from the 1970s, when the widespread adoption came in the '90s [62]. LIBs operate on the principle of lithium ions moving between the cathode and anode during charging and discharging cycles, allowing energy storage and release [62], [66]. LIBs are applied to a wide range of devices such as phones, laptops, Electric Vehicles (EVs) and large-scale ESS (BES), and more than 85% of new energy storage distribution installations from 2016 are using Li-ion batteries [67]. Storage systems using LIBs have the advantages of long life, lightweight and high adaptability and therefore, these systems are preferred in BESS [34]. Furthermore, LIBs have high power density and high efficiency [63]. Disadvantages are high production cost and special charging circuit requirements [63]. Furthermore, the cycle-life of LIBs will significantly increase when the limit is 89% of the rated capacity [62]. However, it significantly decreases when the temperature is above 45°C due to the temperature sensitivity of LIBs.

2.3.4. Conclusion

Based on the previous sub-sections, different types of batteries were discussed and compared to each other. The summary can be seen in Table 2.1. It can be concluded, based on Table 2.1, that Lithium-Ion can be best applied for this thesis. First of all, the application of lithium-ion batteries is widely adopted. This means that the technological readiness of those batteries is higher than that of other battery types. Also, the battery energy/power density, the specific energy/power and efficiency are high. The only disadvantages are investment and operational costs, but those are expected to decrease in the future. Therefore, this is the best option to use at this moment for a BSM.

Table 2.1: Comparison of available batteries to store renewable energy

	Energy Density (kWh/m^3)	**Power Density** (kW/m^3)	**Specific Energy** (kW/kg)	**Specific Power** (W/kg)	**Round-trip Efficiency** (%)	**Serive Life** ($years$)	**Technology Maturity** (-)	**Environmental Impact** (-)	**Energy Costs** ($\$/kWh$)	**Power Costs** ($\$/kW$)
Pb-Acid (CH2.3.1)	80 [62] 100 [33] 50 - 80 [68] 50 - 80 [72] 50 - 90 [25] 100 [62] 30 - 50 [70]	10 - 400 [68] 10 - 400 [72] 10 - 700 [73]	30 - 50 [69] 25 - 32 [73] 20 - 35 [75] 15 - 40 [76]	75 - 300 [68] 180 - 200 [69] 74 - 415 [76] 25 [75]	65 - 80 [70] 70 - 90 [68] 85 [77] 70 - 80 [69]	5 - 15 [68] 5 - 15 [69]	Commercialized [71]	High [72]	120 - 150 [73] 54 - 337 [74] 200 - 400 [73] 200 - 400 [78]	300 - 600 [73] 326 - 651 [74] 200 - 300 [72]
Ni-Cd (CH2.3.2)	60 - 150 [68] 30 - 150 [76] 60 - 150 [73]	150 - 300 [73] 100 - 450 [25]	50 - 75 [68] 50 - 75 [79] 50 - 75 [70] 30 - 80 [69] 40 - 60 [75]	150 - 300 [68] 100 - 160 [69] 140 - 180 [75] 150 - 300 [79] 50 - 150 [76]	72 [69] 60 - 70 [79]	10 - 20 [68] 13 - 20 [69] 10 [76] 5 - 20 [79]	Commercialized [72]	High [72]	800 - 1500 [25] 400 - 2400 [73]	500 - 1500 [73]
Li-Ion (CH2.3.3)	200 - 500 [68] 200 - 500 [82] 150 - 400 [25] 170 - 300 [69]	50 - 800 [80] 1000 - 5000 [68] >5000 [79]	200 [70] 75 - 200 [68] 75 - 200 [79] 80 - 200 [69] 100 - 200 [75] 90 - 200 [76]	150 - 315 [68] 80 - 200 [67] 185 - 370 [69]	95 [70] 85 - 98 [79] 78 - 88 [69] 85 [83]	5 - 15 [68] 5 - 15 [79] 14 - 16 [69] 6 - 20 [76]	Demonstration [77] Proven [72] Commercialized [72]	Medium/low [72]	600 - 2500 [81] 600 - 1300 [72]	1300 - 4342 [74] 1200 - 4000 [72] 900 - 4000 [73]

The literature also shows that Lithium-Ion is applied more. Liu et al. [84] have predicted that in the coming years, nickel- and lead-acid-based batteries will be replaced by LIBs and that those batteries will dominate the market in powering and transportation in the next decade(s). This aligns with the literature found and displayed in Table 2.1. Muslimin et al. [58] also concluded that Li-ion batteries are the most common used batteries in EVS because of the long cycle life, high energy capacity, high safety level and lack of toxic gassing problems. The only disadvantage of Li-Ion batteries is their cost, which is higher than that of other battery types. However, studies suggest that the energy and power costs of Li-Ion batteries will decrease in the future [85].

However, the battery market is evolving and several studies have indicated that more energy-dense batteries could enter the market in the coming years [86]. For example, the solid state batteries which promise higher energy densities, excellent safety, and longer lifespans than traditional lithium-ion batteries due to their solid electrolyte (replacing the liquid/gel electrolytes in conventional Li-ion batteries) [87]. Disadvantages are the slow kinetics of ion diffusion, chemical instabilities, local mechanical and structural instabilities, and the necessity of renewing the existing Li-ion assembly [87], [88]. Furthermore, solid-state batteries are more expensive to produce than traditional lithium-ion batteries [89]. However, Solid-state batteries are still in the development and testing phases and have not been widely commercialised [90]. The technology is advancing, but there are challenges related to manufacturing at scale, cost and ensuring consistent performance across a wide range of temperatures and usage conditions [91]. But, these battery types should be followed.

2.4. Charging Station

A part of the BSM is Battery Charging Stations (BCS). A BCS is a station where the depleted batteries are stored and charged to be swapped at a later stadium when an EV wants a swap. This process can be seen in Figure 2.9. The BCS is not newly introduced for the BSM; it was already applied for PHEVs. The difference, however, is that the batteries, in combination with the BSM, are stored and charged separately. In this way, the EV does not have to wait until the batteries are fully charged.

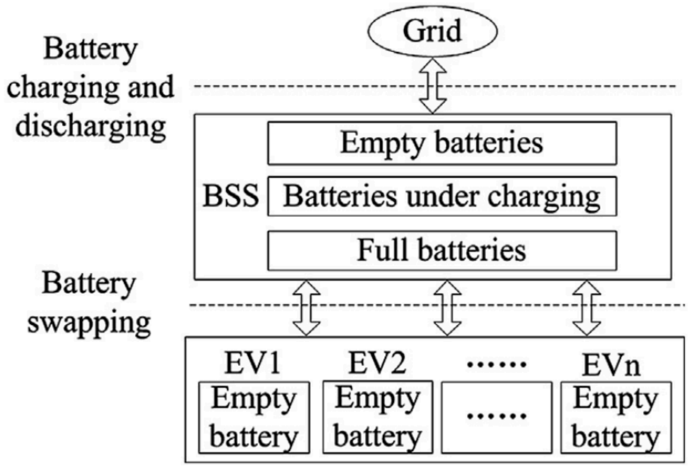

Figure 2.9: Structure of EVs power supply through BSS [92].

2.4.1. Charging strategies

Leijon and Boström [46] researched different charging strategies for different EVs since there was an expected increase in used EVs. There are two types of charging, by cables and conductive charging [46]. Leijon and Boström [46] concluded that the preferred charging strategy depends on the type of electric vehicles and other factors where battery data is crucial for charging strategies. Charging can be divided into three different charging modes. Level 1 (AC) charging with speeds up to $5kW$, level 2 charging (AC) with speeds typically ranging from $5kW - 50kW$ and Direct Current Quick Charging (DCQC) or DCFC (Direct Current Fast Charge) with typical speeds ranging from $50kW$ and higher[38], [93]. However, types of EVs (especially PHEVs) and batteries may have different charging service requirements. Therefore, it is difficult to have one charging station which could facilitate a multi-class of customers and service quality [38]. This would be different if one type of battery is used in the BSM. In this way, the charging can be optimised for BCS.

Wu et al. [55] mentioned that the charging time varies depending on different charging technologies and equipment types. Fast charging is a solution, but it can potentially cause damage/ battery degradation to batteries and give rise to a heavy load on the power grid [38], [93]. This is higher than slower AC charging, especially with the DCFC of Li-ion battery cells. Timilsina et al. [94] researched the degradation mechanism in lithium-ion batteries for EVs and PHEVs. Also, these high charging speeds can lead to unsustainable load spikes on the distribution grid [52]. Different operating conditions affect the ageing mechanism differently. Timilsina et al. [94] focused on the physical and chemical changes, and they concluded that the battery's operating condition and environment are essential for the charging strategy. Therefore, slow charging is still dominant [86]. Furthermore, Infante et al. [45] mentioned that the charging strategy is highly correlated to battery degradation and service time.

Feng et al. [39] have discussed the three different charging strategies. The first one is reducing the grid load. The charging costs can be reduced significantly if a charging model is making load predictions [95], which can reduce the grid load. Secondly is the Queuing theory, which influences the main indicators considered to be the blocking degree at the service level. The last is the economic perspective, which aims to achieve the maximum benefit or lowest cost of BSSs and, thus, BCSs.

2.4.2. Battery degradation

Battery degradation refers to the process by which a battery loses its capacity and efficiency over time, losing its ability to store and deliver power effectively [96]. This phenomenon is particularly relevant in lithium-ion batteries for EVs and renewable ESSs [97]. The primary mechanisms driving battery degradation include physical changes such as the growth of the solid electrolyte interphase (SEI) layer, lithium plating, and mechanical stresses within the cell, as well as chemical changes like electrolyte decomposition and active material dissolution [98]. These degradation processes are influenced by charge/discharge cycles, depth of discharge, operating temperature, and current intensity. As a result, battery degradation reduces the battery's usable life in terms of performance, safety, and economic viability [99]. Understanding and mitigating battery degradation is crucial for improving battery systems' cycle life and efficiency [100].

Since battery degradation affects the performance of the batteries, it is important to indicate this to elaborate this with the customer. This is done with the State of Health (SOH). The SOH is essential because if batteries are delivered to customers when their performance (the amount of energy delivered) is lower, it will affect their acceptance eventually. Yang et al. [101] proposed a battery allocation strategy where batteries were divided into different levels. The first level ($SOH < 0.6$), the second level ($0.6 \leq SOH < 0.8$) and the third level ($0.8 \leq SOH \leq 1$). In this way, the batteries are continuously recycled between the BSS (and thus BCS) and the customers. This can be seen in the following figure, Figure 2.10.

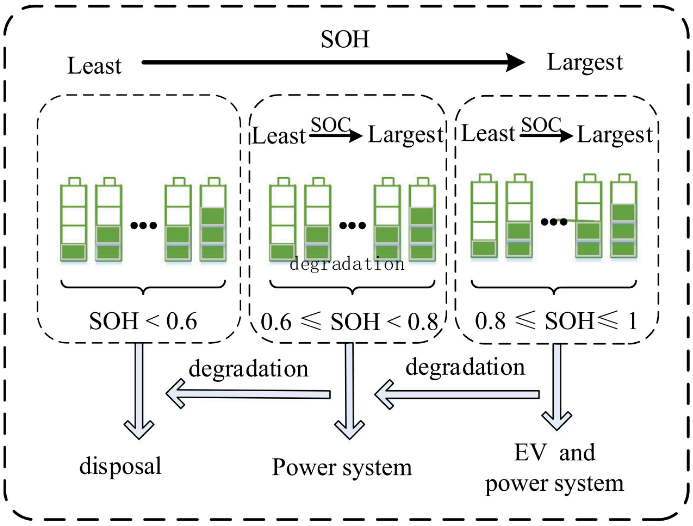

Figure 2.10: Battery Allocation strategy [101].

2.4.3. (De)Centralised charging infrastructure

There are two different charging infrastructures; centralised and decentralized charging structures [53]. In Centralized Battery Charging Stations (CBCS), depleted batteries are collected and transported to centralised facilities or sites for recharging [102], [103]. They are often located away from the swapping station, leading to logistical challenges such as higher operational costs due to warehouse rents. This model benefits from economies of scale in energy management and can integrate seamlessly with existing power grid systems [103], but also has a low utilisation rate of charging facilities.

The Decentralised Battery Charging Stations (DBCS) approach addresses some of the inefficiencies seen in CBCS. In this model, the BCS is stationed near the BSS so that fully charged batteries can quickly be deployed, empty batteries can quickly be charged, and it has a local inventory that can be easily accessed. DS also significantly cuts down on the costs of renting large warehouse spaces and increases the utilisation rates of recharging facilities. On the other hand, decentralised systems involve numerous smaller, strategically placed swapping stations that offer flexibility and access across a broader area. These stations typically support the localised charging of batteries, and reduce the centralised grid load[35], [104]. A drawback of the DC Stations is the need for perfectly coordinated swapping station requirements, the scheduling of charging operations and battery logistics [105].

2.4.4. Impact on electricity grid

Rao et al. [106] discussed how EV drivers' behaviour in battery swapping affects the power grid, suggesting that optimal charging management (OCM) could minimise adverse impacts on the power grid and generation. Sarker et al. [107] investigated the business case and optimisation model for EV battery swapping stations, emphasising their benefits to the power system by providing better energy management solutions and balancing demand and supply on the grid. Wu [35] surveyed operational modes and decision scenarios in battery swapping stations, pointing out the direct influences on power grid performance and the need for strategic planning to accommodate the growing number of EVs. Li et al. [108] discussed a centralised scheduling strategy for battery swapping, which could potentially improve the stability and reliability of power grid operations by mitigating the erratic nature of EV charging demands.

2.4.5. Safety

The safety of charging is highly important, which includes the EV itself, batteries, electrical systems, fire, electrical shocks and cyber-security [46]. Acharya et al. [109] are mentioning that the charging infrastructure can be attacked by spoofing (disguising as a legitimate source or process), tampering (unauthorised alteration or destruction of data or a process), repudiation (irresponsibility of actions performed), information disclosure (unauthorised acquisition and dissemination of information), Denial-of-service (D0D) (state where any authorised entry is deprived of reliable and timely access to services and information) and elevation of privilege (attacker gains extra privileges circumventing standard authorisation protocols). Nowadays, those types of cyber-securities are relevant and should be considered.

2.4.6. Conclusion

In this section of the literature review, the BCS was discussed. Several strategies have been presented for charging the batteries. The benefit of BSSs, and thus charging stations, is that batteries can be charged as optimally as possible. This can reduce battery degradation, improving the SOH and optimal use of the BCS. However, the advantage of slower charging also has a downside. Slower battery charging results in fewer batteries being available if there are a lot of EVs demanding batteries. One advantage of slower battery charging is that it extends the battery's lifetime. However, the optimisation between battery lifetime and charging speed is not within the scope of this thesis. For this thesis, a specific (constant) charging speed will be chosen. This can be modified if the optimisation model indicates that the BSM cannot be applied. The primary focus is on the general applicability of the BSM and the potential for applying the RPA vessel with this method.

The centralised and decentralised charging infrastructure were discussed as well. Applying (large) battery modules on RPA vessels is the best way to do this in decentralised in combination with the BSS. To move the batteries to a centralised facility or site is, from the perspective of the BSM, not the most ideal option for this application of the BSM. Therefore, in this thesis, a decentralised BCS in combination with a BSS will be used. Optimal charging management could be introduced to optimise this. However, for this thesis, this is not within the scope.

This is more complicated when looking at the impact on the electricity grid. The battery charging is correlated with the demand of the electricity grid. This can be solved by optimal charging management. Also, safety is important since the batteries are within the Port of Rotterdam. The BSS can also have two additional benefits for the power grid: the reliability of unsustainable penetration of the grid and a controlled/scheduled charging of depleted batteries and charging those batteries at peak hours. Also, charged batteries can be used as storage aggregators and the application of smart grids [52]. In this way, it can be solved. However, this is not directly within the scope of the thesis.

2.5. Swapping Concepts

From a market perspective, the BSM is already applied in the maritime industry, but not specifically for vessels with an uncertain sailing profile like the RPA vessels. This section discusses the application of three different Battery Swapping Concepts. The first is the ZES-pack container concept, which uses containerised energy modules that are already operational for container barges. The second battery-swapping concept is based on the ZES-pack containerised energy modules. However, it has another application (container barges differ from RPA vessels) and is in an early design phase. The last one is a concept that uses cranes to load and unload battery modules on the vessel.

2.5.1. ZES-pack containers (Zero Emission Services)

Zero Emission Services (ZES) is a company with the objective of accelerating the energy transition for sustainable inland waterway transport. ZES uses BSSs to facilitate swapping depleted battery containers for fully charged batteries (within 15 minutes) [21]. This technology is currently applied at container barges to reduce charging downtime. ZES facilitates the pay-per-use of 20-foot containers (2000 kWh) with renewable energy, which can be easily scaled and are available at different locations in the Netherlands and some parts of Belgium and Germany. This pay-per-use method minimises the upfront costs for ship owners, reduces financial barriers, and promotes the widespread adoption of sustainability in the maritime sector. The containers have control, safety and cooling systems and are fire-safe. When the containers are not in use, the ZES-pack containers can stabilise or balance the energy demand and supply for the electricity grid. Furthermore, these containers can be used for purposes other than the shipping industry, such as events or construction sites. Additionally, different energy sources could be used for the same concept in the future. The ZES-pack concept can be seen in Figure 2.11.

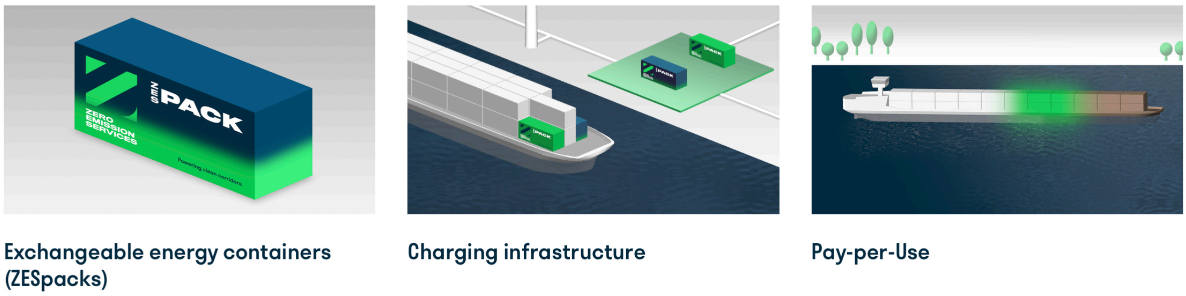

Figure 2.11: Zero Emission Services (ZES) [21]

2.5.2. Pontoon concept (with ZES-containers) (Port of Rotterdam)

Based on the ZES-pack concept, the Port of Rotterdam has explored the market and came up with an alternative. This is an implementation where the ZES-packs play a significant role. Since the ZES-pack is based on container barges, the RPA vessel design should need an adoption where the containers can be (un)loaded to the RPA vessel. The idea is to use a floating pontoon, where the ZES-pack containers are stationed and charged, to move containers (automatically) to and from the vessel. One of the disadvantages is that this concept is not yet applied in the industry and, therefore, needs to be researched. The concept can be seen in Figure 2.12.

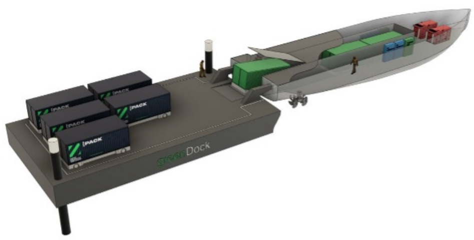

Figure 2.12: Port of Rotterdam concept (internal source)

2.5.3. Cranes (SHIFTR)

SHIFTR has a system where battery packs are interchanged on deck with a crane. SHIFTR is a company that aims to enable zero-emission operations for ferries in Norway through an autonomous battery swap system. This system reduces time at the quay and allows for continuous operation at high speeds, benefiting ship owners, passengers, and the environment. SHIFTR's technology can also suit new vessels and retrofits, including wave tide compensation. The technology aims to keep vessels running efficiently without charging during peak hours. SHIFTR does not yet have an operational functioning system, but SHIFTR's autonomous battery-swapping solution with a cutting-edge autonomous battery swap has the potential. SHIFTR plans to apply this system to Norway's fast-ferry industry, where the crane system can revolutionise this branch. Also, the batteries' footprint is smaller than that of ZES-pack containers since the batteries are designed specifically for this system. The concept can be seen in 2.13 and Figure 2.14.

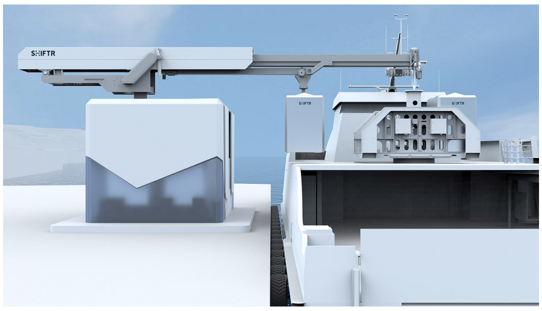

Figure 2.13: SHIFTR concept for interchangeable batteries (1) [22]

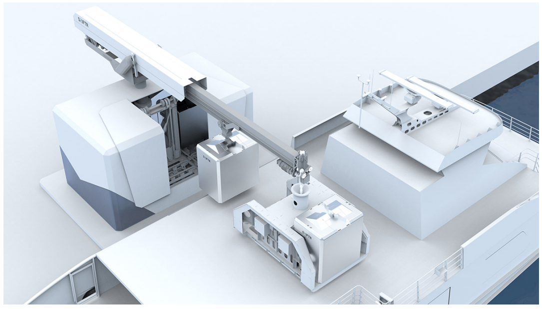

Figure 2.14: SHIFTR concept for interchangeable batteries (2) [22]

2.5.4. Conclusion

Based on the three different BSM applications, the concept of the Port of Rotterdam is not likely to be applied during this thesis. The main reason is the early design phase and the resources (e.g. money, time and infrastructure) needed to further design this concept, which is not within the scope of the thesis. Also, the practical application of the BSM is different from that of RPA vessels compared to container barges since RPA vessels are not designed to accommodate 20-foot containers. Furthermore, the main station (where the RPAs are stationed) will need a pontoon (design) from which the containers are charged and swapped. This is different compared to container barges, which already have the necessary infrastructure available on their route. Also, the technology readiness level (TRL) from the ZES-pack-based concept of the Port of Rotterdam is less than the SHIFTR concept. The SHIFTR concept also requires modifications to the current RPA design since the energy containers will be placed on the deck (e.g. stability). However, the SHIFTR concept is more likely to be used compared to the other concepts.

The choice of the SHIFTR concept is mainly due to the practical application based on the current design of the RPA vessels. However, it should be mentioned that every concept is effectively related to parameters. This parameter-based approach defines various concepts, applying one concept to the optimisation model. This approach allows flexibility, as the model can be hypothetically adjusted to accommodate new concepts as the market evolves. In Chapter 4, the SHIFTR concept and the used parameters for the optimisation model will be discussed.

2.6. Operational Research Methodology

From the previous sections, it was concluded that a BESS (CH2.1) could be used in this thesis, in combination with a BSS (CH2.2) with Lithium-Ion batteries (CH2.3). Furthermore, a BCS (CH2.4) was researched to facilitate the BSM. The combination resulted in the SHIFTR concept (CH2.5). Based on this technical part of applying a BSM, the operational part is discussed in this section. It is essential to research how the BSM can be optimised. From this point forward, the literature review is used to research potential optimisation methodologies. This can be divided into four different types of optimisation based on the already discussed literature:

1. **Swapping Stations**
   There are two views of the BSS: the view of the customer and the BSS operator. From the perspective of BSS, optimal sizing and siting are important for BSS operators since the accessibility of BSS is an important service for customers. From a customer perspective, fast service time is important since longer waiting times reduce the operational time of the customers.
2. **Energy Modules**
   The energy modules in the system can be optimised independently; too many energy modules will affect the cost, but fewer energy modules will increase the service time since customers cannot swap batteries instantly.
3. **Charging Stations**
   For the BCS, effective charging could be the main optimisation method.
4. **Vehicle related (Shortest path and optimal scheduling)**
   From the perspective of the customers, going to the swapping station, swapping and going back to the original tasks can be minimized to maximize operational time.

Based on these four topics, different literature is research and displayed in Table 2.2. In this table, the relevant studies (including references), objectives, subjects and used optimisation methods can be seen. In this table, six different optimisation methods were found: Linear Programming (LP), Mixed Integer Linear Programming (MILP), Mixed Integer Programming (MIP), Robust Optimization (RO), Markov Decision Process (MDP) and General Algorithm (GA). These optimisation methods will be first explained, and in 2.6.6 in the following section, followed by the Table 2.2 in Chapter 2.6.6.

2.6.1. Linear Programming

Linear programming (LP) is a mathematical method used to optimise a linear objective function, which includes decision variables and linear (in)equality constraints applied for different fields such as transportation and production planning [110]. LP has multiple advantages such as quality decision, maximisation of resources, complex problems, multiple constraints, simplicity, and multi-purpose [111]. The downsides of LP are the assumption of constant parameters, integer values, single objective, linear objective functions and constraints and certainty is needed for objectives and constraints which might not be known beforehand [111]. LP models are primarily categorised into two types: deterministic and stochastic. Deterministic LP assumes that all parameters are known with certainty, simplifying problem formulation and solution. In contrast, stochastic LP deals with uncertainty in data, incorporating scenarios or probability distributions within constraints or the objective function [112].

2.6.2. Mixed Integer (Linear) Programming

Mixed Integer Programming (MIP) is a mathematical optimisation technique that involves problems where some variables are constrained to be integers while others can be non-integers [113]. A specific form of MIP is mixed integer linear programming (MILP), which is restricted to a linear objective function and its constraints. These models are formulated with a linear objective function to be optimised (maximised or minimised) subject to a set of linear constraints [114]. The integration of integer variables allows these techniques to handle complex scheduling, resource allocation, and network design tasks effectively, making MIP and MILP powerful tools in operational research and various industrial applications [115], [116]. For example, in supply chain optimisation, MILP can determine the most cost-effective way to transport goods while adhering to capacity constraints [113], [117]. MIP problems typically involve advanced algorithms such as branch-and-bound, cutting planes, and heuristic methods [118]. These algorithms use an iterative method to explore feasible solutions and improve them to find the optimal solution. MIP is a powerful tool for decision-making involving continuous and discrete choices in real-world scenarios [118].

2.6.3. Markov decision process

A Markov Decision Process (MDP) is a mathematical framework utilised for modelling decision-making scenarios where the outcomes are influenced by randomness and the decisions made by the decision maker [119]. MDPs are characterised by a set of states, actions, transition probabilities that define the likelihood of moving from one state to another given an action, and a reward function which assigns a value to each transition between states [120]. The objective of an MDP is to find a policy, which is a rule that the decision maker follows in selecting actions based on the current state, that maximises the cumulative reward over time, often under conditions of uncertainty [119]. This framework is widely used in various fields such as robotics, automated control, economics, and artificial intelligence, particularly in stochastic control and reinforcement learning, where an agent learns to make decisions by interacting with a complex, uncertain environment [120].

2.6.4. Robust optimization

Robust optimisation is a branch of optimisation that deals with decision-making under uncertainty [121], [122]. It aims to provide solutions immune to input data variations within specified bounds. Traditional optimisation methods often assume precise and deterministic input data, which is not always realistic in many practical applications (e.g. supply chain management) [123], finance [124], and engineering [125]. Robust optimisation counters this by incorporating uncertainty directly into the optimisation model. The method focuses on constructing feasible solutions for all possible variations of the uncertain parameters defined within a prescribed uncertainty set [126]. The key feature of robust optimisation is its ability to offer solutions that guarantee performance against the worst-case scenario, thus ensuring greater reliability and stability of the outcomes in unpredictable environments [121]. This approach is precious when it is difficult to accurately estimate the uncertain parameters' probability distributions, making it a conservative yet convenient tool for decision-makers facing uncertain conditions [125].

2.6.5. Generic Algorithms

Genetic algorithms (GAs) are heuristic optimisation methods inspired by the principles of natural selection and genetics [127]. These algorithms are particularly effective for solving complex optimisation problems where traditional methods may falter due to the non-linearity, high dimensionality, or discontinuity of the solution space [128]. A typical GA operates by maintaining a population of potential solutions encoded as chromosomes [127]. Through iterative selection, crossover, and mutation processes, GAs evolve this population towards optimal solutions [55]. The selection emphasises fitter solutions, enhancing their likelihood of propagating their characteristics to subsequent generations. Crossover combines pairs of solutions to explore new regions of the solution space, while mutation introduces random alterations to maintain genetic diversity and avoid premature convergence [129]. The robustness of GAs in exploring diverse solution landscapes makes them valuable in various fields, including engineering, economics, and biological research [129]. Their adaptability and efficiency in handling multi-objective and constrained optimisation problems underscore their significance in contemporary optimisation models [130].

2.6.6. Relevant literature

In this section, the considered studies are discussed based on the discussed optimisation methods: Linear Programming (LP), Mixed Integer Linear Programming (MILP), Mixed Integer Programming (MIP), Robust Optimization (RO), Markov Decision Process (MDP) and General Algorithm (GA). If the optimisation method is used, it is indicated with a green checkmark.

Table 2.2: Different optimisation studies from the literature

Reference	Objective	Subject	LP	MILP	MIP	RO	MDP	GA
Kuby and Lim (2005) [131]	Maximise traffic flow	Refueling range-limited AFVs			✓			
Kuby and Lim (2007) [132]	Maximise traffic flow	Candidates site along arcs for range-limited vehicles			✓			
Kim and Kuby (2013) [133]	Maximise traffic flow	Refueling range-limited AFVs		✓				
Chung (2015) [134]	Maximise traffic flow	Multi-period optimisation for charging station location planning for EVs		✓				
Wang and Lin (2009) [135]	Minimise total costs	Battery Charging Stations EVs			✓			
Wang and Wang (2010) [136]	Minimise costs and maximise coverage	Refueling range-limited AFVs			✓			
Tu et al. (2016) [137]	Maximise (charging) service	Battery Charging stations EVs (ET)			✓			
Mak et al. (2013) [138]	Minimise worst-case costs, maximise worst-case probability	Infrastructure planning EVs Battery Swapping				✓		
Yang et Sun (2015) [92]	Minimise travel/ investment cost	BSS locating-routing problem for EVs		✓				
Hof et al [139]	Minimise travel/ investment cost	BSS locating-routing problem for EVs		✓				
Yang et al. (2017) [140]	Maximise total profit	Optimising planning of BSS/BCS		✓				
Chen et al. (2016) [141]	Minimise social costs	Optimising deployment of charging lanes for EVs		✓				
Xi et al. (2013) [142]	Maximise the number of charged EVs	Location of (public) BCS infrastructure	✓					
Dong et al. (2014) [143]	Minimise missed trips	EVs BCS location and siting	✓					
Cavades et al. (2015) [144]	Maximise satisfied demand	EVs BCS location and siting			✓			
Asamer et al. (2016) [145]	Maximise total trips	EVs BCS location		✓				
Chen et al. (2017) [146]	Minimise total costs	Planning PHEVs for BSCs		✓				
Flath et al. (2014) [147]	Minimise total charging costs	Improving EVs Charging Coordination	✓					
Qi et al. (2014) [148]	Maximise total utility	Coordination of charging PHEVs		✓				
Iversen et al. (2014) [149]	Maximise revenue	Optimal charging of EVs					✓	
Nurre et al. (2014) [150]	Maximise profit	BSS for PHEVs	✓					
Boyaci et al. (2014) [151]	Maximise net revenue	Relocation problem one-way (sharing) EV		✓				
Bruglieri et al. (2014) [152]	Maximise satisfied request	Relocation problem one-way (sharing) EV		✓				
Kim and Kuby (2011) [153]	Station location optimization model	Hydrogen Stations		✓				
An et al. (2020) [104]	Minimise total investment BSS	BSS planning electric buses with local charging	✓					
Sarker et al. (2015) [107]	Maximise operator profit	Limited EV range vehicles		✓				
Armstrong et al. (2013) [154]	Maximise operator profit	Optimal recharging strategy BSS EVs		✓		✓		
Wu et al. (2015) [55]	Maximizing batteries in stock, minimise battery costs	Optimisation for EVs for BSSs						✓
Wu et al. (2018) [50]	Minimizing the number of batteries	Optimisation for EVs for BSSs						✓
Infante et al. (2020) [45]	Minimizing battery degradation costs	Coordinated management and ration assessment of EVs BCS		✓				
Sepetanc et al. (2020) [155]	Maximise number of batteries, minimizing charging power	EVs BSSs		✓				
Zhang et al. (2014) [156]	Minimizing charging costs	Optimal scheduling of EVs BSS		✓				
Mahoor et al. (2019) [157]	Minimizing operation costs	Least-cost operation for BSS with random customer request		✓				

2.6.7. Conclusion

Optimising on four different topics requires more advanced optimisation models. Since the RPA vessel should have a maximal operation profile, the optimisation will be based on minimising the time a vessel is busy with the swapping process (so vehicle related). Based on the studied literature, most optimisations were executed with MILP and thefore this optimisation method will be used in this thesis.

2.7. Literature Gap

Based on the literature discussed in this chapter, the literature gap can be formulated. In this literature review, both the technical as the operation issue for a BSM was discussed. For the technical part, the ESS (CH2.1), the swapping station (CH2.2), the energy modules (CH2.3, the charging station (CH2.4 and concepts for applying the BSM (CH2.5) were discussed.

It was concluded that a BESS (CH2.1) could be best applied for this research, in combination with a swapping method explained in Chapter 2.2. The Battery Swapping Stations were introduced as an alternative to PHEVs, which had several problems in the past. In the transportation sector, it was already applied to different types of vehicles, such as electric cars, buses, taxis, and steps and was discussed in Chapter 2.2.1. However, little to no literature was available for the application of the BSM for vessels (CH2.2.2) and if available, this would have been with specific sailing paths instead of uncertain sailing paths.

In Chapter 2.3.4, the energy modules were discussed. Based on a comparison of different batteries (Table 2.1), it was concluded that lithium-ion batteries could be best applied in this research for the BSM. From a literature perspective, there is enough research available on lithium-ion batteries, and there is no specific literature gap in this field for applying those batteries.

In the fourth section (CH2.4), the Battery Charging Station (BCS) was discussed. This section discussed multiple topics such as the charging strategies (CH2.4.1), battery degradation (H2.4.2), centralised or decentralised charging infrastructure, the impact on the electricity grid (CH2.4.4) and safety (CH2.4.5). Battery degradation, the impact on the electricity grid, and the safety of BCS are important, but they are not directly relevant to the scope of the thesis. The integration with the BSS is important for this thesis, especially if the BSS and the BCS are combined (decentralised) or not (centralised). A centralised infrastructure was not feasible for applying the BSM for RPA vessels. Combined with lithium-ion batteries, it was concluded that the BSS and BCS should be combined; thus, a decentralised structure was needed. From a literature perspective, the combination of BSSs and BCSs was discussed in different papers, but not specifically for vessels with uncertain sailing paths.

In the fifth section (CH2.5), the different potential concepts were discussed based on the first four sections. The company ZES, a variant of the ZES concept and the SHIFTR company were discussed. None of the companies applied the BSM for vessels with an uncertain sailing path. However, the SHIFTR concept can potentially be used for this thesis because the integration with the cranes can be better implemented than in the case of the cranes and ZES-pack containers. Little to no literature was available on the application of those systems. Some applications were applied, like the company ZES, which uses the BSM for inland container barges with a specific sailing path. Again, the application for vessels with an uncertain sailing path was unavailable. In conclusion, for the technical part of the literature, it was concluded that there is a literature gap for the application of renewable energy sources for vessels with an uncertain sailing path, with a relatively small footprint.

The second part of the literature discussed the operational part of applying the BSM (CH2.6). In this section, the discussed technical parts of the BSM were considered and used to research different optimisation methods based on several relevant studies (Table 2.2). Since the application of uncertain sailing paths for vessels was (mostly) unavailable, similar studies were researched. In line with the technical part of the literature, little to no literature was available for the application of optimisation methods for this type of research. However, it was concluded that for this type of research, MILP is most suitable for this thesis.

The overall conclusion is that the combination of BESS, lithium-ion batteries, BSS, BCS, the SHIFTR concept and the optimisation model is not yet researched in literature. The topics are not specifically a literature gap, but combined, they are. From this point, the thesis is performed to investigate whether the BSM can be applied for RPA vessels in the Port of Rotterdam.

3 Methods

This thesis researches the application of the BSM for RPA vessels in the Port of Rotterdam where the objective is to minimise the total swapping time time. Based on the technical part of the literature review, a BES system with Li-Ion batteries and a decentralised BCS in combination with a BSS is used to evaluate this. Additionally, the operational part was discussed and a MILP optimisation model will be made to identify the most optimal configuration of the BSM.

This chapter describes the methodology and is divided into three sections. Firstly, the scope of the thesis is discussed (CH3.1). Since the thesis is in the early stages of the renewal/refitting of the RPA vessels, it should be defined correctly. Then, the conceptual process (CH3.2) is discussed. This is mainly based on the tasks of the vessel, the decisions that should be made, and the primary process for both vessel types (blue and red). Finally, the mathematical model (CH3.3) is discussed, which includes everything which is needed to make the optimisation model (sets, decision variables, parameters, objective function and functional constraints). Each section has its research question:

1. *What is the scope of this research? (CH3.1)*
2. *What is the current conceptual process and how can a BSM be applied to this? (CH3.2)*
3. *How can the mathematical model be formulated to make an optimisation model for this specific research for RPA vessels in the Port of Rotterdam? (CH3.3)*

3.1. Scope

Since the refitting/renewal of RPA vessels is in an early stage, with uncertain parameters, the thesis must be well-scoped. Based on the technical part of the literature review (CH2.1 - CH2.5), the scope is formulated to research the operational part of the thesis: Minimising the downtime due to swapping for RPA vessels. As mentioned in the literature review, some of the discussed topics will be outside the scope of this thesis. The scope of this thesis is defined as follows:

1. **Swapping Stations**
    - Physical swapping of energy modules onto the RPA vessel, is assumed to be working. The explained Shiftr concept is working.
    - The layout of the swapping station is only implemented in the way that model-based parameters are used and could be changed if necessary.
    - The average service time of swapping energy modules is a constant as an input parameter.
    - Energy module strategies are not applied; the energy modules stationed the longest at the swapping station are not explicitly used first (First In, First Out).
2. **Energy Modules**
    - Batteries are used (CH2.3) to store energy in the energy module and their characteristics are assumed constant.
    - Battery degradation is not considered.
    - Energy modules have the same dimensions and the same power output.
    - The batteries' State of Health (SOH) is the same during the optimisation.
    - Linear charging speed.
3. **Battery Charging Stations (BCSs)**
    - Battery strategies are not considered as explained in the literature.
4. **Vessels**
    - The sailing profile is a pre-defined set based on AIS data.
    - The connection between the swapping station/crane, from a vessel's perspective, is feasible and assumed to be working.
    - Modular design is available for the application of energy modules. However, the modular design of the RPA itself is not within the scope.
    - The energy consumption is pre-defined from a data set based on the AIS data.
    - If a swap is made, a predefined vessel speed is used to go to and from swapping stations.
    - The vessel's design, including any system for swapping (e.g. the battery carousel as seen in the SHIFTR concept) for swapping, is outside the scope of this thesis.
    - The operating area of the RPAs remains the same.
    - Distances to other swapping stations are calculated in the pre-processing.

3.2. Conceptual process

The conceptual process of the RPA vessels is discussed in this section. In the current operation, each RPA vessel (red or blue) starts at its main harbour, which is the Pistoolhaven, Madroelhaven or Duivelseiland (an outpost in Dordrecht, which is under the jurisdiction of the Port of Rotterdam). Furthermore, a bunker location is located in the Eemhaven. From these main harbours, the vessels will sail and do tasks such as inspecting vessels or responding to incidents (e.g. fire, man overboard or (dangerous) goods in the water). The RPA vessels have 24/7 availability and operate three shifts (during the day) with a different crew. The duty starts and ends at the same harbour, and the vessels have enough energy onboard to complete the shifts (conventional power). The operating area for each location can be seen in Figure 3.1.

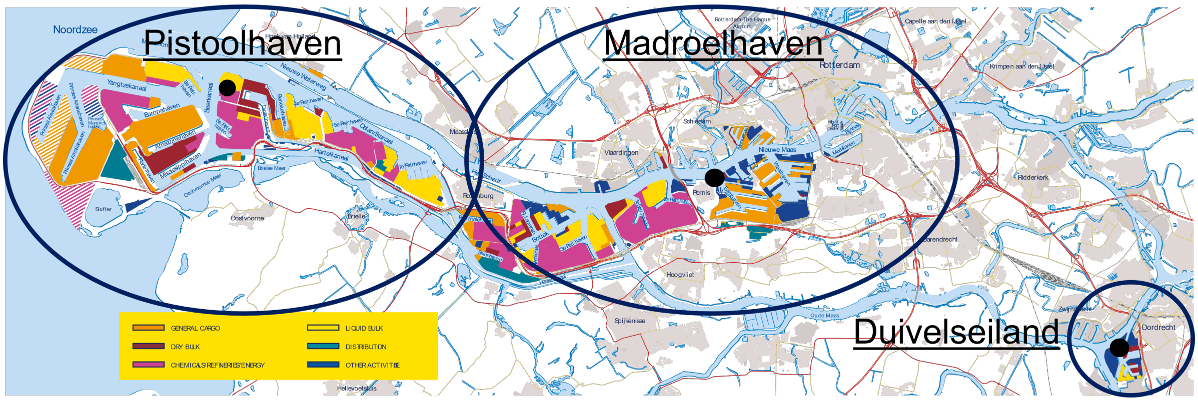

Figure 3.1: Operational area RPA vessels Port of Rotterdam [Internal source/own work]

However, when a swapping method is applied to those vessels, the operating pattern will be affected by this method since the vessel's total energy is significantly less than conventional energy sources, which means that the vessels most likely need a swap during the current shift. Figure 3.2 gives an example. At time $= 6$ the vessel has two empty (red) modules and cannot sail further. Therefore, the vessel should initiate a swap going to the swapping where the empty modules can be swapped for fully charged modules (green). After the swapping of the modules, the vessel should sail back to the original path. The implementation can be seen in the mathematical model which will be discussed in the next section (CH3.3).

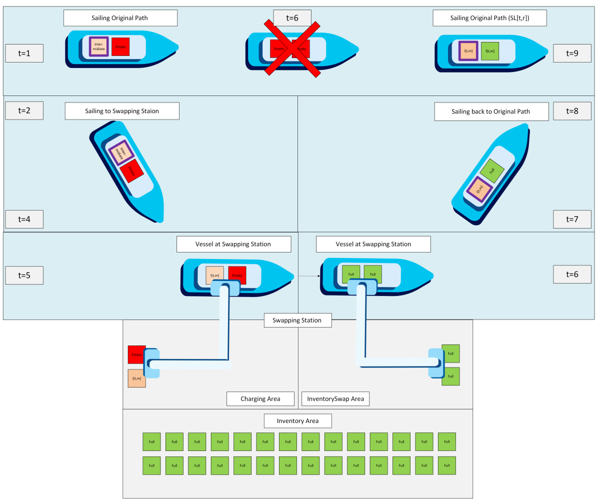

Figure 3.2: Swapping concept

3.3. Mathematical model

Based on the conceptual process and the scope, this section discusses the mathematical model. The summarised version of the mathematical model can be seen in Appendix A. In this section, the sets and indices (CH3.3.1), the (decision) variables (CH3.3.2), the parameters (CH3.3.3), the objective function (CH3.3.4) and the (functional) constraints (CH3.3.5) will be discussed.

3.3.1. Sets and indices

Based on the scope and the conceptual process, the sets and indices are discussed. In this optimisation model, both the vessel r and the energy modules m should be tracked for each time t. Furthermore, the swapping areas s should be indicated since different zones will be used during this thesis. Due to the decentralised structure of the BSM, the swapping station, charging station and inventory area are indicated with index s. The reason why this same index s is used for these different sub-locations is to make the optimisation smaller in terms of indices, which could improve the structure of the model (otherwise, an index for charging c and an index for the inventory i would have been introduced). The different sets are summarised in Table 3.1.

Table 3.1: Sets and indices for the optimisation model

Sets and indices for the optimisation model		
M	Set of Energy Modules m	$m \in M$
R	Set of RPA Vessels r	$r \in R$
S	Set of Swapping Area s	$s \in S$
T	Set of time t	$t \in T$

3.3.2. (Decision) Variables

For this optimisation model, different (decision) variables are used. These variables can be divided into two levels: the module and vessel level, where the module level has at least an index m, and the vessel level has exclusive indices r and t. The module level can be divided into different subjects: modules m located on the vessel r or located in the swapping area s, the energy level (and state) of module m and an indication that the module is used for energy consumption for a specific vessel state. This can be seen in Table 3.2. In this table, one continuous variable is used ($l_{t,m}$) to indicate the actual energy level of each module m at time t while the other variables are binary variables, meaning those variables can either be zero or one. Figure 3.4, in Chapter 3.3.5, shows the variables in an example.

Table 3.2: (Decision) Variables for the optimisation model

(Decision) Variables			Explanation
Module Level	Vessel	$x_{t,m,r}$	Indicating module m is located on vessel r at time t
		$u_{t,m,r}$	Indicating module m is used for propulsion on vessel r at time t
Module Level	Swapping Area	$y_{t,m,s}$	Indicating module m is located at swapping station s at time t
		$\theta_{t,m,s}$	Indicating module m is at the swapping station s at time t, comes from the vessel r
		$\Delta_{t,m,s}$	Indicating module m in swapping station s at time t, comes from the swapping area s
		$SWAP_{t,m,s}$	Variable used to ensure module m is for exactly T_{swap} period at the swapping station s
		$Ch_{t,m,s}$	Indicating module m is at the charging station s at time t
		$In_{t,m,s}$	Indicating module m is in inventory area, within the swapping area s, at time t
		$InS_{t,m,s}$	Indicating module m is in InventorySwap area, within the swapping area s, at time t
Module Level	Energy Modules (EM)	$l_{t,m}$	Continuous variable for the energy level of module m at time t
		$e_{t,m}$	Indicating module m is below SF_{min} at time t
		$i_{t,m}$	Indicating module m has a intermediate power level at time t
		$f_{t,m}$	Indicating module m has a fully charged energy module m at time t
Module Level	Energy Consumption	$PSL_{t,m,r}$	Indicating module m is used at vessel r during sailing the original path at time t
		$PStS_{t,m,r}$	Indicating module m is used at vessel r during sailing to the swapping station at time t
		$PSbOP_{t,m,r}$	Indicating module m is used at vessel r during sailing back to the original path at time t
Vessel Level	Vessel State	$SL_{t,r}$	Indicating vessel r is at a swapping station s at time t
		$StS_{t,r}$	Indicating vessel r is sailing to a swapping station s at time t
		$VS_{t,r}$	Indicating vessel r is at swapping station s at time t
		$SbOP_{t,r}$	Indicating vessel r is sailing back to the original path at time t
		$StartSbOP_{t,r}$	Indicating vessel r starts sailing back to the original path at t
		$StartStS_{t,r}$	Indicating vessel r starts sailing to a swapping station at t

3.3.3. Parameters

There are two different types of parameters, where the first parameters are constant for the optimisation model. The second set of parameters depends on time t for a particular vessel r or swapping area s. This can be seen in Table 3.3. The meaning of the parameters is discussed in this chapter, but this will be explained further in the chapter pre-processing (CH4).

Table 3.3: Parameters

Parameters for the optimisation model			
T_{period}	The (actual) timestep for one timestep in the model	CH4.1	[min]
T_{swap}	The time it takes to swap	CH4.6	[min]
EM_N	The number of modules m on each vessel r	CH4.6	[-]
EM_{total}	Total modules m in the system	-	[-]
$EM_{capacity}$	The total capacity of an energy module m	CH4.6	[kWh]
EM_{start}	The set of modules starting at each inventory s	-	[-]
SF_{min}	The minimum safety level of modules m	CH4.6	[-]
SF_{max}	The maximum safety level of modules m	CH4.6	[-]
P_{StS}	The energy consumption for sailing to the swapping station s	CH4.4.2	[kWh]
P_{SbOP}	The energy consumption for sailing back to the original path s	CH4.4.2	[kWh]
$v_{max,StS}$	The speed for sailing to the swapping station	CH4.4.2	[km/h]
$v_{max,SbOP}$	The speed for sailing back to the original path	CH4.4.2	[km/h]
CS	Charging speed for a certain time period t	CH4.6	[kWh]
$P_{t,r}$	Energy consumption for sailing the original path for time t for vessel r	CH4.4.1	[kWh]
$RinZ_{t,r,s}$	The vessel r is in zone s at time t	CH4.4.1	[-]
$DT_{StS_{t,r}}$	The time it takes to go to a swapping station at a certain time t for vessel r	CH4.5	[min]
$DT_{StS,actual_{t,r}}$	The actual time it takes to go to a swapping station at a certain time t for vessel r	CH4.5	[min]
$DT_{SbOP_{t,r}}$	The time it takes to go back to the original path at a certain time t for vessel r	CH4.5	[min]
$DT_{SbOP,atual_{t,r}}$	The actual time it takes to go to a swapping station at a certain time t for vessel r	CH4.5	[min]
$SPos_{t,r}$	The possibility to swap for vessel r at time t	CH4.7.1	[-]
$RB_{t,r}$	Parameter which is used to indicate a vessel r is doing a task at time t	CH4.7.2	[-]
$T_{toal_{t,r}}$	The total duration of a swap for vessel r at time t	CH4.8	[min]

A more detailed explanation can be found in CH4, pre-processing. The first parameter is the energy consumption of the vessel r, $P_{t,r}$, which time and vessel depended. Also, the vessel location (latitude and longitude) is used to specify where the vessel r is in a specific zone ($RinZ_{t,r,s}$), which can only be one for a particular location s. If the optimisation is considering every time to any station, this will affect the computational time, which is not needed. Based on the objective of this thesis and the wide span of the Port of Rotterdam, reducing the possibility of swapping (calculating the time) can reduce the computational time. Therefore, the input parameter $RinZ_{t,r,s}$ is introduced which is used for a vessel r sailing in a specific zone s. This parameter is essential since if all the zones s are considered, computational time is increasing. Each zone s consists of one swapping station, charging station, inventory and one InventorySwap are due to its decentralised structure as explained in Chapter 2.4.3. For example, if the vessel is positioned at the Maasvlakte, it would not make sense to calculate all the times to each swapping station besides the closest swapping area s.

Besides the locations of each vessel r for each time t, the optimisation model should determine for each timestep t what time it takes to reach the swapping station or return to the original path. For this specific zone, the time it takes to reach a swapping station is calculated ($DT_{StS,actual_{t,r}}$) and rounded to the timestep (T_{period}), which results in $DT_{StS_{t,r}}$. Sailing back to the original path is more complicated, but for now, the only important thing to mention is that this is the time to sail back to the original path. This will be further elaborated in Chapter 4.5.

For some timesteps t, data is unavailable. To prevent the model from giving an infeasible result, parameter $SPos_{t,r}$ excludes this timestep t for vessel r for the optimisation model. Furthermore, if the RPA is outside the main harbour and is stationary for more than two executive timesteps t, the vessel r is most likely busy. This results in the parameter $RB_{t,r}$. As said earlier, this will be explained in more detail in the pre-processing chapter (CH4). But since those parameters are used in the mathematical model, at least the main concept of those should be explained.

3.3.4. Objective function

The objective of the mathematical model is to spend the least time as possible for swapping to improve the operation time of the vessels. Suppose that a vessel r is sailing ($SL_{t,r}$) which can be seen in Figure 3.3. The vessel r has two modules m ($x_{t,r,m}$) on the vessel r where one module m is empty ($e_{t,m}$), indicated with red and the other module m is intermediate ($i_{t,m}$), indicated with orange. At some point in time, at $t = 6$, the modules m will both be empty. Therefore, the vessel r should have started at an earlier timestep t with sailing to the swapping station ($StS_{t,r}$), which takes $DT_{StS_{t,r}}$ periods. After this time, the vessel r reaches the swapping station s ($VS_{t,r}$) and the modules m for the vessel r can be swapped for fully charged energy modules ($f_{t,m}$) (indicated with green) which takes exactly T_{swap} periods. After the swapping sequence, the vessel r can sail back to the original path ($SbOP_{t,r}$) which takes $DT_{SbOP_{t,r}}$ periods to eventually arrive at a certain point in time of the original sailing path ($SL_{t,r}$).

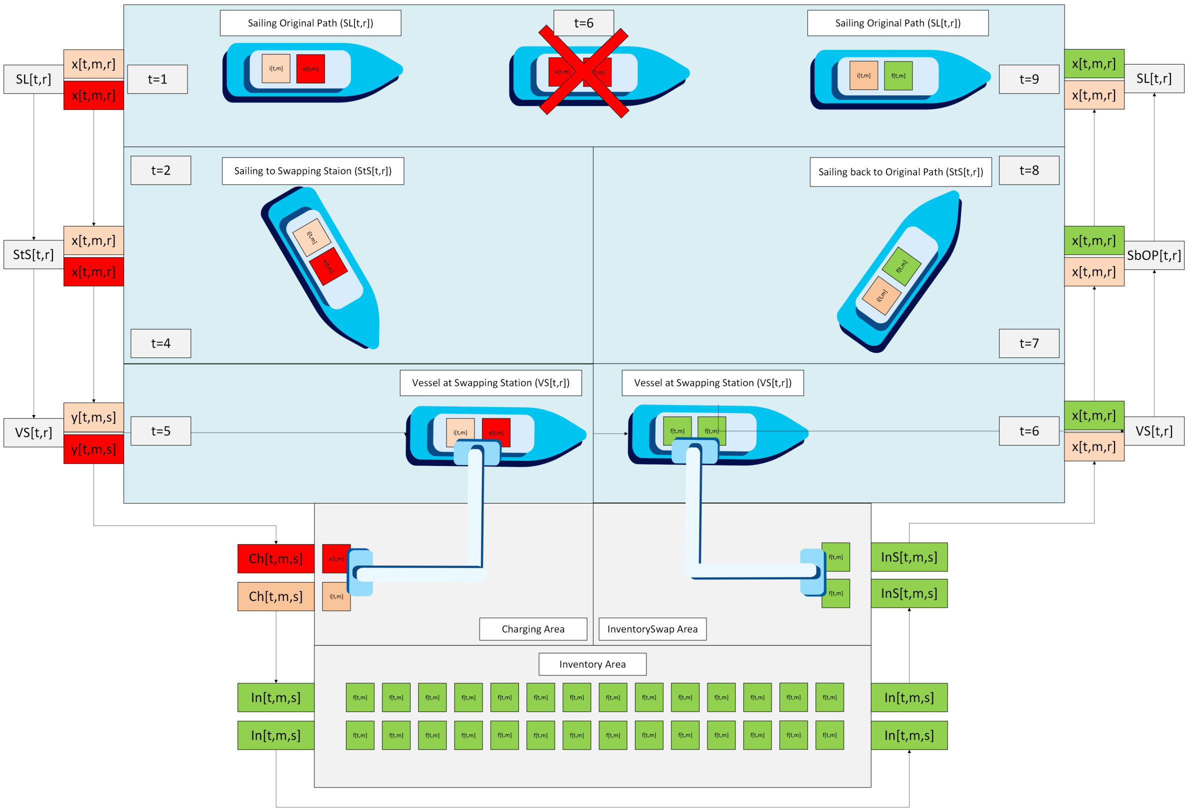

Figure 3.3: Summary of the mathematical model

Due to swapping sequence, the vessel r spends time which is not used for operational purposes. This time that the vessel r is not sailing its original path ($SL_{t,r}$), is considered as downtime and this downtime should be minimised. Therefore, the objective of this thesis is as following:

$$\min \sum_{t \in T} \sum_{r \in R} \left(StS_{start_{t,r}} \cdot DT_{StS_{t,r}} + VS_{t,r} + SbOP_{start_{t,r}} \cdot DT_{SbOP_{t,r}} \right) \tag{3.1}$$

3.3.5. (Functional) Constraints

Based on the indices (Table 3.1), the variables (Table 3.2), the parameters (Table 3.3), the objective function (Equation 3.1) and the conceptual process (Figure 3.2) the functional constraints can be defined. As discussed in Figure 3.2, the vessels r will eventually run out of energy, and a swap is required. Figure 3.4 shows an example for a vessel r, sailing with two modules m. In this example, a fictive time t is used. The blue parts refer to binary variables where the index r is used for either the vessels state ($SL_{t,r}$, $StS_{t,r}$, $VS_{t,r}$ and $SbOP_{t,r}$) or a module m located on the vessel r ($x_{t,m,r}$, and $u_{t,m,r} = 1$ if used for propulsion). At the vessel level, two additional colours can be seen referring to binary variables $InS_{t,m,s}$ and $y_{t,m,s}$, which are not directly related to the vessel r (in means of the index r). If the vessel r is sailing to the swapping station s ($StS_{t,r}$), an module m should be reserved for $DT_{StS_{t,m,r}}$ periods at the InventorySwap ($InS_{t,m,s}$) which is indicated with gray. Furthermore, when the vessel r is at the swapping station ($VS_{t,r}$), the module m should be swapped which is indicated with green. In this figure, one module m will be swapped while the other is still on the vessel r. However, it is possible in this optimisation model to swap both the modules m. The reason why the colour for $VS_{t,r}$ is green and blue, is that one module m is still on the vessel r. The green colour indicates that the vessel r is physically at the swapping station s where at least one module m of the vessel r is swapped for another module m (coming from the InventorySwap $InS_{t,m,s}$).

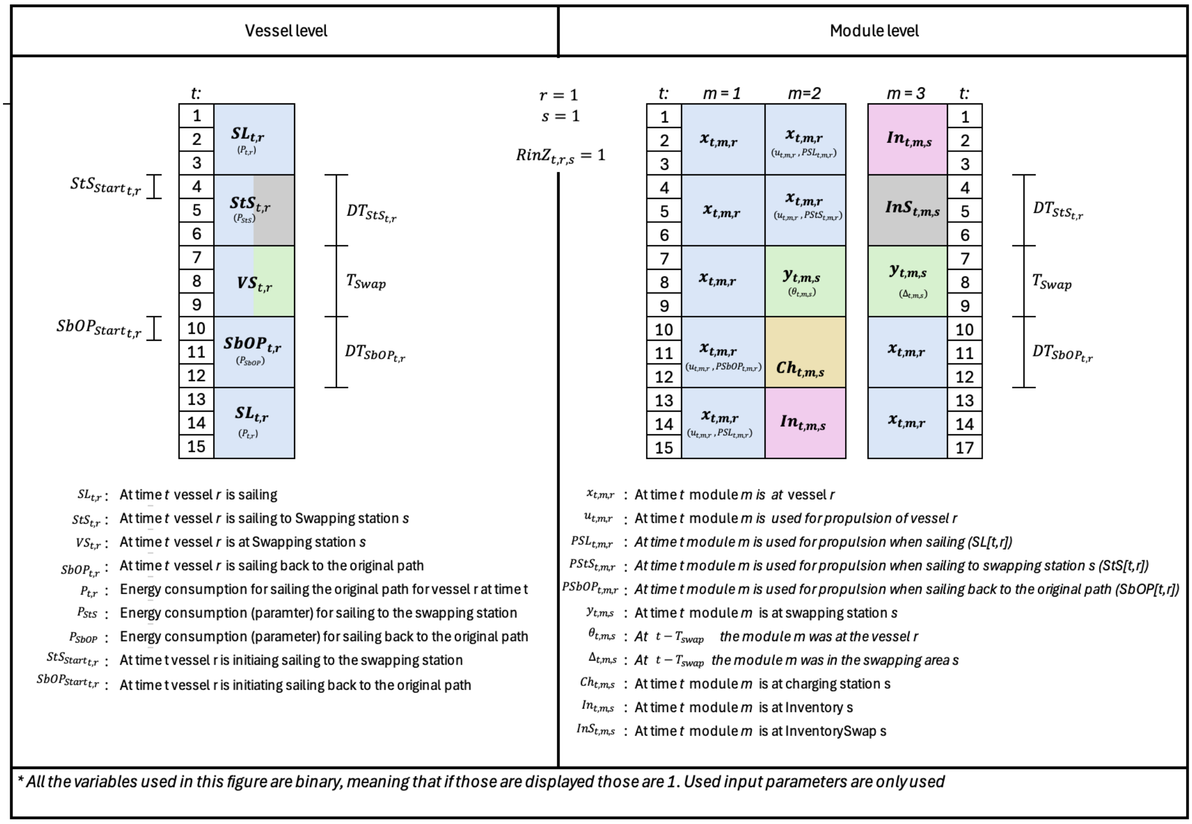

Figure 3.4: Module level

Lets suppose that a vessel r is sailing ($SL_{t,r}$) in zone s ($RinZ_{t,r,s} = 1$) with two modules m ($x_{t,m,r}$). During this sailing ($SL_{t,r}$), one energy module m is located on the vessel r ($x_{t,m,r}$) and used for propulsion ($u_{t,m,r} = 1$) with a specific energy consumption of $P_{t,r}$. Eventually, the module m on the vessel r ($x_{t,m,r}$) will be empty. Therefore, the optimisation model should initiate a swap ($StSStart_{t,r}$) to prevent the vessel r from being empty. After initiating this swap, the vessel r sails to the swapping station s ($StS_{t,r}$), with an energy consumption of P_{StS}, for $DT_{StS_{t,r}}$ periods of time. During this $DT_{StS_{t,r}}$ periods of time, a module m from the InventorySwap ($InS_{t,m,s}$) is reserved until the vessels r reaches the swapping station s ($VS_{t,r}$). When the vessel r arrives at the swapping station s ($VS_{t,r}$), at least one module m from the vessel r ($x_{t,m,r}$) is transferred to the swapping station s ($y_{t,m,s}$) (indicated with $\Delta_{t,m,s}$). On the other hand, one module m should be transferred from the InventorySwap ($InS_{t,m,s}$) (indicated with $\theta_{t,m,s}$). Both the modules m should be at the swapping station s for exactly T_{swap} periods of time. Now the modules m are swapped at the swapping station s, the modules m should correctly move to the next location based on where the modules m came from. The module m coming from the InventorySwap ($InS_{t,m,s}$) is transferred by the swapping station s to the vessel r. After swapping the module m, the vessel r initiates ($SbOP_{Start_{t,r}}$) sailing back to the original path ($SbOP_{t,r}$) for $DT_{SbOP_{t,r}}$ periods. The other module ($m = 2$) on the vessel r, which was not swapped, is now used for propulsion ($u_{t,m,r} = 1$), using an energy consumption of $P_S bOP$. When the vessel r finishes sailing to sailing back to the original path ($SbOP_{t,r}$), it reaches the original path ($SL_{t,r}$) and sails further with the power consumption $P_{t,r}$. The module m coming from the vessel r goes through the swapping station to the charging station ($CH_{t,m,s}$), where this module m is charged. Eventually, the energy module is fully charged and stored in the Inventory ($In_{t,m,s}$), waiting until it is needed for the next swap.

In Figure 3.4, the energy level $l_{t,m}$ is not defined. The energy level $l_{t,m}$ decreases or increases depending on the location of the module m at time t. There are three different levels which are used in this thesis, which will be explained later in the constraints. The modules can be full ($f_{t,m}$), intermediate ($i_{t,m}$) or empty ($e_{t,m}$). In Table 3.4 the restrictions can be seen for the state of the energy modules m for different locations. Modules m at the vessels r or at the swapping station s can be full, intermediate or empty, but if the module m is used for propulsion ($u_{t,m,r}$), the module m cannot be empty. When looking to the swapping area s, modules at the charging area ($Ch_{t,m,s}$) cannot be fully charged. Modules m in either the Inventory ($In_{t,m,s}$) or the InventorySwap ($InS_{t,m,s}$) cannot be empty ($e_{t,m}$) or intermediate ($i_{t,m}$) since those modules should be fully charged.

State	**Energy range**	**Vessel r**		**Swapping area s**			
		$x_{t,m,r}$	$u_{t,m,r}$	$y_{t,m,s}$	$Ch_{t,m,s}$	$In_{t,m,s}$	$InS_{t,m,s}$
$e_{t,m}$	$0 \leq l_{t,m} \leq$ SF$_{min}$	✓	✗	✓	✓	✗	✗
$i_{t,m}$	$SF_{min} \leq l_{t,m} \leq SF_{max}$	✓	✓	✓	✓	✗	✗
$f_{t,m}$	$SF_{max} \leq l_{t,m} \leq EM_{capacity}$	✓	✓	✓	✗	✓	✓

Table 3.4: The indication of different states of modules with a certain energy level $l_{t,m}$

The previous explanation was a high level summary of the working of the constraints. The actual (functional) constraints are divided in different parts, where each part will be discussed separately (the overall constraints can also be seen in Appendix A):

1. *Module position (Chapter 3.3.5.a)*
2. *Logical flow of modules (Chapter 3.3.5.b)*
3. *Modules at Swapping Station (Module level) (Chapter 3.3.5.c)*
4. *Energy level and module state(Chapter 3.3.5.d)*
5. *Vessel state (Chapter 3.3.5.e)*
6. *The correct indication of the energy level of modules (Chapter 3.3.5.f)*

a. Module position

The modules m can only be located at one specific location for each time t. The modules m can either be at the vessel r ($x_{t,m,r}$) or in the swapping area s ($Ch_{t,m,s}$, $In_{t,m,s}$ or $InS_{t,m,s}$) which can be seen in Constraint 3.2. Furthermore, the sum of all the modules m at a certain location r or s should be equal to the total energy modules EM_{total} in the system, which can be seen in Constraint 3.3.

$$\sum_{r\in R} x_{t,m,r} + \sum_{s\in S} y_{t,m,s} + \sum_{s\in S} Ch_{t,m,s} + \sum_{s\in S} In_{t,m,s} + \sum_{s\in S} InS_{t,m,s} = 1 \qquad \forall\, t\in T, m\in M \tag{3.2}$$

$$\sum_{r\in R}\sum_{m\in M} x_{t,m,r} + \sum_{s\in S}\sum_{m\in M} y_{t,m,s} + \sum_{s\in S}\sum_{m\in M} Ch_{t,m,s} + \sum_{s\in S}\sum_{m\in M} In_{t,m,s} + \sum_{s\in S}\sum_{m\in M} InS_{t,m,s} = EM_{total} \qquad \forall\, t\in T, m\in M \tag{3.3}$$

b. Logical flow of modules

The specific module flow, as can be seen in Figure 3.4, is essential since the modules should follow this flow at all times. Therefore, the following constraints discuss the flow of modules for a specific location.

Vessel
As can be seen in Figure 3.4 the modules m have a specific flow. A module m coming from a vessel r ($x_{t-1,m,r}$) can only stay at the vessel r ($x_{t,m,r}$) or go to the swapping station s ($y_{t,m,s}$), realised by Constraint 3.4. Constraint 3.5 ensures that an module m at the vessel r ($x_{t,m,r}$) could only have come from the vessel r ($x_{t-1,m,r}$) or a swapping station s ($y_{t-1,m,r}$). Constraints 3.6 - 3.7 ensure that the modules m cannot move directly between the vessel r to the charging area ($Ch_{t,m,s}$), inventory ($In_{t,m,s}$) or InventorySwap ($InS_{t,m,s}$).

$$\sum_{r\in R} x_{t-1,m,r} \leq \sum_{r\in R} x_{t,m,r} + \sum_{s\in S} y_{t,m,s} \qquad \forall\, t \in \{1,\dots,T\}, m \in M \quad (3.4)$$

$$\sum_{r\in R} x_{t,m,r} \leq \sum_{r\in R} x_{t-1,m,r} + \sum_{s\in S} y_{t-1,m,s} \qquad \forall\, t \in \{1,\dots,T\}, m \in M \quad (3.5)$$

$$\sum_{r\in R} x_{t,m,r} \leq 1 - \sum_{s\in S} Ch_{t-1,m,s} - \sum_{s\in S} In_{t-1,m,s} - \sum_{s\in S} InS_{t-1,m,s} \qquad \forall\, t \in \{1,\dots,T\}, m \in M \quad (3.6)$$

$$\sum_{r\in R} x_{t-1,m,r} \leq 1 - \sum_{s\in S} Ch_{t,m,s} - \sum_{s\in S} In_{t,m,s} - \sum_{s\in S} InS_{t,m,s} \qquad \forall\, t \in \{1,\dots,T\}, m \in M \quad (3.7)$$

When the module m is on the vessel r, one extra binary variable is introduced, $u_{t,m,r}$, which is the usage of a specific module m on a vessel r, for time t. This variable can only be one if the module m is on the vessel r, so that $x_{t,m,r} = 1$. This can be seen in Constraint 3.8. The vessels r can have multiple energy modules m onboard. However, at most, one module can be used at time t for vessel r. This can be seen in Constraint 3.9.

$$u_{t,m,r} \leq x_{t,m,r} \qquad \forall\, t \in T, m \in M, r \in R \quad (3.8)$$

$$\sum_{r\in R} u_{t,m,r} \leq 1 \qquad \forall\, t \in T, m \in M \quad (3.9)$$

Swapping station
Looking at Figure 3.4 the modules at the swapping station ($y_{t,m,s}$) can come from two different locations either the vessel($x_{t-1,m,r}$) or the InventorySwap ($InS_{t-1,m,s}$). Similarly, the modules from swapping ($y_{t-1,m,s}$: green) can either go to the vessel ($x_{t,m,r}$) or the charging area ($Ch_{t,m,s}$). The swapping station s then serves as a crossing point for modules m and therefore logic of the flow is different from the flow of the vessel r. This logic is formulated in Constraint 3.10 - 3.11. If a module m was in the charging area ($Ch_{t-1,m,s}$) or the Inventory ($In_{t-1,m,s}$), it cannot go to the swapping station ($y_{t,m,s}$) (Constraint 3.12). Also, if a module m was at the swapping station ($y_{t-1,m,s}$), it cannot go directly to the InventorySwap ($InS_{t,m,s}$) or Inventory ($In_{t,m,s}$) (Constraint 3.13).

$$\sum_{s\in S} y_{t,m,s} \leq \sum_{r\in R} x_{t-1,m,r} + \sum_{s\in S} y_{t-1,m,s} + \sum_{s\in S} InS_{t-1,m,s} \qquad \forall\, t \in \{1,\dots,T\}, m \in M \quad (3.10)$$

$$\sum_{s\in S} y_{t-1,m,s} \leq \sum_{r\in R} x_{t,m,r} + \sum_{s\in S} y_{t,m,s} + \sum_{s\in S} Ch_{t,m,s} \qquad \forall\, t \in \{1,\dots,T\}, m \in M \quad (3.11)$$

$$\sum_{s\in S} y_{t,m,s} \leq 1 - \sum_{s\in S} Ch_{t-1,m,s} - \sum_{s\in S} In_{t-1,m,s} \qquad \forall\, t \in \{1,\dots,T\}, m \in M \quad (3.12)$$

$$\sum_{s\in S} y_{t-1,m,s} \leq 1 - \sum_{s\in S} InS_{t,m,s} - \sum_{s\in S} In_{t,m,s} \qquad \forall\, t \in \{1,\dots,T\}, m \in M \quad (3.13)$$

Charging, inventory and InventorySwap
The logical flow of the modules at the charging station, inventory and InventorySwap are similar to the logical flow of the modules m onboard the vessel r. The constraints for the flow of those energy modules m can be seen in the appendices. For the flow of modules m for the charging area in Constraint A.16 - A.19, for the modules m in the charging area Constraint A.20 - A.23, for modules m going for the Inventory in Constraint A.24 - A.27 and modules m for the InventorySwap Constraint A.24 - A.27.

Additional
In the addition of the logical flow of the energy modules, the modules can only go to swapping station if the vessel r is in the correct swapping area s, so the parameter $RinZ_{t,r,s} = 1$ (CH3.3.3). This can be seen in Constraint 3.14 - 3.15 for the vessel. Furthemore, the same is true for modules in the swapping area and can be seen in Constraint 3.16 - 3.17.

$$x_{t,m,r} \leq x_{t-1,m,r} + \sum_{s \in S} (y_{t-1,m,s} \cdot RinZ_{t,r,s}) \qquad \forall\, t \in \{1, \ldots, T\}, m \in M, r \in R \quad (3.14)$$

$$x_{t-1,m,r} \leq x_{t,m,r} + \sum_{s \in S} (y_{t,m,s} \cdot RinZ_{t,r,s}) \qquad \forall\, t \in \{1, \ldots, T\}, m \in M, r \in R \quad (3.15)$$

$$y_{t,m,s} \leq \sum_{r \in R} (x_{t-1,m,r} \cdot RinZ_{t,r,s}) + InS_{t-1,m,s} + y_{t-1,m,s} \qquad \forall\, t \in \{1, \ldots, T\}, m \in M, s \in S \quad (3.16)$$

$$y_{t-1,m,s} \leq \sum_{r \in R} (x_{t,m,r} \cdot RinZ_{t,r,s}) + Ch_{t,m,s} + y_{t,m,s} \qquad \forall\, t \in \{1, \ldots, T\}, m \in M, s \in S \quad (3.17)$$

The constraints for the flow of specific modules in the swapping area s (Charging, inventory and InventorySwap) can be seen in Appendix A in Constraint A.37 - A.42.

There are more specific constraints for the flow of the modules m, especially those modules m leaving the swapping station $y_{t,m,s}$ in the swapping area s. Therefore, additional constraints are introduced to ensure the swapping of modules m is correctly performed. This is because a module m could, in theory, come from the vessel ($x_{t,m,r}$), go to the swapping station ($y_{t,m,s}$), and eventually return to the same vessel ($x_{t,m,r}$) (or, worse, another vessel $x_{t,m,r}$). Therefore, Constraint 3.18 and 3.19 are introduced, preventing a module m from coming from the vessel ($x_{t,m,r}$), going to the swapping station ($y_{t,m,s}$), and returning to the same vessel r or a vessel r in general. When a module is at the vessel ($x_{t,m,r}$) and came from the swapping station ($y_{t-T_{Swap},m,s}$), the module cannot be at the same vessel at the time step $t - T_{Swap} - 1$ ($x_{t-T_{Swap}-1,m,s}$) since this constraint does not allow to be higher or equal to two which prevent this situation from happening. Since the module m should stay for at least one period of time t at the vessel ($x_{t,m,r}$), this constraint is always working.

$$RinZ_{t,r,s} \left(x_{t-T_{swap}-1,m,r} + y_{t-T_{swap},m,s} + x_{t,m,r} \right) \leq 2 \qquad \forall\, t \in \{T_{swap}+1, \ldots, T\}, m \in M, r \in R, s \in S \quad (3.18)$$

$$\sum_{r \in R} x_{t-T_{swap}-1,m,r} + y_{t-T_{swap},m,s} + \sum_{r \in R} x_{t,m,r} \leq 2 \qquad \forall\, t \in \{T_{swap}+1, \ldots, T\}, m \in M, s \in S \quad (3.19)$$

As discussed earlier, there are two distinct flows of modules going to the swapping station ($y_{t,m,s}$), the modules m coming from the vessel $x_{t,m,r}$ and the modules m coming from the InventorySwap ($InS_{t,m,s}$). The modules m from the InventorySwap ($InS_{t,m,s}$) also need a similar constraint. If the module m was at time $t - T_{swap} - 1$ in the InventorySwap ($InS_{t-T_{Swap}-1,m,s}$), it cannot be at the charging station ($Ch_{t,m,s}$) at time t. This constraint can be seen in Constraint 3.20).

$$InS_{t-T_{swap}-1,m,s} + Ch_{t,m,s} \leq 1 \qquad \forall\, t \in \{T_{swap}+1, \ldots, T\}, m \in M, s \in S \quad (3.20)$$

$$InS_{t-T_{swap}-1,m,s} + y_{t-T_{swap},m,s} + Ch_{t,m,s} \leq 2 \qquad \forall\, t \in \{T_{swap}+1, \ldots, T\}, m \in M, s \in S \quad (3.21)$$

c. Modules at Swapping Station

In Figure 3.4 the crossing point of modules m in the swapping station s can be seen. To ensure this, the binary variables $\theta_{t,m,s}$ and $\Delta_{t,m,s}$ are used. If a module m is at swapping station s at time t ($y_{t,m,s} = 1$), one of these new variables must be one. This can be seen in Constraint 3.22. At the swapping station s, one module m should come from the vessel$r$ ($x_{t,m,r}$) which is indicated with $\theta_{t,m,s}$. The other module m should come from the InventorySwap ($InS_{t,m,s}$), which is indicated with $\Delta_{t,m,s}$. These modules m should stay for exactly T_{swap} periods at the swapping station s. After this T_{Swap} period, the modules m should flow to the next (correct) location as also indicated in the logical flow of modules m.

$$\theta_{t,m,s} + \Delta_{t,m,s} = y_{t,m,s} \qquad \forall\, t \in T, m \in M, s \in S \tag{3.22}$$

To ensure the introduced variables are correctly indicated, extra constraints are introduced. First, lets discuss the variable $\theta_{t,m,s}$, which can only be 1 if a module m is coming from the vessel $x_{t-T_{swap},m,r}$. This can only be true if the vessel r is sailing in the correct zone s ($RinZ_{t,r,s} = 1$), which can be seen in Constraint 3.23. Constraint 3.24 - 3.22 force this variable zero if the module m was not at the vessel r ($Ch_{t-T_{swap},m,s}$, $In_{t-T_{swap},m,s}$ or $InS_{-T_{swap}t,m,s}$). These constraints can only work if the module m was at the vessel r for at least T_{swap} periods, which results in a restriction. However, this is considered not a problem since the module m will be longer on the vessel r.

$$\theta_{t,m,s} \leq \sum_{r \in R} \left(x_{t-T_{swap},m,r} \cdot RinZ_{t,r,s} \right) \qquad \forall\, t \in \{T_{swap}, \dots, T\}, m \in M, s \in S \tag{3.23}$$

$$\theta_{t,m,s} \leq 1 - Ch_{t-T_{swap},m,s} - In_{t-T_{swap},m,s} \qquad \forall\, t \in \{T_{swap}, \dots, T\}, m \in M, s \in S \tag{3.24}$$

$$\theta_{t,m,s} \leq 1 - InS_{t-T_{swap},m,s} - y_{t-T_{swap},m,s} \qquad \forall\, t \in \{T_{swap}, \dots, T\}, m \in M, s \in S \tag{3.25}$$

For the variable $\Delta_{t,m,s}$, the module m should come from the InventorySwap ($InS_{t,m,s}$). However, to reduce the problem as indicated in the previous constraints, the constraints are slightly different formulated. Since the flow of the modules m in the swapping area s is defined, it does not matter where the module m was in the swapping area s (($Ch_{t-T_{swap},m,s}$, $In_{t-T_{swap},m,s}$ or $InS_{-T_{swap}t,m,s}$) as long as the module m was not at the vessel r ($x_{t-T_{swap},m,r}$). This can be seen in the following constraints, Constraint 3.26 and Constraint 3.27. However, this does not solve the problem, in theory, entirely. If the swapping $T_{swap} \geq 3$, it can in theory result in a restriction. But, in practice, charging will normally will take longer than one t.

$$\Delta_{t,m,s} \leq Ch_{t-T_{swap},m,s} + In_{t-T_{swap},m,s} + InS_{t-T_{swap},m,s} \quad \forall\, t \in \{T_{swap}, \dots, T\}, m \in M, s \in S \tag{3.26}$$

$$\Delta_{t,m,s} \leq 1 - \sum_{r \in R} \left(x_{t-T_{swap},m,r} \cdot RinZ_{t,r,s} \right) - y_{t-T_{swap},m,s} \quad \forall\, t \in \{T_{swap}, \dots, T\}, m \in M, s \in S \tag{3.27}$$

To ensure the correct number of modules m at the swapping station s, additional constraints are introduced. Constraint 3.28 ensures that the same number of modules m are coming from the vessel r as the modules m coming from the swapping area s. Furthermore, there cannot be more than EM_N modules m coming from the vessel r, which can be seen in Constraint 3.29.

$$\sum_{m \in M} \theta_{t,m,s} = \sum_{m \in M} \Delta_{t,m,s} \qquad \forall\, t \in T, s \in S \tag{3.28}$$

$$\sum_{m \in M} \theta_{t,m,s} \leq EM_N \qquad \forall\, t \in T, s \in S \tag{3.29}$$

Furthermore, the variables $\theta_{t,m,s}$ and $\Delta_{t,m,s}$) should be coupled to the modules m at the swapping station s ($y_{t,m,s}$). The sum of the both the variables should equal the total sum of modules m at the swapping station s, which can be seen in Constraint 3.30. Since the number of both the variables should be equal to each other, constraint 3.31 is added to maintain this. At last, in general, there cannot be more than $2 \cdot EM_N$ at the swapping station s which is defined in Constraint 3.32.

$$\sum_{m\in M} \Delta_{t,m,s} + \sum_{m\in M} \theta_{t,m,s} \geq \sum_{m\in M} y_{t,m,s} \qquad \forall\, t \in T, s \in S \tag{3.30}$$

$$2\sum_{m\in M} \Delta_{t,m,s} \leq \sum_{m\in M} y_{t,m,s} \qquad \forall\, t \in T, s \in S \tag{3.31}$$

$$\sum_{m\in M} y_{t,m,s} \leq 2 \cdot EM_N \qquad \forall\, t \in T, s \in S \tag{3.32}$$

Besides the origin of the modules m in the swapping station s, the modules m in the swapping station s ($y_{t,m,s}$) should stay for exactly T_{swap} periods in the swapping station s. Binary variable $SWAP_{t,m,s}$ is used to force this which is one if the module m is first located at the swapping station s ($y_{t,m,s}$), since $y_{t,m,s} - y_{t-1,m,s} = 1$ (Constraint 3.33). This binary variable $SWAP_{t,m,s}$ will stay 1 (Constraint 3.34) until the T_{swap} is reached (Constraint 3.35). This way, the modules m stay in the swapping station s for exactlyT_{swap} periods.

$$SWAP_{t,m,s} \geq y_{t,m,s} - y_{t-1,m,s} \qquad \forall\, t \in \{1,\dots,T\}, m \in M, r \in R, s \in S \tag{3.33}$$

$$y_{t+dt,m,s} \geq SWAP_{t,m,s} \qquad \forall\, t \in \{0,\dots,T - T_{swap}\}, m \in M, s \in S, dt \in \{0,\dots,T_{swap}\} \tag{3.34}$$

$$y_{t+T_{swap},m,s} \leq 1 - SWAP_{t,m,s} \qquad \forall\, t \in \{0,\dots,T - T_{swap}\}, r \in R \tag{3.35}$$

d. Energy level and module states

In Table 3.4, the indication of the state of the energy modules m was discussed ($e_{t,m}$, $i_{t,m}$ and $f_{t,m}$). This is necessary because the location of modules m depends on the energy level $l_{t,m}$, which must have an state for each time t, which can be seen in Constraint 3.36. For now suppose a energy level of $l_{t,m}$, the actual constraints for the definition of $l_{t,m}$ are discussed in CH3.3.5.f.

$$e_{t,m} + i_{t,m} + f_{t,m} = 1 \qquad \forall\, t \in T, m \in M \tag{3.36}$$

To actually indicate the energy level ($l_{t,m}$) for each state of the module m, the Big M method is used. The Big-M method is a method that is used to force binary variables to a certain level to be activated (one) or deactivated (zero). Big M should not be taken too large, but should also not be taken small. If big M M_1 is too high, this can result in numerical instability, resulting in infeasible solutions of the optimisation model. Also, the constraint coefficients are substantial, which can slow down the solver significantly. Making big M too small will result in not working at all. Big M is taken as $1.5 \cdot EM_{capacity}$ which can be changed in the optimisation model if necessary. This can be seen in the following constraints: Constraint 3.37 - Constraint 3.40.

$$l_{t,m} \leq SF_{min} + M_1 \cdot (1 - e_{t,m}) \qquad \forall\, t \in T, m \in M \tag{3.37}$$

$$l_{t,m} \geq SF_{min} - M_1 \cdot e_{t,m} \qquad \forall\, t \in T, m \in M \tag{3.38}$$

$$l_{t,m} \geq SF_{max} - M_1 \cdot (1 - f_{t,m}) \qquad \forall\, t \in T, m \in M \tag{3.39}$$

$$l_{t,m} \leq SF_{max} + M_1 \cdot f_{t,m} \qquad \forall\, t \in T, m \in M \tag{3.40}$$

With the definition of the the states of the modules m, the restrictions of Table 3.36 can be formulated in constraints (indicated with the red crosses). For the modules m at the vessel $r(x_{t,m,r})$ and in the swapping station s ($y_{t,m,s}$), each state ($e_{t,m}$, $i_{t,m}$ or $f_{t,m}$) can be assigned. However, when a module m is used for for propulsion ($u_{t,m,r}$), the module m cannot be empty ($e_{t,m}$). This can be seen in Constraint 3.41. In the charging area ($Ch_{t,m,s}$) modules m cannot be full ($f_{t,m}$), which can be seen in Constraint 3.42. At last, for both the inventory ($In_{t,m,s}$) and the InventorySwap ($InS_{t,m,s}$), the modules m cannot be empty which can be seen in Constraint 3.43.

$$\sum_{r \in R} u_{t,m,r} \leq 1 - e_{t,m} \qquad \forall\, t \in T, m \in M \tag{3.41}$$

$$\sum_{s \in S} Ch_{t,m,s} \leq 1 - f_{t,m} \qquad \forall\, t \in T, m \in M \tag{3.42}$$

$$\sum_{s \in S} In_{t,m,s} + \sum_{s \in S} InS_{t,m,s} \leq 1 - e_{t,m} - i_{t,m} \qquad \forall\, t \in T, m \in M \tag{3.43}$$

Besides the previous constraints, one set of constraint is defined extra for the intermediate state ($i_{t,m}$). If a module m is intermediate ($i_{t,m}$), the module m can only be used for propulsion on the vessel r ($u_{t,m,r} = 1$), at the charging station ($Ch_{t,m,s}$) or at the swapping station ($y_{t,m,s}$). This ensures a module m is used until it is empty ($e_{t,m}$), which can be seen in Constraint 3.44.

$$i_{t,m} \leq \sum_{r \in R} u_{t,m,r} + \sum_{s \in S} Ch_{t,m,s} + \sum_{s \in S} y_{t,m,s} \qquad \forall\, t \in T, \forall m \in M \tag{3.44}$$

It should be mentioned that the state of the modules m, based on the energy level of module m ($l_{t,m}$), has one flaw. Since big M ensures that the constraints correctly indicate the modules m, there is one exception: When the energy module m has exactly SF_{max} or SF_{min} energy. The module m can be theoretical in multiple states (in terms of either in location a or either in location b, since a module m can be only in one specific location). However, this does not matter since the constraints are also coupled to the state of the modules m, to a specific location. For example, a module m cannot be fully ($f_{t,m}$) charged in the charging station $Ch_{t,m,s}$. This is also verified in the verification chapter (CH5).

e. Vessel state

In Figure 3.4 the vessel level can be seen for the vessel level, which also has a specific logical flow for each vessel r. First, the vessel r can only have one state ($SL_{t,r}$, $StS_{t,r}$, $VS_{t,r}$ or $SbOP_{t,r}$) at one time t, which can be seen in Constraint 3.45. However, it is not always possible to initiate a swap or being in the swapping process ($StS_{t,r}$, $VS_{t,r}$ or $SbOP_{t,r}$). This is depended on the input parameter $SPos_{t,r}$ (CH4.7) and $RB_{t,r}$ (CH4.7.2) and explained in the beginning of this chapter in the Chapter 3.3.3. Therefore, Constraint 3.46 - 3.47 are introduced.

$$SL_{t,r} + StS_{t,r} + VS_{t,r} + SbOP_{t,r} = 1 \qquad \forall\, t \in T, r \in R \tag{3.45}$$

$$StS_{t,r} + VS_{t,r} + SbOP_{t,r} \leq SPos_{t,r} \qquad \forall\, t \in T, r \in R \tag{3.46}$$

$$StS_{t,r} + VS_{t,r} + SbOP_{t,r} \leq 1 - RBt, r \qquad \forall t \in T, r \in R \tag{3.47}$$

First, the logical flow of the vessels r are discussed. When a vessel r is sailing its original sailing path $SL_{t,r}$, the vessel r can either stay in this state or sail to the swapping station $StS_{t,r}$ (Constraint 3.48). On the other hand, the vessel r could come from sailing back to the original path $SbOP_{t,r}$ (Constraint 3.49). Furthermore, the other states are not possible, which can be seen in Constraint 3.50 - Constraint 3.51. The other states ($StS_{t,r}$, $VS_{t,r}$ and $SbOP_{t,r}$) have an similar logical flow, and are discussed in Appendix A ($StS_{t,r}$ in Constraint A.99 - A.102, $VS_{t,r}$ in Constraint A.103 - A.106 and $SbOP_{t,r}$ in Constraint A.107 - A.110). One important note is that each vessel r is sailing at the first time step, so $SL_{0,r} = 1$.

$$SL_{t-1,r} \leq SL_{t,r} + StS_{t,r} \qquad \forall\, t \in \{1, \ldots, T\}, r \in R \tag{3.48}$$

$$SL_{t,r} \leq SL_{t-1,r} + SbOP_{t-1,r} \qquad \forall\, t \in \{1, \ldots, T\}, r \in R \tag{3.49}$$

$$SL_{t,r} \leq 1 - VS_{t-1,r} - StS_{t-1,r} \qquad \forall\, t \in \{1, \ldots, T\}, r \in R \tag{3.50}$$

$$SL_{t-1,r} \leq 1 - VS_{t,r} - SbOP_{t,r} \qquad \forall\, t \in \{1, \ldots, T\}, r \in R \tag{3.51}$$

To ensure the vessel can exclusively be at a certain swapping station s, for T_{swap} periods, four additional constraints are introduced. A vessel can only be at a swapping station if the vessel is in the correct zone ($RinZ_{t,r,s}$) to prevent the vessel r swapping in an swapping area s where the vessel r is not located at a given time t. Furthermore, the vessel cannot be at the swapping station for more extended than T_{swap} period. These constraints can be seen in Constraint 3.52 - 3.54. At last, a minimum of two modules should be at the swapping station if the vessel r is at the swapping staiton s, which can be seen in Constraint 3.56.

$$VS_{t,r} \leq \sum_{s \in S} RinZ_{t,r,s} \qquad \forall\, t \in T, r \in R \tag{3.52}$$

$$\sum_{r \in R} (VS_{t,r} \cdot RinZ_{t,r,s}) \leq 1 \qquad \forall\, t \in T, s \in S \tag{3.53}$$

$$\sum_{s \in S} (VS_{t,r} \cdot RinZ_{t,r,s}) \leq 1 \qquad \forall\, t \in T, r \in R \tag{3.54}$$

$$VS_{t,r} + VS_{t-T_{Swap}} \leq 1 \qquad \forall\, t \in \{T_{swap}, \ldots, T\}, r \in R \tag{3.55}$$

$$\sum_{m \in M} y_{t,m,s} \geq 2 \cdot RinZ_{t,r,s} \cdot VS_{t,r} \qquad \forall\, t \in T, r \in R, s \in S \tag{3.56}$$

In Figure 3.4, it can be seen that one module m is still on the vessel r which is not swapped at swapping station s. could be seen that two states of the vessel r ($StS_{t,r}$ and $VS_{t,r}$) have an dependency to the module level. If a swap is initiated, a module m should be available for the vessel r to be swapped when the vessel arrives at the swapping station ($VS_{t,r}$). The constraints to ensure this can be seen in Constraint 3.57 - 3.58. The first constraint ensures that the at least one module m is reserved if a vessel is sailing to the swapping station ($StS_{t,r}$) for $DT_{StS_{t,r}}$ time. The second constraint ensures that the maximum number of modules can be at the InventorySwap ($InS_{t,m,s}$), where the total amount of vessels r sailing to the swapping station s is multiplied with EM_N modules m. This works because of the flow of the modules m, the module m cannot go back and thus the correct number of modules m is reserved by the optimisation model.

$$\sum_{m \in M} InS_{t,m,s} \geq \sum_{r \in R} (RinZ_{t,r,s} \cdot StS_{t,r}) \qquad \forall\, t \in T, s \in S \tag{3.57}$$

$$\sum_{m \in M} InS_{t,m,s} \leq EM_N \cdot \sum_{r \in R} (RinZ_{t,r,s}(1 - VS_{t,r} - SbOP_{t,r} - SL_{t,r})) \qquad \forall\, t \in T, s \in S \tag{3.58}$$

In Figure 3.4, if the vessel r is at the swapping station ($VS_{t,r}$), is coupled. At least one module m should be swapped, so at time t there can be at most $EM_N - 1$ modules m on the vessel r. Since the vessel r at the swapping station s is indicated with the binary variable $VS_{t,r}$, this can be used to define constraint 3.59. On the other hand, alle the modules may be at the swapping station s, resulting in no modules m on the vessel r ($x_{t,m,r} = 0$. Constraint 3.61 states that if the vessel is sailing ($SL_{t,r}$), sailing to the swapping sation ($StS_{t,r}$) or sailing back to the original path ($SbOP_{t,r}$) there should alwasy be EM_N modules m on the vessel r. Also, a module m cannot be used ($u_{t,m,r}$) for propulsion if the vessel r is at the swapping station (Constraint 3.62).

$$\sum_{m \in M} x_{t,m,r} \leq EM_N - VS_{t,r} \qquad \forall\, t \in T, r \in R \tag{3.59}$$

$$\sum_{m \in M} x_{t,m,r} \geq EM_N \cdot (1 - VS_{t,r}) \qquad \forall\, t \in T, r \in R \tag{3.60}$$

$$\sum_{m \in M} x_{t,m,r} \geq EM_N \cdot (SL_{t,r} + StS_{t,r} + SbOP_{t,r}) \qquad \forall\, t \in T, r \in R \tag{3.61}$$

$$\sum_{m \in M} u_{t,m,r} = 1 - VS_{t,r} \qquad \forall\, t \in T, r \in R \tag{3.62}$$

In Figure 3.4 two variables indicate the first time a vessel r is sailing to ($StS_{t,r}$) the swapping station s, indicated with $StS_{Start_{t,r}}$ and sailing back to the original path ($SbOP_{t,r}$), $SbOP_{Start_{t,r}}$ is used. Both variables are related to the objective function (Equation 3.1), and are therefore important. First of all, similar to Constraint 3.46 - 3.47, the variables are couple to the input parameters $SPos_{t,r}$ and $RB_{t,r}$, which can be seem in in Constraint 3.63 - 3.63. Both the variables have similar constraints, so only $StS_{Start_{t,r}}$ will be discussed in this section. The constraints for $SbOP_{t,r}$ can be found in Appendix A. The start $StS_{Start_{t,r}}$ is indicated with Constraint 3.65, and Constraint 3.66 is used to prevent that two executive time steps $StS_{Start_{t,r}}$ are both one.

$$StS_{start_{t,r}} + SbOP_{start_{t,r}} \leq SPos_{t,r} \qquad \forall\, t \in T, r \in R \tag{3.63}$$
$$StS_{start_{t,r}} + SbOP_{start_{t,r}} \leq 1 - RB_{t,r} \qquad \forall\, t \in T, r \in R \tag{3.64}$$
$$StS_{Start_{t,r}} \geq StS_{t,r} - StS_{t-1,r} \qquad \forall\, t \in \{1,\ldots,T\}, r \in R \tag{3.65}$$
$$StS_{Start_{t,r}} + StS_{Start_{t-1,r}} \leq 1 \qquad \forall\, t \in \{1,\ldots,T\}, r \in R \tag{3.66}$$

If the vessel r is starting its journey (either $StS_{t,r}$ or $SbOP_{t,r}$) the vessel r should sail for exactly $DT_{StS_{t,r}}$ or $DT_{SbOP_{t,r}}$ time periods (input parameter, explained in more detail in CH4.5). The constraints to ensure the correct time of a vessel r being in a certain state can be seen in Constraint 3.70 - Constraint 3.69.

$$StS_{t+dt,r} \geq StS_{Start_{t,r}} \qquad \forall\, t \in \{1,\ldots,T - DT_{StS_{t,r}}\}, r \in R, dt \in \{0,\ldots,DT_{StS_{t,r}}\} \tag{3.67}$$
$$StS_{t+DT_{StS_{t,r}},r} \leq 1 - StS_{Start_{t,r}} \qquad \forall\, t \in \{1,\ldots,T - DT_{StS_{t,r}}\}, r \in R \tag{3.68}$$
$$VS_{t+DT_{StS_{t,r}},r} \geq StS_{Start_{t,r}} \qquad \forall\, t \in \{1,\ldots,T - DT_{StS_{t,r}}\}, r \in R \tag{3.69}$$

One extra constraint should be added to these constraints. When no data is available, there is also no value for the data, which can introduce problems that could potentially make the model infeasible. The value for the data used in the Constraint 3.71 should be an integer. When this has a $none$ value, it will introduce problems. Therefore, this is solved by having the maximum for the data set plus one. This ensures that the data is higher than the actual data. When this is the case, the vessel cannot begin sailing to or from the swapping station. Therefore, this error is used to force the $StS_{start_{t,r}} = 0$ and is not forcing the model infeasible if it has a value lower or equal to the maximum value for $StS_{DATA_{t,r}}$.

$$Error_{TSbOP} = \max\left(StS_{DATA_{t,r}}\right) + 1 \qquad \forall\, t \in T, r \in R \tag{3.70}$$
$$Error_{TSbOP} - StS_{DATA_{t,r}} \geq StS_{Start_{t,r}} \qquad \forall\, t \in T, r \in R \tag{3.71}$$

Number of required swaps

From the input, the total energy is known and it is also known what the maximum usable energy level of the energy modules is. With this information, a lower bound can be introduced which may improve the computational time. When a vessel r has for example a usage of 2000 kWh, and the energy modules have a combined (EM_N) capacity of 1000 kWh, at least one swap should occur.

$$SWAP_{required,r} = \left(\frac{1}{EM_{capacity} \cdot EM_N}\right) \cdot \sum_{t \in T} P_{r,t} \qquad \forall r \in R \tag{3.72}$$

With this said, the model does not need to search possibilities for swapping without at least one swap. In this way, the model decreases its solution space, which can result in less computational time

$$\sum_{t \in T} StS_{Start_{t,r}} \geq SWAP_{required,r} \qquad \forall\, t \in T, r \in R \tag{3.73}$$
$$\sum_{t \in T} VS_{Start_{t,r}} \geq SWAP_{required,r} \cdot T_{Swap} \qquad \forall\, t \in T, r \in R \tag{3.74}$$
$$\sum_{t \in T} SbOP_{Start_{t,r}} \geq SWAP_{required,r} \qquad \forall\, t \in T, r \in R \tag{3.75}$$

Furthermore, one full cycle of the swapping process, including the sailing to the swapping station, swapping the modules and sailing back to the original path, should be aligned with each other. This can be seen in Constraint 3.76 until Constraint 3.78.

$$\sum_{t\in T} StS_{Start_{t,r}} = \sum_{t\in T} SbOP_{Start_{t,r}} \qquad \forall\, t\in T, r\in R \tag{3.76}$$

$$\sum_{t\in T} VS_{Start_{t,r}} = T_{swap}\cdot \sum_{t\in T} StS_{Start_{t,r}} \qquad \forall\, t\in T, r\in R \tag{3.77}$$

$$\sum_{t\in T} VS_{Start_{t,r}} = T_{swap}\cdot \sum_{t\in T} SbOP_{Start_{t,r}} \qquad \forall\, t\in T, r\in R \tag{3.78}$$

f. The correct indication of the energy level of modules

In Figure 3.4, each sailing state of the vessel $r(SL_{t,r}$, $StS_{t,r}$ and $SbOP_{t,r})$ has an energy consumption ($P_{t,r}$), P_{StS} or P_{SbOP}) which should be subtracted from the energy level $l_{t,m}$ for the module m which is used on the vessel r ($u_{t,m,r}=1$). Each vessel state has its energy consumption, which should be defined. First, only one state can be applied when the module m is at the vessel r where the power consumption for sailing ($P_{t,r}$), explained in CH4.4), for sailing to the swapping station (P_{StS}) and at last for the modules on the vessel sailing back to the original path (P_{SbOP}) are defined. The only time-dependent input parameter is $P_{t,r}$, where the others are defined as constant input parameters.

Quadratic Energy level of modules

To define the energy level $l_{t,m}$ for a module m with the current binary variables, this will result in quadratic constraints, which can be seen Constraint 3.79.

$$\begin{aligned} l_{t+1,m} = l_{t,m} &- \sum_{r\in R}(SL_{t,r}\cdot P_{t,r}\cdot u_{t,m,r}) - \sum_{r\in R}(StS_{t,r}\cdot P_{StS}\cdot u_{t,m,r}) \\ &- \sum_{r\in R}(SbOP_{t,r}\cdot P_{SbOP}\cdot u_{t,m,r}) + CS\cdot \sum_{s\in S} Ch_{t,m,s} \qquad \forall\, t\in T, m\in M \end{aligned} \tag{3.79}$$

Constraint 3.79 is not linear since the multiplication of binary variables is used. Therefore, this constraint needs a linearisation. Since the problem, from the literature perspective, is a MILP, the quadratic constraints will be linearised. Furthermore, Gurobi is highly optimised for linear constraints. The optimisation model will contain the option to use these quadratic constraints if needed. Gurobi can handle the multiplication of binary variables, but with large problems, this may slow down the optimisation.

Linearisation of the Energy level of modules

For the linearisation, the variables are used to indicate a vessel r is used for propulsion, $PSL_{t,m,r}$ for sailing the original path, $PStS_{t,m,r}$ for sailing to the swapping station s and $PSbOP_{t,m,r}$ for sailing back to the original path. At each time t, only one of these binary variables can be one which can be seen in Constraint 3.80. Evermore, when the vessel is using a module m ($u_{t,m,r}=1$) to propel the vessel r, one of these variables should be one. This can be seen in Constraint 3.81.

$$\sum_{m\in M} PSL_{t,m,r} + \sum_{m\in M} PStS_{t,m,r} + \sum_{m\in M} PSbOP_{t,m,r} \le 1 \qquad \forall\, t\in T, r\in R \tag{3.80}$$

$$PSL_{t,m,r} + PStS_{t,m,r} + PSbOP_{t,m,r} = u_{t,m,r} \qquad \forall\, t\in T, m\in M, r\in R \tag{3.81}$$

Futhermore, the indication of the usage of energy should be couple to the state of the vessel r ($SL_{t,r}$, $StS_{t,r}$ and $SbOP_{t,r}$). Constraint 3.82 - Constraint 3.84 show that if a vessel r is, for example sailing, the variable for the energy usage should also be one, resulting in $PSL_{t,r}=1$.

$$SL_{t,r} \le \sum_{m\in M} PSL_{t,m,r} \qquad \forall\, t\in T, r\in R \tag{3.82}$$

$$StS_{t,r} \le \sum_{m\in M} PStS_{t,m,r} \qquad \forall\, t\in T, r\in R \tag{3.83}$$

$$SbOP_{t,r} \le \sum_{m\in M} PSbOP_{t,m,r} \qquad \forall\, t\in T, r\in R \tag{3.84}$$

After linearising the problem, the energy level $l_{t,m}$ can be formulated again with the linearised constraints which can be seen in Constraint 3.85.

$$\begin{aligned} l_{t+1,m} = l_{t,m} - \sum_{r \in R} (PSL_{t,m,r} \cdot P_{t,r}) - \sum_{r \in R} (PStS_{t,m,r} \cdot P_{StS}) \\ - \sum_{r \in R} (PSbOP_{t,m,r} \cdot P_{SbOP}) + CS \cdot \sum_{s \in S} Ch_{t,m,s} \qquad \forall\, t \in T, m \in M \end{aligned} \tag{3.85}$$

3.4. Conclusion

After the literature review, the methods section was discussed (CH2.6). This chapter consisted of the scope (3.1), conceptual process (CH3.2) and the mathematical model (CH3.3). The mathematical model was used to make the optimisation model in Gurobi (python). The optimisation model is able to track the vessels and modules for every timestep, to minimise the downtime due to the swapping process based on data of specific sailing profiles with an energy consumption. For this chapter, it can be concluded that the model is implemented as needed. However, verification and validation should be performed. This is discussed in Chapter 5.

4 Pre-Processing

After defining the mathematical model, the described input parameters should be established to proceed with the verification/validation process (Chapter 5) and to perform case studies. This chapter comprehensively explains all the requirements for running the Gurobi optimisation model in Python. While the input parameters were briefly mentioned in (Table 3.3) of the mathematical model (Chapter 3.3), this chapter elaborates on their definitions and implementation for both the constant as the time, vessel, and swapping area dependent input parameters.

A critical reason why this chapter is important is to reduce computational time. Everything which can be calculated upfront will make the optimisation model less heavy. Since optimisation can take a long computational time, pre-processing is performed to calculate all the necessary data upfront, which is not needed in optimisation. This chapter will explain those and how vessel and swapping are dependent parameters for the time. This chapter aims to remove every unnecessary computational step the optimisation model has to make to decrease the computational time for the model.

Before actually discussing the input parameters, it should be mentioned that A Python script is made where the data can be decreased to a specific time step and time frame. This is based on different parameters such as the maximum speed (and thus travelling distance), the sailing profile, the estimated energy consumption, the shifts of the RPAs and the location data (if a vessel is stationary due to repair or other situations). The estimated energy consumption is based on the PRA data, where the velocity is translated to used energy consumption. Since the vessels will be renewed, the energy demand will also differ from the old vessels. The preprocessing is done at the servers of the Port of Rotterdam, which means that this data is preprocessed in DataBricks. As briefly explained in the chapter (CH3), where the mathematical model is discussed, there is the input needed for the preprocessing. These input parameters will be discussed in this chapter.

This chapters answers the sub-question of what is needed to actually define the input parameters, and what is used to define these parameters. This can be seen in the following sub-questions:

1. *Which RPA vessels are used? (CH4.1)*
2. *How is the location data retrieved of the RPA vessels (CH4.2)*
3. *How is the Port of Rotterdam divided, in zones? (CH4.3)*
4. *How is the power estimation performed for RPA vessels? (CH4.4)*
5. *How is swapping duration defined? (CH4.5)*
6. *Which swapping method is applied for this thesis? (CH4.6)*
7. *Possible swap (CH4.7)*
8. *Time-intervals (CH4.8)*

Every parameter defined in this chapter could, in theory, be different when other data is used. From this chapter and forward, if not explicitly noted, this chapter is leading for the used data. From the verification chapter, it is said that the parameters are changed to test the optimisation model and to verify this. More can be found in Chapter 5.2 and Chapter 6 for the verification validation and the case studies, respectively.

4.1. RPA vessels

The vessels used for the case study and the validation are specified in this chapter. Usually, three patrolling (blue-)vessels and three Incident Response (IRV) (Red-)vessels are sailing in the Port of Rotterdam from two different main harbours (Pistoolhaven/Madroelhaven) which can be seen in Figure 4.1

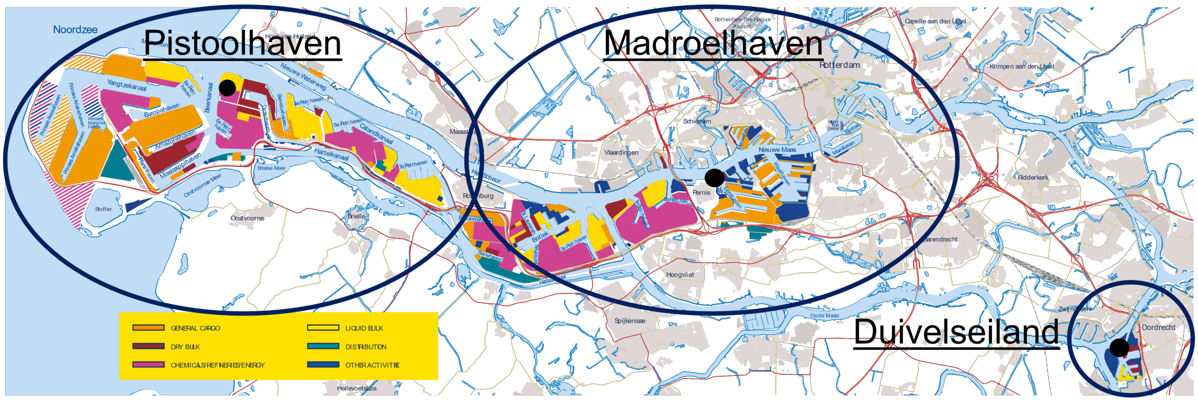

Figure 4.1: Used operational areas for RPA vessels (Pistoolhaven/Madroelhaven) [Internal source/own work]

The choice of the actual data was based on several factors. The first factor is that there was enough available AIS data (vacation periods, weather conditions, available vessels, events etc.). Furthermore, the vessel should be sailing for most of the time considered. This was quite difficult since the vessels had shifted and were out of use, for example, due to docking or repairs at the 'Eemhaven'. The actual window for the different vessels r can be seen in Table, table 4.1. The used data windows can be seen in Figure 4.1. Three vessels were chosen to start in the Madroelhaven and three vessels in the Pitstoolhaven. It can be seen in Table 4.1 that the RPA6 and the RPA16 have a different day compared to the other vessels. One of the arguments is that at least three blue and three red vessels should be used, which is not more than for the general application of those vessels. The reason why this was chosen was to make sure the vessels were sailing. The choice was made to have at least three vessels in a specific area since the vessels operate in their own harbours.

Vessel	Type	MSSI	Date Time	Begin Time	End Harbour	Main Eemhaven	Visit Eemhaven
RPA6	Blue	245127000	4/24/23	0:00	23:59	Madroelhaven	✓
RPA7	Blue	245549000	4/5/23	0:00	23:59	Pistoolhaven	✗
RPA10	Blue	244050426	4/5/23	0:00	23:59	Madroelhaven	✓
RPA13	Red	244070288	4/5/23	0:00	23:59	Madroelhaven	✓
RPA15	Red	245209000	4/5/23	0:00	23:59	Pistoolhaven	✗
RPA16	Red	244757000	4/24/23	0:00	23:59	Pistoolhaven	✗

Table 4.1: Chose of RPA vessels, and time frame for those vessels

4.2. Location data RPA vessels

The RPA vessels have historical Automated Identification System (AIS) data. AIS data refers to a standardized data format where the movement of vessels is monitored and tracked. AIS is used for safety, navigation, and operational efficiency and operates through VHF radio frequencies. The AIS data consists of two different types of information: dynamic data (position, course over ground, speed over ground, heading, rate of turn, navigational status and time of transmission) and static voyage data (vessel's name, IMO number, MMSI number, ship type, size, destination, ETA and draught). The latter are more manually entered information and are more constant over time. The Port of Rotterdam uses this AIS data to automatically track their RPA vessels, where the position and velocity of each vessel are shared every three seconds, which results in large databases. This data is stored and used for different purposes.

Since there will be different vessels r in the optimisation model, where every vessel r shares its position (not necessarily at the same time), the data should be aligned with all the vessels r for a specific time t. As the mathematical model explains, CH3.3, the data points should be aligned for each time t to have a working optimisation model to have a location of each vessel r at a specific time t. This is done by linear interpolating two points closest to the specifically defined time t and determining the theoretical location of that specific location for time t. For example, if the time step is one minute, it should be known exactly every minute for each vessel r (12:00:00, 12:01:00 and so on).

The actual choice of the timestep is more nuanced since Implementing (large) AIS-data sets will impact the computational time. Therefore, it is necessary to quantify the data carefully to avoid unnecessary computation time for the optimisation model. The optimisation model does not need to determine every 3 seconds if the vessels r need a swap. On the other hand, increasing the time steps will result in less accuracy, especially when the RPA vessels are sailing at higher speeds. Also, the estimated power over a larger time step is more uncertain because the vessel could have changed its cruising speed, for this thesis has determined that the smallest timestep is one minute. From now on, all the data will be pre-processed using this timestep. However, based on this input, it is possible to increase the timestep. This is only possible if the timestep is a certain number of times within 60 minutes. Therefore, one, two, three and six minutes can be, for example, increased timesteps, which can be interesting when the computation time is increased. This is determined for each case, depending on the time needed for a swap compared to the total time a vessel is sailing.

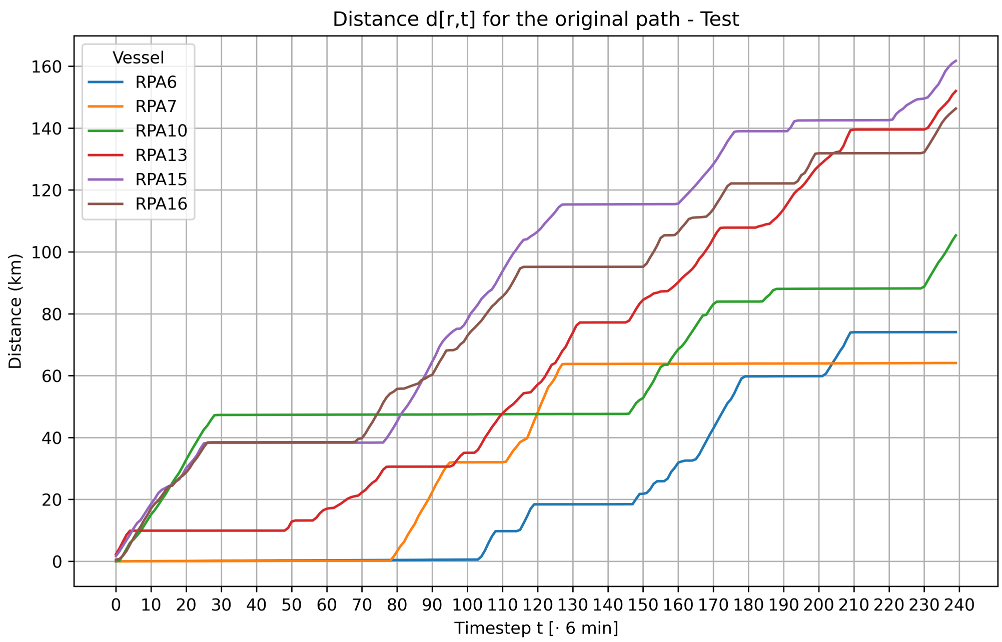

Figure 4.2: Sailing distance for each RPA vessel validation test case

4.3. Zones

As discussed in Chapter 3.3.3, the zones are needed to decrease the swapping possibilities. In this chapter, the specific locations of the swapping stations s are discussed. Based on internal communication with the Port of Rotterdam, a total of fourteen different swapping areas are considered (Table 4.2 - 4.3). Each swapping area consist of its 'own' swapping station, charging station, inventory and InventorySwap due to its decentralised structure (CH2.4.3). Note that the swapping station locations in this thesis are fictive, which means that these locations are not definitive to be used in the future (see the discussion chapter, CH7.3). From those different locations, the 'Pistoolhaven' and 'Madroel Haven' are harbours where the crew does their crew changes for each shift and therefore have a large potential. Also, the Eemhaven is a bunker/repair location where vessels come more often. Those locations are highly likely to be swapping locations since the RPA vessels are at least three times a day at those crew-changing locations. The 'Eemhaven' is also expected to have a swapping station, for the same reason.

Zone	Name	X-COR	Y-COR
1	Margriet Haven	60358.82	442139.2
2	Pistool Haven	65775.00	442189.00
3	Monding Hartelkanaal	65065.45	439708
4	Dintel Haven	67936.51	441168.2
5	Geul Haven	81161.46	433993
6	Stormvloedkering	71455.29	441266.7
7	Scheur Haven	69219.81	442222.1

Table 4.2: Zones 1-7 for the optimisation model

Zone	Name	X-COR	Y-COR
8	4e Petroleum Haven	69600.75	441232.9
9	Madroel Haven	85700.00	434480.00
10	Eem Haven	88335.00	433805.00
11	RDM	88611	434904
12	LekHaven/Radar post	89117.36	435569.3
13	SS Rotterdam	92159.07	434946
14	Bunker Noordereiland	93947.77	436899.3

Table 4.3: Zones 8-14 for the optimisation model

These swapping areas s are fixed and not variable. The reason for this is that optimising potential swapping areas is also an optimisation problem itself. Since the renewal of the fleet is in an early stage, adding an extra variable will make the model more complex. The names and locations of the swapping stations can be seen in, and these corresponding zones can be seen in Figure 4.3 (including the AIS location of all the vessels based on Chapter 4.2). The zones could, in theory, be adjusted since an Excel script is made to import the correct polygons in the Python script. In this Excel sheet, adjustments can be made to the (polygon) zones, and Python reads this file automatically. However, when the zones are changed, this will affect the pre-processing and the data, meaning that the zones will greatly impact the optimisation since changing this will affect the optimisation. From now on, those 14 different locations are used for this thesis.

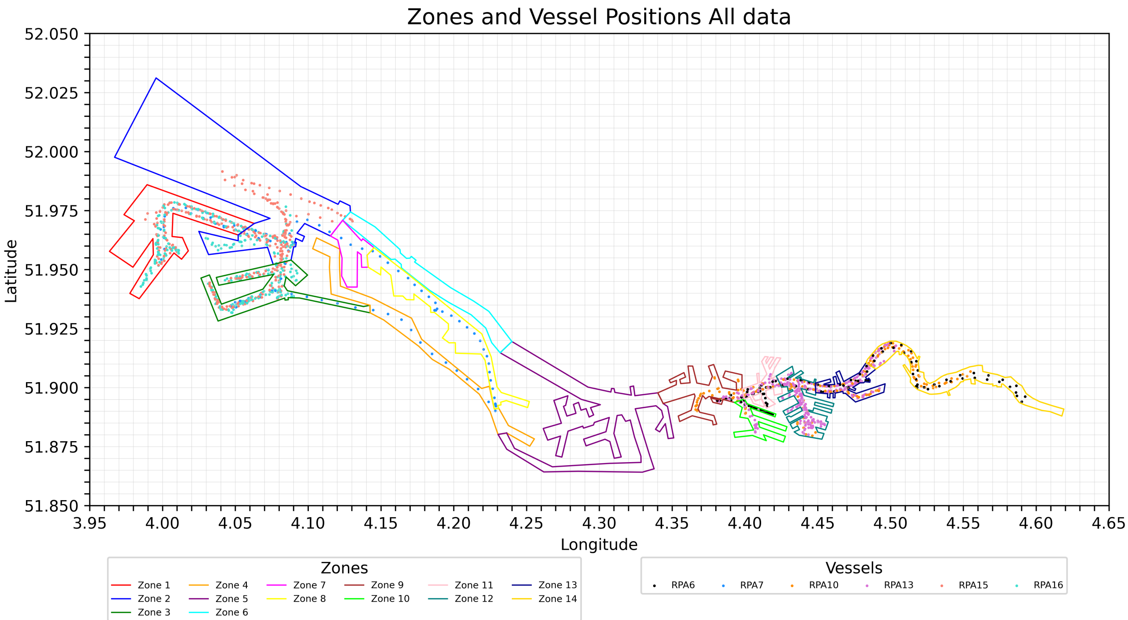

Figure 4.3: Zones for the RPA vessels

4.4. Power estimation of the RPA vessels

The power estimation of the RPA vessels can be divided into two different estimations, one for the original path (CH4.4.1) and the power consumption for the sailing to and from the swapping station (CH4.4.2).

4.4.1. Original path

The power estimation of each RPA vessel should be known to determine if a vessel r needs a swap. As described in CH4.1, six different vessels (shape, engines, power consumptions, etc.) are used for this thesis. Normally, the equation to calculate the power for a vessel can be seen in Equation 4.1. However, the torque T is not known for each timestep used in the optimisation model. The RPM, however, (which can be translated to an angular velocity ω) is known. But, as can be seen in Equation 4.1, the torque T and the angular velocity ω depend on each other and therefore this equation cannot be used. Therefore, another method should be considered to estimate the power consumption.

$$P = \frac{T \cdot \omega}{1000}\ kW \tag{4.1}$$

So, another way is introduced to estimate the power consumption of the RPA vessels. Data is available on the engine load EL, a percentage of the engine used to propel the vessel at a certain speed. These data points can be plotted, and an (average) function of the speed versus the engine load can be made with a scatter diagram. Based on the AIS data (travelled distance, CH4.2), the (average) speed of the vessel r sailing its original path ($SL_{t,r}$) can be calculated for each Δt. This speed is then translated to an engine load using the scatter diagram. Unfortunately, this data is not available for all the vessels. The RPA10 and RPA13 already had a sensor installed on the vessel where the engine load is saved. An extra sensor is installed onto the RPA16 to have more data for this thesis. The scatter diagrams can be seen in Figure 4.6 - 4.6 for RPA10, RPA13 and RPA16, respectively.

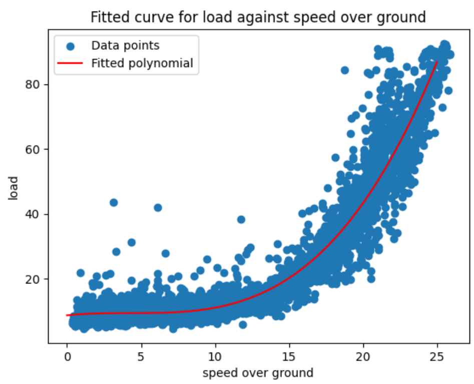

Figure 4.4: Engine load for RPA 10

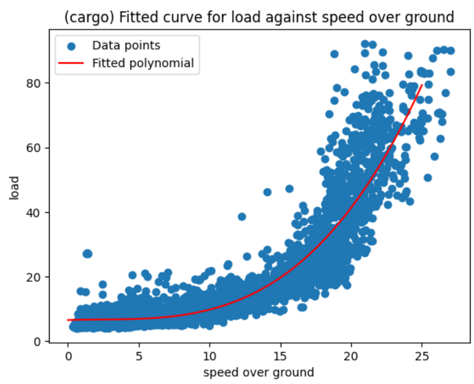

Figure 4.5: Engine load for RPA 13

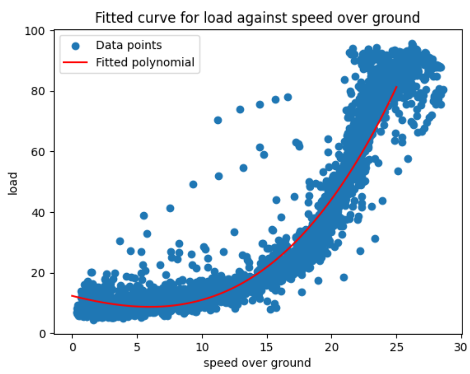

Figure 4.6: Engine load for RPA 16

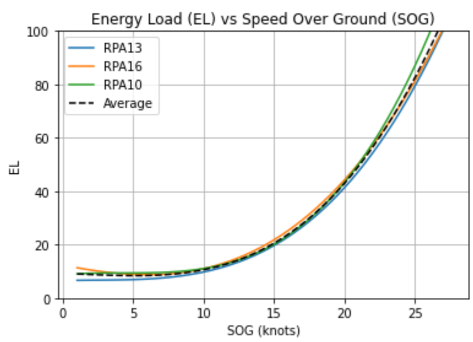

Figure 4.7: Combined engine load

The scatter diagrams are used to make polynomial fits, as seen in the previous figures. The actual equations for these polynomial fits can be seen in Equation 4.2 - 4.4.

$$EL_{RPA10}(SOG) = 6.1651 \cdot 10^{-3} \cdot SOG^3 - 4.3394 \cdot 10^{-2} \cdot SOG^2 + 1.4067 \cdot 10^{-1} \cdot SOG + 6.5348 \quad (4.2)$$

$$EL_{RPA13}(SOG) = 3.9572 \cdot 10^{-3} \cdot SOG^3 + 5.4067 \cdot 10^{-2} \cdot SOG^2 - 1.0718 \cdot 10^{-1} \cdot SOG + 1.2368 \quad (4.3)$$

$$EL_{RPA16}(SOG) = 8.6772 \cdot 10^{-3} \cdot SOG^3 - 1.1111 \cdot 10^{-2} \cdot SOG^2 + 4.7908 \cdot 10^{-1} \cdot SOG + 8.7017 \quad (4.4)$$

$$EL_{combine}(SOG) = 6.2665 \cdot 10^{-3} \cdot SOG^3 - 3.3480 \cdot 10^{-2} \cdot SOG^2 - 1.5067 \cdot 10^{-1} \cdot SOG + 9.2015 \quad (4.5)$$

Looking at the polynomial fits of the scatter diagram (Equation 4.2 - 4.4), it can be seen (Figure 4.4 - 4.6) that the vessels have an increasing engine load when the vessel is sailing faster, but also consumes energy when stationary. These patterns align with the expectations since if a vessel has a low velocity, the vessel's acceleration from zero will consume more energy to overcome the resistance, drag and other external forces/ factors. Also, when the vessel is sailing faster, the power should increase non-linear, as seen in the Figures. Note that the auxiliary is not considered in these figures since the auxiliary does not come from the main engine on which this data is based. However, when the vessel is stationary (not accelerating), the vessel will also consume power, which can compensate for this auxiliary data. Since the estimation is not the main objective of the thesis, these values will be used for all the vessels. In the discussion, CH7.2 this will be elaborated further.

In Figure 4.7, the polynomials for the engine loads are combined to have a general engine load for all the vessels. The combined graph and the polynomial fit in Equation 4.6 and in Figure 4.7. Based on the engine load, the actual power for a particular speed can be calculated using the specifications of the engines of the RPA vessels. It is chosen to use an engine with a power output of $P_{SB} = 485\ kW$. The PRA vessels have two engines, producing a total power output of $P_{total} = 2 \cdot 485 = 970\ kW$. The power output for RPA10, RPA13 and RPA16 can be seen in Figure 4.8 and the actual power output for the combined engine load can be seen in Equation 4.6.

$$P_{vessel}(SOG) = EL_{combine}(SOG) \cdot P_{total} \quad (4.6)$$

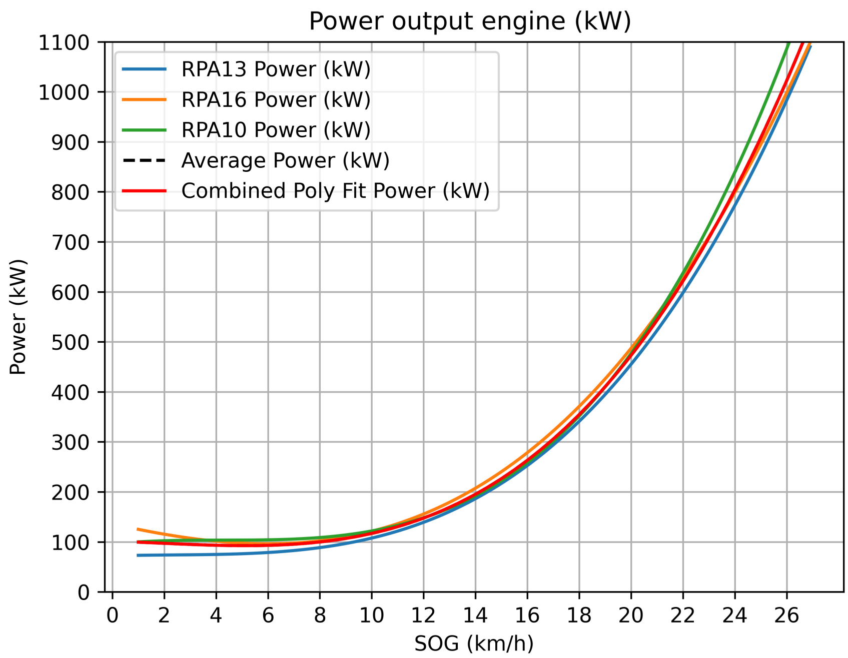

Figure 4.8: Combined power output

4.4.2. Sailing to and from the swapping station

Based on the power output for the vessels (Figure 4.8) , the power consumption for sailing the original path ($P_{t,r}$) can be defined. For the power consumption for sailing to (P_{StS}) and from the swapping station (P_{SbOP}), this is different from the power consumption for sailing the original path. The power consumption sailing to P_{StS} and from P_{SbOP} the swapping station is a constant input parameter and only based on a certain velocity of vessel, related to the power output for that speed ($V_{max,StS}$ and $V_{max,SbOP}$).

To make a make a better decission on the actual power consumption of the vessel, and to better understand the vessel's energy efficiency, the energy consumption in kWh/km is calculated using Equation 4.7. This metric reflects the energy consumed to travel one kilometre at a given speed SOG. The combined power consumption (Equation 4.6, $P_{vessel}(SOG)$) for a specific SOG by the SOG in km/h, resulting in the unit kWh/km. The combined power consumption equation (Equation 4.6) as a function of the speed (SOG) is divided by the actual speed which can be seen in Equation 4.7 .

$$EnergyConsumption = \frac{P_{vessel}(SOG)}{SOG} \; [kWh/km] \tag{4.7}$$

The power consumption curve, as discussed earlier, shows that increasing speed leads to higher power consumption (Figure 4.8). However, equation 4.7 shows how much energy is needed to travel one kilometre, which gives additional insight which can be seen in Figure 4.9. For slower speeds, the vessel takes longer to finish one kilometre, leading to higher total energy consumption. From a certain point, the increased speed will result in a higher energy consumption for one kilometre, where the most opitimal speed for one kilometre can be seen in this Figure.

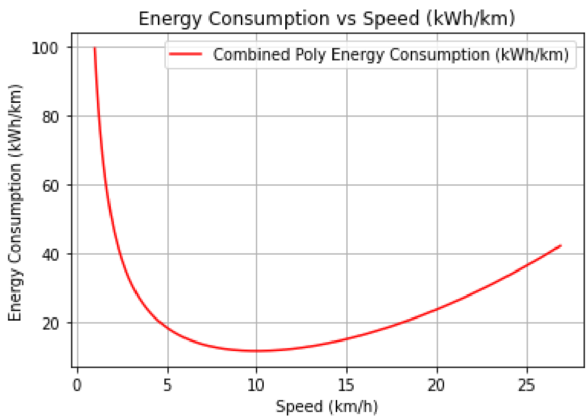

Figure 4.9: Energy consumption for one kilometre

It can be seen in Figure 4.9 that based on the power consumption (Equation 4.6), the most optimal speed to finish one kilometre is approximately $10\ km/h$. Sailing at the maximum speed ($25\ km/h$) will impact the power consumption four times more than $10\ km/h$. Figure 4.9 shows the impact of sailing faster, which increases power consumption and should be considered thoroughly, especially when this will be different in the following research.

Based on the objective of minimising the time a vessel is busy with swapping, more priority is given to faster sailing to reduce the total swapping time than saving power consumption. Therefore, this thesis uses a speed of $25\ km/h$, which is the most conservative choice. As mentioned, the time it takes to go to or from the swapping station is rounded up (Chapter 4.5), implying a higher power consumption because of the longer duration due to the increased timesteps. This is even more conservative.

4.5. Swapping duration

If a vessel r needs a swap, it will differ from its original path. This time should be calculated upfront to prevent the optimisation model from having more calculations. This is possible since the AIS data locations, the zones, and the parameter $RinZ_{t,r,s}$ are known. With this information, the distance and time to get to ($DT_{StS_{t,r}}$) or go from ($DT_{SbOP_{t,r}}$) a swapping station s can be calculated. To determine the path of each vessel r within a specific area $RinZ_{t,r,s}$, the shortest path algorithm by Dijkstra is used (which is already available from the Port of Rotterdam). Since the optimisation model depends on time-synchronised time steps t, it is necessary to precisely calculate those times to prevent time-shifts in the optimisation model.

At each time step, if the vessel r is in a specific zone ($RinZ_{t,r,s} = 1$), both the distance to get to the swapping station and the distance to get back to the original path should be calculated. For calculating the distance to the swapping station, at each time t, the distance to the swapping station is calculated. This distance is then used to calculate the time to the swapping station ($DT_{StS_{t,r}}$) based on a certain speed v_{max}. This actual time ($DT_{StS,actual_{t,r}}$) is then rounded up to the nearest (integer) timestep.

Calculating the time to reach the original path is somewhat different. The problem is that the vessel r should return to a certain point in time to avoid a time-shift. Since the distance to a certain point in time will vary, from the moment a vessel r completes the swapping at swapping sataion s, each point in time should be considered to know where the vessel r should return to. Therefore, an extra step in the calculation is performed to ensure the vessel r reaches a specific point in time with a given maximum speed v_{max}. This calculates where the vessel r should return to, and the value of $DT_{SbOP_{t,r}}$ is used if a vessel r leaves the swapping station at a certain point t in time.

Figure 4.10 shows an example of how this is calculated. The original path (upper part), the path to the swapping station, and the swapping station and sailing back to the original path (lower part) can be seen. Especially for the time to get back to the original path ($DT_{SbOP_{t,r}}$), an example is discussed in Figure 4.10. A vessel r initiates sailing to the swapping area s ($StS_{t,r} = 1$). In this case, this takes the vessel r 1.6 timesteps rounded to two timesteps t. When the vessel r arrives at the swapping station s ($VS_{t,r} = 1$), the vessel r will stay there for exactly $T_{swap} = 1$ periods. After the swap is complete, an additional algorithm is used to decide where the vessel r can rejoin the original path. The first considered location where the vessel can return to is $t + n$ (only for $RinZ_{t,r,s} = 1$). However, the time to arrive there in time ($DT_{SbOP_{t,r}} = 2.6$) is higher than the considered timestep. Therefore, the following point in time ($n = 2$) is considered. This next point ($t = 5$) is as well not suited, $DT_{SbOP_{t,r}} = 2.6 > 2$. This calculation is performed until the bound is satisfied (with a maximum of 12 timesteps), increasing n with one each time until the bound is satisfied, where $DT_{SbOP_{t,r}} < n$. For this exmaple, the bound is satisfied at $t = 4$ ($DT_{SbOP_{t,r}} = 3.2 < 4$). The value used for ($DT_{SbOP_{t,r}}$) should always be in line with the timestep t used in the optimisation model, in this case, rounded to the nearest integer number.

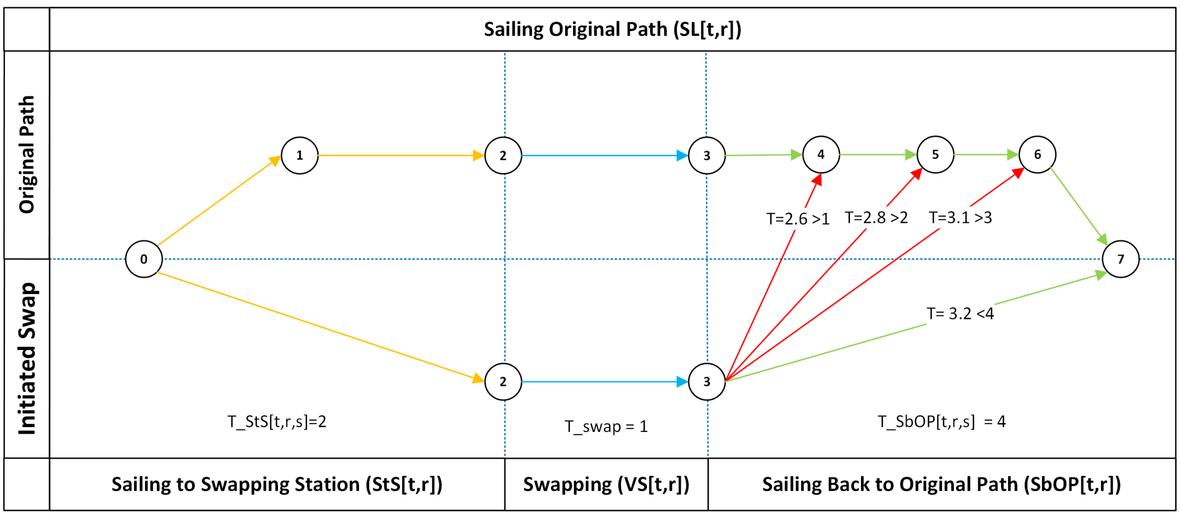

Figure 4.10: Time synchronization for the vessel

4.6. Swapping method

Based on the literature, the Shiftr method will be applied in this thesis (CH2.5.3). However, there should be a decision on the number of energy modules m on the vessel r, which will impact the optimisation model. The modules used by the shifter have a capacity of $980\ kW$, where the safety factor of $SF_{max,Shiftr} = 0.7$ and $SF_{min,Shiftr} = 0.1$ (depth of charge is 0.6) is used resulting in a usable capacity of $588\ kW$ for each module m. Based on the mathematical model (CH3.3), at least two modules should be used to maintain the possibility of only swapping one module m to have more possibilities for swapping in the optimisation model. For the Shfitr concept, four modules could be installed on the vessel. According to calculations of both the Port of Rotterdam and Shfitr, four modules should be enough to have shifts of eight hours, where swaps only happen at the main harbours. This approach is redundant, but it might be too redundant for this thesis because the other swapping locations besides the main harbour will be irrelevant. Also, this exclusive swapping in main harbours can result in a bottlenecks when charging the modules m. To accommodate the decision of the number of modules, an estimation is made for the correct number of moudles for the purpose of this thesis. This can be seen in Equation 4.8.

$$T_{sailing,SOG} = \frac{EM_N \cdot C_{capcity}}{P_{vessel}(SOG)}\ [h] \tag{4.8}$$

The equation's results are presented in Figure 4.11. This figure shows the duration an RPA vessel can sail (at a constant speed) with a specific number of modules m. The RPA vessels have shifts of eight hours, so if looking at one module m, this cannot be used at any speed for eight hours, and in combination with redundancy and the mathematical model, at least two modules should be used. If two modules m are used, the RPA vessel can have a constant speed of approximately (up to) $12\ km/h$ to finish an eight-hour shift. When an extra module m is used, this duration is increased to approximately (up to) $15\ km/h$. Since the shifter concept has either two or four modules (as can be seen in Figure 2.13 - 2.14), two modules are used for this thesis to have a more challenging optimisation model. The capacity of two modules is displayed to each vessel's initial cumulative power consumption. When doing this, the vessel should at least swap three times, as shown in Figure 4.12 (indicated with red lines). Note that the actual power consumption will be higher because if a vessel differs from its original path, a higher power consumption is more likely to be used, see Chapter 4.4.2.

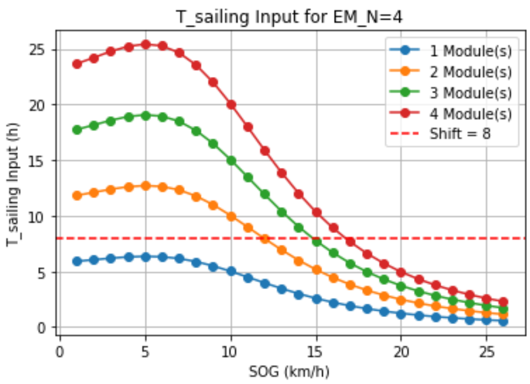

Figure 4.11: Engine load for RPA 10

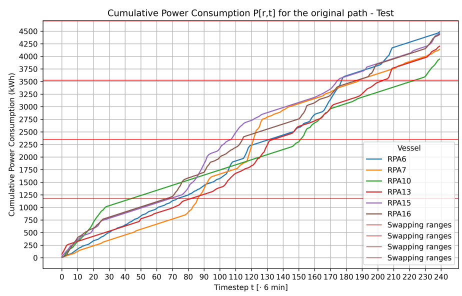

Figure 4.12: The initial power consumption with the

Figure 4.11, needs more explanation. The power consumption does not increase linearly with speed. Typically, power consumption increases exponentially with velocity because of factors such as drag (air resistance for vehicles or water resistance for ships), which grows roughly with the cube of the speed. If the power consumption is increased by increasing speed, the time to drain the battery decreases, but not as quickly as might intuitively be expected. This is because dividing by a larger power value results in a slower decrease in time. Because power consumption scales with the cube of speed (or another non-linear factor), the energy module m drain time will decrease slower for higher speeds. Therefore, the relationship between speed and sailing time is non-linear, and the 'odd' curvature can be seen.

4.7. Possible Swap

The input for the possible swap can be divided into two different parameters on a specific vessel r and a particular time t. The first one is defined if there is no data (Chapter 4.7.1), and the other is an estimation when an RPA vessel is busy doing a swap (Chapter 4.7.2).

4.7.1. Data gaps

In the previous sections, the data is considered. The data points should not be considered if the data is missing for one of those input parameters. Therefore, the input parameter $SPos_{t,r}$ is introduced, which is one if there are no data gaps and zero when there are data gaps. When there is a gap in the data, the vessel r cannot be sailing to ($StS_{t,r}$), from ($SbOP_{t,r}$) or being at the swapping station ($VS_{t,r}$) which is also explained in Constraint 3.46 - 3.64 in the methods chapter (CH3.3).

This preprocessing is done in the Excel file, those gaps are indicated with $null$ values, meaning no data is available for that specific vessel r for a particular time t. As the mathematical model indicates, those missing data have at least a value to prevent the model from being infeasible due to $null$ values. Due to this parameter $SPos_{t,r}$, it prevents these values from being used in the optimisation model ($SPos_{t,r} = 0$). As discussed in the mathematical model, this parameter is zero for the constraints depending on specific times. For example, the first T_{swap} periods, where some constraints are not defined due to time-dependent constraints. This is done in the optimisation itself by applying certain rules to the data frame for this specific parameter $SPos_{t,r}$. This parameter will decrease the possibility of swapping and should improve the computational time needed to solve.

4.7.2. RPAs doing tasks

The other input parameter used for an RPA vessel when a swap, or the process, is excluded is the input parameter where the RPA vessel is doing tasks, $RB_{t,r}$, which is also time t and vessel r dependent. Suppose the vessel r is doing a particular task; the vessel r cannot do anything that has to do with swapping. In that case, this should also not be part of the optimisation. This is for sailing to ($StS_{t,r}$), from ($SbOP_{t,r}$) or being at a swapping station ($VS_{t,r}$). When a vessel r is at the exact location, outside the main harbours, for more than two time steps, it is most likely that a vessel is doing a task. Since the AIS data does not contain information about the tasks of vessels r, this is the only way to include some tasks a vessel r can do. One important note is that if the time step is increased, this can result in less accuracy. Conversely, when fewer options are available, the computational time could decrease. For the tasks of the RPA vessels, it is essential to know if a vessel r is doing a task since if the vessel r is doing tasks, it should not initiate a swap, sailing to a swapping station or sailing back to the original path.

4.8. Time-intervals

There is one more step important for the pre-processing. This step is not directly an input parameter for the optimisation model based on a particular index or constant value but will impact all the other input parameters when changed. This is increasing or decreasing the actual time step. Reducing the time steps can reduce the computational time since fewer considered time steps will result in fewer data points to be considered. The input from the Port of Rotterdam is defined for each minute during the day (Table 4.1), based on the input of the Port of Rotterdam.

Based on this input, another data-based is made. These databases are used to calculate different timesteps. The swapping method is Shiftr, which has a six-minute swapping time for two modules (Chapter 4.6. This timestep is the largest timestep that can be used in the model, where the smallest timestep is one minute. Since the data is based on this one minute, this will be the minimum timestep. The other considered timesteps are two and three minutes since those can be divided by six to indicate the timesteps correctly. The choice of the time steps is case-dependent, but they can only be considered time steps, as discussed in this chapter. Note that increasing the timestep will affect the accuracy of the data, but the decreased computational time can be worth it.

4.9. Conclusion

In this chapter, the pre-processing steps required to define and prepare both constant and time-dependent input parameters for the optimisation model were explained (as also described in the mathematical model, Table 3.3). Pre-processing ensures the model functions efficiently by minimizing computational load, enabling faster and more accurate runtime performance.

This chapter specified and discussed everything which is needed to perform verification, validation and the case studies in the following chapters. This chapter outlined the necessary steps to prepare input data, including the choice of the vessels r (Chapter 4.1), the location data of the vessels (Chapter 4.2), AIS-data of the vessels (Chapter 4.3), the critical role of zones and swapping areas (Chapter 4.3, the power consumptions (Chapter 4.4), the swapping duration (Chapter 4.5) and method (Chapter 4.6), the possibilities to actual swap (Chapter 4.7) and the particular time interval which can be used for this specific thesis (Chapter 4.8). The main purpose was aligning the (time-dependent) input parameters, and structuring vessel-specific attributes.

All the used data in the pre-processing is considered the best available data at this point. However, it should be mentioned that this can be more detailed, and the pre-processing has limitations. First, the data is based on conventional vessels with traditional power consumption. Future RPA vessels will not have a conventional power supply, which will differ. However, this is not yet defined, and no specific design has been suggested. While the optimisation model is using this data, if the optimisation model is working as expected (Chapter 5), this will result in less accurate results. But since this is the first research for these type of vessels for the Port of Rotterdam, this is considerede enough to have at least an beginning. Future work should aim to refine these estimates, particularly for electric-driven vessels or next-generation designs.

Furthermore, The pre-processing is based on the best availba data. this data is important for the output because the more accurate the input, the better the optimisation model results. Since it is known that this is an estimation, it can be calculated in more detail in the future. A working optimisation model is the main objective of this thesis. If there is more specific information, this can be used as input, and the power consumption can be estimated, for example, for the electrical-driven vessels.

This pre-processing will impact the optimisation model since those calculations upfront will not be calculated again in the optimisation model. Firstly, when looking at the used vessels (and the data), it should be mentioned that this data is based on conventional vessels with a traditional power consumption of marine engines. The power consumption estimations are therefreo based on conventional vessels, but for the purpose of this thesisi this data is an beginning since no data of the actual desing of the RPA vessels is known. For the optimisation model, it does not matter what the input is for the power consumption since it will calculate when a specific vessel r needs a swap. However, it affects the outcome, but this pre-processing will be used due to the lack of (detailed) data.

Based on the available information, this is the best data which can now be used for this thesis. However, it should be noted that this data can be more detailed. However, more research is needed to determine this. However, the mathematical and optimisation models can also be used for other cases. Therefore, it is concluded that this data is, for now, enough to proceed.

5
Verification & Validation

While the mathematical model chapter describes the optimisation model and how it should function theoretically, the verification section demonstrates that the model is accurately implemented in Gurobi and that every constraint behaves as expected within the Python environment. On the other hand, validation is used to validate real-world scenarios or theoretical expectations. Typically, validation involves comparing test data with actual data or findings from other studies. Both are important, since the. BSM has not yet been implemented for this type of vessels. For the validation of this research, it is checked whether an individual RPA vessel can perform battery swaps independently, ensuring that when RPA vessels are combined for the case study discussed in the next chapter (CH6), an potential infeasible model result is due to one specific RPA vessel.

1. *How can the model be verified? (CH5.1)*
2. *How can the model be validated? (CH5.1.2)*

5.1. Verification

The verification is used to verify that the mathematical model aligns with the optimisation model. The Python Gurobi optimisation model has a particular testing mode for this verification phase. An Excel file is coupled to the model where the (random) input can be generated to test and verify the mathematical model. It should be mentioned that the testing mode is built so that every (verification) test case is saved automatically to a certain path to prevent data loss and (human) errors. This automatic saving is also used during building the model, meaning that the model was verified for each next step of the optimisation. In this sub-chapter, the final verification checks are performed. Based on the mathematical model (CH3.3), there are six different subjects where the verification checks are performed on.

1. *Module position (Chapter 3.3.5.a)*
2. *Logical flow of modules (Chapter 3.3.5.b)*
3. *Modules at Swapping Station (Module level) (Chapter 3.3.5.c)*
4. *Energy level and module state(Chapter 3.3.5.d)*
5. *Vessel state (Chapter 3.3.5.e)*
6. *The correct indication of the energy level of modules (Chapter 3.3.5.f)*

Each subject (number) corresponds to specific constraints from the mathematical model (letters), which can be seen in Table 5.1. This number-letter combination will be used as a reference in this chapter.

Check	Verification	Constraints
$1\,(a-b)$	(a) One module m should be assigned to the one location ($x_{t,m,r}$, $y_{t,m,s}$, $Ch_{t,m,s}$, $I_{t,m,s}$ or $InS_{t,m,s}$). (b) Modules m cannot be located at multiple locations at the same time t.	Constraint (3.2 - 3.3)
$2\,(a-f)$	(a) The logical flow of modules m, where each module m is at least in one location before going to the next location, is correctly applied. (b) Additional logical flow constraints for the modules m, restricting modules m can only flow to the swapping station s if the vessel r is in the correct zone $RinZ_{t,r,s}$. (c) Modules m can only flow to the charging area ($Ch_{t,m,s}$), Inventory ($In_{t,m,s}$) or the InventorySwap ($InS_{t,m,s}$) if the module m are in the same swapping area s. (d) A module m cannot came from the vessel r, going to the swapping station $y_{t,m,s}$ and then go to a vessel r. (e) A module m can not go from the InventorySwap $InS_{t,m,s}$ to the swapping station $y_{t,m,s}$ to the charging area $Ch_{t,m,s}$. (f) Modules cannot jump from locations.	Constraint (3.4 - 3.21)
$3\,(a-e)$	(a) In the swapping station, there should be at least two modules m, one coming from the vessel r ($\theta_{t,m,s}$) and one from the swapping area s ($\Delta_{t,m,s}$). (b) A module m in the swapping station $y_{t,m,s}$ has a correct indication of where it came from. (c) A module m coming from the vessel r is correclty assigned. (d) A module m coming from the swapping area s is correclty applied. (e) There can be at most $2 \cdot EM_N$ modules m in the swapping stations for each time t. (f) Modules m are staying for exactly T_{swap} periods of time at the swapping station.	Constraint (3.22 - 3.35)
$4\,(a-f)$	(a) Each module m should be indicated with a correct energy level state ($f_{t,m}$, $i_{t,m}$ and $e_{t,m}$. (b) Each state can only be assigned once. (c) The energy level $l_{t,m}$ is correctly coupled to a specific state. (d) If the module m is full ($f_{t,m}$), it cannot be at the charging area ($Ch_{t,m,s}$). (e) If the module m is intermediate ($i_{t,m}$), it cannot e a the Inventory ($In_{t,m,s}$) or the InventorySwap ($InS_{t,m,s}$). (f) If the module m is empty ($e_{t,m}$) it cannot be propelling the vessel r ($u_{t,m,r}$) or being at the Inventory ($In_{t,m,s}$) or the InventorySwap ($InS_{t,m,s}$). g An energy module m is allowed to go over or beneath the safety factors (SF_{min} and SF_{max}) but can never be lower than either zero or the maximum capacity of the energy modules m.	Constraint (3.36 - 3.44)
$5\,(a-i)$	(a) The state of the vessel r is correctly applied ($SL_{t,r}$, $StS_{t,r}$, $VS_{t,r}$ or $SbOP_{t,r}$), where only one state is applied at each time t. (b) When the vessel r is at the swapping station ($VS_{t,r}$), modules m cannot be used for the propulsion of vessel r. (c) The logical flow of the vessel states is correct, where each state is visited at least once before going to the next state. (d) If the vessel r is sailing tot the swapping station ($StS_{t,r}$), the correct number of modules m should be at the InventorySwap during this time t. (e) If the vessel r is not at the swapping station ($VS_{t,r}$), and thus sailing, there are always EM_N modules m on the vessel r. (f) If the vessel r is at the swapping station ($VS_{t,r}$), at most $EM_N - 1$ modules m are on the vessel r. (g) When the vessel r is at the swapping station ($VS_{t,r}$) there are at least two modules m located at the swapping station and at most $2\dot{E}M_N$ modules m. (h) When the vessel r either starts to sail to ($StS_{t,r}$) or sail back ($SbOP_{t,r}$), it should take the correct time based on the input parameters ($DT_{StS_{t,r}}$ or $DT_{SbOP_{t,r}}$. (i) When there no swap possible ($Spos_{t,r} = 1$) or a vessel r is doing task $RB_{t,r} = 0$, the vessel cannot do anything with swapping ($StS_{t,r} = 0$, $VS_{t,r} = 0$ and $SbOP_{t,r} = 0$.	Constraint (3.45 - 3.78)
$6\,(a-c)$	(a) The modules m have a correct indication of the energy module level $l_{t,m}$. (b) The variables ($PSL_{t,m,r}$, $PStS_{t,m,r}$ and $PSbOP_{t,m,r}$) for indicating which energy consumption is taken is correctly applied, where at most one of these variables can be one at the same time t. c If the vessel r has a module m which is being used ($u_{t,m,r} = 1$), either one of the energy consumption variables ($PSL_{t,m,r}$, $PStS_{t,m,r}$ and $PSbOP_{t,m,r}$) is one.	Constraint (3.79 - 3.85).

Table 5.1: Verification checks based on the mathematical model

5.1.1. Test Base Case

Before doing the verification tests where parameters are varied, a base case (TC_B) is introduced. This base case explains the formatting the tables and the results. It provides a benchmark for comparing the actual test cases to assess the impact of parameter changes and verify the model's behaviour based on the mathematical model. The verification checks, as explained in Table 5.1, are then discussed. To do this, two table types are generated. One is for the vessel and module level, and the other only for the vessel level and the objective function output.

The first table is presented in Table 5.2, where the vessel state (left side) and the modules m on a certain location (right side) can be seen. For TC_B, two vessels r and two swapping areas s are used. Each state of the vessel r ($SL_{t,r}$, $StS_{t,r}$, $VS_{t,r}$ and $SbOP_{t,r}$) is denoted with the corresponding zone s the vessel r is sailing in ($RinZ_{t,r,s}$) for each time t (indicated after the state within brackets). The energy consumption ($P_{t,r}$, P_{StS} or P_{SbOP}) for a vessel r at time t is kept constant, with a value of 10. The run will have a duration of 17 timesteps t to ensure at least one swap is initiated ($170 > 160$). When a swap is initiated both the input parameter $DT_{StS_{t,r}}$ and $DT_{SbOP_{t,r}}$ are kept constant, with the value one. When the vessel r reaches the swapping station s, the vessel r will be kept for exactly $T_{swap} = 2$ periods at the swapping station s.

For the module level (right side of the table), the location of the modules m ($x_{t,m,r}$, $y_{t,m,s}$, $Ch_{t,m,s}$, $In_{t,m,s}$ and $InS_{t,m,s}$), the energy level ($l_{t,m}$) and the state of the energy module m ($e_{t,m}$, $i_{t,m}$, $f_{t,m}$) can be seen. When looking first at the location of the modules m at the vessel r, this is indicated with R. When a specific module m is used on the vessel ($u_{t,m,r} = 1$), this is indicated $'R$ were the energy level $l_{t,m}$ should decrease with $P_{t,r}$, P_{StS} or P_{SbOP} depending on the state of the vessel r until the minimum safety factor SF_{min} is reached. When this value is reached, the module m cannot be used any more. All the modules m have an energy module capacity ($EM_{capaicity}$) of 100, where a safety factor of 0.8 (SF_{max}) and 0.2 (SF_{min}) are used. Note that each module m has one extra unit (81) to ensure the module is full. The energy level $l_{t,mr}$ is indicated for each module m (full=F, intermediate=I and empty=E).

Looking to the modules m located at the swapping station s, this is indicated with Δ or θ. This can only be true if the vessel r is at the swapping station s ($VS_{t,r}$), for T_{Swap} periods both for the modules m coming from the vessel ($\theta_{t,m,s}$) and the modules coming from the swapping area s ($\Delta_{t,m,s}$). The module m from the swapping station s should go to the charging station s ($Ch_{t,m,s}$). When the module m makes a swap, and the module m is going to the charging area ($Ch_{t,m,s}$), the charging speed (Ch_{speed}) is taken as 10. If a module m is charging ($Ch_{t,m,s}$) this is denoted with C. After the module m is fully charged, it flows to the inventory ($In_{t,m,s}$) indicated with I, which is only possible when the module m is above SF_{max}. Furthermore, there are two modules m starting at each inventor s. When the vessel r is sailing to a swapping station s ($StS_{t,r}$), there should be the correct number of modules m at the vessel.

t	Vessel r		Module m with energy level $l_{t,m}$							
	R1	R2	0	1	2	3	4	5	6	7
0	SL (1)	SL (2)	R1 81.0 (F)	’R1 81.0 (F)	R2 81.0 (F)	’R2 81.0 (F)	I1 81.0 (F)	I1 81.0 (F)	I2 81.0 (F)	I2 81.0 (F)
1	SL (1)	SL (2)	R1 81.0 (F)	’R1 71.0 (I)	R2 81.0 (F)	’R2 71.0 (I)	I1 81.0 (F)	I1 81.0 (F)	I2 81.0 (F)	I2 81.0 (F)
2	SL (1)	SL (2)	R1 81.0 (F)	’R1 61.0 (I)	R2 81.0 (F)	’R2 61.0 (I)	I1 81.0 (F)	I1 81.0 (F)	I2 81.0 (F)	I2 81.0 (F)
3	SL (1)	SL (2)	R1 81.0 (F)	’R1 51.0 (I)	R2 81.0 (F)	’R2 51.0 (I)	I1 81.0 (F)	I1 81.0 (F)	I2 81.0 (F)	I2 81.0 (F)
4	SL (1)	SL (2)	R1 81.0 (F)	’R1 41.0 (I)	R2 81.0 (F)	’R2 41.0 (I)	I1 81.0 (F)	I1 81.0 (F)	I2 81.0 (F)	I2 81.0 (F)
5	SL (1)	SL (2)	R1 81.0 (F)	’R1 31.0 (I)	R2 81.0 (F)	’R2 31.0 (I)	I1 81.0 (F)	I1 81.0 (F)	I2 81.0 (F)	I2 81.0 (F)
6	SL (1)	SL (2)	R1 81.0 (F)	’R1 21.0 (I)	R2 81.0 (F)	’R2 21.0 (I)	I1 81.0 (F)	I1 81.0 (F)	I2 81.0 (F)	I2 81.0 (F)
7	SL (1)	StS (2)	’R1 81.0 (F)	R1 11.0 (E)	’R2 81.0 (F)	R2 11.0 (E)	I1 81.0 (F)	I1 81.0 (F)	IS2 81.0 (F)	IS2 81.0 (F)
8	StS (1)	VS (2)	’R1 71.0 (I)	R1 11.0 (E)	θS2 71.0 (I)	θS2 11.0 (E)	IS1 81.0 (F)	IS1 81.0 (F)	ΔS2 81.0 (F)	ΔS2 81.0 (F)
9	VS (1)	VS (2)	θS1 61.0 (I)	θS1 11.0 (E)	θS2 71.0 (I)	θS2 11.0 (E)	ΔS1 81.0 (F)	ΔS1 81.0 (F)	ΔS2 81.0 (F)	ΔS2 81.0 (F)
10	VS (1)	SbOP (2)	θS1 61.0 (I)	θS1 11.0 (E)	C2 71.0 (I)	C2 11.0 (E)	ΔS1 81.0 (F)	ΔS1 81.0 (F)	R2 81.0 (F)	’R2 81.0 (F)
11	SbOP (1)	SL (2)	C1 61.0 (I)	C1 11.0 (E)	I2 81.0 (F)	C2 21.0 (I)	R1 81.0 (F)	’R1 81.0 (F)	R2 81.0 (F)	’R2 71.0 (I)
12	SL (1)	SL (2)	C1 71.0 (I)	C1 21.0 (I)	I2 81.0 (F)	C2 31.0 (I)	R1 81.0 (F)	’R1 71.0 (I)	R2 81.0 (F)	’R2 61.0 (I)
13	SL (1)	SL (2)	I1 81.0 (F)	C1 31.0 (I)	I2 81.0 (F)	C2 41.0 (I)	R1 81.0 (F)	’R1 61.0 (I)	R2 81.0 (F)	’R2 51.0 (I)
14	SL (1)	SL (2)	I1 81.0 (F)	C1 41.0 (I)	I2 81.0 (F)	C2 51.0 (I)	R1 81.0 (F)	’R1 51.0 (I)	R2 81.0 (F)	’R2 41.0 (I)
15	SL (1)	SL (2)	I1 81.0 (F)	C1 51.0 (I)	I2 81.0 (F)	C2 61.0 (I)	R1 81.0 (F)	’R1 41.0 (I)	R2 81.0 (F)	’R2 31.0 (I)
16	SL (1)	SL (2)	I1 81.0 (F)	C1 61.0 (I)	I2 81.0 (F)	C2 71.0 (I)	R1 81.0 (F)	’R1 31.0 (I)	R2 81.0 (F)	’R2 21.0 (I)

Table 5.2: Verification TCB

In Table 5.2 the actual results can also be seen. For this base test case the verification checks as explained in Table 5.1 are checked. The first checks, $1(a-b)$, have a positive result where the modules m are at each time step t are correctly assigned to the vessels r. When multiple modules m, or none, are assigned to a location, this would be indicated with '-', which is not the case. Also every module m has a correct flow (Table 5.2 $2(a-f)$). This base test case also passes when zooming in to the swapping station s, indicated with the verification checks $3(a-e)$. As expected, the vessels r should swap at least once, which can be seen at $t=10$ for vessel $R1$ and at $t=9$ for vessel $R2$, where each vessel r is swapping in the correct zone $RinZ_{t,r,s}$. To zoom further in the swapping station s, there is indeed a correct indication of the modules m coming from the vessel r ($\theta_{t,m,s}$) and modules m coming from the swapping area s ($\Delta_{t,m,s}$). For both the vessels r, there is a swap with a maximum of $2 \cdot EM_N$ modules m at the swapping station s, which takes exactly T_{swap} periods. The verification checks for the energy level $l_{t,m}$ of the modules $l_{t,m}$ and the states of the modules m ($e_{t,m}$, $i_{t,m}$ and $f_{t,m}$), with verification checks $4(a-f)$ are also passing. Every module m does indicate the energy module level $l_{t,m}$, which is also in line with the energy consumption for each vessel r for each time t. This can be seen with vessel $R1$, where module $m=1$ is used because it is indicated with $'$, and it indeed decreases in energy level $l_{t,m}$. However, due to the constant value of the energy consumption, this should have a separate test case since it can not be verified if the correct energy consumption is taken. All the modules m have a correct indication of the energy level state ($e_{t,m}$, $i_{t,m}$ and $f_{t,m}$). Furthermore, the level is never higher than 100 or less than 0, which would give an infeasible result.

The second table type can be seen in Table 5.3 - 5.4. The first column indicated the time t, followed by the possibility of a swap (either $SPos_{t,r}$ or $RB_{t,r}$). The possibility of a swap (CH4.7), is indicated with a green check mark or a red cross. Additionally, if a vessel r is within the area of a main harbour (based on latitude and longitude) at time t this is indicated with $*$ after $SPos_{t,r}$. The other columns represent the objective function. This shows whether a vessel r is initiating sailing to ($Start_{StS_{t,r}}$) or initiates sailing back to the original path ($Start_{SbOP_{t,r}}$) and is indicated with $\mid time \mid$ based on the time t it takes ($DT_{StS_{t,r}}$ or $DT_{SbOP_{t,r}}$). Note that this can only be true if $RinZ_{t,r,s}=1$, and that after t time steps the start was initiated, it vessel r is in the next state. Furthermore, the first time a vessel r is at the swapping station s, indicated with the corresponding T_{swap} is indicated as well. For each timestep, the total time a vessel would need to swap from that point in time, can be seen with T_total.

For this specific test base case T_{BC}, there is no restriction on additional timesteps t where the vessel r cannot swap. Due to the constraints (CH3.3), the first and last $T_{swap}+1$ timesteps t are excluded. This means the vessel r can be used in 11 different time steps for this test base case, from $t=3$ to $t=13$. This is relevant because the main harbour has most likely a short sailing to ($DT_{StS_{t,r}}$) and sailing from ($DT_{SbOP_{t,r}}$).

t	$SPos_{t,r}$	$StS_{t,r}$	$VS_{t,r}$	$SbOP_{t,r}$	T_{total}
0	✗*	1	2	1	4
1	✗*	1	2	1	4
2	✗*	1	2	1	4
3	✓*	1	2	1	4
4	✓*	1	2	1	4
5	✓*	1	2	1	4
6	✓*	1	2	1	4
7	✓*	1	2	1	4
8	✓*	| 1 |	2	1	| 4 |
9	✓*	1	| 2 |	1	4
10	✓*	1	2	1	4
11	✓*	1	2	| 1 |	4
12	✓*	1	2	1	4
13	✓*	1	2	1	4
14	✗*	1	2	1	4
15	✗*	1	2	1	4
16	✗*	1	2	1	4

Table 5.3: Verification TC_B for $R1$

t	$SPos_{t,r}$	$StS_{t,r}$	$VS_{t,r}$	$SbOP_{t,r}$	T_{total}
0	✗*	1	2	1	4
1	✗*	1	2	1	4
2	✗*	1	2	1	4
3	✓*	1	2	1	4
4	✓*	1	2	1	4
5	✓*	1	2	1	4
6	✓*	1	2	1	4
7	✓*	| 1 |	2	1	| 4 |
8	✓*	1	| 2 |	1	4
9	✓*	1	2	1	4
10	✓*	1	2	| 1 |	4
11	✓*	1	2	1	4
12	✓*	1	2	1	4
13	✓*	1	2	1	4
14	✗*	1	2	1	4
15	✗*	1	2	1	4
16	✗*	1	2	1	4

Table 5.4: Verification TC_B for $R2$

5.1.2. Test cases

After defining the test base case T_{BC} and explaining the results in the tables, the actual verification with eleven specific test case scenarios can be performed. This is done to evaluate the optimisation model's behaviour and ensure alignment with the expected results of the mathematical model. The input parameters for the test cases can be categorized into two types: those defined in the optimisation model (T_{total}, $EM_{capacity}$, SF_{max}, SF_{min}, Ch_{speed}, P_{StS}, P_{SbOP}, T_{swap}, $EM_{start,inventory}$, EM_N, r and s) and those from the Excel file ($P_{t,r}$, $RinZ_{t,r,s}$, $SPos_{t,r}$, $RB_{t,r}$, $DT_{StS_{t,r}}$, $DT_{StS,actual_{t,r}}$, $DT_{SbOP_{t,r}}$ and $DT_{SbOP,actual_{t,r}}$). These parameters can be adjusted during testing and can be seen in Table 5.5.

In the second part of Table 5.5, the input parameters for the Excel file can be seen. This Excel file has several tabs with time t, vessels r or swapping area s dependent parameters which can be kept constant or randomised within a specified range. This allows for more thorough model testing where randomisation is particularly useful for testing diverse scenarios and stress-testing the optimisation model. It should be noted that all the inputs have integer values.

Model input	TC_B	TC_1	TC_2	TC_3	TC_4	TC_5	TC_6	TC_7	TC_8	TC_9	TC_{10}	TC_{11}
T_{total}	17	34	"	34	"	34	"	"	"	"	"	34
$EM_{capacity}$	100	"	200	"	"	"	"	"	"	"	"	"
SF_{max}	0.8	"	"	"	"	"	"	"	"	"	"	"
SF_{min}	0.2	"	"	"	"	"	"	"	"	"	"	"
Ch_{speed}	10	"	"	5	"	"	"	"	"	"	"	5
P_{StS}	10	"	"	"	40	"	"	"	"	"	"	20
P_{SbOP}	10	"	"	"	40	"	"	"	"	"	"	20
T_{swap}	2	"	"	"	"	4	"	"	"	"	"	"
$EM_{start,inventory}$	2	"	"	"	"	"	3	1	"	"	"	"
EM_N	2	"	"	"	"	"	1	"	"	"	"	"
r	2	"	"	"	"	"	"	3	"	"	"	3
s	2	"	"	"	"	"	"	1	"	"	"	3
Excel input	TC_B	TC_1	TC_2	TC_3	TC_4	TC_5	TC_6	TC_7	TC_8	TC_9	TC_{10}	TC_{11}
$P_{r,t}$	[10]	"	"	"	"	"	"	[5,10]	"	"	"	[5,10]
$RinZ_{t,r,s}$	[0,1][1]	"	"	"	"	"	"	"	[1][1]	"	"	[0,2]
$SPos_{t,r}$	[0]	"	"	"	"	"	"	"	"	[0,1]	"	"
$RB_{t,r}$	[1]	"	"	"	"	"	"	"	"	[0,1]	"	"
$DT_{StS_{t,r}}$	[1]	"	"	"	"	"	"	"	"	"	[1,3]	[1,3]
$DT_{StS,actual_{t,r}}$	[0,1]	"	"	"	"	"	"	"	"	"	[1,3]	[1,3]
$DT_{SbOP_{t,r}}$	[1]	"	"	"	"	"	"	"	"	"	[1,3]	[1,3]
$DT_{SbOP,actual_{t,r}}$	[0,1]	"	"	"	"	"	"	"	"	"	[1,3]	[1,3]

[1] $s = r$

Table 5.5: Overall verification test cases

a. Test case 1: TC_1

For the first test case (Appendix B.1), the optimisation's total time T_{total} is increased from 17 to 34 timesteps to verify if a vessels r can swap multiple times. The other parameters will be the same as those in the base test case. Due to the energy consumption of the vessels r and the time the vessels r are sailing, it is expected that both the vessels r should swap at least twice. This is confirmed with Table B.1, where both vessels r are swapping twice. What is interesting to see is that both the vessels r do not necessarily swap all the modules m at the swapping station s. For example, vessel $R1$ at timesteps 7 and 8 only swaps one module m. In the test base case, it could not be verified whether one module m could be at the vessel r and the other module m at the swapping station s without having an incorrect logical flow of the modules m in general. Also the modules m at the swapping station s stay for $T_{swap} = 2$ periods at the swapping station s where one module m came from the inventory ($\Delta_{t,m,s}$) while the other module m came from the vessel r ($\theta_{t,m,s}$). It can be concluded that all the other verification checks, as can be seen in Table 5.1, are passing the criteria.

Test case 2: TC_2

For the second test case, the capacity of the energy modules (EM_N) is varied (higher and lowered) (Appendix B.2). Increasing the capacity of the modules m to a level where no swapping should happen (200) will result in no swaps (Table B.4 - B.12). On the other hand, reducing the energy modules' capacity should result in more swapping of modules m, which will increase total swapping time (Table B.7 - B.12). For the increased energy modules capacity, the vessels r are not swapping. Besides that, the vessels r are not swapping; the usage of modules and the energy consumptions are still until the modules m reach the safety factors, so this is correctly applied. The decrease in the capacity of the modules m is indeed resulting in more swapping. This can be seen in Table B.7. It can be seen that both vessel are swapping twice. All the other verification checks are also verified.

Test case 3: TC_3
The third verification test case is used to decrease the availability of modules m at the swapping stations s due to the longer charging times of the energy modules m. Due to these longer charging times, modules m will stay longer at the charging area ($Ch_{t,m,s}$) before going to the Inventory area ($Ins_{t,m,s}$). The other parameters will stay the same compared to the base test case. However, the optimisation time (T_{total}) is increased to 34 to compensate for the decrease in charging speed. Since the vessel r will have a energy consumption of 10, the vessel r should visit the swapping station s at least two times to keep the vessel r sailing. The outcomes can be seen in Appendix B.3. Table B.10 indeed shows that both the vessels r are swapping two times, where charging of the modules m is considered (with the decreased charging speed). It is interesting to see that the modules m in the swapping area s are more frequently used than the base test case. Figure B.1 shows the percentage of modules in the swapping area s for the charging, inventory, and InventorySwap area. In Figure B.2, this can be seen for test case TC_1, where also a time step $T_{total} = 34$ is used (charging capacity is 10). It can be seen that the interaction can indeed result in a more optimal usage of the modules m in the system.

Test case 4: TC_4
In the fourth test case, the energy consumption for sailing to (P_{StS}) and sailing from (P_{SbOP}) the swapping station is increased to 40 (four times the value for the base test case) (Appendix B.4). This verification test is needed for energy consumption. This will be as fast as possible for real-world scenarios when sailing to or from a swapping station. This is to decrease the maximum operation time and thus minimise downtime due to the swapping process (as discussed in CH4, pre-processing). When increasing this energy consumption, the optimisation model also challenges whether a swap can be made. This means the vessels r can only swap if an energy module m capacity is at least 60 or higher. This reduces the timesteps t where a vessel r can swap. Test case 4 does pass the verification checks.

Test case 5: TC_5
For the fifth test case, the swapping time T_{swap} is increased to four (Appendix B.5), which is two times more compared to the test base case TC_B. Since the swapping time T_{swap} is used in multiple constraints, mainly for the bounds where the restrictions apply, testing and verifying whether the optimisation model can correctly use these swapping time T_{swap} is necessary. One of these constraints is the possibility of swapping ($SPos_{t,r}$). If the swapping time T_{swap} is increased, this will result in fewer swapping options for at least the first and last T_{swap} periods of the optimisation model. It can indeed be seen that this is correct in Table B.17 - B.18. Furthermore, the modules m coming from the swapping station ($\theta_{t,m,s}$) and modules m coming from the swapping area s ($\Delta t, m, s$) should be stationed at the swapping station for exactly T_{swap} periods resulting in more total time T_{total} which can be seen in Table B.16. It can indeed be seen that the indication of the modules m coming from the vessel r ($x_{t,m,r}$) are indicated correctly with $\theta_{t,m,s}$ for exactly T_{swap} periods each time the vessel $r$is the swapping station $VS_{t,r}$. Since the time of swapping T_{swap} is adjusted the possibility of exchanging modules m for the first $T_{swap} + max(DT_{StS_{t,r}})$ and for the last part of the optimisation is correctly indicated. Furthermore, the correct indication of $StS_{start_{t,r}}$ and $SbOP_{start_{t,r}}$ as the first time a module m is at the swapping station, is correctly.

Test case 6: TC_6
Test case 6 is used to verify that one module m can also be used on the vessel r (Appendix B.6). This should result in more initiated swaps because there is simply less energy onboard the vessel r. Due to the expected increases in swapping, the number of modules m starting at the inventory has also increased for this test case to three. Based on the actual checks of the model, it can also be concluded that this test case does pass. However, this test case will be probably rare since, due to redundancy, at least two energy modules m should be on a vessel r. When a module m cannot deliver energy for some reason, there should always be an extra module m to propel the vessel r. Besides the redundancy, this case does show that it is possible for the model to sail with one model m. This case can be used to

run a model with an increased capacity where two modules m are represented by one model m. This can be interesting when the model should swap, for example, in pairs of two.

Test case 7: TC_7
For test case 7 (Appendix B.22), the energy consumption $P_{t,r}$ of the vessel r is randomised in a range of $[5, 20]$. This is important because the vessel r should then consider when to swap. To verify that the correct energy consumption is used for each vessel r, an additional table is made for a specific module m, Table B.22, which shows that this indeed happens. It can be concluded that the verification for this test case indeed passes. This means that the optimisation incorporates individual needs for swapping based on the mathematical model and that swapping highly depends on each vessel's energy consumption resulting that the consumption is a critical input parameter and should be as accurate as possible to achieve a precise optimisation result.

Test case 8: TC_8
For test case 8, the vessels r are located in the same swapping area s (Appendix B.8). In combination with the charging rate of the modules m, the optimisation should determine the correct initiated swap. There is a high probability of multiple vessels r within the swapping area s for actual cases. Initially, three vessels r were added to the optimisation model with the same number of modules m and charging speed with the same total time T_{total}. The optimisation was infeasible, due to the energy consumption. Therefore, the total time T_{total} is increased with one. Each vessel r should swap with one module m at least once. This test case also passes the verification checks.

Test case 9: TC_9
For the ninth test case, the possibility of swapping (either $SPos_{t,r}$ or $RB_{t,r}$) is tested (Appendix B.9). This is not randomised since this would probably impact the entire optimisation model. In the mathematical model, if data is not available or the vessel r is doing a task, the vessel r can not sail to a swapping station $StS_{t,r}$, not being at a swapping station $VS_{t,r}$ or sailing back to the original path $SbOP_{t,r}$. This means those parameter will highly impact the model if too much data is missing. On the other hand, if a random input is applied for testing, the model will be infeasible most of the time. The model should have a corresponding time window to initiate or begin a swap. Therefore, it is chosen to have a specific range deleted, in terms of $SPos_{t,r} = 0$ and $RB_{t,r} = 1$, to indicate time windows. This can be seen in Table B.29. Test case 9 is passing the verification checks. Table B.30 - B.31 shows that, indeed the vessel is not doing or initiating a swap when there cannot be a swap (red crosses).

Test case 10: TC_{10}
For this test, there is a random input for the time it takes to sail to ($DT_{StS_{t,r}}$) and sailing back to the original path ($DT_{SbOP_{t,r}}$) with a range of $[1, 3]$. The actual data can be seen in the following table, Table B.32. This test passes the verification checks as well. In Table B.33 and Table B.34, the objective can be seen for every initiated swap. It can be seen that, indeed, the correct time is initiated for a swap. Both vessels r initiate a swap where the total time is the lowest to have the most optimal operational time.

Test case 11: TC_{11}
For the last case, multiple parameters are adjusted (Appendix B.11). This will challenge the optimisation model in a way that combines most of the test cases, as seen in the previous tests. First, the total time T_{total} is increased since this will allow other parameters or input for Excel to be changed. Then, the charging speed is lowered. Since sailing to and from the swapping station will be done as fast as possible, this has been increased to 20 (doubled). The energy consumption is random $[5, 10]$ and the swapping areas s and the number of vessels r is increased to three. The swapping area s of the vessel r is randomised, meaning there can be multiple vessels r in a specific swapping area s. At last, the sailing to the swapping station ($DT_{StS_{t,r}}$) and the time to get to the original path ($DT_{SbOP_{t,r}}$) is also be randomised $[1, 3]$. This will likely challenge the optimisation model, and the computational time should also increase. The last test case also passes the verification test. This test case did challenge the optimisation model more in terms of computational time. Since this is a somehow controlled space where parameters are used as input, this will most likely impact the model if real-world scenarios are applied, which will be done in the next chapter validation (CH5.2).

5.2. Validation

The validation section aims to validate if the optimisation model can be used for real-world applications despite the novelty of this swapping method for this specific type of vessel. Since no direct historical data exists for comparison (e.g. other studies), alternative validation approaches are required. The primary objective (obj) of this section is to confirm whether the data from the pre-processing chapter (CH4 for each individual vessel (Table 4.1) can be used. In this pre-processing chapter, the used vessels (CH4.1), the AIS location data (CH4.2), the power estimation (CH4.4), the swapping (method) (CH4.5 - 4.6) were discussed and this data will will be used in this section. Each RPA vessel will be used for one run to see if it can swap independently to ensure that if multiple RPA vessels are introduced for one optimisation, it cannot be one vessel, which could result in an infeasible optimisation result.

For this validation, the parameters of the pre-processing are used, with a timestep of 6 minutes, resulting in a total of 240 timesteps (for the 24-hour run). This specific timestep is chosen because if swapping is valid for these timesteps, it is also possible with a smaller timestep. After all, there are more options to swap. The six different validation checks are summarised in Table 5.9 where the specific vessel, the data, the zones the RPA vessel is sailing in, the (main) harbours the vessel is visiting, the travelled distance, the energy consumption and estimation of swaps can be seen. Also, in the pre-processing, the zones (Figure 4.3), the distance (Figure 4.2) and the initial energy consumption including the estimated swaps (Figure 4.12) can be seen in the pre-processing chapter (CH4).

Appendix	**Vessel**	**Zones**		**Travelled Distance [km]**		**Initial energy Consumption [kwh]**		**Estimated Swaps**
C.1.1	RPA6	9-13	(Figure C.1)	75	(Figure C.2)	4,485	(Figure C.3)	3
C.2.1	RPA7	1-4, 7-8	(Figure C.9)	65	(Figure C.10)	4,138	(Figure C.11)	3
C.3.1	RPA10	9-14	(Figure C.17)	110	(Figure C.18)	3,944	(Figure C.19)	3
C.4.1	RPA13	9-14	(Figure C.25)	150	(Figure C.26)	4,201	(Figure C.27)	3
C.5.1	RPA15	1-3, 5	(Figure C.33)	161	(Figure C.34)	4,455	(Figure C.35)	3
C.6.1	RPA16	1-3	(Figure C.41)	148	(Figure C.42)	4,434	(Figure C.43)	3

Table 5.6: Input for validation cases

The summary of the results can be seen in Table 5.7. This table shows the appendix for each RPA vessel with the results and figures. First of all, all the vessels are swapping optimally. It was expected that the vessels should have at least swapped three times, and this is also happening, with an objective function value of 54 minutes for each vessel. Since the timestep is chosen as six, and the vessels have a minimum of 18 minutes for one swap, resulting in a total of 54 minutes. This validation validates that the vessel can indeed swap individuals with a correct output. Note that the actual energy consumption will be slightly higher (compared to Table 5.9), the actual energy consumption differs because the vessel has another energy consumption when sailing to and sailing from the swapping station as discussed in the pre-processing chapter (CH4.4.2).

Appendix	**Vessel**	**Obj [min]**	**Runtime [s]**	**Estimated/ actual swaps**	**Swaps in Zone**	**Correct Charging/correct Inventory/ Optimal usage modules**
C.1.2	RPA6	54	11,947	3 / 3 ✓(Figure C.4 - C.5)	9 / 9 /10	✓/ ✓/ ✗(Figure C.6 - C.8)
C.2.2	RPA7	54	136,028	3 / 3 ✓(Figure C.12 - C.13)	9 / 9/10	✓/ ✓/ ✗(Figure C.14 - C.16)
C.3.2	RPA10	54	5,385	3 / 3 ✓(Figure C.20 - C.21)	1 / 2 / 3	✓/ ✓/ ✗(Figure C.22 - C.24)
C.4.2	RPA13	54	18,106	3 / 3 ✓(Figure C.28 - C.29)	9 /9 /9	✓/ ✓/ ✗(Figure C.30 - C.32)
C.5.2	RPA15	54	16,632	3 / 3 ✓(Figure C.36 - C.37)	9 /11/12	✓/ ✓/ ✗(Figure C.38 - C.40)
C.6.2	RPA16	54	15,731	3 / 3 ✓(Figure C.44 - C.45)	1 /2 / 2	✓/ ✓/ ✗(Figure C.46 - C.48)

Table 5.7: Results for validation cases

This chapter confirms that the individual vessels can swap optimal. Also, when looking at the swapping area, where modules are charged and stored in the inventory when fully charged, this is also as predicted. The modules charge in the correct swapping area s and are correctly stored in the inventory s. To look at the efficiency of the modules, a figure is displayed where the percentage of modules in the swapping area can be seen. Since the vessels are only individually in the optimisation, it is expected that this efficiency of modules will improve in when more vessel are added. This will be done in the next chapter Case Study.

5.3. Conclusion

In this chapter, the verification and the validation were performed where it was concluded that the verification of the mathematical model was successfully. The verification summary can be seen in Table 5.8 where eleven different test cases were performed.

Appendix	Test Case	Verification (Table 5.5)	Result	Check
-	TC_B		At least one swap for each vessel r, which is happening.	✓
B.1	TC_1	T_{total}	The total time is increased from 17 to 34, which should increase the number of swaps for each vessel r (at least two swaps). Results show that indeed the vessels r are swapping twice, but not necessarily all the modules m on the vessel r. This verification therefore also shows that swapping one module m is possible, which could not be seen in the test base case.	✓
B.2	TC_2	$EM_{Capacity}$	The capacity of one modules m is increased to 200, and decreased to 50. Resulting in no swaps and twice the number of swaps, as expected.	✓
B.3	TC_3	T_{total}, Ch_{speed}	The charging speed is decreased to 5, twice as low. Modules m will stay longer at the charging station, and fewer modules are available for certain timesteps t. To facilitate this, the total time was increased to 34. The results show that indeed modules m charge longer, without having infeasible flows of modules.	✓
B.4	TC_4	P_{StS}, P_{SbOP}	The energy consumption when sailing to and from the swapping station s is increased. Modules m should decrease in power more rapidly. Results show that this indeed happens.	✓
B.5	TC_5	T_{total}, T_{swap}	In the fifth case, the swapping time of a module m is increased to 4. Also, the total time is increased to see what is happening. It can be concluded that the swapping of modules is indeed as expected, with everything needed.	✓
B.6	TC_6	$EM_{start,Inv}$ EM_N	The number of modules m at the vessels r is decreased to 1, with an increase in starting modules at the inventory. Results show that it is possible to have one module m onboard of the vessel r.	✓
B.22	TC_7	$EM_{start,Inv}$, r, s	Randomised energy usage, which will impact the number of swaps of individual vessels. The verification checks pass.	✓
B.8	TC_8	$RinZ_{t,r,s}$	In this test case three vessels are within the same swapping area. This is possible.	✓
B.9	TC_9	$SPos_{t,r}$ $RB_{t,r}$	The state of the swapping stations $SPos_{t,r}$ and the $RB_{t,r}$ is indeed showing that these are excluded for the possibility of swapping.	✓
B.10	TC_{10}	$DT_{StS_{t,r}}$, $DT_{StS,actual_{t,r}}$ $DT_{SbOP_{t,r}}$ $DT_{SbOP,actual_{t,r}}$	Random input for sailing to and from the swapping station, where the model should determine the most optimal total swapping time. This test passes the criteria.	✓
B.11	TC_{11}	Combined	Combined case or TC_{1-11} to test the model. Resutls show a correct verfication.	✓

Table 5.8: Summary verification

After verification of the optimisation model, the validation is performed. This validation was done with each individual RPA vessel. The input for these validation cases was explained in the prep-processing (CH4). The summary of the input for the validation and the actual results can be seen in Table 5.9. In this table, the results show that the vessel can indeed be swapped individually. However, the efficiency of the usage of modules is low, meaning that there are more modules in the system for too many swapping stations. Adding more vessels should improve the usage of the modules.

Appendix	Vessel	Zones	Travelled Distance [km]	Initial Energy [kWh]	Estimated/ actual Swap	Obj [min]	Runtime [s]	Swap in Zones	Correct Ch/In / optimal usage	Check
C.1	RPA6	9-13	75	4,485	3 / 3 ✓	54	11,947	9 / 9 / 10	✓/ ✓/ ✗	✓
C.2	RPA7	1-4, 7-8	65	4,138	3 / 3 ✓	54	136,028	9 / 9 / 10	✓/ ✓/ ✗	✓
C.3	RPA10	9-14	110	3,944	3 / 3 ✓	54	5,385	1 / 2 / 2	✓/ ✓/ ✗	✓
C.4	RPA13	9-14	150	4,201	3 / 3 ✓	54	18,106	9 / 9 / 9	✓/ ✓/ ✗	✓
C.5	RPA15	1-3, 5	161	4,455	3 / 3 ✓	54	16,632	9 / 11 / 12	✓/ ✓/ ✗	✓
C.6	RPA16	1-3	148	4,434	3 / 3 ✓	54	4,434	1 / 2 / 2	✓/ ✓/ ✗	✓

Table 5.9: Summary Validation

6
Case study

In the previous chapter, the validation and verification were performed. With the insights of these chapters, actual case studies can be performed with different vessels based on the preprocessing chapter (CH4). For the validation, it was seen that the computational time was already high. So, adding more vessels will result in ever more computation time. Therefore, not all the six vessels are added to the optimisation model. Because the preprocessing had already been performed, which took significant time, it was chosen to consider only the area from the Pistoolhaven. Therefore, one case study is performed with two vessels (CH6.1) and one with three vessels (CH6.2) where all three vessels are sailing within the area of the Pistoolhaven.

6.1. Caste study 1: two RPA vessels

Based on the validation, it was concluded that the vessels could swap separately with an optimal result. In this case study, more vessels are added to the optimisation model. Two RPA vessels are chosen based on the sailing profile, where RPA15 and RPA16 sail within three overlapping zones, zones 1,2 and 3. For both the vessels, the Pistoolhaven is their main harbour. RPA15 also sails within zone 5 but has just one data point. This case study is performed for 720 minutes, with an actual timestep of 6 minutes, resulting in 120 timesteps for the optimisation model. The sailing profile for this case study can be seen in both the vessels, RPA15 and RPA16, in Figure 6.1.

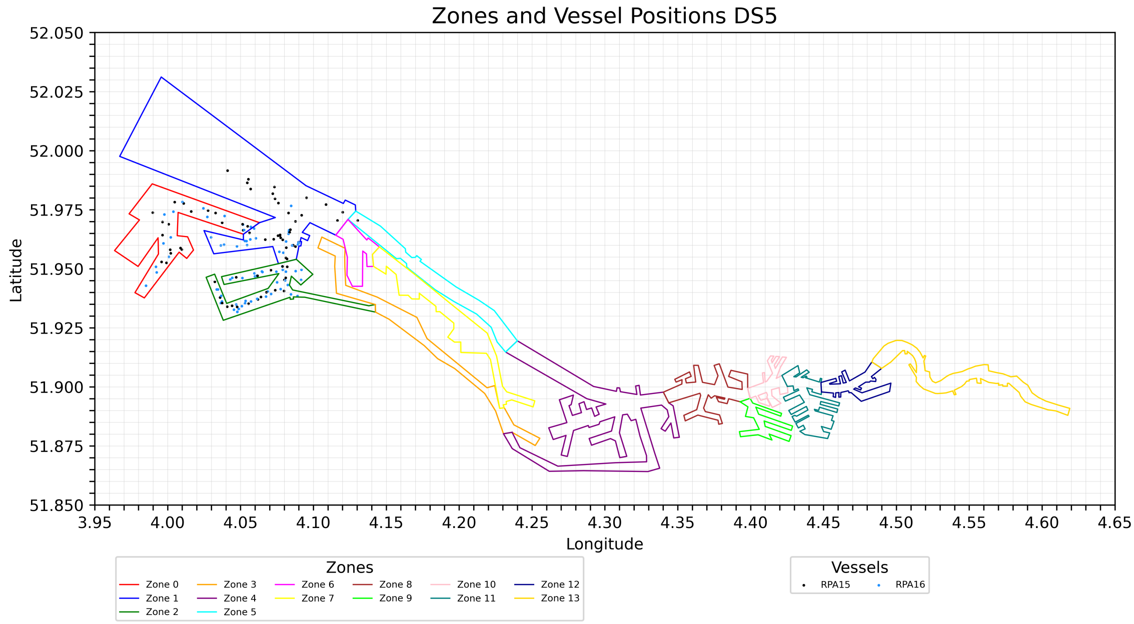

Figure 6.1: RPA15 and RPA16 locations (timestep = 6)

Also, for the case study, the distance for each RPA can be seen, which can be seen in Figure 6.2. In this graph, it can be seen that both vessels are stationed at the Pistoolhaven between approximately timestep 25-70. For the rest of the time, both vessels sail. For the initial power usage, this can also be seen in Figure 6.3. The RPA15 has a power initial usage of 2,717 kWh, meaning the vessels should have at least two swaps. For the RPA16, the vessel consumes 2,443 kWh, so the vessels should swap twice.

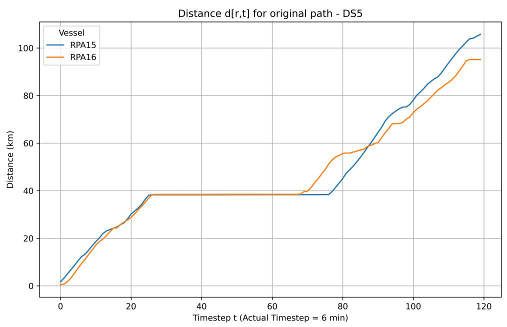

Figure 6.2: Cumulative distance for RPA15 and RPA16

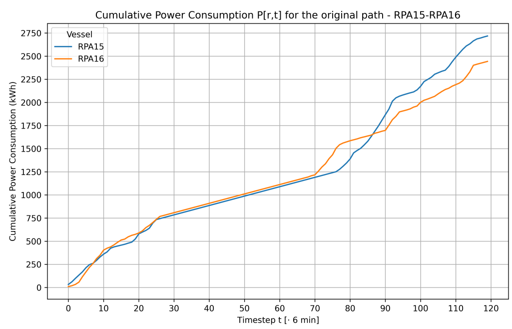

Figure 6.3: Cumulative energy consumption for RPA15 and RPA16

In the following two figures, the swapping for both the RPA vessels (Figure 6.4) and the actual power level for each RPA vessel (Figure 6.5) can be seen. This run took 17,426 seconds, which is almost 5 hours. Both the vessels were swapped two times, which was expected due to the pre-processing of the vessels with the given energy consumption.

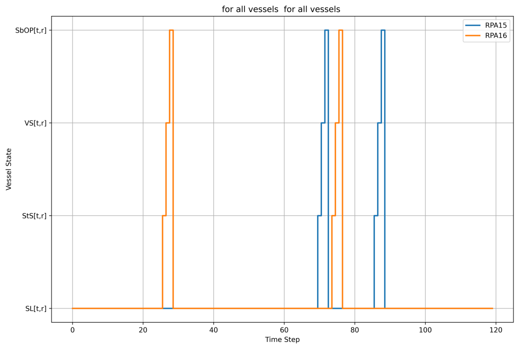

Figure 6.4: Swapping state RPA vessels for case study 1

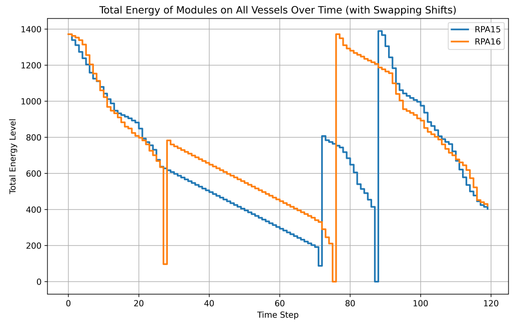

Figure 6.5: Power level RPA vessels Case Study 1

Looking at the charging (Figure 6.6 and inventory area (Figure 6.7), the correct swapping areas s are used. The vessels are swapping in swapping zone 2 and 3.

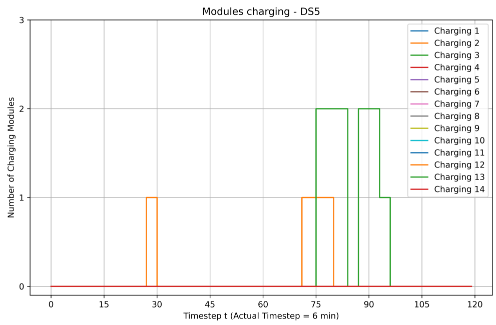

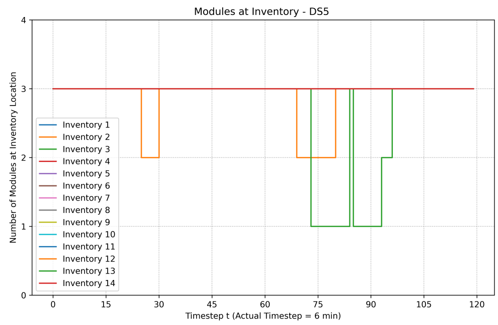

Figure 6.6: Charging area Case Study 1

Figure 6.7: Inventory area Case Study 1

For this case study, again, the modules in the system are not efficiently used. There is still a low percentage of the time the modules are used in the swapping area. For the areas where both vessels are not sailing, this is straightforward. However, the zones where the vessels are located are used relatively less. This can be seen in Figure 6.8.

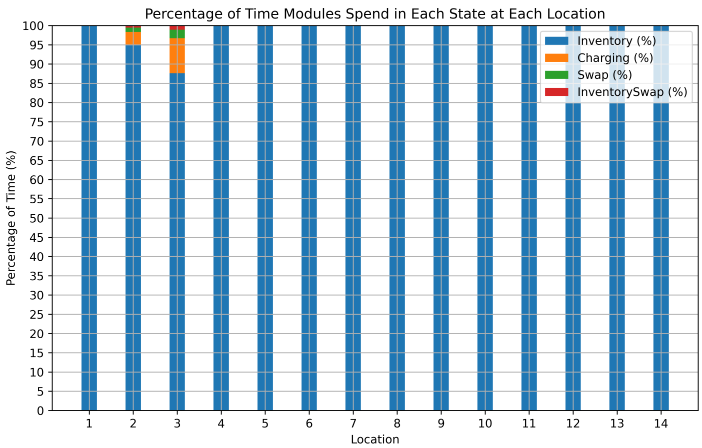

Figure 6.8: Percentage of modules for each location in different swapping stations s for RPA10

6.2. Case study 2: Three RPA vessels

For the second case study, one addition vessel (RPA7) is added to the optimisation model, which will result in more computational time. However, this case study suggests that the efficiency of the modules can be increased for the modules in the swapping section. Due to this expected increased computational time, the optimisation is ran for the same timesteps. Therefore, the model has an actual timestep of 6 minutes, where 120 timesteps were used for the optimisation model. The RPA7, RPA15 and RPA16 locations can be seen in the following figure, Figure 6.9.

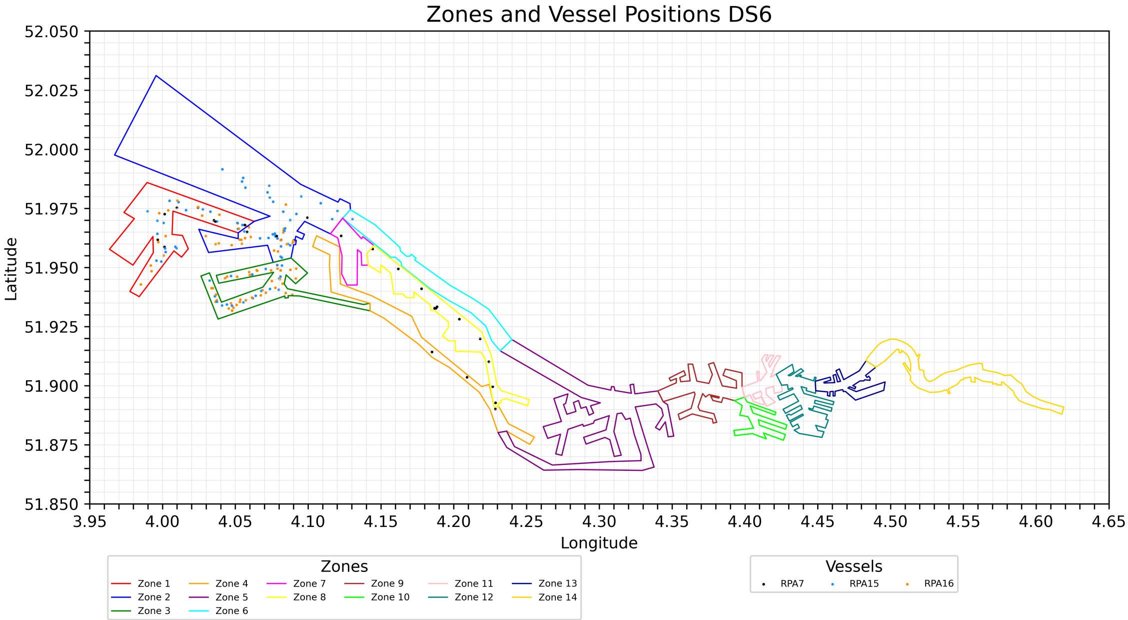

Figure 6.9: RPA locations for Case Study 1 (timestep = 6)

The sailed distance for all the vessels can be seen in Figure 6.10. The RPA7 is also at the Pistoolhaven, as are the RPA15 and RPA16. The RPA7 sails less compared to the RPA15 and the RPA16 for these timesteps, approximately two hours, between steps 80-90 and 110-120. RPA7 has a power consumption of 2,113 kWh, the RPA15 2,717 kWh and RPA16 2,443 kWh, where it is expected that the RPA15 and RPA16 should swap at least two times and the RPA7 at least once. Since the vessels also consume energy when stationary, these values are high when not used, especially for the RPA7. This can be seen in Figure 6.11.

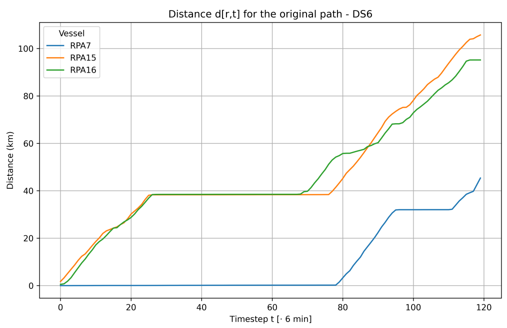

Figure 6.10: Cumulative distance for Case Study 2

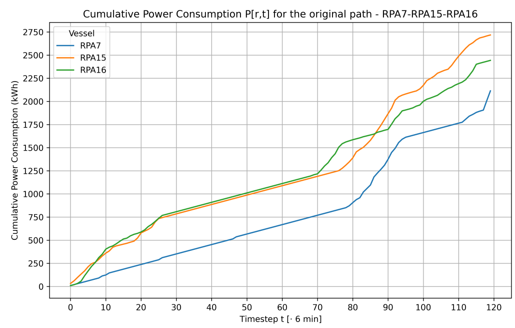

Figure 6.11: Cumulative power consumption for Case Study 2

The actual results for the swapping for all three RPA vessels can be seen in Figure 6.12. The optimisation ran for 340,390 seconds, which is almost 4 days. This is a significant increase in computational time compared to the first case study, which ran for nearly 5 hours. There could be several reasons, such as a specific solution that is hard to converge with the actual value in Gurobi. There are just more possibilities to swap with different vessels where the actual swapping of a vessel has an impact on the rest of the model. The energy level of each RPa vessel can be seen in Figure 6.13.

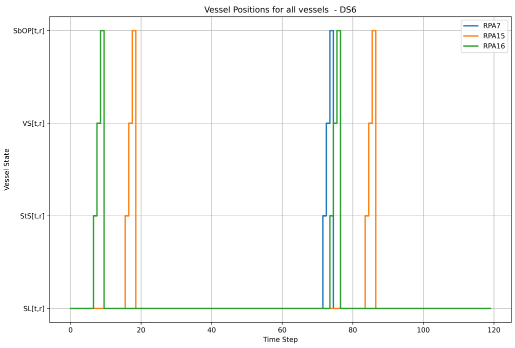

Figure 6.12: Vessel state RPA vessels Case Study 2

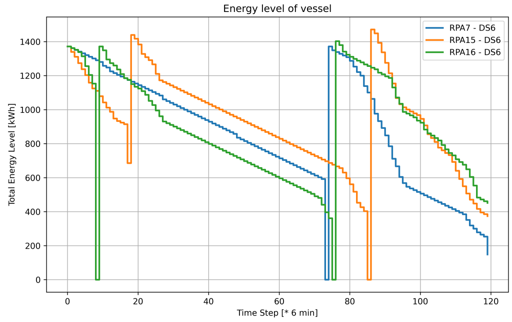

Figure 6.13: Power level RPA vessels Case Study 2

In the following two figures, the modules m in the charging area (Figure 6.14) and the modules m in the inventory (Figure 6.15) can be seen. As can be seen, the modules are only swapping in two zones, zone 2 and zone 3. When looking at the swapping behaviour, it can be concluded that the time in the zones will affect this swapping. For example, the RPA7 sailing in zone 7 (Figure 6.9) has only one step before the vessel moves to the next zone. Thus, the timesteps do have an impact on the place of swapping, especially when the time to go to the swapping station $DT_{StS_{t,r}}$ and the time to go back to the original path $DT_{SbOP_{t,r}}$ will take longer which is the case if RPA7 is swapping in zone 7.

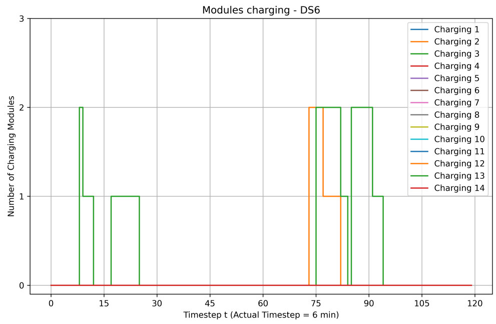

Figure 6.14: Charging area Case Study 2

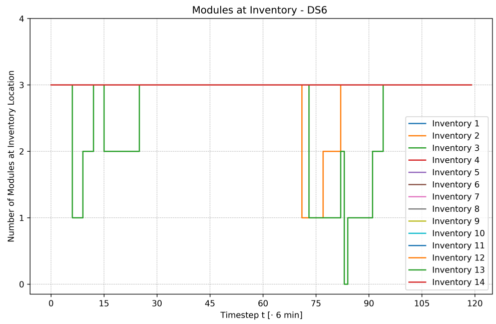

Figure 6.15: Inventory area Case Study 2

For this specific case, it can be seen that the modules are slightly more efficient, but there is also an extra vessel. Therefore, this the usage of modules is still inefficent.

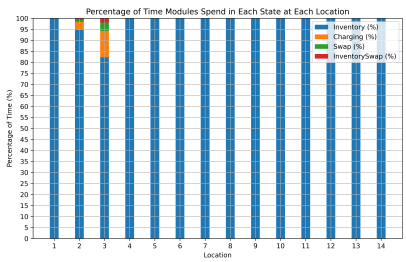

Figure 6.16: Percentage of modules for each location in different swapping stations s for RPA10

6.3. Conclusion

The conclusion of these studies were that the number of swaps was in line with the expectations of each case. However, no optimal usage of modules was seen. The reason for this, was that a vessel takes multiple hours to deplete an energy module, while the swapping of an module was in minutes which resulted in an inefficient usage of modules in the system. Adding more vessels to the system would result in more efficient usage of modules. However, the optimisation model needs significant more computational if more vessels are added to the system. An other conclusion from the case study, was that there too many swapping stations in the model for the used configuration. Despite constraints that exclude zones from being considered (if $RinZ_{t,r,s} = 0$), this is most likely not enough. In the following research, it may be better to shrink the zones or apply less zones across the entire harbour, which could potentially increase the computational time. At last, the decision was made to have three energy modules at each swapping station.

7 Conclusion & Discussion

7.1. Conclusion

For this thesis, a study is performed to model an optimisation model capable of tracking energy modules m and vessels r. First, there was literature research on the implementation of such a system for both the technical and the operational issues. Followed by a mathematical model, implementing the actual optimisation model in Python (Gurbobi). Finally, verification and validation were performed to check whether the mathematical model and, thus, the optimisation model could optimise where it was built. In this chapter, the main research question is answered which is:

What is the optimal configuration (number of energy modules, swapping stations and charging stations) for the swapping concept for patrol and incident-response vessels (RPAs) in the Port of Rotterdam?

The optimisation model successfully tracks the module and vessel level with different vessels r and (decentralised) swapping areas s (swapping and charging stations). The mathematical model is verified and validated with the Port of Rotterdam input data. It is concluded that it is possible (with the provided data) to swap energy modules for the RPA vessels if those conventional RPA vessels are equipped with energy modules. However, the optimisation took extensive time to solve when more data input was applied. This was because of the ratio of the actual time considered in the optimisation and the total time a swap took place. Therefore, an actual answer to a specific configuration cannot be found within this thesis. However, the optimisation model is successful in minimising the total swapping time.

Due to this increasing computation time, it was difficult to determine the sensitivity of the input parameters and the variables. Thus, this has not been researched in detail because of the time available for this thesis. For example, the combination of the number of energy modules at the swapping stations and the charging speed impacts the overall efficiency of modules in comparison with the actual swapping of vessels. What can be said with certainty is that too many swapping stations are included in this research. In all the validation tests, it can be seen that modules were not efficiently used. Based on this, there can be fewer swapping/charging stations and thus swapping areas in the model. If there are fewer swapping stations, it cannot be stated that this also means decreased computational time. Less swapping areas will increase vessels' visits to each swapping station. This could result in bottlenecks. Furthermore, applying fewer zones will affect the pre-processing but can be adjusted (with the pre-processing and automatic scripts for Python and Excel). However, this sensitivity has not been researched.

7.2. Discussion

Since this thesis is based on early research for the optimisation of specific vessels, the discussion chapter is used to look back and discuss the thesis. After concluding that the optimisation model is working for the designed purpose, but the main research question could not be answered fully, an discussion is needed.

In the literature review, the conclusion was made that for this specific case for the Port of Rotterdam, the application of batteries was the most promising and that Li-Ion batteries were the best possible storage medium for the new RPA vessels. Since the conventional RPA vessels will be replaced in the future, which will take multiple years from now on, there could be a shift in the specific storage medium for the application of energy modules. For this thesis, an actual choice of the storage medium is not needed since the optimisation model only needs a certain energy consumption input. As well, the charging speed, the depth of charge, and certain safety limits (SF_{min} and SF_{max}) should be known. The main discussion part is that the application of a storage medium is case-dependent and that, in future research, this can be easily adjusted because of the generic optimisation model.

Furthermore, the Battery Swapping Method (BSM) was discussed (based on batteries). The implication of this method was discussed for specific markets, with an example of a case where it is applied to the maritime industry but not for vessels with a response task, meaning that for this type of vessel, this swapping mechanism is not yet used. This thesis assumes that the (physical) swapping mechanism is working, meaning that this is implemented correctly for the RPA vessel. However, this is not the case at the moment since the conventional RPA vessels are not sailing with energy modules, and even more, those vessels have no system onboard to load these modules. This means that the parameters used in this thesis for swapping modules are purely based on theoretical methods to use the energy modules on vessels. Companies like ZES-Pack and Shifter are working on these types of systems, but neither of them used these systems for vessels with 24/7 response tasks. On the other hand, if there is an actual indication that it is possible to apply these types of (different) swapping mechanisms, it can be used to test this for each specific case with the optimisation model.

For the optimisation model, the charging of modules is also incorporated. As discussed in the literature, there are different strategies to optimise the charging so that the energy modules will last as long as possible. However, the basic charging structure is only applied in this optimisation model. The model does take into account the depth of charge, with the safety level, but does not apply specific charging strategies such as the First in, First out (FIFO) principle or the keeping track of the State of Health (SOH) of energy modules. This means that an energy module is not ranked into a state, where energy modules are not used if those energy modules are below a specific value. Since the maximum time an energy module is used for the validation chapter is, at most, 24 hours this will not affect this. However, when longer runs are considered, this should be incorporated.

One important yet critical assumption is that the electricity grid can handle the increased energy demand. For this thesis, it is assumed that this increased energy demand can be met. In the Port of Rotterdam, and also in general, there is an increase in energy demand due to the energy transition, where energy congestion could occur. In this thesis, 14 different swapping locations are introduced, and each of those swapping stations should be connected to the energy grid with this increased energy demand. Again, this fleet renewal will cost multiple years, and the energy demand could potentially have been increased in the coming years. Therefore, it is hard to say if this energy demand can be met, and therefore, for this thesis, this will be assumed to be working.

As discussed in this thesis, the vessels on which this thesis is based are conventional RPA vessels with conventional energy consumptions. Since there are no newly built RPA vessels or at least concrete plans for the actual design, the question is whether the power consumption can be more accurate. Therefore, conventional RPA vessels and their power consumption (without having actual energy modules installed on the vessel) were used as a starting point to look at the operational profiles of the RPA vessels in the Port of Rotterdam. Another assumption was that newly built vessels would probably have a more energy-efficient design, which should justify the decision to use the conventional vessels since those vessels had actual sailing profiles. However, this new design will affect, for example, what type of swapping method can be used or the actual power consumption. Since this design parallels this master thesis, it was essential that those changes could be incorporated into the actual optimisation model if this information is available.

Another input parameter is the zone where a vessel r is sailing in ($RinZ_{t,r,s}$), which depends on the choice of total swapping stations s in the Port of Rotterdam. The number of swapping stations will also define the number of zones a vessel r can sail in. This constant input parameter of the swapping stations s will impact the total optimisation model for different input parameters, such as the time it takes a vessel r to go to ($DT_{StS_{t,r}}$) or return from ($DT_{SbOP_{t,r}}$) a swapping station which are calculated in the pre-processing. If the number of zones are reduced, this will result in more vessels in the same zone s. Since the vessels have a limit for those sailing times, possiblity of swapping is affected ($SPos_{t,r} = 0$).

For the pre-processing, the zones are based on possible locations. As can be read in the conclusion, there are too many swapping stations compared to the number of vessels in this optimisation model, which results in a less efficient usage of the energy modules. This is a discussion point since this parameter will heavily impact the optimisation model and computational time. Again, the Port of Rotterdam is at the start of its fleet renewal. Therefore, the choice of swapping station locations is difficult. However, the locations of the swapping stations can be changed, including the range of the zones, if more data is available. On the other hand, applying fewer swapping stations will introduce more traffic in zones, which can also increase the computational time of the optimisation model. So, this relation is not as straightforward as it might seem, and more research is needed for the exact locations of the swapping stations.

Looking at the actual optimisation model, this should be discussed as well. First, the timestep is discussed for the optimisation model, where an increase in the number of timesteps will result in an increased computational time in general. On the other hand, decreasing the timesteps will reduce the computational time, but since this is not linear, it is hard to say what the actual impact is. This relation was reported, but could not be tested. On the other hand, when applying larger timesteps (fewer timesteps in the model), this decreased accuracy.

Since there was an increase in computation time, it was chosen to maximise the timestep used (six minutes), which significantly reduced the computational time but impacted the accuracy of the model. For a working model, each module location must be visited at least once timestep t before going to the following location. If the time is increased, a module could be longer in a specific location than necessary. A way to get insights was to have an output displaying the actual time, which could be compared to the values of the used timestep in the optimisation model. Furthermore, this increase in time also impacts the constraints of the mathematical model. For example, the vessel consumes more power to and from the swapping station since there is a larger timestep.

Zooming into the charging area, there are also discussion points for the optimisation model. The charging of modules is working because the energy modules will charge until the actual capacity, to have a correct state, of the energy module is (at least) higher than SF_{max}. But in reality, SF_{max} should be the maximum due to degradation and the state of health of energy modules. This is not implemented because the way the model works now would result in the infeasibility of the optimisation model. For example, if an energy module is charged for 79%, it cannot go to the Inventory $In_{t,m,s}$ but cannot go to the charging area. In this optimisation mode, the first time t the module m is above this value, it will move on to the Inventory $In_{t,m,s}$. Since the charging speed is a constant value, it should be allowed to go slightly above this value or below, with the maximum bound of the energy modules in place. An extra measurement could be to lower the SF_{max} by changing this parameter in the Gurobi model, but that should be case-dependent.

In the optimisation, settings are incorporated to tweak the way Gurboi handles the optimisation. These settings can be changed, such as the cutting planes, the heuristics, the optimality gap, or the specific method applied for optimisation. Since the computational time of the model was substantial, it was challenging to research the effect of changing these parameters. This can potentially decrease the computational time, but it was hard to research due to the significant computational time it could not be researched in detail.

7.3. Future Research

Based on the conclusion and the discussion, more research can be applied. This sub chapter will describe this.

7.3.1. Vessels

First, the future research for the vessels is discussed. For the vessels, the energy consumption is critical since the power consumption is directly related to the optimisation model; the better the power consumption is estimated, the better the optimisation model can optimise the problem. In this thesis, the energy consumption is based on the RPA10, RPA13 and RPA16, with an average for all the vessels considered. This is done with sensors to relate the given engine load to the speed of the vessel, which is explained in CH4. Since the vessels are all different and have different designs and thus resistance, as described in the discussion, this should be researched further to better estimate the energy consumption for each vessel r. The RPA vessels will be replaced in the future, impacting the actual design and, therefore, the energy consumption. At this moment, an overestimation can result in swapping more than needed, or worse, an underestimation would result in less swapping. The latter is most likely not the problem within this thesis. In conclusion, the power estimation can be better estimated if the new design of the RPA vessels is known and should be researched.

Moreover, the power consumption estimation is based on conventional propulsion power in this thesis. Since there is a difference in power consumption between conventional and electrically driven vessels, this can be researched in the future. An option is to look at the RPA8, a hybrid vessel. This can help get insights into the electrification process and, thus, the energy consumption. This hybridisation does not involve energy modules with a swapping method. However, this might be useful and result in a better prediction of energt usage for the vessels.

Besides the vessel's energy consumption, the RPA vessels' operational time is essential since this is the main objective of the thesis. When the RPA vessels are doing these tasks, the vessels should not initiate a swap or being in the swapping process. The problem is that, at this moment, this data cannot be retrieved. Therefore, an estimation is performed when the AIS data shows that a specific RPA vessel is stationary outside the main harbour for more than two executive time steps. As described in the discussion, the timesteps impact this estimation. Doing more research will better predict whether a vessel should swap or not if a vessel is doing tasks, which will result in a more accurate swapping sequence.

7.3.2. Swapping Stations

In this thesis, 14 different potential swapping locations are proposed. However, as explained in CH4.3 and the discussion (CH7.2, the actual choice of the swapping station is more nuanced. The location of the swapping station should be available; the electricity grid should be present; permits should be arranged, etc. Since the place of these swapping stations impacts the results, future research should be performed to have a more detailed plan for locating these swapping stations.

Also, the swapping stations now have one swapping possibility for each time t for a maximum of EM_M modules for a particular vessel r. When this is expanded further, this will affect the mathematical model but will allow swapping with more vessels at the same time. This has not yet been implemented in the optimisation model, but it would be interesting to see if there are more vessels in the optimisation model.

7.3.3. Charging Stations

In the literature review, charging stations and strategies for these charging stations were discussed (CH2.4). This thesis does not consider charging strategies (except for applying a specific range for maximum depletion and an upper bound). However, these charging strategies are essential when energy modules m are used for a more extended period of time. This will reduce battery degradation, and if energy modules are no longer used, the State of Health (SOH) will be more important and should be considered. Since this thesis is only considered, at most, 24 hours, this is unnecessary but should be incorporated when doing longer runs.

Looking at the charging stations, there should be enough electricity available. When a swapping mechanism is introduced, this can significantly impact the electric grid. Some studies suggest using smart grids, where ESS can charge when electricity demands are low. This can also be combined with already built facilities, and looking at this from a "smart" perspective can create a solution. This problem is complex and, therefore, not studied in this thesis. However, this should be researched when planning to apply the swapping method.

7.3.4. Inventory area

In this thesis, the inventory has a dedicated area for the actual inventory ($In_{t,m,s}$) and an area where the modules m are kept for swapping if a swap is initiated by a particular vessel r. For this InventorySwap area, there is no specific order in which module m is used first. Again, with a maximal estimation model time of 24 hours, this will not affect the energy module states. But, if longer, more extended periods are used, it should be incorporated.

7.3.5. Optimisation model

The optimisation model consists of various options, but this can be expanded even further. In a way, this will impact the working way of the optimisation model. For example, the model can be integrated with the internal programming environment to have an update on the vessels. This will update the model as much as possible. Also, a sequence can be introduced so that a particular day is calculated. After this day, the settings are saved (which module m is at the vessel, how many modules m are at a specific charging station ($Ch_{t,m,s}$), Inventory area ($In_{t,m,s}$) or an InventorySwap are ($InS_{t,m,s}$). To break down the optimisation model. This could be an option since the vessel are sailing in time shifts.

In this thesis, there are different variables. With the verification and validation, those variables are checked and researched. However, due to large computational times, the variables' actual dependency could not be researched in detail. In future research, a detailed sensitivity analysis can be performed. In this way, the exact choice of certain variables can be more thorough.

For this research, the operational time was the objective. This was chosen since this would be the basis to actually see if this method could be applied. However, the costs of battery swapping stations and the modules can also be an objective to minimise expenses. Since the optimisation model consists of the locations of the swapping stations, the number of modules, the charging rates, and so on, this can be coupled with an actual price. In this way, the system can be optimised from the perspective of the energy module supplier. In most cases, this is a pay-to-use construction, which means that these optimisations are more interesting for supplies of the energy modules and the system itself. This is not implemented, but could be researched in the future.

References

[1] Port of Rotterdam, *The port that will take you ahead*. [Online]. Available: https://www.portofrotterdam.com/en/why-rotterdam/port-will-take-you-ahead.

[2] European Commission, *European Climate Law*. [Online]. Available: https://climate.ec.europa.eu/eu-action/european-climate-law_en#.

[3] European Environment Agency, *EEA greenhouse gases — data viewer*. [Online]. Available: https://www.eea.europa.eu/data-and-maps/data/data-viewers/greenhouse-gases-viewer.

[4] European Environmental Agency, *Transport and mobility*. [Online]. Available: https://www.eea.europa.eu/en/topics/in-depth/transport-and-mobility#.

[5] European Environmental Agency, *High time to shift gear in transport sector*. [Online]. Available: https://www.eea.europa.eu/signals-archived/signals-2022/articles/high-time-to-shift-gear.

[6] European Commission, *Reducing emissions from the shipping sector*. [Online]. Available: https://climate.ec.europa.eu/eu-action/transport/reducing-emissions-shipping-sector_en.

[7] European Environmental Agency and European Maritime Safety Agency, "European Maritime Transport Environmental Report 2021," European Environmental Agency, Luxembourgh, Tech. Rep., 2021. [Online]. Available: https://www.eea.europa.eu/publications/maritime-transport.

[8] M. Z. Jacobson, M. A. Delucchi, Z. A. Bauer, *et al.*, "100% Clean and Renewable Wind, Water, and Sunlight All-Sector Energy Roadmaps for 139 Countries of the World," *Joule*, vol. 1, no. 1, pp. 108–121, Sep. 2017, ISSN: 25424351. DOI: 10.1016/j.joule.2017.07.005. [Online]. Available: http://www.cell.com/article/S2542435117300120/fulltext%20http://www.cell.com/article/S2542435117300120/abstract%20https://www.cell.com/joule/abstract/S2542-4351(17)30012-0.

[9] Port of Amsterdam, *Sustainable port*. [Online]. Available: https://www.portofamsterdam.com/en/discover/sustainable-port.

[10] Port of Antwerp-Bruges, *Sustainability and SDGs*. [Online]. Available: https://www.portofantwerpbruges.com/en/sustainability-and-sdgs.

[11] Port of Rotterdam, *Sustainable Port*. [Online]. Available: https://www.portofrotterdam.com/en/building-port/sustainable-port.

[12] Eurostat, *Rotterdam: the largest freight port in the EU*. [Online]. Available: https://ec.europa.eu/eurostat/web/products-eurostat-news/-/ddn-20200402-2.

[13] *Havenbedrijf Rotterdam versnelt reductie eigen CO2-uitstoot - Duurzaam Ondernemen*. [Online]. Available: https://www.duurzaam-ondernemen.nl/havenbedrijf-rotterdam-versnelt-reductie-eigen-co2-uitstoot/.

[14] *"Onze haven moet een veilige haven zijn" - Onze Haven*. [Online]. Available: https://onzehaven.nl/2019/09/09/onze-haven-moet-een-veilige-haven-zijn/.

[15] W. Jie, J. Yang, M. Zhang, and Y. Huang, "The two-echelon capacitated electric vehicle routing problem with battery swapping stations: Formulation and efficient methodology," *European Journal of Operational Research*, vol. 272, pp. 879–904, 2019. DOI: 10.1016/j.ejor.2018.07.002. [Online]. Available: https://doi.org/10.1016/j.ejor.2018.07.002.

[16] X. Zhang, L. Peng, Y. Cao, S. Liu, H. Zhou, and K. Huang, "Towards holistic charging management for urban electric taxi via a hybrid deployment of battery charging and swap stations," *Renewable Energy*, 2020. DOI: 10.1016/j.renene.2020.03.093. [Online]. Available: https://doi.org/10.1016/j.renene.2020.03.093.

[17] J. Bischoff and M. Maciejewski, “Electric taxis in Berlin – analysis of the feasibility of a large-scale transition,” in *Communications in Computer and Information Science*, vol. 531, 2015. DOI: 10.1007/978-3-319-24577-5{_}34.

[18] A. E. Torkayesh and M. Deveci, “A mulTi-noRmalization mUlti-distance aSsessmenT (TRUST) approach for locating a battery swapping station for electric scooters,” *Sustainable Cities and Society*, 2021. DOI: 10.1016/j.scs.2021.103243. [Online]. Available: https://doi.org/10.1016/j.scs.2021.103243.

[19] L. Li, Y. Li, R. Liu, Y. Zhou, and E. Pan, “A Two-stage Stochastic Programming for AGV scheduling with random tasks and battery swapping in automated container terminals,” *Transportation Research Part E*, vol. 174, p. 103 110, 2023. DOI: 10.1016/j.tre.2023.103110. [Online]. Available: https://doi.org/10.1016/j.tre.2023.103110.

[20] Y. Zhang, L. Sun, T. Fan, F. Ma, and Y. Xiong, “Speed and energy optimization method for the inland all-electric ship in battery-swapping mode,” *Ocean Engineering*, 2023. DOI: 10.1016/j.oceaneng.2023.115234. [Online]. Available: https://doi.org/10.1016/j.oceaneng.2023.115234.

[21] ZES, *Emissieloos varen met Zero Emission Services voor de binnenvaart*. [Online]. Available: https://zeroemissionservices.nl/en/homepage/.

[22] SHIFTR, *SHIFTR is an autonomous battery swap solution which enables seamless, zero-emission express boat operation*, 2024. [Online]. Available: https://shiftr.no/.

[23] G. J. May, A. Davidson, and B. Monahov, “Lead batteries for utility energy storage: A review,” *Journal of Energy Storage*, Nov. 2017. DOI: 10.1016/j.est.2017.11.008. [Online]. Available: https://doi.org/10.1016/j.est.2017.11.008.

[24] P. D. Lund, J. Lindgren, J. Mikkola, and J. Salpakari, “Review of energy system flexibility measures to enable high levels of variable renewable electricity,” *Renewable and Sustainable Energy Reviews*, 2015. DOI: 10.1016/j.rser.2015.01.057. [Online]. Available: http://dx.doi.org/10.1016/j.rser.2015.01.057.

[25] X. Luo, J. Wang, M. Dooner, and J. Clarke, “Overview of current development in electrical energy storage technologies and the application potential in power system operation,” *Applied Energy*, vol. 137, pp. 511–536, Jan. 2015, ISSN: 0306-2619. DOI: 10.1016/J.APENERGY.2014.09.081.

[26] I. Staffell, D. Scamman, A. V. Abad, *et al.*, “The role of hydrogen and fuel cells in the global energy system,” *Energy Environ. Sci*, vol. 12, p. 463, 2019. DOI: 10.1039/c8ee01157e.

[27] M. Aziz, “Liquid Hydrogen: A Review on Liquefaction, Storage, Transportation, and Safety,” *Energies 2021, Vol. 14, Page 5917*, vol. 14, no. 18, p. 5917, Sep. 2021, ISSN: 1996-1073. DOI: 10.3390/EN14185917. [Online]. Available: https://www.mdpi.com/1996-1073/14/18/5917/htm%20https://www.mdpi.com/1996-1073/14/18/5917.

[28] K. Mazloomi and C. Gomes, “Hydrogen as an energy carrier: Prospects and challenges,” *Renewable and Sustainable Energy Reviews*, vol. 16, pp. 3024–3033, 2012. DOI: 10.1016/j.rser.2012.02.028.

[29] S. Atilhan, S. Park, M. M. El-Halwagi, M. Atilhan, M. Moore, and R. B. Nielsen, “Green hydrogen as an alternative fuel for the shipping industry,” 2021. DOI: 10.1016/j.coche.2020.100668. [Online]. Available: https://doi.org/10.1016/j.coche.2020.100668.

[30] A. Ozarslan, “Large-scale hydrogen energy storage in salt caverns,” 2012. DOI: 10.1016/j.ijhydene.2012.07.111. [Online]. Available: http://dx.doi.org/10.1016/j.ijhydene.2012.07.111.

[31] J. L. Fernandez Soto, R. Garay Seijo, J. A. Fraguela Formoso, G. Gregorio Iglesias, and L. Carral Couce, “Alternative Sources of Energy in Shipping,” *The Journal of Navigation*, vol. 63, no. 3, pp. 435–448, Jul. 2010, ISSN: 1469-7785. DOI: 10.1017/S0373463310000111. [Online]. Available: https://www-cambridge-org.tudelft.idm.oclc.org/core/journals/journal-of-navigation/article/alternative-sources-of-energy-in-shipping/B2B2E50FF1113946C84F11C9F110E367.

[32] H. M. Barkholtz and D. J. Liu, "Advancements in rationally designed PGM-free fuel cell catalysts derived from metal–organic frameworks," *Materials Horizons*, vol. 4, no. 1, pp. 20–37, Jan. 2017, ISSN: 20516355. DOI: 10.1039/C6MH00344C. [Online]. Available: https://pubs-rsc-org.tudelft.idm.oclc.org/en/content/articlehtml/2017/mh/c6mh00344c%20https://pubs-rsc-org.tudelft.idm.oclc.org/en/content/articlelanding/2017/mh/c6mh00344c.

[33] C.-Y. Hsu, Y. Ajaj, G. Kamil Ghadir, *et al.*, "Rechargeable batteries for energy storage: A review," *e-Prime - Advances in Electrical Engineering, Electronics and Energy*, 2024. DOI: 10.1016/j.prime.2024.100510. [Online]. Available: https://doi.org/10.1016/j.prime.2024.100510.

[34] K. Yang, Y. Li, J. Yuan, *et al.*, "A thermal management system for an energy storage battery container based on cold air directional regulation," *Journal of Energy Storage*, vol. 61, p. 106 679, 2023. DOI: 10.1016/j.est.2023.106679. [Online]. Available: https://doi.org/10.1016/j.est.2023.106679.

[35] H. Wu, "A Survey of Battery Swapping Stations for Electric Vehicles: Operation Modes and Decision Scenarios," *IEEE Transactions on Intelligent Transportation Systems*, vol. 23, no. 8, pp. 10 163–10 185, Aug. 2022, ISSN: 15580016. DOI: 10.1109/TITS.2021.3125861.

[36] D. Qiu, Y. Ye, D. Papadaskalopoulos, and G. Strbac, "A Deep Reinforcement Learning Method for Pricing Electric Vehicles with Discrete Charging Levels," *IEEE Transactions on Industry Applications*, vol. 56, no. 5, pp. 5901–5912, Sep. 2020, ISSN: 19399367. DOI: 10.1109/TIA.2020.2984614.

[37] R. Xie, W. Wei, Q. Wu, T. Ding, and S. Mei, "Optimal Service Pricing and Charging Scheduling of an Electric Vehicle Sharing System," *IEEE Transactions on Vehicular Technology*, vol. 69, no. 1, pp. 78–89, Jan. 2020, ISSN: 19399359. DOI: 10.1109/TVT.2019.2950402.

[38] Y. Zhang, P. You, and L. Cai, "Optimal Charging Scheduling by Pricing for EV Charging Station with Dual Charging Modes," *IEEE Transactions on Intelligent Transportation Systems*, vol. 20, no. 9, pp. 3386–3396, Sep. 2019, ISSN: 15580016. DOI: 10.1109/TITS.2018.2876287.

[39] Y. Feng and X. Lu, "Construction Planning and Operation of Battery Swapping Stations for Electric Vehicles: A Literature Review," *Energies 2021, Vol. 14, Page 8202*, vol. 14, no. 24, p. 8202, Dec. 2021, ISSN: 1996-1073. DOI: 10.3390/EN14248202. [Online]. Available: https://www.mdpi.com/1996-1073/14/24/8202/htm%20https://www.mdpi.com/1996-1073/14/24/8202.

[40] A. Alsabbagh, B. Wu, and C. Ma, "Distributed Electric Vehicles Charging Management Considering Time Anxiety and Customer Behaviors," *IEEE Transactions on Industrial Informatics*, vol. 17, no. 4, pp. 2422–2431, Apr. 2021, ISSN: 19410050. DOI: 10.1109/TII.2020.3003669.

[41] G. Zhang, S. T. Tan, and G. Gary Wang, "Real-Time Smart Charging of Electric Vehicles for Demand Charge Reduction at Non-Residential Sites," *IEEE Transactions on Smart Grid*, vol. 9, no. 5, pp. 4027–4037, Sep. 2018, ISSN: 19493053. DOI: 10.1109/TSG.2016.2647620.

[42] Z. Wei, Y. Li, and L. Cai, "Electric vehicle charging scheme for a park-and-charge system considering battery degradation costs," *IEEE Transactions on Intelligent Vehicles*, vol. 3, no. 3, pp. 361–373, Sep. 2018, ISSN: 23798858. DOI: 10.1109/TIV.2018.2843126.

[43] H. Wang, G. Zhou, R. Xue, Y. Lu, and J. A. McCann, "A Driving-Behavior-Based SoC Prediction Method for Light Urban Vehicles Powered by Supercapacitors," *IEEE Transactions on Intelligent Transportation Systems*, vol. 21, no. 5, pp. 2090–2099, May 2020, ISSN: 15580016. DOI: 10.1109/TITS.2019.2912501.

[44] Y. Xiong, J. Gan, B. An, C. Miao, and A. L. Bazzan, "Optimal electric vehicle fast charging station placement based on game theoretical framework," *IEEE Transactions on Intelligent Transportation Systems*, vol. 19, no. 8, pp. 2493–2504, Aug. 2018, ISSN: 15249050. DOI: 10.1109/TITS.2017.2754382.

[45] W. Infante and J. Ma, "Coordinated Management and Ratio Assessment of Electric Vehicle Charging Facilities," *IEEE Transactions on Industry Applications*, vol. 56, no. 5, pp. 5955–5962, Sep. 2020, ISSN: 19399367. DOI: 10.1109/TIA.2020.2987773.

[46] S. Nski, R. D. Pace, A. Coppola, J. Leijon, and C. Boström, "Charging Electric Vehicles Today and in the Future," *World Electric Vehicle Journal 2022, Vol. 13, Page 139*, vol. 13, no. 8, p. 139, Jul. 2022, ISSN: 2032-6653. DOI: 10.3390/WEVJ13080139. [Online]. Available: https://www.mdpi.com/2032-6653/13/8/139/htm%20https://www.mdpi.com/2032-6653/13/8/139.

[47] Cambridge Dictionary, *Cambridge Dictionary - Range anxiety*. [Online]. Available: https://dictionary.cambridge.org/dictionary/english/range-anxiety.

[48] L. Noel, G. Zarazua de Rubens, B. K. Sovacool, and J. Kester, "Fear and loathing of electric vehicles: The reactionary rhetoric of range anxiety," *Energy Research & Social Science*, vol. 48, pp. 96–107, Feb. 2019, ISSN: 2214-6296. DOI: 10.1016/J.ERSS.2018.10.001.

[49] H. Wu, G. Kwok-Hung Pang, K. Lun Choy, and H. Yan Lam, "A charging-scheme decision model for electric vehicle battery swapping station using varied population evolutionary algorithms," *Applied Soft Computing*, vol. 61, pp. 905–920, 2017. DOI: 10.1016/j.asoc.2017.09.008. [Online]. Available: http://dx.doi.org/10.1016/j.asoc.2017.09.008.

[50] H. Wu, G. K. H. Pang, K. L. Choy, and H. Y. Lam, "An Optimization Model for Electric Vehicle Battery Charging at a Battery Swapping Station," *IEEE Transactions on Vehicular Technology*, vol. 67, no. 2, pp. 881–895, Feb. 2018, ISSN: 00189545. DOI: 10.1109/TVT.2017.2758404.

[51] S. Schmidt, "Use of battery swapping for improving environmental balance and price-performance ratio of electric vehicles," 2021. DOI: 10.1016/j.etran.2021.100128. [Online]. Available: https://doi.org/10.1016/j.etran.2021.100128.

[52] F. Adegbohun, A. von Jouanne, and K. Y. Lee, "Autonomous Battery Swapping System and Methodologies of Electric Vehicles," *Energies 2019, Vol. 12, Page 667*, vol. 12, no. 4, p. 667, Feb. 2019, ISSN: 1996-1073. DOI: 10.3390/EN12040667. [Online]. Available: https://www.mdpi.com/1996-1073/12/4/667/htm%20https://www.mdpi.com/1996-1073/12/4/667.

[53] W. Zhan, Z. Wang, L. Zhang, P. Liu, D. Cui, and D. G. Dorrell, "A review of siting, sizing, optimal scheduling, and cost-benefit analysis for battery swapping stations," *Energy*, 2022. DOI: 10.1016/j.energy.2022.124723. [Online]. Available: https://doi.org/10.1016/j.energy.2022.124723.

[54] Y. Gao, J. Yang, M. Yang, and Z. Li, "Deep Reinforcement Learning Based Optimal Schedule for a Battery Swapping Station Considering Uncertainties," *IEEE Transactions on Industry Applications*, vol. 56, no. 5, pp. 5775–5784, Sep. 2020, ISSN: 19399367. DOI: 10.1109/TIA.2020.2986412.

[55] T. H. Wu, G. K. Pang, K. L. Choy, and H. Y. Lam, "An optimization model for a battery swapping station in Hong Kong," *2015 IEEE Transportation Electrification Conference and Expo, ITEC 2015*, Jul. 2015. DOI: 10.1109/ITEC.2015.7165769.

[56] "Swappable Container Waterborne Transport Battery," European Union's Horizon 2020, Tech. Rep., 2021. [Online]. Available: https://cordis.europa.eu/project/id/963603.

[57] *How a battery works*. [Online]. Available: https://www.science.org.au/curious/technology-future/batteries#.

[58] S. Muslimin, Z. Nawawi, B. Y. Suprapto, and T. Dewi, "Comparison of Batteries Used in Electrical Vehicles," *Proceedings of the 5th FIRST T1 T2 2021 International Conference (FIRST-T1-T2 2021)*, vol. 9, pp. 421–425, Feb. 2022, ISSN: 2589-4943. DOI: 10.2991/AHE.K.220205.074. [Online]. Available: https://www.atlantis-press.com/proceedings/first-t1-t2-21/125970344.

[59] W. Arsadiando, M. Jopri, S. Tole, *et al.*, "Comprehensive Analysis of Current Research Trends in Battery Technologies as Electricity Storage Devices for Electric Bikes: A Review," *Article in Journal of Electrical and Electronics Engineering*, vol. 15, no. 2, 2022. [Online]. Available: https://www.researchgate.net/publication/376810202.

[60] P. Asef, M. Milan, A. Lapthorn, and S. Padmanaban, "Future Trends and Aging Analysis of Battery Energy Storage Systems for Electric Vehicles," *Sustainability 2021, Vol. 13, Page 13779*, vol. 13, no. 24, p. 13 779, Dec. 2021, ISSN: 2071-1050. DOI: 10.3390/SU132413779. [Online]. Available: https://www.mdpi.com/2071-1050/13/24/13779/htm%20https://www.mdpi.com/2071-1050/13/24/13779.

[61] Y. Zhang, C.-G. Zhou, J. Yang, *et al.*, "Advances and challenges in improvement of the electrochemical performance for lead-acid batteries: A comprehensive review," *Journal of Power Sources*, vol. 520, p. 230 800, 2022. DOI: 10.1016/j.jpowsour.2021.230800. [Online]. Available: https://doi.org/10.1016/j.jpowsour.2021.230800.

[62] G. Albright Jake Edie Said Al-Hallaj, “A Comparison of Lead Acid to Lithium-ion in Stationary Storage Applications Published by AllCell Technologies LLC,” 2012.

[63] A. Poullikkas, “A comparative overview of large-scale battery systems for electricity storage,” 2013. DOI: 10.1016/j.rser.2013.07.017. [Online]. Available: http://dx.doi.org/10.1016/j.rser.2013.07.017.

[64] K. Varshney, P. K. Varshney, K. Gautam, M. Tanwar, and M. Chaudhary, “Current trends and future perspectives in the recycling of spent lead acid batteries in India,” *Materials Today: Proceedings*, 2019. DOI: 10.1016/j.matpr.2019.12.168. [Online]. Available: https://doi.org/10.1016/j.matpr.2019.12.168.

[65] P. Bernard and M. Lippert, “NickeleCadmium and NickeleMetal Hydride Battery Energy Storage,” DOI: 10.1016/B978-0-444-62616-5.00014-0. [Online]. Available: http://dx.doi.org/10.1016/B978-0-444-62616-5.00014-0.

[66] J. Jaguemont, L. Boulon, and Y. Dubé, “A comprehensive review of lithium-ion batteries used in hybrid and electric vehicles at cold temperatures,” 2015. DOI: 10.1016/j.apenergy.2015.11.034. [Online]. Available: http://dx.doi.org/10.1016/j.apenergy.2015.11.034.

[67] A. A. Kebede, T. Kalogiannis, J. Van Mierlo, and M. Berecibar, “A comprehensive review of stationary energy storage devices for large scale renewable energy sources grid integration,” 2022. DOI: 10.1016/j.rser.2022.112213. [Online]. Available: https://doi.org/10.1016/j.rser.2022.112213.

[68] H. Chen, T. N. Cong, W. Yang, C. Tan, Y. Li, and Y. Ding, “Progress in electrical energy storage system: A critical review,” *Progress in Natural Science*, vol. 19, no. 3, pp. 291–312, Mar. 2009, ISSN: 1002-0071. DOI: 10.1016/J.PNSC.2008.07.014.

[69] F. Díaz-González, A. Sumper, O. Gomis-Bellmunt, and R. Villafáfila-Robles, “A review of energy storage technologies for wind power applications,” *Renewable and Sustainable Energy Reviews*, vol. 16, no. 4, pp. 2154–2171, May 2012, ISSN: 13640321. DOI: 10.1016/j.rser.2012.01.029. [Online]. Available: https://linkinghub.elsevier.com/retrieve/pii/S1364032112000305.

[70] M. Beaudin, H. Zareipour, A. Schellenberglabe, and W. Rosehart, “Energy storage for mitigating the variability of renewable electricity sources: An updated review,” 2010. DOI: 10.1016/j.esd.2010.09.007.

[71] F. Nadeem, S. M. Hussain, P. K. Tiwari, A. K. Goswami, and T. S. Ustun, “Comparative review of energy storage systems, their roles, and impacts on future power systems,” *IEEE Access*, vol. 7, pp. 4555–4585, 2019, ISSN: 21693536. DOI: 10.1109/ACCESS.2018.2888497.

[72] A. K. Rohit and S. Rangnekar, “An overview of energy storage and its importance in Indian renewable energy sector: Part II-energy storage applications, benefits and market potential,” 2017. DOI: 10.1016/j.est.2017.07.012. [Online]. Available: http://dx.doi.org/10.1016/j.est.2017.07.012.

[73] C. K. Das, O. Bass, G. Kothapalli, T. S. Mahmoud, and D. Habibi, “Overview of energy storage systems in distribution networks: Placement, sizing, operation, and power quality,” 2018. DOI: 10.1016/j.rser.2018.03.068. [Online]. Available: https://doi.org/10.1016/j.rser.2018.03.068.

[74] A. K. S. Maisanam, A. Biswas, and K. K. Sharma, “An innovative framework for electrical energy storage system selection for remote area electrification with renewable energy system: Case of a remote village in India,” *Journal of Renewable and Sustainable Energy*, vol. 12, no. 2, p. 24 101, Jan. 2020, ISSN: 19417012. DOI: 10.1063/1.5126690/284617. [Online]. Available: /aip/jrse/article/12/2/024101/284617/An-innovative-framework-for-electrical-energy.

[75] S. Vazquez, S. M. Lukic, E. Galvan, L. G. Franquelo, and J. M. Carrasco, “Energy storage systems for transport and grid applications,” *IEEE Transactions on Industrial Electronics*, vol. 57, no. 12, pp. 3881–3895, Dec. 2010, ISSN: 02780046. DOI: 10.1109/TIE.2010.2076414.

[76] S. Mccluer and J.-F. Christin, “Comparing Data Center Batteries, Flywheels, and Ultracapacitors Revision 2,”

[77] O. Palizban and K. Kauhaniemi, “Energy storage systems in modern grids-Matrix of technologies and applications,” 2016. DOI: 10.1016/j.est.2016.02.001. [Online]. Available: http://dx.doi.org/10.1016/j.est.2016.02.001.

[78] M. Khalid, “A Review on the Selected Applications of Battery-Supercapacitor Hybrid Energy Storage Systems for Microgrids,” *Energies 2019, Vol. 12, Page 4559*, vol. 12, no. 23, p. 4559, Nov. 2019, ISSN: 1996-1073. DOI: 10.3390/EN12234559. [Online]. Available: https://www.mdpi.com/1996-1073/12/23/4559/htm%20https://www.mdpi.com/1996-1073/12/23/4559.

[79] K. Bradbury, “Energy Storage Technology Review,” 2010.

[80] “Capacitors age and capacitors have an end of life, A white Paper,” 2005. [Online]. Available: www.liebert.com..

[81] S. B. Elghali, R. Outbib, and M. Benbouzid, “Selecting and optimal sizing of hybridized energy storage systems for tidal energy integration into power grid,” *Journal of Modern Power Systems and Clean Energy*, vol. 7, 2019. DOI: 10.1007/s40565-018-0442-0. [Online]. Available: https://doi.org/10.1007/s40565-018-0442-0.

[82] M. Aneke and M. Wang, “Energy storage technologies and real life applications-A state of the art review,” 2016. DOI: 10.1016/j.apenergy.2016.06.097. [Online]. Available: http://dx.doi.org/10.1016/j.apenergy.2016.06.097.

[83] C. Schaber, P. Mazza, and R. Hammerschlag, “Utility-Scale Storage of Renewable Energy,” *The Electricity Journal*, vol. 17, no. 6, pp. 21–29, Jul. 2004. DOI: 10.1016/j.tej.2004.05.005. [Online]. Available: www.climatesolutions.org..

[84] W. Liu, T. Placke, and K. T. Chau, “Overview of batteries and battery management for electric vehicles,” *Energy Reports*, vol. 8, pp. 4058–4084, 2022. DOI: 10.1016/j.egyr.2022.03.016. [Online]. Available: https://doi.org/10.1016/j.egyr.2022.03.016.

[85] John Fitzgerald Weaver, *Battery prices collapsing, grid-tied energy storage expanding – pv magazine USA*, 2024. [Online]. Available: https://pv-magazine-usa.com/2024/03/06/battery-prices-collapsing-grid-tied-energy-storage-expanding/.

[86] X. Yang, C. Shao, C. Zhuge, M. Sun, P. Wang, and S. Wang, “Deploying battery swap stations for shared electric vehicles using trajectory data,” 2021. DOI: 10.1016/j.trd.2021.102943. [Online]. Available: https://doi.org/10.1016/j.trd.2021.102943.

[87] R. M. Salgado, F. Danzi, J. E. Oliveira, A. El-Azab, P. P. Camanho, and M. H. Braga, “The Latest Trends in Electric Vehicles Batteries,” *Molecules 2021, Vol. 26, Page 3188*, vol. 26, no. 11, p. 3188, May 2021, ISSN: 1420-3049. DOI: 10.3390/MOLECULES26113188. [Online]. Available: https://www.mdpi.com/1420-3049/26/11/3188/htm%20https://www.mdpi.com/1420-3049/26/11/3188.

[88] N. Boaretto, I. Garbayo, S. Valiyaveettil-SobhanRaj, *et al.*, “Lithium solid-state batteries: State-of-the-art and challenges for materials, interfaces and processing,” *Journal of Power Sources*, vol. 502, p. 229 919, Aug. 2021, ISSN: 0378-7753. DOI: 10.1016/J.JPOWSOUR.2021.229919.

[89] W. D. Richards, L. J. Miara, Y. Wang, J. C. Kim, and G. Ceder, “Interface Stability in Solid-State Batteries,” *Chemistry of Materials*, vol. 28, no. 1, pp. 266–273, Jan. 2016, ISSN: 15205002. DOI: 10.1021/ACS.CHEMMATER.5B04082. [Online]. Available: https://www.asme.org/topics-resources/content/advancing-battery-technology-for-modern-innovations.

[90] D. H. S. Tan, Y. S. Meng, and J. Jang, “Scaling up high-energy-density sulfidic solid-state batteries: A lab-to-pilot perspective,” *Joule*, 2022. DOI: 10.1016/j.joule.2022.07.002. [Online]. Available: https://doi.org/10.1016/j.joule.2022.07.002.

[91] K. J. Huang, G. Ceder, and E. A. Olivetti, “Manufacturing scalability implications of materials choice in inorganic solid-state batteries,” *Joule*, vol. 5, pp. 564–580, 2021. DOI: 10.1016/j.joule.2020.12.001. [Online]. Available: https://doi.org/10.1016/j.joule.2020.12.001.

[92] J. Yang and H. Sun, “Battery swap station location-routing problem with capacitated electric vehicles,” 2014. DOI: 10.1016/j.cor.2014.07.003. [Online]. Available: http://dx.doi.org/10.1016/j.cor.2014.07.003.

[93] R. Collin, Y. Miao, A. Yokochi, P. Enjeti, and A. Von Jouanne, “Advanced Electric Vehicle Fast-Charging Technologies,” *Energies 2019, Vol. 12, Page 1839*, vol. 12, no. 10, p. 1839, May 2019, ISSN: 1996-1073. DOI: 10.3390/EN12101839. [Online]. Available: https://www.mdpi.com/1996-1073/12/10/1839/htm%20https://www.mdpi.com/1996-1073/12/10/1839.

[94] L. Timilsina, P. R. Badr, P. H. Hoang, G. Ozkan, B. Papari, and C. S. Edrington, “Battery Degradation in Electric and Hybrid Electric Vehicles: A Survey Study,” *IEEE Access*, vol. 11, pp. 42 431–42 462, 2023, ISSN: 21693536. DOI: 10.1109/ACCESS.2023.3271287.

[95] Q. Dai, T. Cai, S. Duan, W. Zhang, and J. Zhao, “A smart energy management system for electric city bus battery swap station,” *IEEE Transportation Electrification Conference and Expo, ITEC Asia-Pacific 2014 - Conference Proceedings*, Oct. 2014. DOI: 10.1109/ITEC-AP.2014.6941107.

[96] D. Ansean, V. M. Garcia, M. Gonzalez, *et al.*, “Lithium-Ion Battery Degradation Indicators Via Incremental Capacity Analysis,” *IEEE Transactions on Industry Applications*, vol. 55, no. 3, pp. 2992–3002, May 2019, ISSN: 19399367. DOI: 10.1109/TIA.2019.2891213.

[97] A. Hoke, A. Brissette, K. Smith, A. Pratt, and D. Maksimovic, “Accounting for lithium-ion battery degradation in electric vehicle charging optimization,” *IEEE Journal of Emerging and Selected Topics in Power Electronics*, vol. 2, no. 3, pp. 691–700, 2014, ISSN: 21686785. DOI: 10.1109/JESTPE.2014.2315961.

[98] S. E. O’Kane, W. Ai, G. Madabattula, *et al.*, “Lithium-ion battery degradation: how to model it,” *Physical Chemistry Chemical Physics*, vol. 24, no. 13, pp. 7909–7922, Mar. 2022, ISSN: 14639076. DOI: 10.1039/D2CP00417H. [Online]. Available: https://pubs-rsc-org.tudelft.idm.oclc.org/en/content/articlehtml/2022/cp/d2cp00417h%20https://pubs-rsc-org.tudelft.idm.oclc.org/en/content/articlelanding/2022/cp/d2cp00417h.

[99] M. Shabani, F. Wallin, E. Dahlquist, and J. Yan, “The impact of battery operating management strategies on life cycle cost assessment in real power market for a grid-connected residential battery application,” *Energy*, vol. 270, p. 126 829, May 2023, ISSN: 0360-5442. DOI: 10.1016/J.ENERGY.2023.126829.

[100] B. Foggo and N. Yu, “Improved battery storage valuation through degradation reduction,” *IEEE Transactions on Smart Grid*, vol. 9, no. 6, pp. 5721–5732, Nov. 2018, ISSN: 19493053. DOI: 10.1109/TSG.2017.2695196.

[101] J. Yang, W. Liu, K. Ma, Z. Yue, A. Zhu, and S. Guo, “An optimal battery allocation model for battery swapping station of electric vehicles,” *Energy*, vol. 272, 2023. DOI: 10.1016/j.energy.2023.127109. [Online]. Available: https://doi.org/10.1016/j.energy.2023.127109.

[102] M. Ban, J. Yu, and Y. Yao, “Joint optimal scheduling for electric vehicle battery swapping-charging systems based on wind farms,” *CSEE Journal of Power and Energy Systems*, vol. 7, no. 3, pp. 555–566, May 2021, ISSN: 20960042. DOI: 10.17775/CSEEJPES.2020.02380.

[103] Q. Kang, J. Wang, M. Zhou, and A. C. Ammari, “Centralized Charging Strategy and Scheduling Algorithm for Electric Vehicles under a Battery Swapping Scenario,” *IEEE Transactions on Intelligent Transportation Systems*, vol. 17, no. 3, pp. 659–669, Mar. 2016, ISSN: 15249050. DOI: 10.1109/TITS.2015.2487323.

[104] K. An, W. Jing, and I. Kim, “Battery-swapping facility planning for electric buses with local charging systems,” *International Journal of Sustainable Transportation*, vol. 14, no. 7, pp. 489–502, Jul. 2020, ISSN: 15568334. DOI: 10.1080/15568318.2019.1573939. [Online]. Available: https://www.tandfonline.com/doi/abs/10.1080/15568318.2019.1573939.

[105] O. Erdinç, “Considering the combinatorial effects of on-site distributed generation and battery-to-X option availability in electric vehicle battery swap station operation,” *Sustainable Energy, Grids and Networks*, vol. 26, p. 100 472, 2021. DOI: 10.1016/j.segan.2021.100472. [Online]. Available: https://doi.org/10.1016/j.segan.2021.100472.

[106] R. Rao, X. Zhang, J. Xie, and L. Ju, “Optimizing electric vehicle users’ charging behavior in battery swapping mode,” *Applied Energy*, vol. 155, pp. 547–559, Oct. 2015, ISSN: 03062619. DOI: 10.1016/J.APENERGY.2015.05.125.

[107] M. R. Sarker, H. Pandžić, and M. A. Ortega-Vazquez, "Optimal operation and services scheduling for an electric vehicle battery swapping station," *IEEE Transactions on Power Systems*, vol. 30, no. 2, pp. 901–910, Mar. 2015, ISSN: 08858950. DOI: 10.1109/TPWRS.2014.2331560.

[108] C. Li, N. Wang, W. Li, Q. Yi, and D. Qi, "A battery centralized scheduling strategy for battery swapping of electric vehicles," *Journal of Energy Storage*, vol. 51, pp. 2352–152, 2022. DOI: 10.1016/j.est.2022.104327. [Online]. Available: https://doi.org/10.1016/j.est.2022.104327.

[109] S. Acharya, Y. Dvorkin, H. Pandzic, and R. Karri, "Cybersecurity of Smart Electric Vehicle Charging: A Power Grid Perspective," *IEEE Access*, vol. 8, pp. 214 434–214 453, 2020, ISSN: 21693536. DOI: 10.1109/ACCESS.2020.3041074.

[110] M. Goemans, "Linear programming," *MIT Mathematics*, vol. 17, 2015.

[111] O. Abraham, J. Abolaji, M. Adekunle, J. Ehimen, and O. Moses, "Application of linear programming in production planning," 2019.

[112] J. R. Birge and F. Louveaux, "Introduction to Stochastic Programming," Springer Series in Operations Research and Financial Engineering, 2011. DOI: 10.1007/978-1-4614-0237-4. [Online]. Available: https://link.springer.com/10.1007/978-1-4614-0237-4.

[113] L. P. Fávero and P. Belfiore, "Integer Programming," *Data Science for Business and Decision Making*, pp. 887–918, Jan. 2019. DOI: 10.1016/B978-0-12-811216-8.00019-7. [Online]. Available: https://linkinghub.elsevier.com/retrieve/pii/B9780128112168000197.

[114] *Optimization Problem Types - Mixed-Integer and Constraint Programming | solver*. [Online]. Available: https://www.solver.com/integer-constraint-programming.

[115] J. C. Smith, Z. Caner, and T. Ta¸skın, "A Tutorial Guide to Mixed-Integer Programming Models and Solution Techniques," 2007.

[116] J. A. Huchette, "Advanced mixed-integer programming formulations: Methodology, computation, and application," 2018.

[117] H. G. Santos and T. A. M. Toffolo, "Mixed Integer Linear Programming with Python," 2020.

[118] *OR-Tools*. [Online]. Available: https://developers.google.com/optimization/mip.

[119] *Markov Decision Processes: Theory & Apps | Vaia*. [Online]. Available: https://www.vaia.com/en-us/explanations/math/probability-and-statistics/markov-decision-processes/.

[120] *Markov Decision Process Definition, Working, and Examples - Spiceworks*. [Online]. Available: https://www.spiceworks.com/tech/artificial-intelligence/articles/what-is-markov-decision-process/.

[121] A. Ben-Tal Laurent El Ghaoui Arkadi Nemirovski, "Robust Optimization," 2009.

[122] J. Wiebe and R. Misener, "ROmodel: A Python Robust Optimization Modeling Toolbox," 2021. DOI: 10.1016/B978-0-323-88506-5.50108-X. [Online]. Available: http://dx.doi.org/10.1016/B978-0-323-88506-5.50108-X.

[123] V. Gabrel, C. Murat, and A. Thiele, "Invited Review Recent advances in robust optimization: An overview q," 2013. DOI: 10.1016/j.ejor.2013.09.036. [Online]. Available: http://dx.doi.org/10.1016/j.ejor.2013.09.036.

[124] J. Goh and M. Sim, "Distributionally Robust Optimization and Its Tractable Approximations," *Source: Operations Research*, vol. 58, no. 4, pp. 902–917, 2010. DOI: 10.1287/opre. [Online]. Available: https://about.jstor.org/terms.

[125] D. Bertsimas, D. B. Brown, and C. Caramanis, "Theory and Applications of Robust Optimization," *Source: SIAM Review*, vol. 53, no. 3, pp. 464–501, 2011. DOI: 10.1137/080734510.

[126] D. Bertsimas and M. Sim, "Robust discrete optimization and network flows," *Mathematical Programming*, vol. 98, no. 1-3, pp. 49–71, May 2003, ISSN: 00255610. DOI: 10.1007/S10107-003-0396-4/METRICS. [Online]. Available: https://link-springer-com.tudelft.idm.oclc.org/article/10.1007/s10107-003-0396-4.

[127] C. Onnen, R. Babuka, U. Kaymak, J. M. Sousa, H. B. Verbruggen, and R. Isermann, "GENETIC ALGORITHMS FOR OPTIMIZATION IN PREDICTIVE CONTROL," *Control Eng. Practice*, vol. 5, no. 10, pp. 1363–1372, 1997.

[128] E. U. Haq, I. Ahmad, A. Hussain, and I. M. Almanjahie, "A novel selection approach for genetic algorithms for global optimization of multimodal continuous functions," *Computational Intelligence and Neuroscience*, vol. 2019, 2019, ISSN: 16875273. DOI: 10.1155/2019/8640218.

[129] J. Mccall, "Genetic algorithms for modelling and optimisation," *Journal of Computational and Applied Mathematics*, vol. 184, pp. 205–222, 2005. DOI: 10.1016/j.cam.2004.07.034. [Online]. Available: www.elsevier.com/locate/cam.

[130] D. E. Goldberg and J. H. Holland, "Genetic Algorithms and Machine Learning," *Machine Learning*, vol. 3, no. 2, pp. 95–99, 1988, ISSN: 15730565. DOI: 10.1023/A:1022602019183/METRICS. [Online]. Available: https://link.springer.com/article/10.1023/A:1022602019183.

[131] M. Kuby and S. Lim, "The flow-refueling location problem for alternative-fuel vehicles," *Socio-Economic Planning Sciences*, vol. 39, pp. 125–145, 2005. DOI: 10.1016/j.seps.2004.03.001.

[132] M. Kuby and S. Lim, "Location of alternative-fuel stations using the Flow-Refueling Location Model and dispersion of candidate sites on Arcs," *Networks and Spatial Economics*, vol. 7, no. 2, pp. 129–152, Jun. 2007, ISSN: 1566113X. DOI: 10.1007/S11067-006-9003-6/METRICS. [Online]. Available: https://link.springer.com/article/10.1007/s11067-006-9003-6.

[133] J.-G. Kim and M. Kuby, "A network transformation heuristic approach for the deviation flow refueling location model," 2012. DOI: 10.1016/j.cor.2012.10.021. [Online]. Available: http://dx.doi.org/10.1016/j.cor.2012.10.021.

[134] S. H. Chung and C. Kwon, "Multi-period planning for electric car charging station locations: A case of Korean Expressways," *European Journal of Operational Research*, vol. 242, pp. 677–687, 2014. DOI: 10.1016/j.ejor.2014.10.029. [Online]. Available: http://dx.doi.org/10.1016/j.ejor.2014.10.029.

[135] Y.-W. Wang and C.-C. Lin, "Locating road-vehicle refueling stations," *Transportation Research Part E*, vol. 45, pp. 821–829, 2009. DOI: 10.1016/j.tre.2009.03.002.

[136] Y.-W. Wang and C.-R. Wang, "Locating passenger vehicle refueling stations," *Transportation Research Part E*, vol. 46, pp. 791–801, 2010. DOI: 10.1016/j.tre.2009.12.001.

[137] W. Tu, Q. Li, Z. Fang, S.-L. Shaw, B. Zhou, and X. Chang, "Optimizing the locations of electric taxi charging stations: A spatial-temporal demand coverage approach," 2015. DOI: 10.1016/j.trc.2015.10.004. [Online]. Available: http://dx.doi.org/10.1016/j.trc.2015.10.004.

[138] H. Y. Mak, Y. Rong, and Z. J. M. Shen, "Infrastructure planning for electric vehicles with battery swapping," *Management Science*, vol. 59, no. 7, pp. 1557–1575, Jul. 2013, ISSN: 00251909. DOI: 10.1287/MNSC.1120.1672.

[139] J. Hof, M. Schneider, and D. Goeke, "Solving the battery swap station location-routing problem with capacitated electric vehicles using an AVNS algorithm for vehicle-routing problems with intermediate stops," *Transportation Research Part B*, vol. 97, pp. 102–112, 2016. DOI: 10.1016/j.trb.2016.11.009. [Online]. Available: http://dx.doi.org/10.1016/j.trb.2016.11.009.

[140] J. Yang, F. Guo, and M. Zhang, "Optimal planning of swapping/charging station network with customer satisfaction," 2017. DOI: 10.1016/j.tre.2017.04.012. [Online]. Available: http://dx.doi.org/10.1016/j.tre.2017.04.012.

[141] Z. Chen and Y. Yin, "Optimal deployment of charging lanes for electric vehicles in transportation networks," *Transportation Research Part B*, vol. 91, pp. 344–365, 2016. DOI: 10.1016/j.trb.2016.05.018. [Online]. Available: http://dx.doi.org/10.1016/j.trb.2016.05.018.

[142] X. Xi, R. Sioshansi, and V. Marano, "Simulation-optimization model for location of a public electric vehicle charging infrastructure," 2013. DOI: 10.1016/j.trd.2013.02.014. [Online]. Available: http://dx.doi.org/10.1016/j.trd.2013.02.014.

[143] J. Dong, C. Liu, and Z. Lin, "Charging infrastructure planning for promoting battery electric vehicles: An activity-based approach using multiday travel data," 2014. DOI: 10.1016/j.trc.2013.11.001. [Online]. Available: http://dx.doi.org/10.1016/j.trc.2013.11.001.

[144] J. Cavadas, G. Homem De Almeida Correia, and J. Gouveia, “A MIP model for locating slow-charging stations for electric vehicles in urban areas accounting for driver tours,” 2015. DOI: 10.1016/j.tre.2014.11.005. [Online]. Available: http://dx.doi.org/10.1016/j.tre.2014.11.005.

[145] J. Asamer, M. Reinthaler, M. Ruthmair, M. Straub, and J. Puchinger, “Optimizing charging station locations for urban taxi providers,” *J. Puchinger). Transportation Research Part A*, vol. 85, pp. 233–246, 2016. DOI: 10.1016/j.tra.2016.01.014. [Online]. Available: http://dx.doi.org/10.1016/j.tra.2016.01.014.

[146] H. Chen, Y. Jia, Z. Hu, G. Wu, and Z. J. M. Shen, “Data-driven planning of plug-in hybrid electric taxi charging stations in urban environments: A case in the central area of Beijing,” *2017 IEEE PES Innovative Smart Grid Technologies Conference Europe, ISGT-Europe 2017 - Proceedings*, vol. 2018-January, pp. 1–6, Jul. 2017. DOI: 10.1109/ISGTEUROPE.2017.8260264.

[147] C. M. Flath, J. P. Ilg, S. Gottwalt, H. Schmeck, and C. Weinhardt, “Improving Electric Vehicle Charging Coordination Through Area Pricing,” *https://doi-org.tudelft.idm.oclc.org/10.1287/trsc.2013.0467*, vol. 48, no. 4, pp. 619–634, Jul. 2013, ISSN: 15265447. DOI: 10.1287/TRSC.2013.0467. [Online]. Available: https://pubsonline-informs-org.tudelft.idm.oclc.org/doi/abs/10.1287/trsc.2013.0467.

[148] W. Qi, Z. Xu, Z. J. M. Shen, Z. Hu, and Y. Song, “Hierarchical coordinated control of plug-in electric vehicles charging in multifamily dwellings,” *IEEE Transactions on Smart Grid*, vol. 5, no. 3, pp. 1465–1474, 2014, ISSN: 19493053. DOI: 10.1109/TSG.2014.2308217.

[149] E. B. Iversen, J. M. Morales, and H. Madsen, “Optimal charging of an electric vehicle using a Markov decision process,” 2014. DOI: 10.1016/j.apenergy.2014.02.003. [Online]. Available: http://dx.doi.org/10.1016/j.apenergy.2014.02.003.

[150] S. G. Nurre, R. Bent, F. Pan, and T. C. Sharkey, “Managing operations of plug-in hybrid electric vehicle (PHEV) exchange stations for use with a smart grid,” 2013. DOI: 10.1016/j.enpol.2013.11.052. [Online]. Available: http://dx.doi.org/10.1016/j.enpol.2013.11.052.

[151] B. Boyacı, K. G. Zografos, and N. Geroliminis, “An optimization framework for the development of efficient one-way car-sharing systems,” 2014. DOI: 10.1016/j.ejor.2014.07.020. [Online]. Available: http://dx.doi.org/10.1016/j.ejor.2014.07.020.

[152] M. Bruglieri, A. Colorni, and A. Luè, “The relocation problem for the one-way electric vehicle sharing,” *Networks*, vol. 64, no. 4, pp. 292–305, Dec. 2014, ISSN: 1097-0037. DOI: 10.1002/NET.21585. [Online]. Available: https://onlinelibrary-wiley-com.tudelft.idm.oclc.org/doi/full/10.1002/net.21585%20https://onlinelibrary-wiley-com.tudelft.idm.oclc.org/doi/abs/10.1002/net.21585%20https://onlinelibrary-wiley-com.tudelft.idm.oclc.org/doi/10.1002/net.21585.

[153] J.-G. Kim and M. Kuby, “The deviation-flow refueling location model for optimizing a network of refueling stations,” 2011. DOI: 10.1016/j.ijhydene.2011.08.108. [Online]. Available: www.elsevier.com/loca.

[154] M. Armstrong, C. El, H. Moussa, J. Adnot, A. Galli, and P. Riviere, “Optimal recharging strategy for battery-switch stations for electric vehicles in France,” *Energy Policy*, 2013. DOI: 10.1016/j.enpol.2013.05.089. [Online]. Available: http://dx.doi.org/10.1016/j.enpol.2013.05.089.

[155] K. Sepetanc and H. Pandzic, “A Cluster-Based Operation Model of Aggregated Battery Swapping Stations,” *IEEE Transactions on Power Systems*, vol. 35, no. 1, pp. 249–260, Jan. 2020, ISSN: 15580679. DOI: 10.1109/TPWRS.2019.2934017.

[156] L. Zhang, S. Lou, Y. Wu, L. Yi, and B. Hu, “Optimal scheduling of electric vehicle battery swap station based on time-of-use pricing,” *Asia-Pacific Power and Energy Engineering Conference, APPEEC*, vol. 2015-March, no. March, Mar. 2014, ISSN: 21574847. DOI: 10.1109/APPEEC.2014.7066014.

[157] M. Mahoor, Z. S. Hosseini, and A. Khodaei, “Least-cost operation of a battery swapping station with random customer requests,” 2019. DOI: 10.1016/j.energy.2019.02.018. [Online]. Available: https://doi.org/10.1016/j.energy.2019.02.018.

A
Appendix

Position of Modules - in general

$$\sum_{r\in R} x_{t,m,r} + \sum_{s\in S} y_{t,m,s} + \sum_{s\in S} Ch_{t,m,s} + \sum_{s\in S} In_{t,m,s} + \sum_{s\in S} InS_{t,m,s} = 1 \qquad \forall\, t \in T, m \in M \tag{A.1}$$

$$\sum_{r\in R} x_{t,m,r} \leq 1 \qquad \forall\, t \in T, m \in M \tag{A.2}$$

$$\sum_{s\in S} y_{t,m,s} \leq 1 \qquad \forall\, t \in T, m \in M \tag{A.3}$$

$$\sum_{s\in S} Ch_{t,m,s} \leq 1 \qquad \forall\, t \in T, m \in M \tag{A.4}$$

$$\sum_{s\in S} In_{t,m,s} \leq 1 \qquad \forall\, t \in T, m \in M \tag{A.5}$$

$$\sum_{s\in S} InS_{t,m,s} \leq 1 \qquad \forall\, t \in T, m \in M \tag{A.6}$$

Updates due to vessel tracking - Position of Modules - for the charging/inventory area

$$\sum_{r\in R}\sum_{m\in M} x_{t,m,r} + \sum_{s\in S}\sum_{m\in M} y_{t,m,s} + \sum_{s\in S}\sum_{m\in M} Ch_{t,m,s} + \sum_{s\in S}\sum_{m\in M} In_{t,m,s} + \sum_{s\in S}\sum_{m\in M} InS_{t,m,s} = EM_{total} \qquad \forall\, t \in T, m \in M \tag{A.7}$$

Position of the modules - Vessel location

$$\sum_{r\in R} x_{t,m,r} \leq 1 - \sum_{s\in S} Ch_{t-1,m,s} - \sum_{s\in S} In_{t-1,m,s} - \sum_{s\in S} InS_{t-1,m,s} \qquad \forall\, t \in \{1,\ldots,T\}, m \in M \tag{A.8}$$

$$\sum_{r\in R} x_{t-1,m,r} \leq 1 - \sum_{s\in S} Ch_{t,m,s} - \sum_{s\in S} In_{t,m,s} - \sum_{s\in S} InS_{t,m,s} \qquad \forall\, t \in \{1,\ldots,T\}, m \in M \tag{A.9}$$

$$\sum_{r\in R} x_{t,m,r} \leq \sum_{r\in R} x_{t-1,m,r} + \sum_{s\in S} y_{t-1,m,s} \qquad \forall\, t \in \{1,\ldots,T\}, m \in M \tag{A.10}$$

$$\sum_{r\in R} x_{t-1,m,r} \leq \sum_{r\in R} x_{t,m,r} + \sum_{s\in S} y_{t,m,s} \qquad \forall\, t \in \{1,\ldots,T\}, m \in M \tag{A.11}$$

Position of the modules - Swapping location

$$\sum_{s\in S} y_{t,m,s} \leq 1 - \sum_{s\in S} Ch_{t-1,m,s} - \sum_{s\in S} In_{t-1,m,s} \qquad \forall\, t \in \{1,\ldots,T\}, m \in M \tag{A.12}$$

$$\sum_{s\in S} y_{t-1,m,s} \leq 1 - \sum_{s\in S} InS_{t,m,s} - \sum_{s\in S} In_{t,m,s} \qquad \forall\, t \in \{1,\ldots,T\}, m \in M \tag{A.13}$$

$$\sum_{s\in S} y_{t,m,s} \leq \sum_{r\in R} x_{t-1,m,r} + \sum_{s\in S} y_{t-1,m,s} + \sum_{s\in S} InS_{t-1,m,s} \qquad \forall\, t \in \{1,\ldots,T\}, m \in M \tag{A.14}$$

$$\sum_{s\in S} y_{t-1,m,s} \leq \sum_{r\in R} x_{t,m,r} + \sum_{s\in S} y_{t,m,s} + \sum_{s\in S} Ch_{t,m,s} \qquad \forall\, t \in \{1,\ldots,T\}, m \in M \tag{A.15}$$

Position of the modules - Charging location

$$\sum_{s\in S} Ch_{t,m,s} \leq 1 - \sum_{s\in S} In_{t-1,m,s} - \sum_{r\in R} x_{t-1,m,r} - \sum_{s\in S} InS_{t-1,m,s} \qquad \forall\, t \in \{1,\ldots,T\}, m \in M \tag{A.16}$$

$$\sum_{s\in S} Ch_{t-1,m,s} \leq 1 - \sum_{s\in S} y_{t,m,s} - \sum_{r\in R} x_{t,m,r} - \sum_{s\in S} InS_{t,m,s} \qquad \forall\, t \in \{1,\ldots,T\}, m \in M \tag{A.17}$$

$$\sum_{s\in S} Ch_{t,m,s} \leq \sum_{s\in S} y_{t-1,m,s} + \sum_{s\in S} Ch_{t-1,m,s} \qquad \forall\, t \in \{1,\ldots,T\}, m \in M \tag{A.18}$$

$$\sum_{s\in S} Ch_{t-1,m,s} \leq \sum_{s\in S} In_{t,m,s} + \sum_{s\in S} Ch_{t,m,s} \qquad \forall\, t \in \{1,\ldots,T\}, m \in M \tag{A.19}$$

Movement of Modules - Inventory location

$$\sum_{s\in S} In_{t,m,s} \leq 1 - \sum_{s\in S} y_{t-1,m,s} - \sum_{r\in R} x_{t-1,m,r} - \sum_{s\in S} InS_{t-1,m,s} \quad \forall\, t \in \{1,\ldots,T\}, m \in M \tag{A.20}$$

$$\sum_{s\in S} In_{t-1,m,s} \leq 1 - \sum_{s\in S} y_{t,m,s} - \sum_{r\in R} x_{t,m,r} - \sum_{s\in S} Ch_{t,m,s} \quad \forall\, t \in \{1,\ldots,T\}, m \in M \tag{A.21}$$

$$\sum_{s\in S} In_{t,m,s} \leq \sum_{s\in S} Ch_{t-1,m,s} + \sum_{s\in S} In_{t-1,m,s} \quad \forall\, t \in \{1,\ldots,T\}, m \in M \tag{A.22}$$

$$\sum_{s\in S} In_{t-1,m,s} \leq \sum_{s\in S} InS_{t,m,s} + \sum_{s\in S} In_{t,m,s} \quad \forall\, t \in \{1,\ldots,T\}, m \in M \tag{A.23}$$

Position of the modules - Inventory for Swapping location

$$\sum_{s\in S} InS_{t,m,s} \leq 1 - \sum_{s\in S} y_{t-1,m,s} - \sum_{r\in R} x_{t-1,m,r} - \sum_{s\in S} Ch_{t-1,m,s} \quad \forall\, t \in \{1,\ldots,T\}, m \in M \tag{A.24}$$

$$\sum_{s\in S} InS_{t-1,m,s} \leq 1 - \sum_{s\in S} In_{t,m,s} - \sum_{r\in R} x_{t,m,r} - \sum_{s\in S} Ch_{t,m,s} \quad \forall\, t \in \{1,\ldots,T\}, m \in M \tag{A.25}$$

$$\sum_{s\in S} InS_{t,m,s} \leq \sum_{s\in S} InS_{t-1,m,s} + \sum_{s\in S} In_{t-1,m,s} \quad \forall\, t \in \{1,\ldots,T\}, m \in M \tag{A.26}$$

$$\sum_{s\in S} InS_{t-1,m,s} \leq \sum_{s\in S} InS_{t,m,s} + \sum_{s\in S} y_{t,m,s} \quad \forall\, t \in \{1,\ldots,T\}, m \in M \tag{A.27}$$

Position of the modules - Prevention movement certain cases

$$InS_{t-T_{swap}-1,m,s} + Ch_{t,m,s} \leq 1 \quad \forall\, t \in \{T_{swap}+1,\ldots,T\}, m \in M, s \in S \tag{A.28}$$

$$RinZ_{t,r,s}\left(x_{t-T_{swap}-1,m,r} + y_{t-T_{swap},m,s} + x_{t,m,r}\right) \leq 2 \quad \forall\, t \in \{T_{swap}+1,\ldots,T\}, m \in M, r \in R, s \in S \tag{A.29}$$

$$\sum_{r\in R} x_{t-T_{swap}-1,m,r} + y_{t-T_{swap},m,s} + \sum_{r\in R} x_{t,m,r} \leq 2 \quad \forall\, t \in \{T_{swap}+1,\ldots,T\}, m \in M, s \in S \tag{A.30}$$

$$InS_{t-T_{swap}-1,m,s} + Ch_{t,m,s} \leq 1 \quad \forall\, t \in \{T_{swap}+1,\ldots,T\}, m \in M, s \in S \tag{A.31}$$

$$InS_{t-T_{swap}-1,m,s} + y_{t-T_{swap},m,s} + Ch_{t,m,s} \leq 2 \quad \forall\, t \in \{T_{swap}+1,\ldots,T\}, m \in M, s \in S \tag{A.32}$$

Order of movement of modules

$$x_{t,m,r} \leq x_{t-1,m,r} + \sum_{s\in S}(y_{t-1,m,s} \cdot RinZ_{t,r,s}) \quad \forall t \in \{1,\ldots,T\}, m \in M, r \in R \tag{A.33}$$

$$x_{t-1,m,r} \leq x_{t,m,r} + \sum_{s\in S}(y_{t,m,s} \cdot RinZ_{t,r,s}) \quad \forall t \in \{1,\ldots,T\}, m \in M, r \in R \tag{A.34}$$

$$y_{t,m,s} \leq \sum_{r\in R}(x_{t-1,m,r}) + InS_{t-1,m,s} + y_{t-1,m,s} \quad \forall t \in \{1,\ldots,T\}, m \in M, s \in S \tag{A.35}$$

$$y_{t-1,m,s} \leq \sum_{r\in R}(x_{t,m,r}) + Ch_{t,m,s} + y_{t,m,s} \quad \forall t \in \{1,\ldots,T\}, m \in M, s \in S \tag{A.36}$$

$$Ch_{t,m,s} \leq Ch_{t-1,m,s} + y_{t-1,m,s} \quad \forall t \in \{1,\ldots,T\}, m \in M, s \in S \tag{A.37}$$

$$Ch_{t-1,m,s} \leq Ch_{t,m,s} + In_{t,m,s} \quad \forall t \in \{1,\ldots,T\}, m \in M, s \in S \tag{A.38}$$

$$In_{t,m,s} \leq In_{t-1,m,s} + Ch_{t-1,m,s} \quad \forall t \in \{1,\ldots,T\}, m \in M, s \in S \tag{A.39}$$

$$In_{t-1,m,s} \leq In_{t,m,s} + InS_{t,m,s} \quad \forall t \in \{1,\ldots,T\}, m \in M, s \in S \tag{A.40}$$

$$InS_{t,m,s} \leq InS_{t-1,m,s} + In_{t-1,m,s} \quad \forall t \in \{1,\ldots,T\}, m \in M, s \in S \tag{A.41}$$

$$InS_{t-1,m,s} \leq InS_{t,m,s} + y_{t,m,s} \quad \forall t \in \{1,\ldots,T\}, m \in M, s \in S \tag{A.42}$$

Energy Modules States (Full/Intermediate/Empty) (no adjustments)

$$l_{t,m} \leq SF_{min} + M_1 \cdot (1 - e_{t,m}) \qquad \forall t \in T, m \in M \qquad \text{(A.43)}$$
$$l_{t,m} \geq SF_{min} - M_1 \cdot e_{t,m} \qquad \forall t \in T, m \in M \qquad \text{(A.44)}$$
$$l_{t,m} \geq SF_{max} - M_1 \cdot (1 - f_{t,m}) \qquad \forall t \in T, m \in M \qquad \text{(A.45)}$$
$$l_{t,m} \leq SF_{max} \cdot f_{t,m} \qquad \forall t \in T, m \in M \qquad \text{(A.46)}$$
$$1 = e_{t,m} + i_{t,m} + f_{t,m} \qquad \forall t \in T, m \in M \qquad \text{(A.47)}$$

Restrictions for the positions of modules

$$\sum_{s \in S} Ch_{t,m,s} \leq e_{t,m} + i_{t,m} \qquad \forall t \in T, \forall m \in M \qquad \text{(A.48)}$$
$$\sum_{s \in S} Ch_{t,m,s} \leq 1 - f_{t,m} \qquad \forall t \in T, \forall m \in M \qquad \text{(A.49)}$$
$$\sum_{s \in S} In_{t,m,s} + \sum_{s \in S} InS_{t,m,s} \leq f_{t,m} \qquad \forall t \in T, \forall m \in M \qquad \text{(A.50)}$$
$$\sum_{s \in S} In_{t,m,s} + \sum_{s \in S} InS_{t,m,s} \leq 1 - e_{t,m} - i_{t,m} \qquad \forall t \in T, \forall m \in M \qquad \text{(A.51)}$$
$$\sum_{r \in R} u_{t,m,r} + \sum_{s \in S} Ch_{t,m,s} + \sum_{s \in S} y_{t,m,s} \geq i_{t,m} \qquad \forall t \in T, \forall m \in M \qquad \text{(A.52)}$$

Usage of modules

$$u_{t,m,r} \leq x_{t,m,r} \qquad \forall t \in T, m \in M, r \in R \qquad \text{(A.53)}$$
$$\sum_{m \in M} u_{t,m,r} = 1 - VS_{t,r} \qquad \forall t \in T, r \in R \qquad \text{(A.54)}$$
$$\sum_{r \in R} u_{t,m,r} \leq 1 - e_{t,m} \qquad \forall t \in T, m \in M \qquad \text{(A.55)}$$
$$\sum_{r \in R} u_{t,m,r} \leq i_{t,m} + f_{t,m} \qquad \forall t \in T, m \in M \qquad \text{(A.56)}$$
$$\sum_{m \in M} u_{t,m,r} \leq 1 \qquad \forall t \in T, r \in R \qquad \text{(A.57)}$$

Modules on the Vessel

$$\sum_{m \in M} x_{t,m,r} \leq EM_N - VS_{t,r} \qquad \forall\, t \in T, r \in R \qquad \text{(A.58)}$$
$$\sum_{m \in M} x_{t,m,r} \geq EM_N \cdot (1 - VS_{t,r}) \qquad \forall\, t \in T, r \in R \qquad \text{(A.59)}$$
$$EM_N \cdot (SL_{t,r} + StS_{t,r} + SbOP_{t,r}) \leq \sum_{m \in M} x_{t,m,r} \qquad \forall\, t \in T, r \in R \qquad \text{(A.60)}$$

Power level - quadratic constraints

$$\begin{aligned} l_{t+1,m} = l_{t,m} &- \sum_{r \in R} (SL_{t,r} \cdot P_{t,r} \cdot u_{t,m,r}) - \sum_{r \in R} (StS_{t,r} \cdot P_{StS} \cdot u_{t,m,r}) \\ &- \sum_{r \in R} (SbOP_{t,r} \cdot P_{SbOP} \cdot u_{t,m,r}) + CS \cdot \sum_{s \in S} Ch_{t,m,s} \qquad \forall t \in T, m \in M \qquad \text{(A.61)} \end{aligned}$$

Power level - linearisation

$$SL_{t,r} \leq \sum_{m \in M} PSL_{t,m,r} \qquad \forall t \in T, r \in R \tag{A.62}$$

$$StS_{t,r} \leq \sum_{m \in M} PStS_{t,m,r} \qquad \forall t \in T, r \in R \tag{A.63}$$

$$SbOP_{t,r} \leq \sum_{m \in M} PSbOP_{t,m,r} \qquad \forall t \in T, r \in R \tag{A.64}$$

$$\sum_{m \in M} PSL_{t,m,r} \leq 1 \qquad \forall t \in T, r \in R \tag{A.65}$$

$$\sum_{m \in M} PStS_{t,m,r} \leq 1 \qquad \forall t \in T, r \in R \tag{A.66}$$

$$\sum_{m \in M} PSbOP_{t,m,r} \leq 1 \qquad \forall t \in T, r \in R \tag{A.67}$$

$$PSL_{t,m,r} + PStS_{t,m,r} + PSbOP_{t,m,r} = u_{t,m,r} \qquad \forall t \in T, m \in M, r \in R \tag{A.68}$$

$$l_{t+1,m} = l_{t,m} - \sum_{r \in R} (PSL_{t,m,r} \cdot P_{t,r}) - \sum_{r \in R} (PStS_{t,m,r} \cdot P_{StS}) - \sum_{r \in R} (PSbOP_{t,m,r} \cdot P_{SbOP}) + CS \cdot \sum_{s \in S} Ch_{t,m,s} \qquad \forall t \in T, m \in M \tag{A.69}$$

Vessel at swapping station

$$VS_{t,r} \leq \sum_{s \in S} RinZ_{t,r,s} \qquad \forall t \in T, r \in R, s \in S \tag{A.70}$$

$$\sum_{s \in S} (VS_{t,r} \cdot RinZ_{t,r,s}) \leq 1 \qquad \forall t \in T, r \in R \tag{A.71}$$

$$\sum_{r \in R} (VS_{t,r} \cdot RinZ_{t,r,s}) \leq 1 \qquad \forall t \in T, s \in S \tag{A.72}$$

Vessel at swapping station (actual lineraizatoin)

$$y_{t,m,s} = \theta_{t,m,s} + \Delta_{t,m,s} \qquad \forall t \in T, m \in M, s \in S \tag{A.73}$$

$$\theta_{t,m,s} \leq \sum_{r \in R} \left(x_{t-T_{swap},m,r} \cdot RinZ_{t,r,s} \right) \qquad \forall t \in \{T_{swap}, \ldots, T\}, m \in M, s \in S \tag{A.74}$$

$$\theta_{t,m,s} \leq 1 - Ch_{t-T_{swap},m,s} - In_{t-T_{swap},m,s} \qquad \forall t \in \{T_{swap}, \ldots, T\}, m \in M, s \in S \tag{A.75}$$

$$\theta_{t,m,s} \leq 1 - InS_{t-T_{swap},m,s} - y_{t-T_{swap},m,s} \qquad \forall t \in \{T_{swap}, \ldots, T\}, m \in M, s \in S \tag{A.76}$$

$$\Delta_{t,m,s} \leq Ch_{t-T_{swap},m,s} + In_{t-T_{swap},m,s} + InS_{t-T_{swap},m,s} \qquad \forall t \in \{T_{swap}, \ldots, T\}, m \in M, s \in S \tag{A.77}$$

$$\Delta_{t,m,s} \leq 1 - \sum_{r \in R} \left(x_{t-T_{swap},m,r} \cdot RinZ_{t,r,s} \right) - y_{t-T_{swap},m,s} \qquad \forall t \in \{T_{swap}, \ldots, T\}, m \in M, s \in S \tag{A.78}$$

Vessel at swapping station (actual lineraizatoin)

$$\sum_{m \in M} \Delta_{t,m,s} = \sum_{m \in M} \theta_{t,m,s} \qquad \forall t \in \{T_{swap}, \ldots, T\}, s \in S \tag{A.79}$$

$$\sum_{m \in M} \theta_{t,m,s} \leq EM_N \qquad \forall \{T_{swap}, \ldots, T\}, s \in S \tag{A.80}$$

$$\sum_{m \in M} \Delta_{t,m,s} + \sum_{m \in M} \theta_{t,m,s} \geq \sum_{m \in M} y_{t,m,s} \qquad \forall t \in \{T_{swap}, \ldots, T\}, s \in S \tag{A.81}$$

$$2 \sum_{m \in M} \Delta_{t,m,s} \leq \sum_{m \in M} y_{t,m,s} \qquad \forall t \in \{T_{swap}, \ldots, T\}, s \in S \tag{A.82}$$

$$\sum_{m \in M} y_{t,m,s} \leq 2 \cdot EM_N \qquad \forall t \in T, s \in S \tag{A.83}$$

Swapping possible

$$VS_{t,r} \leq SPos_{t,r} \quad \forall t \in T, r \in R \tag{A.84}$$
$$StS_{t,r} \leq SPos_{t+DT_{StS_{t,r}}} \quad \forall t \in \{0,\dots,T-DT_{StS_{t,r}}\}, r \in R \tag{A.85}$$
$$VS_{t,r} \leq 1 - DT_{RB_{t,r}} \quad \forall t \in T, r \in R \tag{A.86}$$
$$StS_{t,r} \leq 1 - DT_{RB_{t,r}} \quad \forall t \in T, r \in R \tag{A.87}$$
$$\tag{A.88}$$

Module swap duration

$$SWAP_{t,m,s} \geq y_{t,m,s} - y_{t-1,m,s} \quad \forall t \in \{1,\dots,T\}, m \in M, r \in R, s \in S \tag{A.89}$$
$$y_{t+dt,m,s} \geq SWAP_{t,m,s} \quad \forall t \in \{0,\dots,T-T_{swap}\}, m \in M, s \in S, dt \in \{0,\dots,T_{swap}\} \tag{A.90}$$
$$y_{t+T_{swap},m,s} \leq 1 - SWAP_{t,m,s} \quad \forall t \in \{0,\dots,T-T_{swap}\}, r \in R \tag{A.91}$$

Vessel tracking

$$SL_{t,r} + StS_{t,r} + VS_{t,r} + SbOP_{t,r} = 1 \quad \forall t \in T, r \in R \tag{A.92}$$
$$VS_{t,r} + VS_{t-T_{Swap},r} \leq 1 \quad \forall t \in \{T_{swap},\dots,T\}, r \in R \tag{A.93}$$
$$SL_{0,r} = 1 \quad \forall r \in R \tag{A.94}$$

Vessel tracking - Sailing original path

$$SL_{t,r} \leq 1 - VS_{t-1,r} - StS_{t-1,r} \quad \forall t \in \{1,\dots,T\}, r \in R \tag{A.95}$$
$$SL_{t-1,r} \leq 1 - VS_{t,r} - SbOP_{t,r} \quad \forall t \in \{1,\dots,T\}, r \in R \tag{A.96}$$
$$SL_{t,r} \leq SL_{t-1,r} + SbOP_{t-1,r} \quad \forall t \in \{1,\dots,T\}, r \in R \tag{A.97}$$
$$SL_{t-1,r} \leq SL_{t,r} + StS_{t,r} \quad \forall t \in \{1,\dots,T\}, r \in R \tag{A.98}$$

Vessel tracking - Vessel sailing to Swapping station

$$StS_{t,r} \leq 1 - SbOP_{t-1,r} - VS_{t-1,r} \quad \forall t \in \{1,\dots,T\}, r \in R \tag{A.99}$$
$$StS_{t-1,r} \leq 1 - SbOP_{t,r} - SL_{t,r} \quad \forall t \in \{1,\dots,T\}, r \in R \tag{A.100}$$
$$StS_{t,r} \leq StS_{t-1,r} + SL_{t-1,r} \quad \forall t \in \{1,\dots,T\}, r \in R \tag{A.101}$$
$$StS_{t-1,r} \leq VS_{t,r} + StS_{t,r} \quad \forall t \in \{1,\dots,T\}, r \in R \tag{A.102}$$

Vessel tracking - Vessel at Swapping Station

$$VS_{t,r} \leq 1 - SL_{t-1,r} - SbOP_{t-1,r} \quad \forall t \in \{1,\dots,T\}, r \in R \tag{A.103}$$
$$VS_{t-1,r} \leq 1 - SL_{t,r} - StS_{t,r} \quad \forall t \in \{1,\dots,T\}, r \in R \tag{A.104}$$
$$VS_{t,r} \leq VS_{t-1,r} + StS_{t-1,r} \quad \forall t \in \{1,\dots,T\}, r \in R \tag{A.105}$$
$$VS_{t-1,r} \leq VS_{t,r} + SbOP_{t,r} \quad \forall t \in \{1,\dots,T\}, r \in R \tag{A.106}$$

Vessel tracking - Sailing back to Original Path

$$SbOP_{t,r} \leq 1 - StS_{t-1,r} - SL_{t-1,r} \quad \forall t \in \{1,\dots,T\}, r \in R \tag{A.107}$$
$$SbOP_{t-1,r} \leq 1 - StS_{t,r} - VS_{t,r} \quad \forall t \in \{1,\dots,T\}, r \in R \tag{A.108}$$
$$SbOP_{t,r} \leq SbOP_{t-1,r} + VS_{t-1,r} \quad \forall t \in \{1,\dots,T\}, r \in R \tag{A.109}$$
$$SbOP_{t-1,r} \leq SbOP_{t,r} + SL_{t,r} \quad \forall t \in \{1,\dots,T\}, r \in R \tag{A.110}$$

Vessel tracking - Sailing to the Swapping Station - Definition

$$\sum_{m \in M} InS_{t,m,s} \geq \sum_{r \in R} (StS_{t,r} \cdot RinZ_{t,r,s}) \forall t \in T, r \in R, s \in S \tag{A.111}$$
$$\sum_{m \in M} InS_{t,m,s} \leq EM_N \sum_{r \in R} ((1 - VS_{t,r} - SbOP_{t,r} - SL_{t,r}) \cdot RinZ_{t,r,s}) \forall t \in T, s \in S \tag{A.112}$$
$$SPos_{t+DTSTS_{t,r},r} \geq StS_{t,r} \forall t \in T, r \in R \tag{A.113}$$

Vessel tracking - Sailing to the swapping station - Indication and duration

$$StS_{Start_{t,r}} \geq StS_{t,r} - StS_{t-1,r} \quad \forall t \in \{1,\dots,T\}, r \in R \tag{A.114}$$

$$StS_{Start_{t,r}} + StS_{Start_{t-1,r}} \leq 1 \quad \forall t \in \{1,\dots,T\}, r \in R \tag{A.115}$$

$$StS_{t+dt,r} \geq StS_{Start_{t,r}} \quad \forall t \in \{1,\dots,T - DT_{StS_{t,r}}\}, r \in R, dt \in \{0,\dots,DT_{StS_{t,r}}\} \tag{A.116}$$

$$StS_{t+DT_{StS_{t,r}},r} \leq 1 - StS_{Start_{t,r}} \quad \forall t \in \{1,\dots,T - DT_{StS_{t,r}}\}, r \in R \tag{A.117}$$

$$VS_{t+DT_{StS_{t,r}},r} \geq StS_{Start_{t,r}} \quad \forall t \in \{1,\dots,T - DT_{StS_{t,r}}\}, r \in R \tag{A.118}$$

Vessel tracking - Sailing back to Original Path - Definition

$$SbOP_{Start_{t,r}} \geq SbOP_{t,r} - SbOP_{t-1,r} \quad \forall t \in \{1,\dots,T\}, r \in R \tag{A.119}$$

$$SbOP_{Start_{t,r}} + SbOP_{Start_{t-1,r}} \leq 1 \quad \forall t \in \{1,\dots,T\}, r \in R \tag{A.120}$$

$$SbOP_{t+DATAT\_SbOP_{t,r},r} \leq 1 - SbOP_{Start_{t,r}} \quad \forall t \in \{1,\dots,T - DT_{SbOP_{t,r}}\}, r \in R \tag{A.121}$$

$$SbOP_{t+dt,r} \geq SbOP_{Start_{t,r}} \quad \forall t \in \{1,\dots,T - DT_{SbOP_{t,r}}\}, r \in R, dt \in \{0,\dots,DT_{SbOP_{t,r}}\} \tag{A.122}$$

(A.123)

Minimum swaps required

$$\sum_{t \in T} StS_{Start_{t,r}} \geq Swap_{min_r} \quad \forall r \in R \tag{A.124}$$

$$\sum_{t \in T} VS_{Start_{t,r}} \geq T_{swap} \cdot Swap_{min_r} \quad \forall r \in R \tag{A.125}$$

$$\sum_{t \in T} SbOP_{Start_{t,r}} \geq Swap_{min_r} \quad \forall r \in R \tag{A.126}$$

B
Appendix

B.1. Verification Test Case 1

t	Vessel r		Module m with energy level $l_{t,m}$							
	R1	R2	0	1	2	3	4	5	6	7
0	SL (1)	SL (2)	R1 81.0 (F)	’R1 81.0 (F)	’R2 81.0 (F)	R2 81.0 (F)	I1 81.0 (F)	I1 81.0 (F)	I2 81.0 (F)	I2 81.0 (F)
1	SL (1)	SL (2)	R1 81.0 (F)	’R1 71.0 (I)	’R2 71.0 (I)	R2 81.0 (F)	I1 81.0 (F)	I1 81.0 (F)	I2 81.0 (F)	I2 81.0 (F)
2	SL (1)	SL (2)	R1 81.0 (F)	’R1 61.0 (I)	’R2 61.0 (I)	R2 81.0 (F)	I1 81.0 (F)	I1 81.0 (F)	I2 81.0 (F)	I2 81.0 (F)
3	SL (1)	SL (2)	R1 81.0 (F)	’R1 51.0 (I)	’R2 51.0 (I)	R2 81.0 (F)	I1 81.0 (F)	I1 81.0 (F)	I2 81.0 (F)	I2 81.0 (F)
4	SL (1)	SL (2)	R1 81.0 (F)	’R1 41.0 (I)	’R2 41.0 (I)	R2 81.0 (F)	I1 81.0 (F)	I1 81.0 (F)	I2 81.0 (F)	I2 81.0 (F)
5	SL (1)	SL (2)	R1 81.0 (F)	’R1 31.0 (I)	’R2 31.0 (I)	R2 81.0 (F)	I1 81.0 (F)	I1 81.0 (F)	I2 81.0 (F)	I2 81.0 (F)
6	StS (1)	SL (2)	R1 81.0 (F)	’R1 21.0 (I)	’R2 21.0 (I)	R2 81.0 (F)	I1 81.0 (F)	IS1 81.0 (F)	I2 81.0 (F)	I2 81.0 (F)
7	VS (1)	SL (2)	R1 81.0 (F)	θS1 11.0 (E)	R2 11.0 (E)	’R2 81.0 (F)	I1 81.0 (F)	ΔS1 81.0 (F)	I2 81.0 (F)	I2 81.0 (F)
8	VS (1)	SL (2)	R1 81.0 (F)	θS1 11.0 (E)	R2 11.0 (E)	’R2 71.0 (I)	I1 81.0 (F)	ΔS1 81.0 (F)	I2 81.0 (F)	I2 81.0 (F)
9	SbOP (1)	StS (2)	’R1 81.0 (F)	C1 11.0 (E)	R2 11.0 (E)	’R2 61.0 (I)	I1 81.0 (F)	R1 81.0 (F)	IS2 81.0 (F)	IS2 81.0 (F)
10	SL (1)	VS (2)	’R1 71.0 (I)	C1 21.0 (I)	θS2 11.0 (E)	θS2 51.0 (I)	I1 81.0 (F)	R1 81.0 (F)	ΔS2 81.0 (F)	ΔS2 81.0 (F)
11	SL (1)	VS (2)	’R1 61.0 (I)	C1 31.0 (I)	θS2 11.0 (E)	θS2 51.0 (I)	I1 81.0 (F)	R1 81.0 (F)	ΔS2 81.0 (F)	ΔS2 81.0 (F)
12	SL (1)	SbOP (2)	’R1 51.0 (I)	C1 41.0 (I)	C2 11.0 (E)	C2 51.0 (I)	I1 81.0 (F)	R1 81.0 (F)	R2 81.0 (F)	’R2 81.0 (F)
13	SL (1)	SL (2)	’R1 41.0 (I)	C1 51.0 (I)	C2 21.0 (I)	C2 61.0 (I)	I1 81.0 (F)	R1 81.0 (F)	R2 81.0 (F)	’R2 71.0 (I)
14	SL (1)	SL (2)	’R1 31.0 (I)	C1 61.0 (I)	C2 31.0 (I)	C2 71.0 (I)	I1 81.0 (F)	R1 81.0 (F)	R2 81.0 (F)	’R2 61.0 (I)
15	SL (1)	SL (2)	’R1 21.0 (I)	C1 71.0 (I)	C2 41.0 (I)	I2 81.0 (F)	I1 81.0 (F)	R1 81.0 (F)	R2 81.0 (F)	’R2 51.0 (I)
16	SL (1)	SL (2)	R1 11.0 (E)	I1 81.0 (F)	C2 51.0 (I)	I2 81.0 (F)	I1 81.0 (F)	’R1 81.0 (F)	R2 81.0 (F)	’R2 41.0 (I)
17	StS (1)	SL (2)	R1 11.0 (E)	IS1 81.0 (F)	C2 61.0 (I)	I2 81.0 (F)	IS1 81.0 (F)	’R1 71.0 (I)	R2 81.0 (F)	’R2 31.0 (I)
18	VS (1)	SL (2)	θS1 11.0 (E)	ΔS1 81.0 (F)	C2 71.0 (I)	I2 81.0 (F)	ΔS1 81.0 (F)	θS1 61.0 (I)	R2 81.0 (F)	’R2 21.0 (I)
19	VS (1)	SL (2)	θS1 11.0 (E)	ΔS1 81.0 (F)	I2 81.0 (F)	I2 81.0 (F)	ΔS1 81.0 (F)	θS1 61.0 (I)	’R2 81.0 (F)	R2 11.0 (E)
20	SbOP (1)	SL (2)	C1 11.0 (E)	’R1 81.0 (F)	I2 81.0 (F)	I2 81.0 (F)	R1 81.0 (F)	C1 61.0 (I)	’R2 71.0 (I)	R2 11.0 (E)
21	SL (1)	SL (2)	C1 21.0 (I)	’R1 71.0 (I)	I2 81.0 (F)	I2 81.0 (F)	R1 81.0 (F)	C1 71.0 (I)	’R2 61.0 (I)	R2 11.0 (E)
22	SL (1)	SL (2)	C1 31.0 (I)	’R1 61.0 (I)	I2 81.0 (F)	I2 81.0 (F)	R1 81.0 (F)	I1 81.0 (F)	’R2 51.0 (I)	R2 11.0 (E)
23	SL (1)	SL (2)	C1 41.0 (I)	’R1 51.0 (I)	I2 81.0 (F)	I2 81.0 (F)	R1 81.0 (F)	I1 81.0 (F)	’R2 41.0 (I)	R2 11.0 (E)
24	SL (1)	SL (2)	C1 51.0 (I)	’R1 41.0 (I)	I2 81.0 (F)	I2 81.0 (F)	R1 81.0 (F)	I1 81.0 (F)	’R2 31.0 (I)	R2 11.0 (E)
25	SL (1)	StS (2)	C1 61.0 (I)	’R1 31.0 (I)	IS2 81.0 (F)	I2 81.0 (F)	R1 81.0 (F)	I1 81.0 (F)	’R2 21.0 (I)	R2 11.0 (E)
26	SL (1)	VS (2)	C1 71.0 (I)	’R1 21.0 (I)	ΔS2 81.0 (F)	I2 81.0 (F)	R1 81.0 (F)	I1 81.0 (F)	θS2 11.0 (E)	R2 11.0 (E)
27	SL (1)	VS (2)	I1 81.0 (F)	R1 11.0 (E)	ΔS2 81.0 (F)	I2 81.0 (F)	’R1 81.0 (F)	I1 81.0 (F)	θS2 11.0 (E)	R2 11.0 (E)
28	SL (1)	SbOP (2)	I1 81.0 (F)	R1 11.0 (E)	’R2 81.0 (F)	I2 81.0 (F)	’R1 71.0 (I)	I1 81.0 (F)	C2 11.0 (E)	R2 11.0 (E)
29	SL (1)	SL (2)	I1 81.0 (F)	R1 11.0 (E)	’R2 71.0 (I)	I2 81.0 (F)	’R1 61.0 (I)	I1 81.0 (F)	C2 21.0 (I)	R2 11.0 (E)
30	SL (1)	SL (2)	I1 81.0 (F)	R1 11.0 (E)	’R2 61.0 (I)	I2 81.0 (F)	’R1 51.0 (I)	I1 81.0 (F)	C2 31.0 (I)	R2 11.0 (E)
31	SL (1)	SL (2)	I1 81.0 (F)	R1 11.0 (E)	’R2 51.0 (I)	I2 81.0 (F)	’R1 41.0 (I)	I1 81.0 (F)	C2 41.0 (I)	R2 11.0 (E)
32	SL (1)	SL (2)	I1 81.0 (F)	R1 11.0 (E)	’R2 41.0 (I)	I2 81.0 (F)	’R1 31.0 (I)	I1 81.0 (F)	C2 51.0 (I)	R2 11.0 (E)
33	SL (1)	SL (2)	I1 81.0 (F)	R1 11.0 (E)	’R2 31.0 (I)	I2 81.0 (F)	’R1 21.0 (I)	I1 81.0 (F)	C2 61.0 (I)	R2 11.0 (E)

Table B.1: Verification TC_1

t	$SPos_{t,r}$	$StS_{t,r}$	$VS_{t,r}$	$SbOP_{t,r}$	T_{total}
0	✗*	1	2	1	4
1	✗*	1	2	1	4
2	✗*	1	2	1	4
3	✓*	1	2	1	4
4	✓*	1	2	1	4
5	✓*	1	2	1	4
6	✓*	| 1 |	2	1	| 4 |
7	✓*	1	| 2 |	1	4
8	✓*	1	2	1	4
9	✓*	1	2	| 1 |	4
10	✓*	1	2	1	4
11	✓*	1	2	1	4
12	✓*	1	2	1	4
13	✓*	1	2	1	4
14	✓*	1	2	1	4
15	✓*	1	2	1	4
16	✓*	1	2	1	4
17	✓*	| 1 |	2	1	| 4 |
18	✓*	1	| 2 |	1	4
19	✓*	1	2	1	4
20	✓*	1	2	| 1 |	4
21	✓*	1	2	1	4
22	✓*	1	2	1	4
23	✓*	1	2	1	4
24	✓*	1	2	1	4
25	✓*	1	2	1	4
26	✓-	1	2	1	4
27	✓-	1	2	1	4
28	✓*	1	2	1	4
29	✓*	1	2	1	4
30	✓*	1	2	1	4
31	✗*	1	2	1	4
32	✗*	1	2	1	4
33	✗*	1	2	1	4

Table B.2: Verification TC_1 for $R1$ - objective

t	$SPos_{t,r}$	$StS_{t,r}$	$VS_{t,r}$	$SbOP_{t,r}$	T_{total}
0	✗*	1	2	1	4
1	✗*	1	2	1	4
2	✗*	1	2	1	4
3	✓*	1	2	1	4
4	✓*	1	2	1	4
5	✓*	1	2	1	4
6	✓*	1	2	1	4
7	✓*	1	2	1	4
8	✓*	1	2	1	4
9	✓*	| 1 |	2	1	| 4 |
10	✓*	1	| 2 |	1	4
11	✓*	1	2	1	4
12	✓*	1	2	| 1 |	4
13	✓*	1	2	1	4
14	✓*	1	2	1	4
15	✓*	1	2	1	4
16	✓*	1	2	1	4
17	✓*	1	2	1	4
18	✓*	1	2	1	4
19	✓*	1	2	1	4
20	✓*	1	2	1	4
21	✓*	1	2	1	4
22	✓*	1	2	1	4
23	✓*	1	2	1	4
24	✓*	1	2	1	4
25	✓*	| 1 |	2	1	| 4 |
26	✓*	1	| 2 |	1	4
27	✓*	1	2	1	4
28	✓*	1	2	| 1 |	4
29	✓*	1	2	1	4
30	✓*	1	2	1	4
31	✗*	1	2	1	4
32	✗*	1	2	1	4
33	✗*	1	2	1	4

Table B.3: Verification TC_1 for $R2$ - objective

B.2. Test Case 2

t	Vessel r		Module m with energy level $l_{t,m}$							
	R1	R2	0	1	2	3	4	5	6	7
0	SL (1)	SL (2)	'R1 161.0 (F)	R1 161.0 (F)	R2 161.0 (F)	'R2 161.0 (F)	I1 161.0 (F)	I1 161.0 (F)	I2 161.0 (F)	I2 161.0 (F)
1	SL (1)	SL (2)	'R1 151.0 (I)	R1 161.0 (F)	R2 161.0 (F)	'R2 151.0 (I)	I1 161.0 (F)	I1 161.0 (F)	I2 161.0 (F)	I2 161.0 (F)
2	SL (1)	SL (2)	'R1 141.0 (I)	R1 161.0 (F)	R2 161.0 (F)	'R2 141.0 (I)	I1 161.0 (F)	I1 161.0 (F)	I2 161.0 (F)	I2 161.0 (F)
3	SL (1)	SL (2)	'R1 131.0 (I)	R1 161.0 (F)	R2 161.0 (F)	'R2 131.0 (I)	I1 161.0 (F)	I1 161.0 (F)	I2 161.0 (F)	I2 161.0 (F)
4	SL (1)	SL (2)	'R1 121.0 (I)	R1 161.0 (F)	R2 161.0 (F)	'R2 121.0 (I)	I1 161.0 (F)	I1 161.0 (F)	I2 161.0 (F)	I2 161.0 (F)
5	SL (1)	SL (2)	'R1 111.0 (I)	R1 161.0 (F)	R2 161.0 (F)	'R2 111.0 (I)	I1 161.0 (F)	I1 161.0 (F)	I2 161.0 (F)	I2 161.0 (F)
6	SL (1)	SL (2)	'R1 101.0 (I)	R1 161.0 (F)	R2 161.0 (F)	'R2 101.0 (I)	I1 161.0 (F)	I1 161.0 (F)	I2 161.0 (F)	I2 161.0 (F)
7	SL (1)	SL (2)	'R1 91.0 (I)	R1 161.0 (F)	R2 161.0 (F)	'R2 91.0 (I)	I1 161.0 (F)	I1 161.0 (F)	I2 161.0 (F)	I2 161.0 (F)
8	SL (1)	SL (2)	'R1 81.0 (I)	R1 161.0 (F)	R2 161.0 (F)	'R2 81.0 (I)	I1 161.0 (F)	I1 161.0 (F)	I2 161.0 (F)	I2 161.0 (F)
9	SL (1)	SL (2)	'R1 71.0 (I)	R1 161.0 (F)	R2 161.0 (F)	'R2 71.0 (I)	I1 161.0 (F)	I1 161.0 (F)	I2 161.0 (F)	I2 161.0 (F)
10	SL (1)	SL (2)	'R1 61.0 (I)	R1 161.0 (F)	R2 161.0 (F)	'R2 61.0 (I)	I1 161.0 (F)	I1 161.0 (F)	I2 161.0 (F)	I2 161.0 (F)
11	SL (1)	SL (2)	'R1 51.0 (I)	R1 161.0 (F)	R2 161.0 (F)	'R2 51.0 (I)	I1 161.0 (F)	I1 161.0 (F)	I2 161.0 (F)	I2 161.0 (F)
12	SL (1)	SL (2)	'R1 41.0 (I)	R1 161.0 (F)	R2 161.0 (F)	'R2 41.0 (I)	I1 161.0 (F)	I1 161.0 (F)	I2 161.0 (F)	I2 161.0 (F)
13	SL (1)	SL (2)	R1 31.0 (E)	'R1 161.0 (F)	'R2 161.0 (F)	R2 31.0 (E)	I1 161.0 (F)	I1 161.0 (F)	I2 161.0 (F)	I2 161.0 (F)
14	SL (1)	SL (2)	R1 31.0 (E)	'R1 151.0 (I)	'R2 151.0 (I)	R2 31.0 (E)	I1 161.0 (F)	I1 161.0 (F)	I2 161.0 (F)	I2 161.0 (F)
15	SL (1)	SL (2)	R1 31.0 (E)	'R1 141.0 (I)	'R2 141.0 (I)	R2 31.0 (E)	I1 161.0 (F)	I1 161.0 (F)	I2 161.0 (F)	I2 161.0 (F)
16	SL (1)	SL (2)	R1 31.0 (E)	'R1 131.0 (I)	'R2 131.0 (I)	R2 31.0 (E)	I1 161.0 (F)	I1 161.0 (F)	I2 161.0 (F)	I2 161.0 (F)

Table B.4: Verification $TC_{2,1}$

t	$SPos_{t,r}$	$StS_{t,r}$	$VS_{t,r}$	$SbOP_{t,r}$	T_{total}
0	✗*	1	2	1	4
1	✗*	1	2	1	4
2	✗*	1	2	1	4
3	✓*	1	2	1	4
4	✓*	1	2	1	4
5	✓*	1	2	1	4
6	✓*	1	2	1	4
7	✓*	1	2	1	4
8	✓*	1	2	1	4
9	✓*	1	2	1	4
10	✓*	1	2	1	4
11	✓*	1	2	1	4
12	✓*	1	2	1	4
13	✓*	1	2	1	4
14	✗*	1	2	1	4
15	✗*	1	2	1	4
16	✗*	1	2	1	4

Table B.5: Verification $TC_{2,1}$ for $R1$ - objective

t	$SPos_{t,r}$	$StS_{t,r}$	$VS_{t,r}$	$SbOP_{t,r}$	T_{total}
0	✗*	1	2	1	4
1	✗*	1	2	1	4
2	✗*	1	2	1	4
3	✓*	1	2	1	4
4	✓*	1	2	1	4
5	✓*	1	2	1	4
6	✓*	1	2	1	4
7	✓*	1	2	1	4
8	✓*	1	2	1	4
9	✓*	1	2	1	4
10	✓*	1	2	1	4
11	✓*	1	2	1	4
12	✓*	1	2	1	4
13	✓*	1	2	1	4
14	✗*	1	2	1	4
15	✗*	1	2	1	4
16	✗*	1	2	1	4

Table B.6: Verification $TC_{2,1}$ for $R2$ - objective

t	Vessel r		Module m with energy level $l_{t,m}$							
	R1	R2	0	1	2	3	4	5	6	7
0	SL (1)	SL (2)	R1 41.0 (F)	’R1 41.0 (F)	R2 41.0 (F)	’R2 41.0 (F)	I1 41.0 (F)	I1 41.0 (F)	I2 41.0 (F)	I2 41.0 (F)
1	SL (1)	SL (2)	R1 41.0 (F)	’R1 31.0 (I)	R2 41.0 (F)	’R2 31.0 (I)	I1 41.0 (F)	I1 41.0 (F)	I2 41.0 (F)	I2 41.0 (F)
2	SL (1)	SL (2)	R1 41.0 (F)	’R1 21.0 (I)	R2 41.0 (F)	’R2 21.0 (I)	I1 41.0 (F)	I1 41.0 (F)	I2 41.0 (F)	I2 41.0 (F)
3	StS (1)	StS (2)	R1 41.0 (F)	’R1 11.0 (I)	R2 41.0 (F)	’R2 11.0 (I)	IS1 41.0 (F)	I1 41.0 (F)	IS2 41.0 (F)	I2 41.0 (F)
4	VS (1)	VS (2)	R1 41.0 (F)	θS1 1.0 (E)	R2 41.0 (F)	θS2 1.0 (E)	ΔS1 41.0 (F)	I1 41.0 (F)	ΔS2 41.0 (F)	I2 41.0 (F)
5	VS (1)	VS (2)	R1 41.0 (F)	θS1 1.0 (E)	R2 41.0 (F)	θS2 1.0 (E)	ΔS1 41.0 (F)	I1 41.0 (F)	ΔS2 41.0 (F)	I2 41.0 (F)
6	SbOP (1)	SbOP (2)	’R1 41.0 (F)	C1 1.0 (E)	’R2 41.0 (F)	C2 1.0 (E)	R1 41.0 (F)	I1 41.0 (F)	R2 41.0 (F)	I2 41.0 (F)
7	SL (1)	SL (2)	’R1 31.0 (I)	C1 11.0 (I)	’R2 31.0 (I)	C2 11.0 (I)	R1 41.0 (F)	I1 41.0 (F)	R2 41.0 (F)	I2 41.0 (F)
8	StS (1)	SL (2)	’R1 21.0 (I)	C1 21.0 (I)	’R2 21.0 (I)	C2 21.0 (I)	R1 41.0 (F)	IS1 41.0 (F)	R2 41.0 (F)	I2 41.0 (F)
9	VS (1)	StS (2)	θS1 11.0 (I)	C1 31.0 (I)	’R2 11.0 (I)	C2 31.0 (I)	R1 41.0 (F)	ΔS1 41.0 (F)	R2 41.0 (F)	IS2 41.0 (F)
10	VS (1)	VS (2)	θS1 11.0 (I)	I1 41.0 (F)	θS2 1.0 (E)	I2 41.0 (F)	R1 41.0 (F)	ΔS1 41.0 (F)	R2 41.0 (F)	ΔS2 41.0 (F)
11	SbOP (1)	VS (2)	C1 11.0 (I)	I1 41.0 (F)	θS2 1.0 (E)	I2 41.0 (F)	’R1 41.0 (F)	R1 41.0 (F)	R2 41.0 (F)	ΔS2 41.0 (F)
12	SL (1)	SbOP (2)	C1 21.0 (I)	I1 41.0 (F)	C2 1.0 (E)	I2 41.0 (F)	’R1 31.0 (I)	R1 41.0 (F)	’R2 41.0 (F)	R2 41.0 (F)
13	SL (1)	SL (2)	C1 31.0 (I)	I1 41.0 (F)	C2 11.0 (I)	I2 41.0 (F)	’R1 21.0 (I)	R1 41.0 (F)	’R2 31.0 (I)	R2 41.0 (F)
14	SL (1)	SL (2)	I1 41.0 (F)	I1 41.0 (F)	C2 21.0 (I)	I2 41.0 (F)	’R1 11.0 (I)	R1 41.0 (F)	’R2 21.0 (I)	R2 41.0 (F)
15	SL (1)	SL (2)	I1 41.0 (F)	I1 41.0 (F)	C2 31.0 (I)	I2 41.0 (F)	R1 1.0 (E)	’R1 41.0 (F)	’R2 11.0 (I)	R2 41.0 (F)
16	SL (1)	SL (2)	I1 41.0 (F)	I1 41.0 (F)	I2 41.0 (F)	I2 41.0 (F)	R1 1.0 (E)	’R1 31.0 (I)	R2 1.0 (E)	’R2 41.0 (F)

Table B.7: Verification $TC_{2,2}$

t	$SPos_{t,r}$	$StS_{t,r}$	$VS_{t,r}$	$SbOP_{t,r}$	T_{total}
0	✗*	1	2	1	4
1	✗*	1	2	1	4
2	✗*	1	2	1	4
3	✓*	| 1 |	2	1	| 4 |
4	✓*	1	| 2 |	1	4
5	✓*	1	2	1	4
6	✓*	1	2	| 1 |	4
7	✓*	1	2	1	4
8	✓*	| 1 |	2	1	| 4 |
9	✓*	1	| 2 |	1	4
10	✓*	1	2	1	4
11	✓*	1	2	| 1 |	4
12	✓*	1	2	1	4
13	✓*	1	2	1	4
14	✗*	1	2	1	4
15	✗*	1	2	1	4
16	✗*	1	2	1	4

Table B.8: Verification $TC_{2,1}$ for $R1$ - objective

t	$SPos_{t,r}$	$StS_{t,r}$	$VS_{t,r}$	$SbOP_{t,r}$	T_{total}
0	✗*	1	2	1	4
1	✗*	1	2	1	4
2	✗*	1	2	1	4
3	✓*	| 1 |	2	1	| 4 |
4	✓*	1	| 2 |	1	4
5	✓*	1	2	1	4
6	✓*	1	2	| 1 |	4
7	✓*	1	2	1	4
8	✓*	1	2	1	4
9	✓*	| 1 |	2	1	| 4 |
10	✓*	1	| 2 |	1	4
11	✓*	1	2	1	4
12	✓*	1	2	| 1 |	4
13	✓*	1	2	1	4
14	✗*	1	2	1	4
15	✗*	1	2	1	4
16	✗*	1	2	1	4

Table B.9: Verification $TC_{2,1}$ for $R2$ - objective

B.3. Test Case 3

t	Vessel r		Module m with energy level $l_{t,m}$							
	R1	R2	0	1	2	3	4	5	6	7
0	SL (1)	SL (2)	’R1 81.0 (F)	R1 81.0 (F)	’R2 81.0 (F)	R2 81.0 (F)	I1 81.0 (F)	I1 81.0 (F)	I2 81.0 (F)	I2 81.0 (F)
1	SL (1)	SL (2)	’R1 71.0 (I)	R1 81.0 (F)	’R2 71.0 (I)	R2 81.0 (F)	I1 81.0 (F)	I1 81.0 (F)	I2 81.0 (F)	I2 81.0 (F)
2	SL (1)	SL (2)	’R1 61.0 (I)	R1 81.0 (F)	’R2 61.0 (I)	R2 81.0 (F)	I1 81.0 (F)	I1 81.0 (F)	I2 81.0 (F)	I2 81.0 (F)
3	StS (1)	SL (2)	’R1 51.0 (I)	R1 81.0 (F)	’R2 51.0 (I)	R2 81.0 (F)	IS1 81.0 (F)	I1 81.0 (F)	I2 81.0 (F)	I2 81.0 (F)
4	VS (1)	SL (2)	θS1 41.0 (I)	R1 81.0 (F)	’R2 41.0 (I)	R2 81.0 (F)	ΔS1 81.0 (F)	I1 81.0 (F)	I2 81.0 (F)	I2 81.0 (F)
5	VS (1)	SL (2)	θS1 41.0 (I)	R1 81.0 (F)	’R2 31.0 (I)	R2 81.0 (F)	ΔS1 81.0 (F)	I1 81.0 (F)	I2 81.0 (F)	I2 81.0 (F)
6	SbOP (1)	SL (2)	C1 41.0 (I)	’R1 81.0 (F)	’R2 21.0 (I)	R2 81.0 (F)	R1 81.0 (F)	I1 81.0 (F)	I2 81.0 (F)	I2 81.0 (F)
7	SL (1)	SL (2)	C1 46.0 (I)	’R1 71.0 (I)	R2 11.0 (E)	’R2 81.0 (F)	R1 81.0 (F)	I1 81.0 (F)	I2 81.0 (F)	I2 81.0 (F)
8	SL (1)	SL (2)	C1 51.0 (I)	’R1 61.0 (I)	R2 11.0 (E)	’R2 71.0 (I)	R1 81.0 (F)	I1 81.0 (F)	I2 81.0 (F)	I2 81.0 (F)
9	SL (1)	SL (2)	C1 56.0 (I)	’R1 51.0 (I)	R2 11.0 (E)	’R2 61.0 (I)	R1 81.0 (F)	I1 81.0 (F)	I2 81.0 (F)	I2 81.0 (F)
10	SL (1)	StS (2)	C1 61.0 (I)	’R1 41.0 (I)	R2 11.0 (E)	’R2 51.0 (I)	R1 81.0 (F)	I1 81.0 (F)	IS2 81.0 (F)	IS2 81.0 (F)
11	SL (1)	VS (2)	C1 66.0 (I)	’R1 31.0 (I)	θS2 11.0 (E)	θS2 41.0 (I)	R1 81.0 (F)	I1 81.0 (F)	ΔS2 81.0 (F)	ΔS2 81.0 (F)
12	SL (1)	VS (2)	C1 71.0 (I)	’R1 21.0 (I)	θS2 11.0 (E)	θS2 41.0 (I)	R1 81.0 (F)	I1 81.0 (F)	ΔS2 81.0 (F)	ΔS2 81.0 (F)
13	SL (1)	SbOP (2)	C1 76.0 (I)	R1 11.0 (E)	C2 11.0 (E)	C2 41.0 (I)	’R1 81.0 (F)	I1 81.0 (F)	’R2 81.0 (F)	R2 81.0 (F)
14	SL (1)	SL (2)	I1 81.0 (F)	R1 11.0 (E)	C2 16.0 (E)	C2 46.0 (I)	’R1 71.0 (I)	I1 81.0 (F)	’R2 71.0 (I)	R2 81.0 (F)
15	SL (1)	SL (2)	I1 81.0 (F)	R1 11.0 (E)	C2 21.0 (I)	C2 51.0 (I)	’R1 61.0 (I)	I1 81.0 (F)	’R2 61.0 (I)	R2 81.0 (F)
16	SL (1)	SL (2)	I1 81.0 (F)	R1 11.0 (E)	C2 26.0 (I)	C2 56.0 (I)	’R1 51.0 (I)	I1 81.0 (F)	’R2 51.0 (I)	R2 81.0 (F)
17	SL (1)	SL (2)	I1 81.0 (F)	R1 11.0 (E)	C2 31.0 (I)	C2 61.0 (I)	’R1 41.0 (I)	I1 81.0 (F)	’R2 41.0 (I)	R2 81.0 (F)
18	StS (1)	SL (2)	IS1 81.0 (F)	R1 11.0 (E)	C2 36.0 (I)	C2 66.0 (I)	’R1 31.0 (I)	IS1 81.0 (F)	’R2 31.0 (I)	R2 81.0 (F)
19	VS (1)	SL (2)	ΔS1 81.0 (F)	θS1 11.0 (E)	C2 41.0 (I)	C2 71.0 (I)	θS1 21.0 (I)	ΔS1 81.0 (F)	’R2 21.0 (I)	R2 81.0 (F)
20	VS (1)	SL (2)	ΔS1 81.0 (F)	θS1 11.0 (E)	C2 46.0 (I)	C2 76.0 (I)	θS1 21.0 (I)	ΔS1 81.0 (F)	R2 11.0 (E)	’R2 81.0 (F)
21	SbOP (1)	SL (2)	’R1 81.0 (F)	C1 11.0 (E)	C2 51.0 (I)	I2 81.0 (F)	C1 21.0 (I)	R1 81.0 (F)	R2 11.0 (E)	’R2 71.0 (I)
22	SL (1)	SL (2)	’R1 71.0 (I)	C1 16.0 (E)	C2 56.0 (I)	I2 81.0 (F)	C1 26.0 (I)	R1 81.0 (F)	R2 11.0 (E)	’R2 61.0 (I)
23	SL (1)	SL (2)	’R1 61.0 (I)	C1 21.0 (I)	C2 61.0 (I)	I2 81.0 (F)	C1 31.0 (I)	R1 81.0 (F)	R2 11.0 (E)	’R2 51.0 (I)
24	SL (1)	StS (2)	’R1 51.0 (I)	C1 26.0 (I)	C2 66.0 (I)	IS2 81.0 (F)	C1 36.0 (I)	R1 81.0 (F)	R2 11.0 (E)	’R2 41.0 (I)
25	SL (1)	VS (2)	’R1 41.0 (I)	C1 31.0 (I)	C2 71.0 (I)	ΔS2 81.0 (F)	C1 41.0 (I)	R1 81.0 (F)	R2 11.0 (E)	θS2 31.0 (I)
26	SL (1)	VS (2)	’R1 31.0 (I)	C1 36.0 (I)	C2 76.0 (I)	ΔS2 81.0 (F)	C1 46.0 (I)	R1 81.0 (F)	R2 11.0 (E)	θS2 31.0 (I)
27	SL (1)	SbOP (2)	’R1 21.0 (I)	C1 41.0 (I)	I2 81.0 (F)	’R2 81.0 (F)	C1 51.0 (I)	R1 81.0 (F)	R2 11.0 (E)	C2 31.0 (I)
28	SL (1)	SL (2)	R1 11.0 (E)	C1 46.0 (I)	I2 81.0 (F)	’R2 71.0 (I)	C1 56.0 (I)	’R1 81.0 (F)	R2 11.0 (E)	C2 36.0 (I)
29	SL (1)	SL (2)	R1 11.0 (E)	C1 51.0 (I)	I2 81.0 (F)	’R2 61.0 (I)	C1 61.0 (I)	’R1 71.0 (I)	R2 11.0 (E)	C2 41.0 (I)
30	SL (1)	SL (2)	R1 11.0 (E)	C1 56.0 (I)	I2 81.0 (F)	’R2 51.0 (I)	C1 66.0 (I)	’R1 61.0 (I)	R2 11.0 (E)	C2 46.0 (I)
31	SL (1)	SL (2)	R1 11.0 (E)	C1 61.0 (I)	I2 81.0 (F)	’R2 41.0 (I)	C1 71.0 (I)	’R1 51.0 (I)	R2 11.0 (E)	C2 51.0 (I)
32	SL (1)	SL (2)	R1 11.0 (E)	C1 66.0 (I)	I2 81.0 (F)	’R2 31.0 (I)	C1 76.0 (I)	’R1 41.0 (I)	R2 11.0 (E)	C2 56.0 (I)
33	SL (1)	SL (2)	R1 11.0 (E)	C1 71.0 (I)	I2 81.0 (F)	’R2 21.0 (I)	I1 81.0 (F)	’R1 31.0 (I)	R2 11.0 (E)	C2 61.0 (I)

Table B.10: Verification TC_3

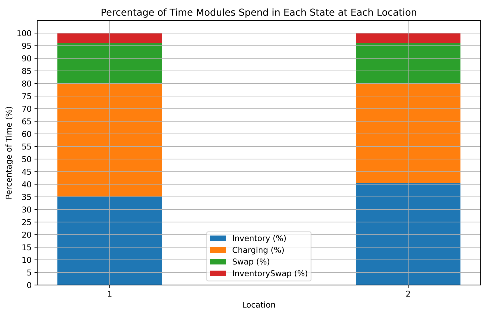

Figure B.1: Verification TC_3 - Optimal usage

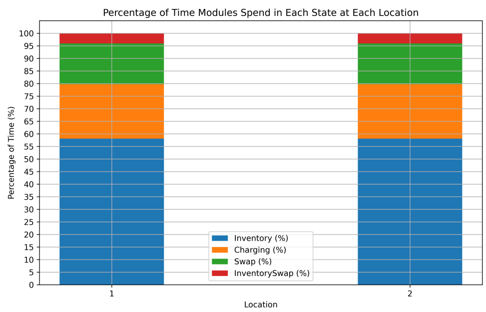

Figure B.2: Verification TC_{BC} - Optimal usage

t	$SPos_{t,r}$	$StS_{t,r}$	$VS_{t,r}$	$SbOP_{t,r}$	T_{total}
0	✗*	1	2	1	4
1	✗*	1	2	1	4
2	✗*	1	2	1	4
3	✓*	| 1 |	2	1	| 4 |
4	✓*	1	| 2 |	1	4
5	✓*	1	2	1	4
6	✓*	1	2	| 1 |	4
7	✓*	1	2	1	4
8	✓*	1	2	1	4
9	✓*	1	2	1	4
10	✓*	1	2	1	4
11	✓*	1	2	1	4
12	✓*	1	2	1	4
13	✓*	1	2	1	4
14	✓*	1	2	1	4
15	✓*	1	2	1	4
16	✓*	1	2	1	4
17	✓*	1	2	1	4
18	✓*	| 1 |	2	1	| 4 |
19	✓*	1	| 2 |	1	4
20	✓*	1	2	1	4
21	✓*	1	2	| 1 |	4
22	✓*	1	2	1	4
23	✓*	1	2	1	4
24	✓*	1	2	1	4
25	✓*	1	2	1	4
26	✓-	1	2	1	4
27	✓-	1	2	1	4
28	✓*	1	2	1	4
29	✓*	1	2	1	4
30	✓*	1	2	1	4
31	✗*	1	2	1	4
32	✗*	1	2	1	4
33	✗*	1	2	1	4

Table B.11: Verification TC_3 for $R1$ - Objective

t	$SPos_{t,r}$	$StS_{t,r}$	$VS_{t,r}$	$SbOP_{t,r}$	T_{total}
0	✗*	1	2	1	4
1	✗*	1	2	1	4
2	✗*	1	2	1	4
3	✓*	1	2	1	4
4	✓*	1	2	1	4
5	✓*	1	2	1	4
6	✓*	1	2	1	4
7	✓*	1	2	1	4
8	✓*	1	2	1	4
9	✓*	1	2	1	4
10	✓*	| 1 |	2	1	| 4 |
11	✓*	1	| 2 |	1	4
12	✓*	1	2	1	4
13	✓*	1	2	| 1 |	4
14	✓*	1	2	1	4
15	✓*	1	2	1	4
16	✓*	1	2	1	4
17	✓*	1	2	1	4
18	✓*	1	2	1	4
19	✓*	1	2	1	4
20	✓*	1	2	1	4
21	✓*	1	2	1	4
22	✓*	1	2	1	4
23	✓*	1	2	1	4
24	✓*	| 1 |	2	1	| 4 |
25	✓*	1	| 2 |	1	4
26	✓*	1	2	1	4
27	✓*	1	2	| 1 |	4
28	✓*	1	2	1	4
29	✓*	1	2	1	4
30	✓*	1	2	1	4
31	✗*	1	2	1	4
32	✗*	1	2	1	4
33	✗*	1	2	1	4

Table B.12: Verification TC_3 for $R2$ - Objective

B.4. Test Case 4

t	Vessel r		Module m with energy level $l_{t,m}$							
	R1	R2	0	1	2	3	4	5	6	7
0	SL (1)	SL (2)	R1 81.0 (F)	’R1 81.0 (F)	’R2 81.0 (F)	R2 81.0 (F)	I1 81.0 (F)	I1 81.0 (F)	I2 81.0 (F)	I2 81.0 (F)
1	SL (1)	SL (2)	R1 81.0 (F)	’R1 71.0 (I)	’R2 71.0 (I)	R2 81.0 (F)	I1 81.0 (F)	I1 81.0 (F)	I2 81.0 (F)	I2 81.0 (F)
2	SL (1)	SL (2)	R1 81.0 (F)	’R1 61.0 (I)	’R2 61.0 (I)	R2 81.0 (F)	I1 81.0 (F)	I1 81.0 (F)	I2 81.0 (F)	I2 81.0 (F)
3	SL (1)	SL (2)	R1 81.0 (F)	’R1 51.0 (I)	’R2 51.0 (I)	R2 81.0 (F)	I1 81.0 (F)	I1 81.0 (F)	I2 81.0 (F)	I2 81.0 (F)
4	SL (1)	SL (2)	R1 81.0 (F)	’R1 41.0 (I)	’R2 41.0 (I)	R2 81.0 (F)	I1 81.0 (F)	I1 81.0 (F)	I2 81.0 (F)	I2 81.0 (F)
5	SL (1)	SL (2)	R1 81.0 (F)	’R1 31.0 (I)	’R2 31.0 (I)	R2 81.0 (F)	I1 81.0 (F)	I1 81.0 (F)	I2 81.0 (F)	I2 81.0 (F)
6	SL (1)	SL (2)	R1 81.0 (F)	’R1 21.0 (I)	’R2 21.0 (I)	R2 81.0 (F)	I1 81.0 (F)	I1 81.0 (F)	I2 81.0 (F)	I2 81.0 (F)
7	SL (1)	SL (2)	’R1 81.0 (F)	R1 11.0 (E)	R2 11.0 (E)	’R2 81.0 (F)	I1 81.0 (F)	I1 81.0 (F)	I2 81.0 (F)	I2 81.0 (F)
8	SL (1)	SL (2)	’R1 71.0 (I)	R1 11.0 (E)	R2 11.0 (E)	’R2 71.0 (I)	I1 81.0 (F)	I1 81.0 (F)	I2 81.0 (F)	I2 81.0 (F)
9	StS (1)	StS (2)	’R1 61.0 (I)	R1 11.0 (E)	R2 11.0 (E)	’R2 61.0 (I)	IS1 81.0 (F)	IS1 81.0 (F)	IS2 81.0 (F)	IS2 81.0 (F)
10	VS (1)	VS (2)	θS1 21.0 (I)	θS1 11.0 (E)	θS2 11.0 (E)	θS2 21.0 (I)	ΔS1 81.0 (F)	ΔS1 81.0 (F)	ΔS2 81.0 (F)	ΔS2 81.0 (F)
11	VS (1)	VS (2)	θS1 21.0 (I)	θS1 11.0 (E)	θS2 11.0 (E)	θS2 21.0 (I)	ΔS1 81.0 (F)	ΔS1 81.0 (F)	ΔS2 81.0 (F)	ΔS2 81.0 (F)
12	SbOP (1)	SbOP (2)	C1 21.0 (I)	C1 11.0 (E)	C2 11.0 (E)	C2 21.0 (I)	’R1 81.0 (F)	R1 81.0 (F)	’R2 81.0 (F)	R2 81.0 (F)
13	SL (1)	SL (2)	C1 31.0 (I)	C1 21.0 (I)	C2 21.0 (I)	C2 31.0 (I)	’R1 41.0 (I)	R1 81.0 (F)	’R2 41.0 (I)	R2 81.0 (F)
14	SL (1)	SL (2)	C1 41.0 (I)	C1 31.0 (I)	C2 31.0 (I)	C2 41.0 (I)	’R1 31.0 (I)	R1 81.0 (F)	’R2 31.0 (I)	R2 81.0 (F)
15	SL (1)	SL (2)	C1 51.0 (I)	C1 41.0 (I)	C2 41.0 (I)	C2 51.0 (I)	’R1 21.0 (I)	R1 81.0 (F)	’R2 21.0 (I)	R2 81.0 (F)
16	SL (1)	SL (2)	C1 61.0 (I)	C1 51.0 (I)	C2 51.0 (I)	C2 61.0 (I)	R1 11.0 (E)	’R1 81.0 (F)	R2 11.0 (E)	’R2 81.0 (F)

Table B.13: Verification TC_4

<table>
<tr><th>t</th><th>$SPos_{t,r}$</th><th>$StS_{t,r}$</th><th>$VS_{t,r}$</th><th>$SbOP_{t,r}$</th><th>T_{total}</th></tr>
<tr><td>0</td><td>✗*</td><td>1</td><td>4</td><td>1</td><td>6</td></tr>
<tr><td>1</td><td>✗*</td><td>1</td><td>4</td><td>1</td><td>6</td></tr>
<tr><td>2</td><td>✗*</td><td>1</td><td>4</td><td>1</td><td>6</td></tr>
<tr><td>3</td><td>✗*</td><td>1</td><td>4</td><td>1</td><td>6</td></tr>
<tr><td>4</td><td>✗*</td><td>1</td><td>4</td><td>1</td><td>6</td></tr>
<tr><td>5</td><td>✓*</td><td>1</td><td>4</td><td>1</td><td>6</td></tr>
<tr><td>6</td><td>✓*</td><td>1</td><td>4</td><td>1</td><td>6</td></tr>
<tr><td>7</td><td>✓*</td><td>1</td><td>4</td><td>1</td><td>6</td></tr>
<tr><td>8</td><td>✓*</td><td>1</td><td>4</td><td>1</td><td>6</td></tr>
<tr><td>9</td><td>✓*</td><td>1</td><td>4</td><td>1</td><td>6</td></tr>
<tr><td>10</td><td>✓*</td><td>1</td><td>4</td><td>1</td><td>6</td></tr>
<tr><td>11</td><td>✓*</td><td>1</td><td>4</td><td>1</td><td>6</td></tr>
<tr><td>12</td><td>✓*</td><td>| 1 |</td><td>4</td><td>1</td><td>| 6 |</td></tr>
<tr><td>13</td><td>✓*</td><td>1</td><td>| 4 |</td><td>1</td><td>6</td></tr>
<tr><td>14</td><td>✓*</td><td>1</td><td>4</td><td>1</td><td>6</td></tr>
<tr><td>15</td><td>✓*</td><td>1</td><td>4</td><td>1</td><td>6</td></tr>
<tr><td>16</td><td>✓*</td><td>1</td><td>4</td><td>1</td><td>6</td></tr>
<tr><td>17</td><td>✓*</td><td>1</td><td>4</td><td>| 1 |</td><td>6</td></tr>
<tr><td>18</td><td>✓*</td><td>1</td><td>4</td><td>1</td><td>6</td></tr>
<tr><td>19</td><td>✓*</td><td>1</td><td>4</td><td>1</td><td>6</td></tr>
<tr><td>20</td><td>✓*</td><td>1</td><td>4</td><td>1</td><td>6</td></tr>
<tr><td>21</td><td>✓*</td><td>1</td><td>4</td><td>1</td><td>6</td></tr>
<tr><td>22</td><td>✓*</td><td>1</td><td>4</td><td>1</td><td>6</td></tr>
<tr><td>23</td><td>✓*</td><td>| 1 |</td><td>4</td><td>1</td><td>| 6 |</td></tr>
<tr><td>24</td><td>✓*</td><td>1</td><td>| 4 |</td><td>1</td><td>6</td></tr>
<tr><td>25</td><td>✓*</td><td>1</td><td>4</td><td>1</td><td>6</td></tr>
<tr><td>26</td><td>✓-</td><td>1</td><td>4</td><td>1</td><td>6</td></tr>
<tr><td>27</td><td>✓-</td><td>1</td><td>4</td><td>1</td><td>6</td></tr>
<tr><td>28</td><td>✓*</td><td>1</td><td>4</td><td>| 1 |</td><td>6</td></tr>
<tr><td>29</td><td>✗*</td><td>1</td><td>4</td><td>1</td><td>6</td></tr>
<tr><td>30</td><td>✗*</td><td>1</td><td>4</td><td>1</td><td>6</td></tr>
<tr><td>31</td><td>✗*</td><td>1</td><td>4</td><td>1</td><td>6</td></tr>
<tr><td>32</td><td>✗*</td><td>1</td><td>4</td><td>1</td><td>6</td></tr>
<tr><td>33</td><td>✗*</td><td>1</td><td>4</td><td>1</td><td>6</td></tr>
</table>

Table B.14: Verification TC_4 for $R1$ - Objective

<table>
<tr><th>t</th><th>$SPos_{t,r}$</th><th>$StS_{t,r}$</th><th>$VS_{t,r}$</th><th>$SbOP_{t,r}$</th><th>T_{total}</th></tr>
<tr><td>0</td><td>✗*</td><td>1</td><td>4</td><td>1</td><td>6</td></tr>
<tr><td>1</td><td>✗*</td><td>1</td><td>4</td><td>1</td><td>6</td></tr>
<tr><td>2</td><td>✗*</td><td>1</td><td>4</td><td>1</td><td>6</td></tr>
<tr><td>3</td><td>✗*</td><td>1</td><td>4</td><td>1</td><td>6</td></tr>
<tr><td>4</td><td>✗*</td><td>1</td><td>4</td><td>1</td><td>6</td></tr>
<tr><td>5</td><td>✓*</td><td>1</td><td>4</td><td>1</td><td>6</td></tr>
<tr><td>6</td><td>✓*</td><td>1</td><td>4</td><td>1</td><td>6</td></tr>
<tr><td>7</td><td>✓*</td><td>1</td><td>4</td><td>1</td><td>6</td></tr>
<tr><td>8</td><td>✓*</td><td>1</td><td>4</td><td>1</td><td>6</td></tr>
<tr><td>9</td><td>✓*</td><td>1</td><td>4</td><td>1</td><td>6</td></tr>
<tr><td>10</td><td>✓*</td><td>| 1 |</td><td>4</td><td>1</td><td>| 6 |</td></tr>
<tr><td>11</td><td>✓*</td><td>1</td><td>| 4 |</td><td>1</td><td>6</td></tr>
<tr><td>12</td><td>✓*</td><td>1</td><td>4</td><td>1</td><td>6</td></tr>
<tr><td>13</td><td>✓*</td><td>1</td><td>4</td><td>1</td><td>6</td></tr>
<tr><td>14</td><td>✓*</td><td>1</td><td>4</td><td>1</td><td>6</td></tr>
<tr><td>15</td><td>✓*</td><td>1</td><td>4</td><td>| 1 |</td><td>6</td></tr>
<tr><td>16</td><td>✓*</td><td>1</td><td>4</td><td>1</td><td>6</td></tr>
<tr><td>17</td><td>✓*</td><td>1</td><td>4</td><td>1</td><td>6</td></tr>
<tr><td>18</td><td>✓*</td><td>1</td><td>4</td><td>1</td><td>6</td></tr>
<tr><td>19</td><td>✓*</td><td>1</td><td>4</td><td>1</td><td>6</td></tr>
<tr><td>20</td><td>✓*</td><td>1</td><td>4</td><td>1</td><td>6</td></tr>
<tr><td>21</td><td>✓*</td><td>1</td><td>4</td><td>1</td><td>6</td></tr>
<tr><td>22</td><td>✓*</td><td>1</td><td>4</td><td>1</td><td>6</td></tr>
<tr><td>23</td><td>✓*</td><td>| 1 |</td><td>4</td><td>1</td><td>| 6 |</td></tr>
<tr><td>24</td><td>✓*</td><td>1</td><td>| 4 |</td><td>1</td><td>6</td></tr>
<tr><td>25</td><td>✓*</td><td>1</td><td>4</td><td>1</td><td>6</td></tr>
<tr><td>26</td><td>✓*</td><td>1</td><td>4</td><td>1</td><td>6</td></tr>
<tr><td>27</td><td>✓*</td><td>1</td><td>4</td><td>1</td><td>6</td></tr>
<tr><td>28</td><td>✓*</td><td>1</td><td>4</td><td>| 1 |</td><td>6</td></tr>
<tr><td>29</td><td>✗*</td><td>1</td><td>4</td><td>1</td><td>6</td></tr>
<tr><td>30</td><td>✗*</td><td>1</td><td>4</td><td>1</td><td>6</td></tr>
<tr><td>31</td><td>✗*</td><td>1</td><td>4</td><td>1</td><td>6</td></tr>
<tr><td>32</td><td>✗*</td><td>1</td><td>4</td><td>1</td><td>6</td></tr>
<tr><td>33</td><td>✗*</td><td>1</td><td>4</td><td>1</td><td>6</td></tr>
</table>

Table B.15: Verification TC_4 for $R2$ - Objective

B.5. Test Case 5

t	Vessel r		Module m with energy level $l_{t,m}$							
	R1	R2	0	1	2	3	4	5	6	7
0	SL (1)	SL (2)	’R1 81.0 (F)	R1 81.0 (F)	R2 81.0 (F)	’R2 81.0 (F)	I1 81.0 (F)	I1 81.0 (F)	I2 81.0 (F)	I2 81.0 (F)
1	SL (1)	SL (2)	’R1 71.0 (I)	R1 81.0 (F)	R2 81.0 (F)	’R2 71.0 (I)	I1 81.0 (F)	I1 81.0 (F)	I2 81.0 (F)	I2 81.0 (F)
2	SL (1)	SL (2)	’R1 61.0 (I)	R1 81.0 (F)	R2 81.0 (F)	’R2 61.0 (I)	I1 81.0 (F)	I1 81.0 (F)	I2 81.0 (F)	I2 81.0 (F)
3	SL (1)	SL (2)	’R1 51.0 (I)	R1 81.0 (F)	R2 81.0 (F)	’R2 51.0 (I)	I1 81.0 (F)	I1 81.0 (F)	I2 81.0 (F)	I2 81.0 (F)
4	SL (1)	SL (2)	’R1 41.0 (I)	R1 81.0 (F)	R2 81.0 (F)	’R2 41.0 (I)	I1 81.0 (F)	I1 81.0 (F)	I2 81.0 (F)	I2 81.0 (F)
5	SL (1)	SL (2)	’R1 31.0 (I)	R1 81.0 (F)	R2 81.0 (F)	’R2 31.0 (I)	I1 81.0 (F)	I1 81.0 (F)	I2 81.0 (F)	I2 81.0 (F)
6	SL (1)	SL (2)	’R1 21.0 (I)	R1 81.0 (F)	R2 81.0 (F)	’R2 21.0 (I)	I1 81.0 (F)	I1 81.0 (F)	I2 81.0 (F)	I2 81.0 (F)
7	SL (1)	SL (2)	R1 11.0 (E)	’R1 81.0 (F)	’R2 81.0 (F)	R2 11.0 (E)	I1 81.0 (F)	I1 81.0 (F)	I2 81.0 (F)	I2 81.0 (F)
8	SL (1)	SL (2)	R1 11.0 (E)	’R1 71.0 (I)	’R2 71.0 (I)	R2 11.0 (E)	I1 81.0 (F)	I1 81.0 (F)	I2 81.0 (F)	I2 81.0 (F)
9	SL (1)	SL (2)	R1 11.0 (E)	’R1 61.0 (I)	’R2 61.0 (I)	R2 11.0 (E)	I1 81.0 (F)	I1 81.0 (F)	I2 81.0 (F)	I2 81.0 (F)
10	SL (1)	StS (2)	R1 11.0 (E)	’R1 51.0 (I)	’R2 51.0 (I)	R2 11.0 (E)	I1 81.0 (F)	I1 81.0 (F)	IS2 81.0 (F)	IS2 81.0 (F)
11	SL (1)	VS (2)	R1 11.0 (E)	’R1 41.0 (I)	θS2 41.0 (I)	θS2 11.0 (E)	I1 81.0 (F)	I1 81.0 (F)	ΔS2 81.0 (F)	ΔS2 81.0 (F)
12	StS (1)	VS (2)	R1 11.0 (E)	’R1 31.0 (I)	θS2 41.0 (I)	θS2 11.0 (E)	I1 81.0 (F)	IS1 81.0 (F)	ΔS2 81.0 (F)	ΔS2 81.0 (F)
13	VS (1)	VS (2)	R1 11.0 (E)	θS1 21.0 (I)	θS2 41.0 (I)	θS2 11.0 (E)	I1 81.0 (F)	ΔS1 81.0 (F)	ΔS2 81.0 (F)	ΔS2 81.0 (F)
14	VS (1)	VS (2)	R1 11.0 (E)	θS1 21.0 (I)	θS2 41.0 (I)	θS2 11.0 (E)	I1 81.0 (F)	ΔS1 81.0 (F)	ΔS2 81.0 (F)	ΔS2 81.0 (F)
15	VS (1)	SbOP (2)	R1 11.0 (E)	θS1 21.0 (I)	C2 41.0 (I)	C2 11.0 (E)	I1 81.0 (F)	ΔS1 81.0 (F)	R2 81.0 (F)	’R2 81.0 (F)
16	VS (1)	SL (2)	R1 11.0 (E)	θS1 21.0 (I)	C2 51.0 (I)	C2 21.0 (I)	I1 81.0 (F)	ΔS1 81.0 (F)	R2 81.0 (F)	’R2 71.0 (I)
17	SbOP (1)	SL (2)	R1 11.0 (E)	C1 21.0 (I)	C2 61.0 (I)	C2 31.0 (I)	I1 81.0 (F)	’R1 81.0 (F)	R2 81.0 (F)	’R2 61.0 (I)
18	SL (1)	SL (2)	R1 11.0 (E)	C1 31.0 (I)	C2 71.0 (I)	C2 41.0 (I)	I1 81.0 (F)	’R1 71.0 (I)	R2 81.0 (F)	’R2 51.0 (I)
19	SL (1)	SL (2)	R1 11.0 (E)	C1 41.0 (I)	I2 81.0 (F)	C2 51.0 (I)	I1 81.0 (F)	’R1 61.0 (I)	R2 81.0 (F)	’R2 41.0 (I)
20	SL (1)	SL (2)	R1 11.0 (E)	C1 51.0 (I)	I2 81.0 (F)	C2 61.0 (I)	I1 81.0 (F)	’R1 51.0 (I)	R2 81.0 (F)	’R2 31.0 (I)
21	SL (1)	SL (2)	R1 11.0 (E)	C1 61.0 (I)	I2 81.0 (F)	C2 71.0 (I)	I1 81.0 (F)	’R1 41.0 (I)	R2 81.0 (F)	’R2 21.0 (I)
22	SL (1)	SL (2)	R1 11.0 (E)	C1 71.0 (I)	I2 81.0 (F)	I2 81.0 (F)	I1 81.0 (F)	’R1 31.0 (I)	’R2 81.0 (F)	R2 11.0 (E)
23	StS (1)	StS (2)	R1 11.0 (E)	I1 81.0 (F)	IS2 81.0 (F)	I2 81.0 (F)	IS1 81.0 (F)	’R1 21.0 (I)	’R2 71.0 (I)	R2 11.0 (E)
24	VS (1)	VS (2)	θS1 11.0 (E)	I1 81.0 (F)	ΔS2 81.0 (F)	I2 81.0 (F)	ΔS1 81.0 (F)	R1 11.0 (E)	θS2 61.0 (I)	R2 11.0 (E)
25	VS (1)	VS (2)	θS1 11.0 (E)	I1 81.0 (F)	ΔS2 81.0 (F)	I2 81.0 (F)	ΔS1 81.0 (F)	R1 11.0 (E)	θS2 61.0 (I)	R2 11.0 (E)
26	VS (1)	VS (2)	θS1 11.0 (E)	I1 81.0 (F)	ΔS2 81.0 (F)	I2 81.0 (F)	ΔS1 81.0 (F)	R1 11.0 (E)	θS2 61.0 (I)	R2 11.0 (E)
27	VS (1)	VS (2)	θS1 11.0 (E)	I1 81.0 (F)	ΔS2 81.0 (F)	I2 81.0 (F)	ΔS1 81.0 (F)	R1 11.0 (E)	θS2 61.0 (I)	R2 11.0 (E)
28	SbOP (1)	SbOP (2)	C1 11.0 (E)	I1 81.0 (F)	’R2 81.0 (F)	I2 81.0 (F)	’R1 81.0 (F)	R1 11.0 (E)	C2 61.0 (I)	R2 11.0 (E)
29	SL (1)	SL (2)	C1 21.0 (I)	I1 81.0 (F)	’R2 71.0 (I)	I2 81.0 (F)	’R1 71.0 (I)	R1 11.0 (E)	C2 71.0 (I)	R2 11.0 (E)
30	SL (1)	SL (2)	C1 31.0 (I)	I1 81.0 (F)	’R2 61.0 (I)	I2 81.0 (F)	’R1 61.0 (I)	R1 11.0 (E)	I2 81.0 (F)	R2 11.0 (E)
31	SL (1)	SL (2)	C1 41.0 (I)	I1 81.0 (F)	’R2 51.0 (I)	I2 81.0 (F)	’R1 51.0 (I)	R1 11.0 (E)	I2 81.0 (F)	R2 11.0 (E)
32	SL (1)	SL (2)	C1 51.0 (I)	I1 81.0 (F)	’R2 41.0 (I)	I2 81.0 (F)	’R1 41.0 (I)	R1 11.0 (E)	I2 81.0 (F)	R2 11.0 (E)
33	SL (1)	SL (2)	C1 61.0 (I)	I1 81.0 (F)	’R2 31.0 (I)	I2 81.0 (F)	’R1 31.0 (I)	R1 11.0 (E)	I2 81.0 (F)	R2 11.0 (E)

Table B.16: Verification TC_5

t	$SPos_{t,r}$	$StS_{t,r}$	$VS_{t,r}$	$SbOP_{t,r}$	T_{total}
0	✗*	1	4	1	6
1	✗*	1	4	1	6
2	✗*	1	4	1	6
3	✗*	1	4	1	6
4	✗*	1	4	1	6
5	✓*	1	4	1	6
6	✓*	1	4	1	6
7	✓*	1	4	1	6
8	✓*	1	4	1	6
9	✓*	1	4	1	6
10	✓*	1	4	1	6
11	✓*	1	4	1	6
12	✓*	| 1 |	4	1	| 6 |
13	✓*	1	| 4 |	1	6
14	✓*	1	4	1	6
15	✓*	1	4	1	6
16	✓*	1	4	1	6
17	✓*	1	4	| 1 |	6
18	✓*	1	4	1	6
19	✓*	1	4	1	6
20	✓*	1	4	1	6
21	✓*	1	4	1	6
22	✓*	1	4	1	6
23	✓*	| 1 |	4	1	| 6 |
24	✓*	1	| 4 |	1	6
25	✓*	1	4	1	6
26	✓-	1	4	1	6
27	✓-	1	4	1	6
28	✓*	1	4	| 1 |	6
29	✗*	1	4	1	6
30	✗*	1	4	1	6
31	✗*	1	4	1	6
32	✗*	1	4	1	6
33	✗*	1	4	1	6

Table B.17: Verification TC_5 for $R1$ - Objective

t	$SPos_{t,r}$	$StS_{t,r}$	$VS_{t,r}$	$SbOP_{t,r}$	T_{total}
0	✗*	1	4	1	6
1	✗*	1	4	1	6
2	✗*	1	4	1	6
3	✗*	1	4	1	6
4	✗*	1	4	1	6
5	✓*	1	4	1	6
6	✓*	1	4	1	6
7	✓*	1	4	1	6
8	✓*	1	4	1	6
9	✓*	1	4	1	6
10	✓*	| 1 |	4	1	| 6 |
11	✓*	1	| 4 |	1	6
12	✓*	1	4	1	6
13	✓*	1	4	1	6
14	✓*	1	4	1	6
15	✓*	1	4	| 1 |	6
16	✓*	1	4	1	6
17	✓*	1	4	1	6
18	✓*	1	4	1	6
19	✓*	1	4	1	6
20	✓*	1	4	1	6
21	✓*	1	4	1	6
22	✓*	1	4	1	6
23	✓*	| 1 |	4	1	| 6 |
24	✓*	1	| 4 |	1	6
25	✓*	1	4	1	6
26	✓*	1	4	1	6
27	✓*	1	4	1	6
28	✓*	1	4	| 1 |	6
29	✗*	1	4	1	6
30	✗*	1	4	1	6
31	✗*	1	4	1	6
32	✗*	1	4	1	6
33	✗*	1	4	1	6

Table B.18: Verification TC_5 for $R2$ - Objective

B.6. Test Case 6

t	Vessel r		Module m with energy level $l_{t,m}$							
	R1	R2	0	1	2	3	4	5	6	7
0	SL (1)	SL (2)	'R1 81.0 (F)	'R2 81.0 (F)	I1 81.0 (F)	I1 81.0 (F)	I1 81.0 (F)	I2 81.0 (F)	I2 81.0 (F)	I2 81.0 (F)
1	SL (1)	SL (2)	'R1 71.0 (I)	'R2 71.0 (I)	I1 81.0 (F)	I1 81.0 (F)	I1 81.0 (F)	I2 81.0 (F)	I2 81.0 (F)	I2 81.0 (F)
2	SL (1)	SL (2)	'R1 61.0 (I)	'R2 61.0 (I)	I1 81.0 (F)	I1 81.0 (F)	I1 81.0 (F)	I2 81.0 (F)	I2 81.0 (F)	I2 81.0 (F)
3	StS (1)	StS (2)	'R1 51.0 (I)	'R2 51.0 (I)	IS1 81.0 (F)	I1 81.0 (F)	I1 81.0 (F)	IS2 81.0 (F)	I2 81.0 (F)	I2 81.0 (F)
4	VS (1)	VS (2)	θS1 41.0 (I)	θS2 41.0 (I)	ΔS1 81.0 (F)	I1 81.0 (F)	I1 81.0 (F)	ΔS2 81.0 (F)	I2 81.0 (F)	I2 81.0 (F)
5	VS (1)	VS (2)	θS1 41.0 (I)	θS2 41.0 (I)	ΔS1 81.0 (F)	I1 81.0 (F)	I1 81.0 (F)	ΔS2 81.0 (F)	I2 81.0 (F)	I2 81.0 (F)
6	SbOP (1)	SbOP (2)	C1 41.0 (I)	C2 41.0 (I)	'R1 81.0 (F)	I1 81.0 (F)	I1 81.0 (F)	'R2 81.0 (F)	I2 81.0 (F)	I2 81.0 (F)
7	SL (1)	SL (2)	C1 51.0 (I)	C2 51.0 (I)	'R1 71.0 (I)	I1 81.0 (F)	I1 81.0 (F)	'R2 71.0 (I)	I2 81.0 (F)	I2 81.0 (F)
8	SL (1)	SL (2)	C1 61.0 (I)	C2 61.0 (I)	'R1 61.0 (I)	I1 81.0 (F)	I1 81.0 (F)	'R2 61.0 (I)	I2 81.0 (F)	I2 81.0 (F)
9	SL (1)	SL (2)	C1 71.0 (I)	C2 71.0 (I)	'R1 51.0 (I)	I1 81.0 (F)	I1 81.0 (F)	'R2 51.0 (I)	I2 81.0 (F)	I2 81.0 (F)
10	StS (1)	StS (2)	I1 81.0 (F)	I2 81.0 (F)	'R1 41.0 (I)	IS1 81.0 (F)	I1 81.0 (F)	'R2 41.0 (I)	IS2 81.0 (F)	I2 81.0 (F)
11	VS (1)	VS (2)	I1 81.0 (F)	I2 81.0 (F)	θS1 31.0 (I)	ΔS1 81.0 (F)	I1 81.0 (F)	θS2 31.0 (I)	ΔS2 81.0 (F)	I2 81.0 (F)
12	VS (1)	VS (2)	I1 81.0 (F)	I2 81.0 (F)	θS1 31.0 (I)	ΔS1 81.0 (F)	I1 81.0 (F)	θS2 31.0 (I)	ΔS2 81.0 (F)	I2 81.0 (F)
13	SbOP (1)	SbOP (2)	I1 81.0 (F)	I2 81.0 (F)	C1 31.0 (I)	'R1 81.0 (F)	I1 81.0 (F)	C2 31.0 (I)	'R2 81.0 (F)	I2 81.0 (F)
14	SL (1)	SL (2)	I1 81.0 (F)	I2 81.0 (F)	C1 41.0 (I)	'R1 71.0 (I)	I1 81.0 (F)	C2 41.0 (I)	'R2 71.0 (I)	I2 81.0 (F)
15	SL (1)	SL (2)	I1 81.0 (F)	I2 81.0 (F)	C1 51.0 (I)	'R1 61.0 (I)	I1 81.0 (F)	C2 51.0 (I)	'R2 61.0 (I)	I2 81.0 (F)
16	SL (1)	SL (2)	I1 81.0 (F)	I2 81.0 (F)	C1 61.0 (I)	'R1 51.0 (I)	I1 81.0 (F)	C2 61.0 (I)	'R2 51.0 (I)	I2 81.0 (F)

Table B.19: Verification TC_6

t	$SPos_{t,r}$	$StS_{t,r}$	$VS_{t,r}$	$SbOP_{t,r}$	T_{total}
0	✗*	1	2	1	4
1	✗*	1	2	1	4
2	✗*	1	2	1	4
3	✓*	| 1 |	2	1	| 4 |
4	✓*	1	| 2 |	1	4
5	✓*	1	2	1	4
6	✓*	1	2	| 1 |	4
7	✓*	1	2	1	4
8	✓*	1	2	1	4
9	✓*	1	2	1	4
10	✓*	| 1 |	2	1	| 4 |
11	✓*	1	| 2 |	1	4
12	✓*	1	2	1	4
13	✓*	1	2	| 1 |	4
14	✗*	1	2	1	4
15	✗*	1	2	1	4
16	✗*	1	2	1	4

Table B.20: Verification TC_6 for $R1$ - Objective

t	$SPos_{t,r}$	$StS_{t,r}$	$VS_{t,r}$	$SbOP_{t,r}$	T_{total}
0	✗*	1	2	1	4
1	✗*	1	2	1	4
2	✗*	1	2	1	4
3	✓*	| 1 |	2	1	| 4 |
4	✓*	1	| 2 |	1	4
5	✓*	1	2	1	4
6	✓*	1	2	| 1 |	4
7	✓*	1	2	1	4
8	✓*	1	2	1	4
9	✓*	1	2	1	4
10	✓*	| 1 |	2	1	| 4 |
11	✓*	1	| 2 |	1	4
12	✓*	1	2	1	4
13	✓*	1	2	| 1 |	4
14	✗*	1	2	1	4
15	✗*	1	2	1	4
16	✗*	1	2	1	4

Table B.21: Verification TC_6 for $R2$ - Objective

B.7. Test Case 7

t	$P_{t,r}$		Module m with energy level $l_{t,m}$							
	R1	R2	0	1	2	3	4	5	6	7
0	12	20	12.0	-	20.0	-	-	-	-	-
1	18	10	18.0	-	10.0	-	-	-	-	-
2	15	13	15.0	-	13.0	-	-	-	-	-
3	5	10	5.0	-	10.0	-	-	-	-	-
4	5	13	5.0	-	13.0	-	-	-	-	-
5	13	19	-	-	-	-	-	-	-	-
6	12	15	-	-	-	-	-	-	-	-
7	18	15	-	18.0	-	15.0	-	-	-	-
8	13	14	-	13.0	-	14.0	-	-	-	-
9	18	17	-	18.0	-	17.0	-	-	-	-
10	17	16	-	17.0	-	-	-	-	-	-
11	5	17	-	5.0	-	-	-	-	-	-
12	10	20	-	-	-	-	-	10.0	20.0	-
13	12	20	-	-	-	-	-	12.0	20.0	-
14	7	7	-	-	-	-	-	7.0	7.0	-
15	9	18	-	-	-	-	-	9.0	18.0	-
16	14	5	-	-	-	-	-	14.0	5.0	-

Table B.22: Verification TC_7 - energy consumption

t	Vessel r		Module m with energy level $l_{t,m}$							
	R1	R2	0	1	2	3	4	5	6	7
0	SL (1)	SL (2)	'R1 81.0 (F)	R1 81.0 (F)	'R2 81.0 (F)	R2 81.0 (F)	I1 81.0 (F)	I1 81.0 (F)	I2 81.0 (F)	I2 81.0 (F)
1	SL (1)	SL (2)	'R1 69.0 (I)	R1 81.0 (F)	'R2 61.0 (I)	R2 81.0 (F)	I1 81.0 (F)	I1 81.0 (F)	I2 81.0 (F)	I2 81.0 (F)
2	SL (1)	SL (2)	'R1 51.0 (I)	R1 81.0 (F)	'R2 51.0 (I)	R2 81.0 (F)	I1 81.0 (F)	I1 81.0 (F)	I2 81.0 (F)	I2 81.0 (F)
3	SL (1)	SL (2)	'R1 36.0 (I)	R1 81.0 (F)	'R2 38.0 (I)	R2 81.0 (F)	I1 81.0 (F)	I1 81.0 (F)	I2 81.0 (F)	I2 81.0 (F)
4	StS (1)	StS (2)	'R1 31.0 (I)	R1 81.0 (F)	'R2 28.0 (I)	R2 81.0 (F)	I1 81.0 (F)	IS1 81.0 (F)	I2 81.0 (F)	IS2 81.0 (F)
5	VS (1)	VS (2)	θS1 21.0 (I)	R1 81.0 (F)	θS2 18.0 (E)	R2 81.0 (F)	I1 81.0 (F)	ΔS1 81.0 (F)	I2 81.0 (F)	ΔS2 81.0 (F)
6	VS (1)	VS (2)	θS1 21.0 (I)	R1 81.0 (F)	θS2 18.0 (E)	R2 81.0 (F)	I1 81.0 (F)	ΔS1 81.0 (F)	I2 81.0 (F)	ΔS2 81.0 (F)
7	SbOP (1)	SbOP (2)	C1 21.0 (I)	'R1 81.0 (F)	C2 18.0 (E)	'R2 81.0 (F)	I1 81.0 (F)	R1 81.0 (F)	I2 81.0 (F)	R2 81.0 (F)
8	SL (1)	SL (2)	C1 31.0 (I)	'R1 71.0 (I)	C2 28.0 (I)	'R2 71.0 (I)	I1 81.0 (F)	R1 81.0 (F)	I2 81.0 (F)	R2 81.0 (F)
9	SL (1)	StS (2)	C1 41.0 (I)	'R1 58.0 (I)	C2 38.0 (I)	'R2 57.0 (I)	I1 81.0 (F)	R1 81.0 (F)	IS2 81.0 (F)	R2 81.0 (F)
10	SL (1)	VS (2)	C1 51.0 (I)	'R1 40.0 (I)	C2 48.0 (I)	θS2 47.0 (I)	I1 81.0 (F)	R1 81.0 (F)	ΔS2 81.0 (F)	R2 81.0 (F)
11	SL (1)	VS (2)	C1 61.0 (I)	'R1 23.0 (I)	C2 58.0 (I)	θS2 47.0 (I)	I1 81.0 (F)	R1 81.0 (F)	ΔS2 81.0 (F)	R2 81.0 (F)
12	SL (1)	SbOP (2)	C1 71.0 (I)	R1 18.0 (E)	C2 68.0 (I)	C2 47.0 (I)	I1 81.0 (F)	'R1 81.0 (F)	'R2 81.0 (F)	R2 81.0 (F)
13	SL (1)	SL (2)	I1 81.0 (F)	R1 18.0 (E)	C2 78.0 (I)	C2 57.0 (I)	I1 81.0 (F)	'R1 71.0 (I)	'R2 71.0 (I)	R2 81.0 (F)
14	SL (1)	SL (2)	I1 81.0 (F)	R1 18.0 (E)	I2 88.0 (F)	C2 67.0 (I)	I1 81.0 (F)	'R1 59.0 (I)	'R2 51.0 (I)	R2 81.0 (F)
15	SL (1)	SL (2)	I1 81.0 (F)	R1 18.0 (E)	I2 88.0 (F)	C2 77.0 (I)	I1 81.0 (F)	'R1 52.0 (I)	'R2 44.0 (I)	R2 81.0 (F)
16	SL (1)	SL (2)	I1 81.0 (F)	R1 18.0 (E)	I2 88.0 (F)	I2 87.0 (F)	I1 81.0 (F)	'R1 43.0 (I)	'R2 26.0 (I)	R2 81.0 (F)

Table B.23: Verification TC_7

t	$SPos_{t,r}$	$StS_{t,r}$	$VS_{t,r}$	$SbOP_{t,r}$	T_{total}
0	✗*	1	2	1	4
1	✗*	1	2	1	4
2	✗*	1	2	1	4
3	✓*	1	2	1	4
4	✓*	$\lvert 1 \rvert$	2	1	$\lvert 4 \rvert$
5	✓*	1	$\lvert 2 \rvert$	1	4
6	✓*	1	$\lvert 2 \rvert$	1	4
7	✓*	1	2	$\lvert 1 \rvert$	4
8	✓*	1	2	1	4
9	✓*	1	2	1	4
10	✓*	1	2	1	4
11	✓*	1	2	1	4
12	✓*	1	2	1	4
13	✓*	1	2	1	4
14	✗*	1	2	1	4
15	✗*	1	2	1	4
16	✗*	1	2	1	4

Table B.24: Verification TC_7 for $R1$ - Objective

t	$SPos_{t,r}$	$StS_{t,r}$	$VS_{t,r}$	$SbOP_{t,r}$	T_{total}
0	✗*	1	2	1	4
1	✗*	1	2	1	4
2	✗*	1	2	1	4
3	✓*	1	2	1	4
4	✓*	$\lvert 1 \rvert$	2	1	$\lvert 4 \rvert$
5	✓*	1	$\lvert 2 \rvert$	1	4
6	✓*	1	$\lvert 2 \rvert$	1	4
7	✓*	1	2	$\lvert 1 \rvert$	4
8	✓*	1	2	1	4
9	✓*	$\lvert 1 \rvert$	2	1	$\lvert 4 \rvert$
10	✓*	1	$\lvert 2 \rvert$	1	4
11	✓*	1	$\lvert 2 \rvert$	1	4
12	✓*	1	2	$\lvert 1 \rvert$	4
13	✓*	1	2	1	4
14	✗*	1	2	1	4
15	✗*	1	2	1	4
16	✗*	1	2	1	4

Table B.25: Verification TC_7 for $R2$ - Objective

B.8. Test Case 8

t	Vessel r			Module m with energy level $l_{t,m}$							
	R1	R2	R3	0	1	2	3	4	5	6	7
0	SL (1)	SL (1)	SL (1)	’R1 81.0 (F)	R1 81.0 (F)	R2 81.0 (F)	’R2 81.0 (F)	R3 81.0 (F)	’R3 81.0 (F)	I1 81.0 (F)	I1 81.0 (F)
1	SL (1)	SL (1)	SL (1)	’R1 71.0 (I)	R1 81.0 (F)	R2 81.0 (F)	’R2 71.0 (I)	R3 81.0 (F)	’R3 71.0 (I)	I1 81.0 (F)	I1 81.0 (F)
2	SL (1)	SL (1)	SL (1)	’R1 61.0 (I)	R1 81.0 (F)	R2 81.0 (F)	’R2 61.0 (I)	R3 81.0 (F)	’R3 61.0 (I)	I1 81.0 (F)	I1 81.0 (F)
3	SL (1)	SL (1)	StS (1)	’R1 51.0 (I)	R1 81.0 (F)	R2 81.0 (F)	’R2 51.0 (I)	R3 81.0 (F)	’R3 51.0 (I)	IS1 81.0 (F)	I1 81.0 (F)
4	SL (1)	SL (1)	VS (1)	’R1 41.0 (I)	R1 81.0 (F)	R2 81.0 (F)	’R2 41.0 (I)	R3 81.0 (F)	θS1 41.0 (I)	ΔS1 81.0 (F)	I1 81.0 (F)
5	SL (1)	SL (1)	VS (1)	’R1 31.0 (I)	R1 81.0 (F)	R2 81.0 (F)	’R2 31.0 (I)	R3 81.0 (F)	θS1 41.0 (I)	ΔS1 81.0 (F)	I1 81.0 (F)
6	SL (1)	StS (1)	SbOP (1)	’R1 21.0 (I)	R1 81.0 (F)	R2 81.0 (F)	’R2 21.0 (I)	R3 81.0 (F)	C1 41.0 (I)	’R3 81.0 (F)	IS1 81.0 (F)
7	SL (1)	VS (1)	SL (1)	R1 11.0 (E)	’R1 81.0 (F)	R2 81.0 (F)	θS1 11.0 (E)	R3 81.0 (F)	C1 51.0 (I)	’R3 71.0 (I)	ΔS1 81.0 (F)
8	SL (1)	VS (1)	SL (1)	R1 11.0 (E)	’R1 71.0 (I)	R2 81.0 (F)	θS1 11.0 (E)	R3 81.0 (F)	C1 61.0 (I)	’R3 61.0 (I)	ΔS1 81.0 (F)
9	SL (1)	SbOP (1)	SL (1)	R1 11.0 (E)	’R1 61.0 (I)	R2 81.0 (F)	C1 11.0 (E)	R3 81.0 (F)	C1 71.0 (I)	’R3 51.0 (I)	’R2 81.0 (F)
10	SL (1)	SL (1)	SL (1)	R1 11.0 (E)	’R1 51.0 (I)	R2 81.0 (F)	C1 21.0 (I)	R3 81.0 (F)	I1 81.0 (F)	’R3 41.0 (I)	’R2 71.0 (I)
11	StS (1)	SL (1)	SL (1)	R1 11.0 (E)	’R1 41.0 (I)	R2 81.0 (F)	C1 31.0 (I)	R3 81.0 (F)	IS1 81.0 (F)	’R3 31.0 (I)	’R2 61.0 (I)
12	VS (1)	SL (1)	SL (1)	R1 11.0 (E)	θS1 31.0 (I)	R2 81.0 (F)	C1 41.0 (I)	R3 81.0 (F)	ΔS1 81.0 (F)	’R3 21.0 (I)	’R2 51.0 (I)
13	VS (1)	SL (1)	SL (1)	R1 11.0 (E)	θS1 31.0 (I)	R2 81.0 (F)	C1 51.0 (I)	’R3 81.0 (F)	ΔS1 81.0 (F)	R3 11.0 (E)	’R2 41.0 (I)
14	SbOP (1)	SL (1)	SL (1)	R1 11.0 (E)	C1 31.0 (I)	R2 81.0 (F)	C1 61.0 (I)	’R3 71.0 (I)	’R1 81.0 (F)	R3 11.0 (E)	’R2 31.0 (I)
15	SL (1)	SL (1)	SL (1)	R1 11.0 (E)	C1 41.0 (I)	R2 81.0 (F)	C1 71.0 (I)	’R3 61.0 (I)	’R1 71.0 (I)	R3 11.0 (E)	’R2 21.0 (I)
16	SL (1)	SL (1)	SL (1)	R1 11.0 (E)	C1 51.0 (I)	’R2 81.0 (F)	I1 81.0 (F)	’R3 51.0 (I)	’R1 61.0 (I)	R3 11.0 (E)	R2 11.0 (E)
17	SL (1)	SL (1)	SL (1)	R1 11.0 (E)	C1 61.0 (I)	’R2 71.0 (I)	I1 81.0 (F)	’R3 41.0 (I)	’R1 51.0 (I)	R3 11.0 (E)	R2 11.0 (E)

Table B.26: Verification TC_8

t	$SPos_{t,r}$	$StS_{t,r}$	$VS_{t,r}$	$SbOP_{t,r}$	T_{total}
0	✗*	1	2	1	4
1	✗*	1	2	1	4
2	✗*	1	2	1	4
3	✓*	1	2	1	4
4	✓*	1	2	1	4
5	✓*	1	2	1	4
6	✓*	1	2	1	4
7	✓*	1	2	1	4
8	✓*	1	2	1	4
9	✓*	1	2	1	4
10	✓*	1	2	1	4
11	✓*	| 1 |	2	1	| 4 |
12	✓*	1	| 2 |	1	4
13	✓*	1	| 2 |	1	4
14	✓*	1	2	| 1 |	4
15	✗*	1	2	1	4
16	✗*	1	2	1	4
17	✗*	1	2	1	4

Table B.27: Verification TC_8 for $R1$ - Objective

t	$SPos_{t,r}$	$StS_{t,r}$	$VS_{t,r}$	$SbOP_{t,r}$	T_{total}
0	✗*	1	2	1	4
1	✗*	1	2	1	4
2	✗*	1	2	1	4
3	✓*	1	2	1	4
4	✓*	1	2	1	4
5	✓*	1	2	1	4
6	✓*	| 1 |	2	1	| 4 |
7	✓*	1	| 2 |	1	4
8	✓*	1	| 2 |	1	4
9	✓*	1	2	| 1 |	4
10	✓*	1	2	1	4
11	✓*	1	2	1	4
12	✓*	1	2	1	4
13	✓*	1	2	1	4
14	✓*	1	2	1	4
15	✗*	1	2	1	4
16	✗*	1	2	1	4
17	✗*	1	2	1	4

Table B.28: Verification TC_8 for $R2$ - Objective

B.9. Test case 9

t	Vessel r		Module m with energy level $l_{t,m}$							
	R1	R2	0	1	2	3	4	5	6	7
0	SL (1)	SL (2)	R1 81.0 (F)	'R1 81.0 (F)	R2 81.0 (F)	'R2 81.0 (F)	I1 81.0 (F)	I1 81.0 (F)	I2 81.0 (F)	I2 81.0 (F)
1	SL (1)	SL (2)	R1 81.0 (F)	'R1 71.0 (I)	R2 81.0 (F)	'R2 71.0 (I)	I1 81.0 (F)	I1 81.0 (F)	I2 81.0 (F)	I2 81.0 (F)
2	SL (1)	SL (2)	R1 81.0 (F)	'R1 61.0 (I)	R2 81.0 (F)	'R2 61.0 (I)	I1 81.0 (F)	I1 81.0 (F)	I2 81.0 (F)	I2 81.0 (F)
3	StS (1)	SL (2)	R1 81.0 (F)	'R1 51.0 (I)	R2 81.0 (F)	'R2 51.0 (I)	I1 81.0 (F)	IS1 81.0 (F)	I2 81.0 (F)	I2 81.0 (F)
4	VS (1)	SL (2)	R1 81.0 (F)	θS1 41.0 (I)	R2 81.0 (F)	'R2 41.0 (I)	I1 81.0 (F)	ΔS1 81.0 (F)	I2 81.0 (F)	I2 81.0 (F)
5	VS (1)	SL (2)	R1 81.0 (F)	θS1 41.0 (I)	R2 81.0 (F)	'R2 31.0 (I)	I1 81.0 (F)	ΔS1 81.0 (F)	I2 81.0 (F)	I2 81.0 (F)
6	SbOP (1)	SL (2)	R1 81.0 (F)	C1 41.0 (I)	R2 81.0 (F)	'R2 21.0 (I)	I1 81.0 (F)	'R1 81.0 (F)	I2 81.0 (F)	I2 81.0 (F)
7	SL (1)	StS (2)	R1 81.0 (F)	C1 51.0 (I)	'R2 81.0 (F)	R2 11.0 (E)	I1 81.0 (F)	'R1 71.0 (I)	IS2 81.0 (F)	IS2 81.0 (F)
8	SL (1)	VS (2)	R1 81.0 (F)	C1 61.0 (I)	θS2 71.0 (I)	θS2 11.0 (E)	I1 81.0 (F)	'R1 61.0 (I)	ΔS2 81.0 (F)	ΔS2 81.0 (F)
9	SL (1)	VS (2)	R1 81.0 (F)	C1 71.0 (I)	θS2 71.0 (I)	θS2 11.0 (E)	I1 81.0 (F)	'R1 51.0 (I)	ΔS2 81.0 (F)	ΔS2 81.0 (F)
10	SL (1)	SbOP (2)	R1 81.0 (F)	I1 81.0 (F)	C2 71.0 (I)	C2 11.0 (E)	I1 81.0 (F)	'R1 41.0 (I)	'R2 81.0 (F)	R2 81.0 (F)
11	SL (1)	SL (2)	R1 81.0 (F)	I1 81.0 (F)	I2 81.0 (F)	C2 21.0 (I)	I1 81.0 (F)	'R1 31.0 (I)	'R2 71.0 (I)	R2 81.0 (F)
12	SL (1)	SL (2)	R1 81.0 (F)	I1 81.0 (F)	I2 81.0 (F)	C2 31.0 (I)	I1 81.0 (F)	'R1 21.0 (I)	'R2 61.0 (I)	R2 81.0 (F)
13	SL (1)	SL (2)	'R1 81.0 (F)	I1 81.0 (F)	I2 81.0 (F)	C2 41.0 (I)	I1 81.0 (F)	R1 11.0 (E)	'R2 51.0 (I)	R2 81.0 (F)
14	SL (1)	SL (2)	'R1 71.0 (I)	I1 81.0 (F)	I2 81.0 (F)	C2 51.0 (I)	I1 81.0 (F)	R1 11.0 (E)	'R2 41.0 (I)	R2 81.0 (F)
15	SL (1)	SL (2)	'R1 61.0 (I)	I1 81.0 (F)	I2 81.0 (F)	C2 61.0 (I)	I1 81.0 (F)	R1 11.0 (E)	'R2 31.0 (I)	R2 81.0 (F)
16	SL (1)	SL (2)	'R1 51.0 (I)	I1 81.0 (F)	I2 81.0 (F)	C2 71.0 (I)	I1 81.0 (F)	R1 11.0 (E)	'R2 21.0 (I)	R2 81.0 (F)

Table B.29: Verification TC_9

t	$SPos_{t,r}$	$StS_{t,r}$	$VS_{t,r}$	$SbOP_{t,r}$	T_{total}
0	✗*	1	2	1	4
1	✗*	1	2	1	4
2	✗*	1	2	1	4
3	✓*	| 1 |	2	1	| 4 |
4	✓*	1	| 2 |	1	4
5	✓*	1	| 2 |	1	4
6	✓*	1	2	| 1 |	4
7	✓*	1	2	1	4
8	✗*	1	2	1	4
9	✗*	1	2	1	4
10	✗*	1	2	1	4
11	✓*	1	2	1	4
12	✓*	1	2	1	4
13	✓*	1	2	1	4
14	✗*	1	2	1	4
15	✗*	1	2	1	4
16	✗*	1	2	1	4

Table B.30: Verification TC_9 for $R1$ - Objective

t	$SPos_{t,r}$	$StS_{t,r}$	$VS_{t,r}$	$SbOP_{t,r}$	T_{total}
0	✗*	1	2	1	4
1	✗*	1	2	1	4
2	✗*	1	2	1	4
3	✓*	1	2	1	4
4	✗*	1	2	1	4
5	✗*	1	2	1	4
6	✗*	1	2	1	4
7	✓*	| 1 |	2	1	| 4 |
8	✓*	1	| 2 |	1	4
9	✓*	1	| 2 |	1	4
10	✓*	1	2	| 1 |	4
11	✓*	1	2	1	4
12	✓*	1	2	1	4
13	✗*	1	2	1	4
14	✗*	1	2	1	4
15	✗*	1	2	1	4
16	✗*	1	2	1	4

Table B.31: Verification TC_9 for $R2$ - Objective

B.10. Test Case 10

t	Vessel r		Module m with energy level $l_{t,m}$							
	R1	R2	0	1	2	3	4	5	6	7
0	SL (1)	SL (2)	'R1 81.0 (F)	R1 81.0 (F)	R2 81.0 (F)	'R2 81.0 (F)	I1 81.0 (F)	I1 81.0 (F)	I2 81.0 (F)	I2 81.0 (F)
1	SL (1)	SL (2)	'R1 71.0 (I)	R1 81.0 (F)	R2 81.0 (F)	'R2 71.0 (I)	I1 81.0 (F)	I1 81.0 (F)	I2 81.0 (F)	I2 81.0 (F)
2	SL (1)	SL (2)	'R1 61.0 (I)	R1 81.0 (F)	R2 81.0 (F)	'R2 61.0 (I)	I1 81.0 (F)	I1 81.0 (F)	I2 81.0 (F)	I2 81.0 (F)
3	SL (1)	StS (2)	'R1 51.0 (I)	R1 81.0 (F)	R2 81.0 (F)	'R2 51.0 (I)	I1 81.0 (F)	I1 81.0 (F)	IS2 81.0 (F)	I2 81.0 (F)
4	SL (1)	VS (2)	'R1 41.0 (I)	R1 81.0 (F)	R2 81.0 (F)	θS2 41.0 (I)	I1 81.0 (F)	I1 81.0 (F)	ΔS2 81.0 (F)	I2 81.0 (F)
5	SL (1)	VS (2)	'R1 31.0 (I)	R1 81.0 (F)	R2 81.0 (F)	θS2 41.0 (I)	I1 81.0 (F)	I1 81.0 (F)	ΔS2 81.0 (F)	I2 81.0 (F)
6	SL (1)	SbOP (2)	'R1 21.0 (I)	R1 81.0 (F)	'R2 81.0 (F)	C2 41.0 (I)	I1 81.0 (F)	I1 81.0 (F)	R2 81.0 (F)	I2 81.0 (F)
7	StS (1)	SL (2)	R1 11.0 (E)	'R1 81.0 (F)	'R2 71.0 (I)	C2 51.0 (I)	IS1 81.0 (F)	IS1 81.0 (F)	R2 81.0 (F)	I2 81.0 (F)
8	VS (1)	SL (2)	θS1 11.0 (E)	θS1 71.0 (I)	'R2 61.0 (I)	C2 61.0 (I)	ΔS1 81.0 (F)	ΔS1 81.0 (F)	R2 81.0 (F)	I2 81.0 (F)
9	VS (1)	SL (2)	θS1 11.0 (E)	θS1 71.0 (I)	'R2 51.0 (I)	C2 71.0 (I)	ΔS1 81.0 (F)	ΔS1 81.0 (F)	R2 81.0 (F)	I2 81.0 (F)
10	SbOP (1)	SL (2)	C1 11.0 (E)	C1 71.0 (I)	'R2 41.0 (I)	I2 81.0 (F)	R1 81.0 (F)	'R1 81.0 (F)	R2 81.0 (F)	I2 81.0 (F)
11	SL (1)	SL (2)	C1 21.0 (I)	I1 81.0 (F)	'R2 31.0 (I)	I2 81.0 (F)	R1 81.0 (F)	'R1 71.0 (I)	R2 81.0 (F)	I2 81.0 (F)
12	SL (1)	SL (2)	C1 31.0 (I)	I1 81.0 (F)	'R2 21.0 (I)	I2 81.0 (F)	R1 81.0 (F)	'R1 61.0 (I)	R2 81.0 (F)	I2 81.0 (F)
13	SL (1)	SL (2)	C1 41.0 (I)	I1 81.0 (F)	R2 11.0 (E)	I2 81.0 (F)	R1 81.0 (F)	'R1 51.0 (I)	'R2 81.0 (F)	I2 81.0 (F)
14	SL (1)	SL (2)	C1 51.0 (I)	I1 81.0 (F)	R2 11.0 (E)	I2 81.0 (F)	R1 81.0 (F)	'R1 41.0 (I)	'R2 71.0 (I)	I2 81.0 (F)
15	SL (1)	SL (2)	C1 61.0 (I)	I1 81.0 (F)	R2 11.0 (E)	I2 81.0 (F)	R1 81.0 (F)	'R1 31.0 (I)	'R2 61.0 (I)	I2 81.0 (F)
16	SL (1)	SL (2)	C1 71.0 (I)	I1 81.0 (F)	R2 11.0 (E)	I2 81.0 (F)	R1 81.0 (F)	'R1 21.0 (I)	'R2 51.0 (I)	I2 81.0 (F)

Table B.32: Verification TC_{10}

t	$SPos_{t,r}$	$StS_{t,r}$	$VS_{t,r}$	$SbOP_{t,r}$	T_{total}
0	✗*	1	2	1	5
1	✗*	3	2	2	6
2	✗*	3	2	3	7
3	✓*	2	2	2	6
4	✓*	2	2	1	5
5	✓*	3	2	3	6
6	✓*	3	2	1	6
7	✓*	| 1 |	2	2	| 4 |
8	✓*	2	| 2 |	1	6
9	✓*	2	| 2 |	2	6
10	✓*	1	2	| 1 |	5
11	✓*	3	2	1	7
12	✗*	1	2	2	8
13	✗*	1	2	2	8
14	✗*	2	2	3	8
15	✗*	1	2	2	8
16	✗*	1	2	2	8

Table B.33: Verification TC_{10} for $R1$ - Objective

t	$SPos_{t,r}$	$StS_{t,r}$	$VS_{t,r}$	$SbOP_{t,r}$	T_{total}
0	✗*	1	2	2	6
1	✗*	2	2	1	6
2	✗*	3	2	2	8
3	✓*	| 1 |	2	3	| 4 |
4	✓*	2	| 2 |	2	7
5	✓*	1	| 2 |	2	6
6	✓*	3	2	| 1 |	7
7	✓*	3	2	3	8
8	✓*	3	2	3	6
9	✓*	2	2	2	5
10	✓*	1	2	2	4
11	✓*	3	2	2	8
12	✗*	3	2	3	8
13	✗*	1	2	1	8
14	✗*	2	2	3	8
15	✗*	3	2	3	8
16	✗*	1	2	3	8

Table B.34: Verification TC_{10} for $R2$ - Objective

B.11. Test Case 11

t	Vessel r			Module m with energy level $l_{t,m}$											
	R1	R2	0	1	2	3	4	5	6	7	8	9	10	11	12
0	SL (2)	SL (1)	SL (3)	R1 81.0 (F)	'R1 81.0 (F)	'R2 81.0 (F)	R2 81.0 (F)	'R3 81.0 (F)	R3 81.0 (F)	I1 81.0 (F)	I1 81.0 (F)	I2 81.0 (F)	I2 81.0 (F)	I3 81.0 (F)	I3 81.0 (F)
1	SL (2)	SL (1)	SL (3)	R1 81.0 (F)	'R1 71.0 (I)	'R2 71.0 (I)	R2 81.0 (F)	'R3 76.0 (I)	R3 81.0 (F)	I1 81.0 (F)	I1 81.0 (F)	I2 81.0 (F)	I2 81.0 (F)	I3 81.0 (F)	I3 81.0 (F)
2	SL (2)	SL (1)	SL (3)	R1 81.0 (F)	'R1 65.0 (I)	'R2 62.0 (I)	R2 81.0 (F)	'R3 66.0 (I)	R3 81.0 (F)	I1 81.0 (F)	I1 81.0 (F)	I2 81.0 (F)	I2 81.0 (F)	I3 81.0 (F)	I3 81.0 (F)
3	SL (2)	SL (1)	SL (3)	R1 81.0 (F)	'R1 59.0 (I)	'R2 57.0 (I)	R2 81.0 (F)	'R3 61.0 (I)	R3 81.0 (F)	I1 81.0 (F)	I1 81.0 (F)	I2 81.0 (F)	I2 81.0 (F)	I3 81.0 (F)	I3 81.0 (F)
4	StS (2)	SL (1)	SL (3)	R1 81.0 (F)	'R1 50.0 (I)	'R2 47.0 (I)	R2 81.0 (F)	'R3 51.0 (I)	R3 81.0 (F)	I1 81.0 (F)	I1 81.0 (F)	I2 81.0 (F)	IS2 81.0 (F)	I3 81.0 (F)	I3 81.0 (F)
5	VS (2)	StS (1)	SL (3)	R1 81.0 (F)	θS2 30.0 (I)	'R2 41.0 (I)	R2 81.0 (F)	'R3 41.0 (I)	R3 81.0 (F)	I1 81.0 (F)	IS1 81.0 (F)	I2 81.0 (F)	ΔS2 81.0 (F)	I3 81.0 (F)	I3 81.0 (F)
6	VS (2)	VS (1)	SL (3)	R1 81.0 (F)	θS2 30.0 (I)	θS1 21.0 (I)	R2 81.0 (F)	'R3 35.0 (I)	R3 81.0 (F)	I1 81.0 (F)	ΔS1 81.0 (F)	I2 81.0 (F)	ΔS2 81.0 (F)	I3 81.0 (F)	I3 81.0 (F)
7	SbOP (2)	VS (1)	StS (3)	'R1 81.0 (F)	C2 30.0 (I)	θS1 21.0 (I)	R2 81.0 (F)	'R3 29.0 (I)	R3 81.0 (F)	I1 81.0 (F)	ΔS1 81.0 (F)	I2 81.0 (F)	R1 81.0 (F)	IS3 81.0 (F)	I3 81.0 (F)
8	SL (2)	SbOP (1)	VS (3)	'R1 61.0 (I)	C2 40.0 (I)	C1 21.0 (I)	'R2 81.0 (F)	θS3 9.0 (E)	R3 81.0 (F)	I1 81.0 (F)	R2 81.0 (F)	I2 81.0 (F)	R1 81.0 (F)	ΔS3 81.0 (F)	I3 81.0 (F)
9	SL (2)	SbOP (1)	VS (3)	'R1 55.0 (I)	C2 50.0 (I)	C1 31.0 (I)	'R2 61.0 (I)	θS3 9.0 (E)	R3 81.0 (F)	I1 81.0 (F)	R2 81.0 (F)	I2 81.0 (F)	R1 81.0 (F)	ΔS3 81.0 (F)	I3 81.0 (F)
10	SL (2)	SL (1)	SbOP (3)	'R1 48.0 (I)	C2 60.0 (I)	C1 41.0 (I)	'R2 41.0 (I)	C3 9.0 (E)	'R3 81.0 (F)	I1 81.0 (F)	R2 81.0 (F)	I2 81.0 (F)	R1 81.0 (F)	R3 81.0 (F)	I3 81.0 (F)
11	SL (2)	SL (1)	SbOP (3)	'R1 38.0 (I)	C2 70.0 (I)	C1 51.0 (I)	'R2 33.0 (I)	C3 19.0 (E)	'R3 61.0 (I)	I1 81.0 (F)	R2 81.0 (F)	I2 81.0 (F)	R1 81.0 (F)	R3 81.0 (F)	I3 81.0 (F)
12	SL (2)	SL (1)	SbOP (3)	'R1 32.0 (I)	I2 80.0 (F)	C1 61.0 (I)	'R2 23.0 (I)	C3 29.0 (I)	'R3 41.0 (I)	I1 81.0 (F)	R2 81.0 (F)	I2 81.0 (F)	R1 81.0 (F)	R3 81.0 (F)	I3 81.0 (F)
13	SL (2)	SL (1)	SL (3)	'R1 27.0 (I)	I2 80.0 (F)	C1 71.0 (I)	R2 14.0 (E)	C3 39.0 (I)	'R3 21.0 (I)	I1 81.0 (F)	'R2 81.0 (F)	I2 81.0 (F)	R1 81.0 (F)	R3 81.0 (F)	I3 81.0 (F)
14	SL (2)	SL (1)	SL (3)	'R1 22.0 (I)	I2 80.0 (F)	I1 81.0 (F)	R2 14.0 (E)	C3 49.0 (I)	R3 13.0 (E)	I1 81.0 (F)	'R2 72.0 (I)	I2 81.0 (F)	R1 81.0 (F)	'R3 81.0 (F)	I3 81.0 (F)
15	SL (2)	SL (1)	SL (3)	R1 15.0 (E)	I2 80.0 (F)	I1 81.0 (F)	R2 14.0 (E)	C3 59.0 (I)	R3 13.0 (E)	I1 81.0 (F)	'R2 64.0 (I)	I2 81.0 (F)	'R1 81.0 (F)	'R3 72.0 (I)	I3 81.0 (F)
16	SL (2)	SL (1)	SL (3)	R1 15.0 (E)	I2 80.0 (F)	I1 81.0 (F)	R2 14.0 (E)	C3 69.0 (I)	R3 13.0 (E)	I1 81.0 (F)	'R2 57.0 (I)	I2 81.0 (F)	'R1 73.0 (I)	'R3 63.0 (I)	I3 81.0 (F)
17	SL (2)	SL (1)	SL (3)	R1 15.0 (E)	I2 80.0 (F)	I1 81.0 (F)	R2 14.0 (E)	C3 79.0 (I)	R3 13.0 (E)	I1 81.0 (F)	'R2 49.0 (I)	I2 81.0 (F)	'R1 65.0 (I)	'R3 54.0 (I)	I3 81.0 (F)
18	SL (2)	StS (1)	SL (3)	R1 15.0 (E)	I2 80.0 (F)	IS1 81.0 (F)	R2 14.0 (E)	I3 89.0 (F)	R3 13.0 (E)	IS1 81.0 (F)	'R2 40.0 (I)	I2 81.0 (F)	'R1 60.0 (I)	'R3 49.0 (I)	I3 81.0 (F)
19	SL (2)	StS (1)	SL (3)	R1 15.0 (E)	I2 80.0 (F)	IS1 81.0 (F)	R2 14.0 (E)	I3 89.0 (F)	R3 13.0 (E)	IS1 81.0 (F)	'R2 20.0 (I)	I2 81.0 (F)	'R1 50.0 (I)	'R3 44.0 (I)	I3 81.0 (F)
20	StS (2)	VS (1)	StS (3)	R1 15.0 (E)	IS2 80.0 (F)	ΔS1 81.0 (F)	θS1 14.0 (E)	IS3 89.0 (F)	R3 13.0 (E)	ΔS1 81.0 (F)	θS1 0.0 (E)	IS2 81.0 (F)	'R1 42.0 (I)	'R3 36.0 (I)	IS3 81.0 (F)
21	VS (2)	VS (1)	VS (3)	θS2 15.0 (E)	ΔS2 80.0 (F)	ΔS1 81.0 (F)	θS1 14.0 (E)	ΔS3 89.0 (F)	θS3 13.0 (E)	ΔS1 81.0 (F)	θS1 0.0 (E)	ΔS2 81.0 (F)	θS2 22.0 (I)	θS3 16.0 (E)	ΔS3 81.0 (F)
22	VS (2)	SbOP (1)	VS (3)	θS2 15.0 (E)	ΔS2 80.0 (F)	'R2 81.0 (F)	C1 14.0 (E)	ΔS3 89.0 (F)	θS3 13.0 (E)	R2 81.0 (F)	C1 0.0 (E)	ΔS2 81.0 (F)	θS2 22.0 (I)	θS3 16.0 (E)	ΔS3 81.0 (F)
23	SbOP (2)	SL (1)	SbOP (3)	C2 15.0 (E)	'R1 80.0 (F)	'R2 61.0 (I)	C1 24.0 (I)	'R3 89.0 (F)	C3 13.0 (E)	R2 81.0 (F)	C1 10.0 (E)	R1 81.0 (F)	C2 22.0 (I)	C3 16.0 (E)	R3 81.0 (F)
24	SbOP (2)	SL (1)	SbOP (3)	C2 25.0 (I)	'R1 60.0 (I)	'R2 56.0 (I)	C1 34.0 (I)	'R3 69.0 (I)	C3 23.0 (I)	R2 81.0 (F)	C1 20.0 (I)	R1 81.0 (F)	C2 32.0 (I)	C3 26.0 (I)	R3 81.0 (F)
25	SL (2)	SL (1)	SL (3)	C2 35.0 (I)	'R1 40.0 (I)	'R2 49.0 (I)	C1 44.0 (I)	'R3 49.0 (I)	C3 33.0 (I)	R2 81.0 (F)	C1 30.0 (I)	R1 81.0 (F)	C2 42.0 (I)	C3 36.0 (I)	R3 81.0 (F)
26	SL (2)	SL (1)	SL (3)	C2 45.0 (I)	'R1 32.0 (I)	'R2 42.0 (I)	C1 54.0 (I)	'R3 42.0 (I)	C3 43.0 (I)	R2 81.0 (F)	C1 40.0 (I)	R1 81.0 (F)	C2 52.0 (I)	C3 46.0 (I)	R3 81.0 (F)
27	SL (2)	SL (1)	SL (3)	C2 55.0 (I)	'R1 25.0 (I)	'R2 32.0 (I)	C1 64.0 (I)	'R3 32.0 (I)	C3 53.0 (I)	R2 81.0 (F)	C1 50.0 (I)	R1 81.0 (F)	C2 62.0 (I)	C3 56.0 (I)	R3 81.0 (F)
28	SL (2)	SL (1)	SL (3)	C2 65.0 (I)	'R1 20.0 (I)	'R2 27.0 (I)	C1 74.0 (I)	'R3 23.0 (I)	C3 63.0 (I)	R2 81.0 (F)	C1 60.0 (I)	R1 81.0 (F)	C2 72.0 (I)	C3 66.0 (I)	R3 81.0 (F)
29	SL (2)	SL (1)	SL (3)	C2 75.0 (I)	R1 15.0 (E)	R2 19.0 (E)	I1 84.0 (F)	R3 18.0 (E)	C3 73.0 (I)	'R2 81.0 (F)	C1 70.0 (I)	'R1 81.0 (F)	I2 82.0 (F)	C3 76.0 (I)	'R3 81.0 (F)
30	SL (2)	SL (1)	SL (3)	I2 85.0 (F)	R1 15.0 (E)	R2 19.0 (E)	I1 84.0 (F)	R3 18.0 (E)	I3 83.0 (F)	'R2 71.0 (I)	I1 80.0 (F)	'R1 72.0 (I)	I2 82.0 (F)	I3 86.0 (F)	'R3 74.0 (I)
31	SL (2)	SL (1)	SL (3)	I2 85.0 (F)	R1 15.0 (E)	R2 19.0 (E)	I1 84.0 (F)	R3 18.0 (E)	I3 83.0 (F)	'R2 66.0 (I)	I1 80.0 (F)	'R1 67.0 (I)	I2 82.0 (F)	I3 86.0 (F)	'R3 68.0 (I)
32	SL (2)	SL (1)	SL (3)	I2 85.0 (F)	R1 15.0 (E)	R2 19.0 (E)	I1 84.0 (F)	R3 18.0 (E)	I3 83.0 (F)	'R2 59.0 (I)	I1 80.0 (F)	'R1 58.0 (I)	I2 82.0 (F)	I3 86.0 (F)	'R3 59.0 (I)
33	SL (2)	SL (1)	SL (3)	I2 85.0 (F)	R1 15.0 (E)	R2 19.0 (E)	I1 84.0 (F)	R3 18.0 (E)	I3 83.0 (F)	'R2 51.0 (I)	I1 80.0 (F)	'R1 51.0 (I)	I2 82.0 (F)	I3 86.0 (F)	'R3 49.0 (I)

Table B.35: Verification TC_{11}

t	$SPos_{t,r}$	$StS_{t,r}$	$VS_{t,r}$	$SbOP_{t,r}$	T_{total}
0	✓*	1	1	2	3
1	✓*	2	1	1	6
2	✓*	2	1	1	5
3	✓*	|1|	1	1	|4|
4	✓*	1	|1|	3	5
5	✓*	3	1	|2|	5
6	✓*	2	1	3	4
7	✗*	1	1	3	3
8	✗*	2	1	2	4
9	✗*	1	1	1	3
10	✗*	3	1	3	7
11	✓*	2	1	1	6
12	✓*	3	1	2	7
13	✗*	2	1	1	4
14	✗*	2	1	3	4
15	✗*	1	1	3	4
16	✗*	3	1	3	4

Table B.36: Verification TC_{11} for $R1$ - Objective

t	$SPos_{t,r}$	$StS_{t,r}$	$VS_{t,r}$	$SbOP_{t,r}$	T_{total}
0	✗*	1	1	1	3
1	✗*	3	1	1	5
2	✗*	1	1	1	4
3	✗*	3	1	2	6
4	✓*	2	1	2	5
5	✓*	3	1	1	7
6	✓*	1	1	1	4
7	✓*	3	1	2	6
8	✓*	|1|	1	2	|4|
9	✓*	3	|1|	3	5
10	✓*	2	1	|2|	4
11	✓*	1	1	2	3
12	✓*	2	1	1	6
13	✗*	1	1	1	4
14	✗*	3	1	1	4
15	✗*	3	1	3	4
16	✗*	1	1	1	4

Table B.37: Verification TC_{11} for $R2$ - Objective

C

Appendix D

C.1. Validation RPA6

C.1.1. Input

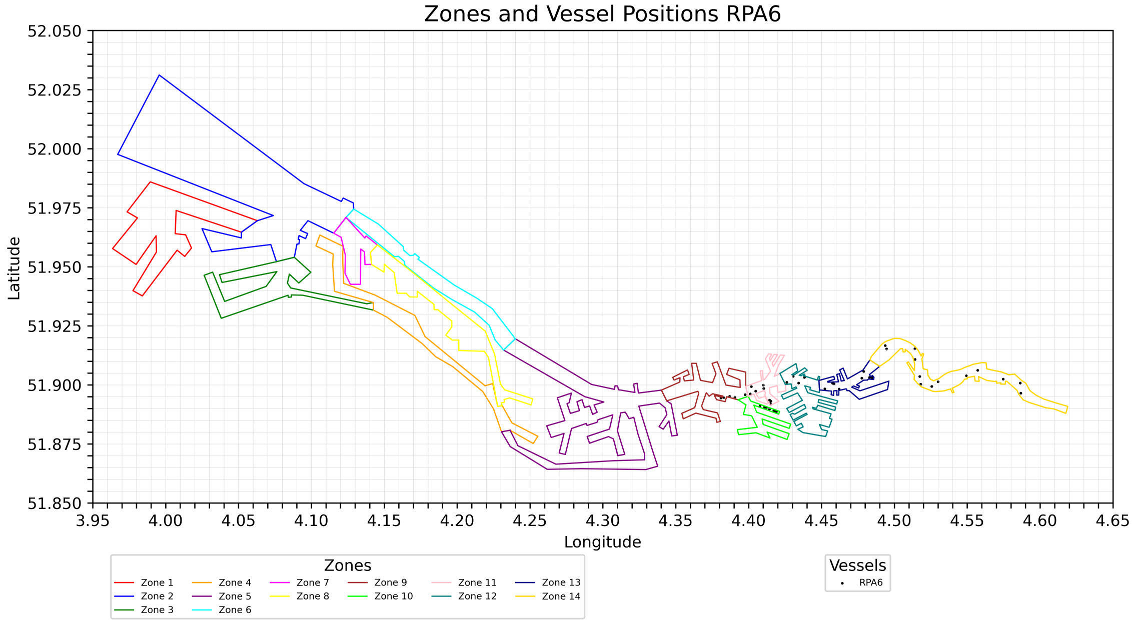

Figure C.1: RPA6 locations (timestep = 6)

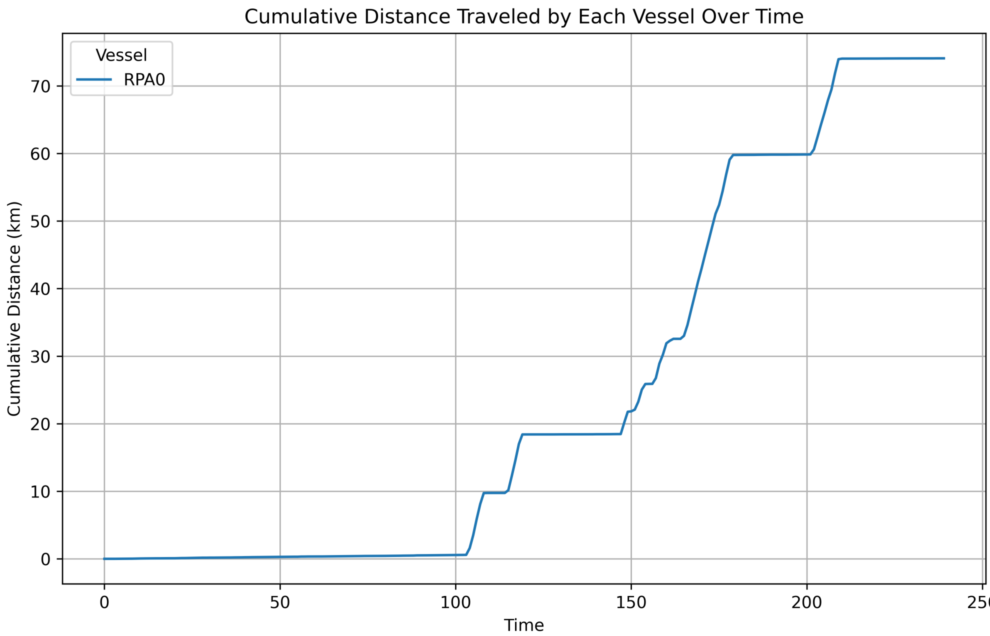

Figure C.2: Cumulative sailed distance for RPA6

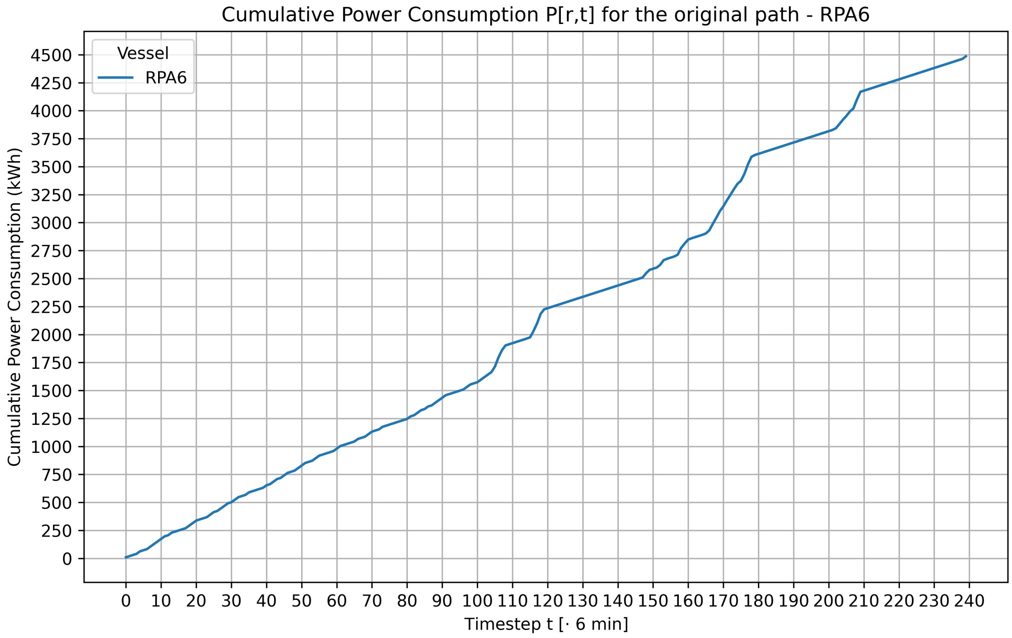

Figure C.3: Cumulative initial power for the RPA6

C.1.2. Results

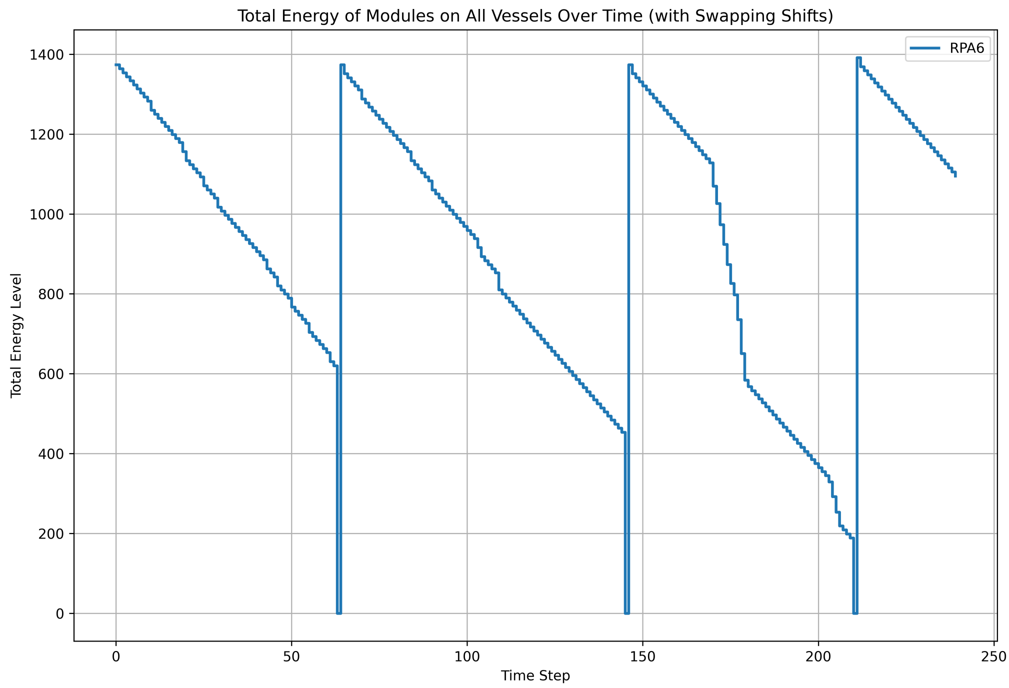

Figure C.4: Power consumption RPA6

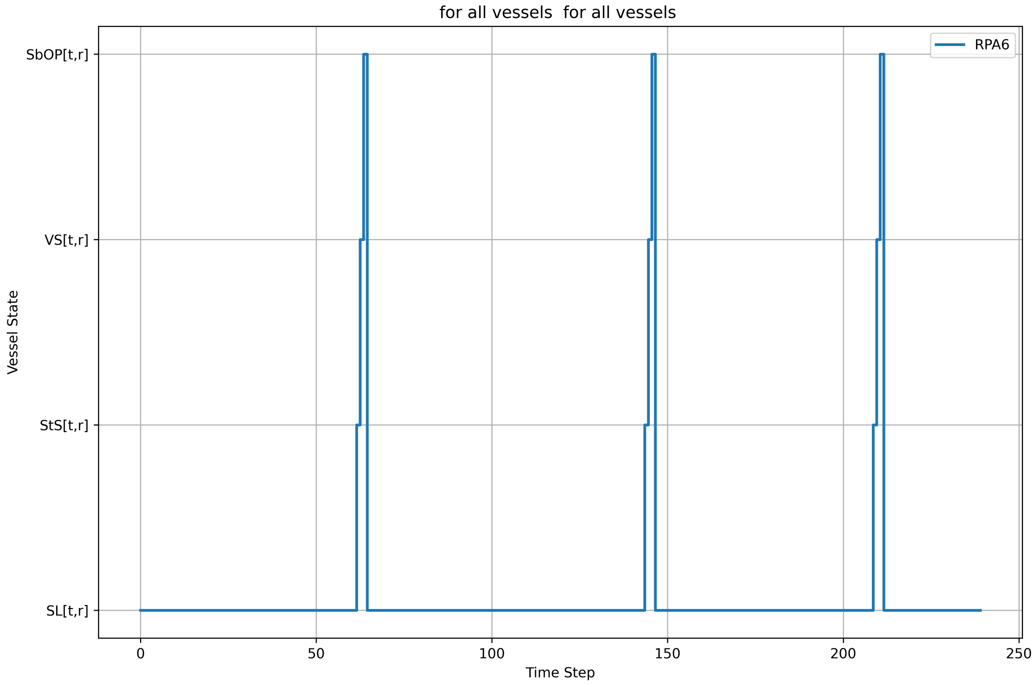

Figure C.5: Swapping states RPA6

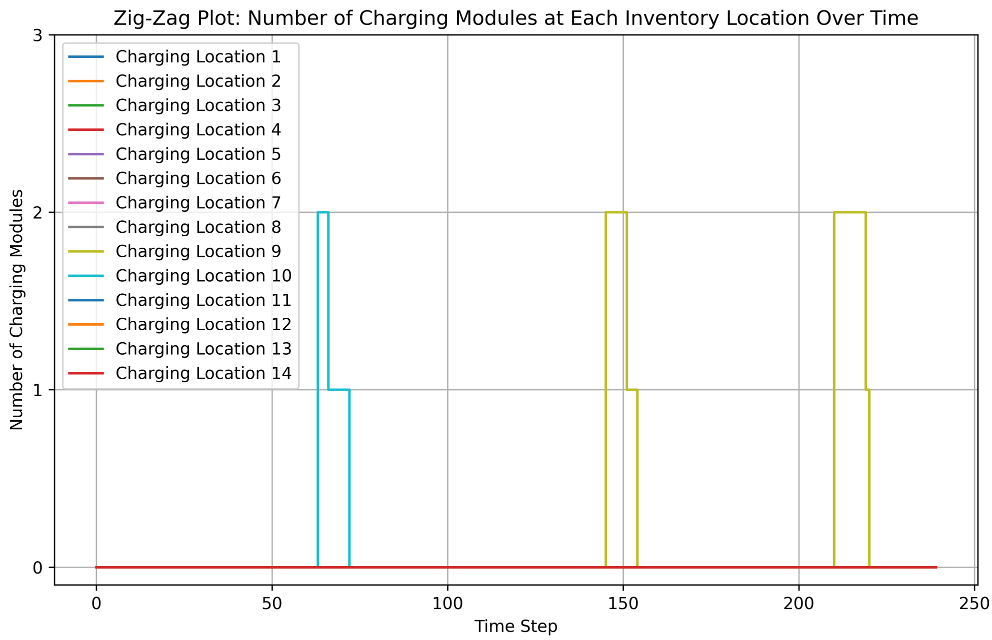

Figure C.6: Charging area for validation RPA6

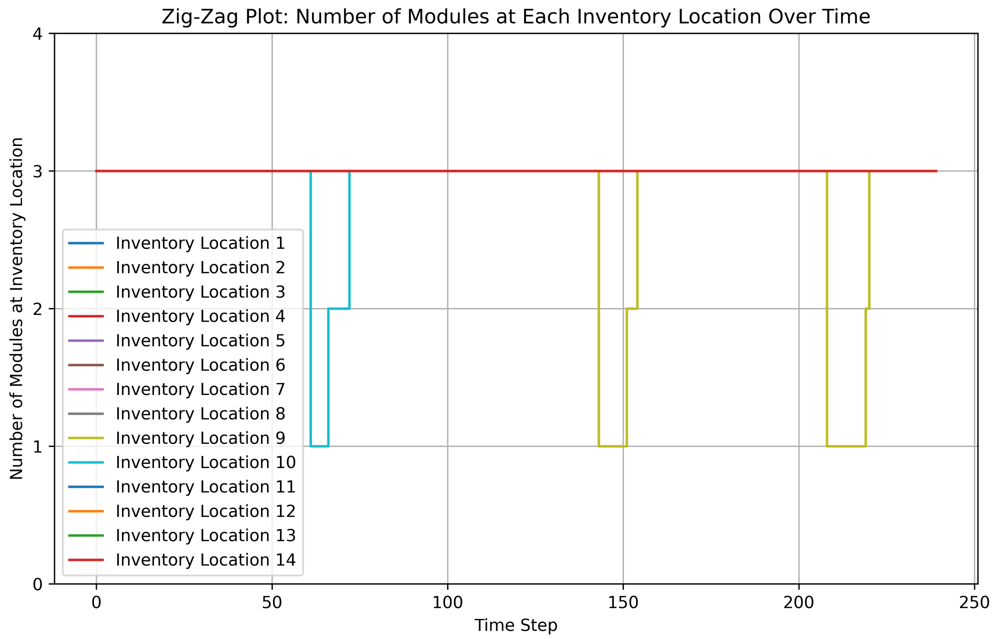

Figure C.7: Inventory area validation RPA6

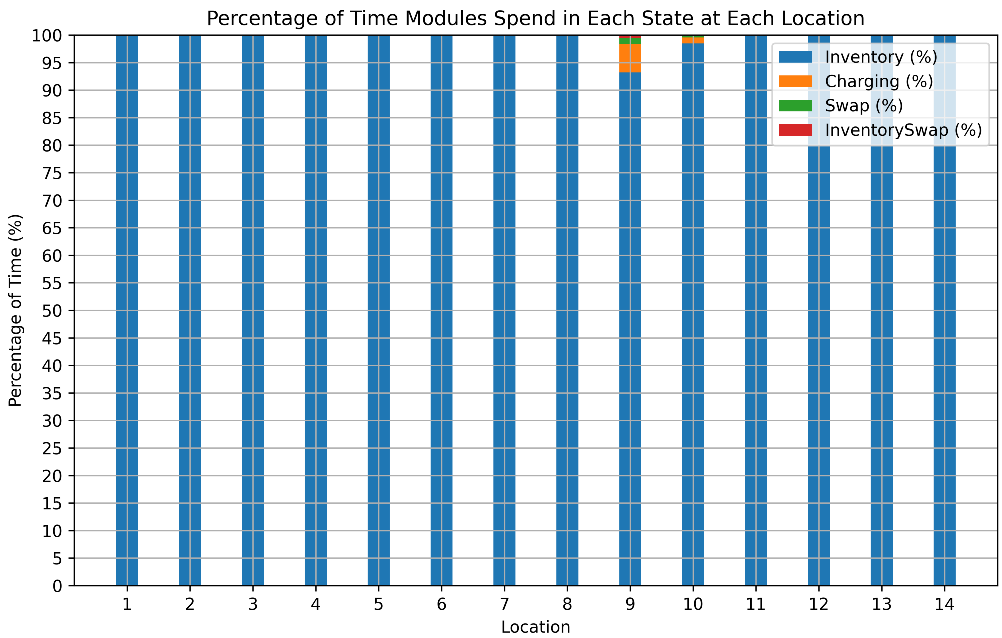

Figure C.8: Percentage of modules for each location in different swapping stations s, validation RPA6

C.2. Validation RPA7

C.2.1. Input

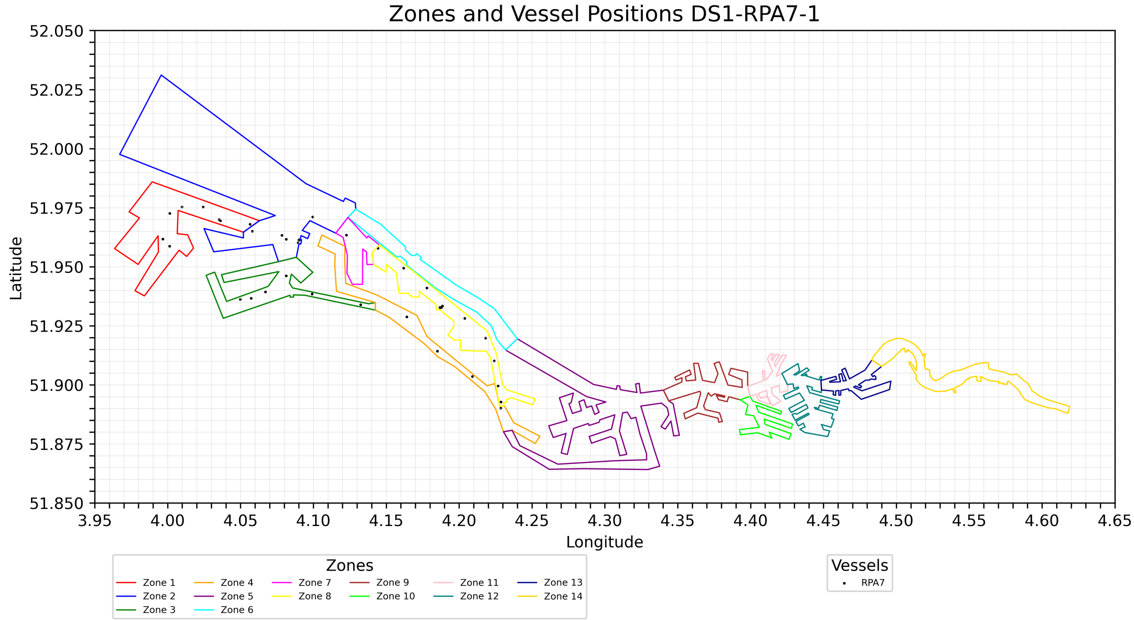

Figure C.9: RPA7 locations (timestep = 6)

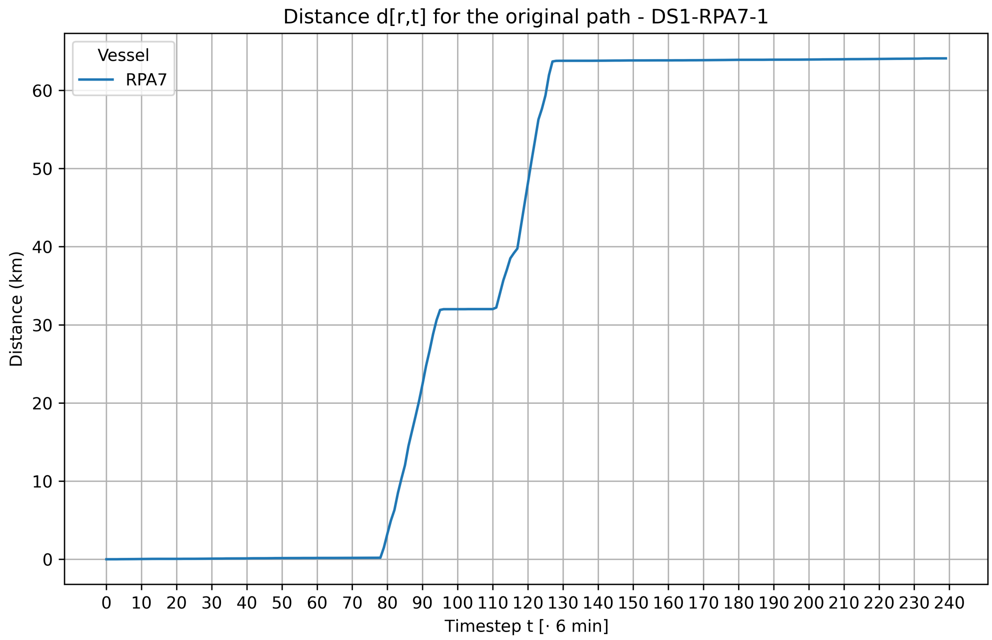

Figure C.10: Cumulative sailed distance for RPA7

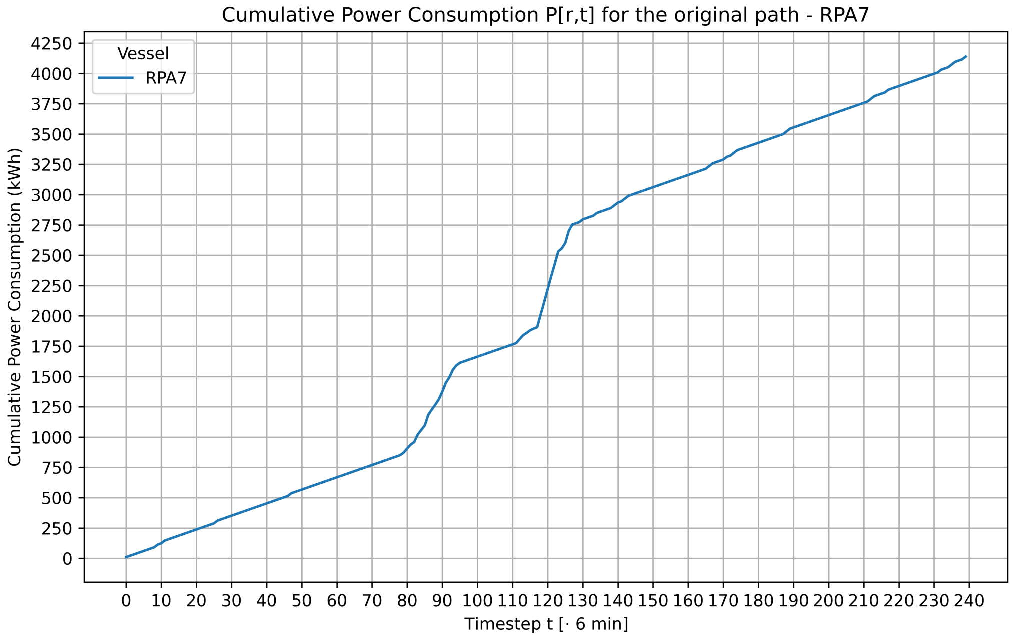

Figure C.11: Cumulative initial power for the RPA7

C.2.2. Results

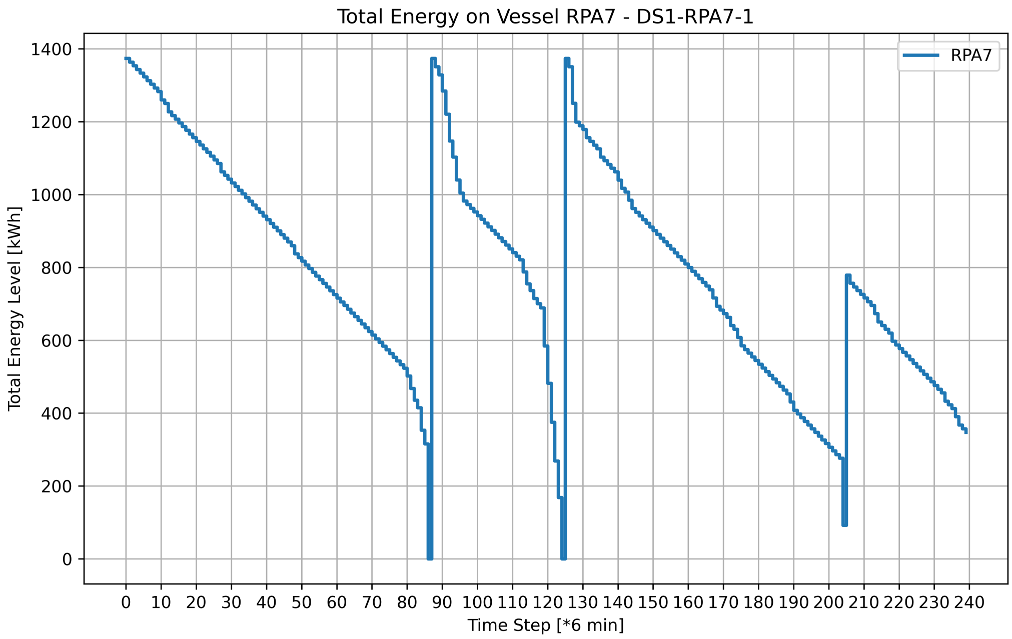

Figure C.12: Power consumption RPA7

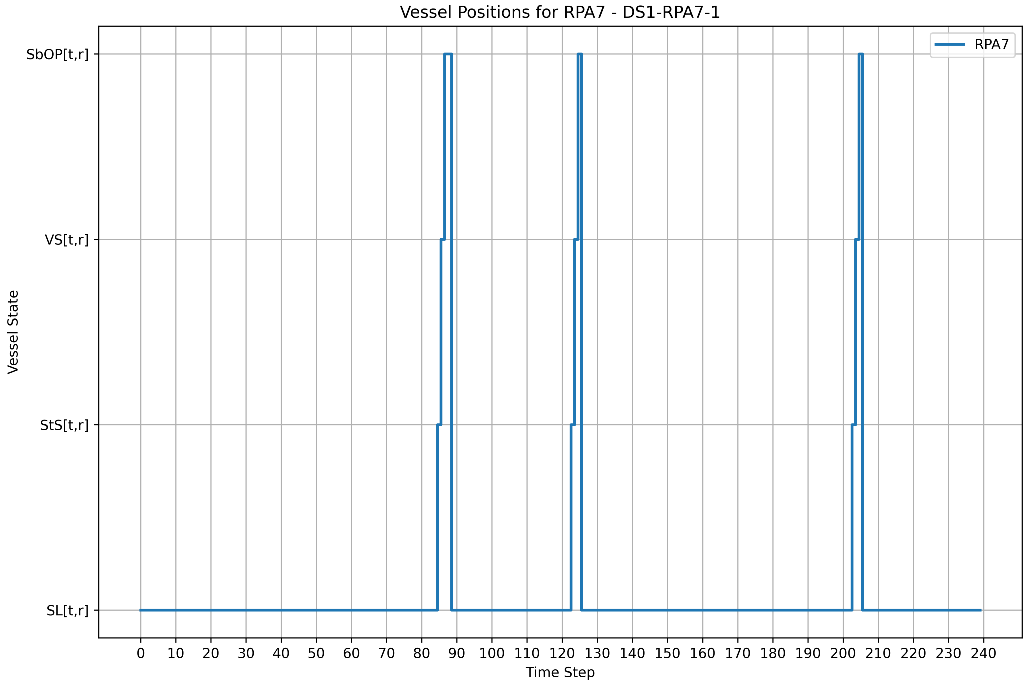

Figure C.13: Power consumption RPA7

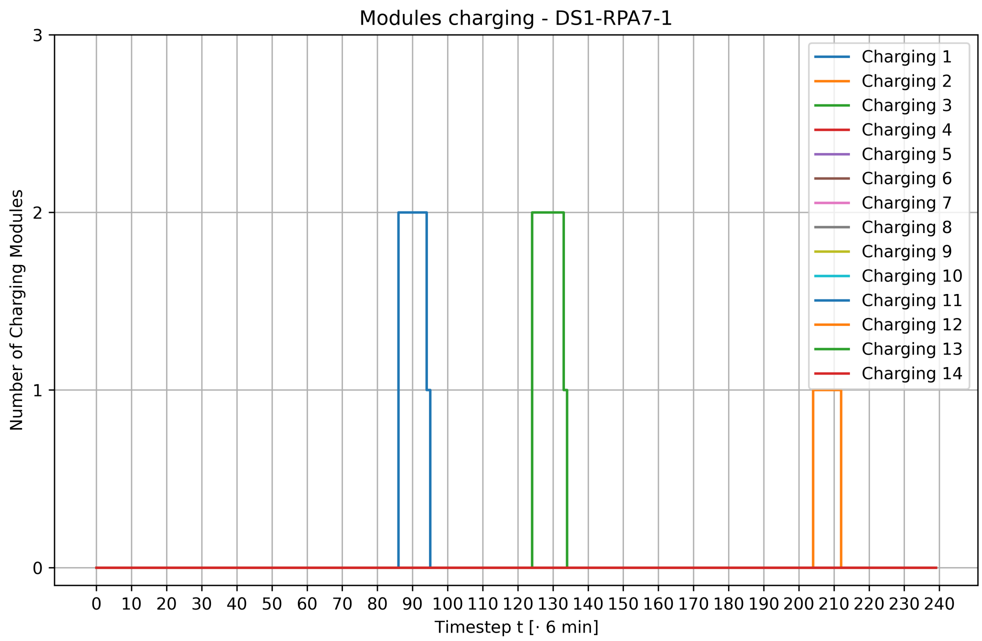

Figure C.14: Charging area for validation RPA7

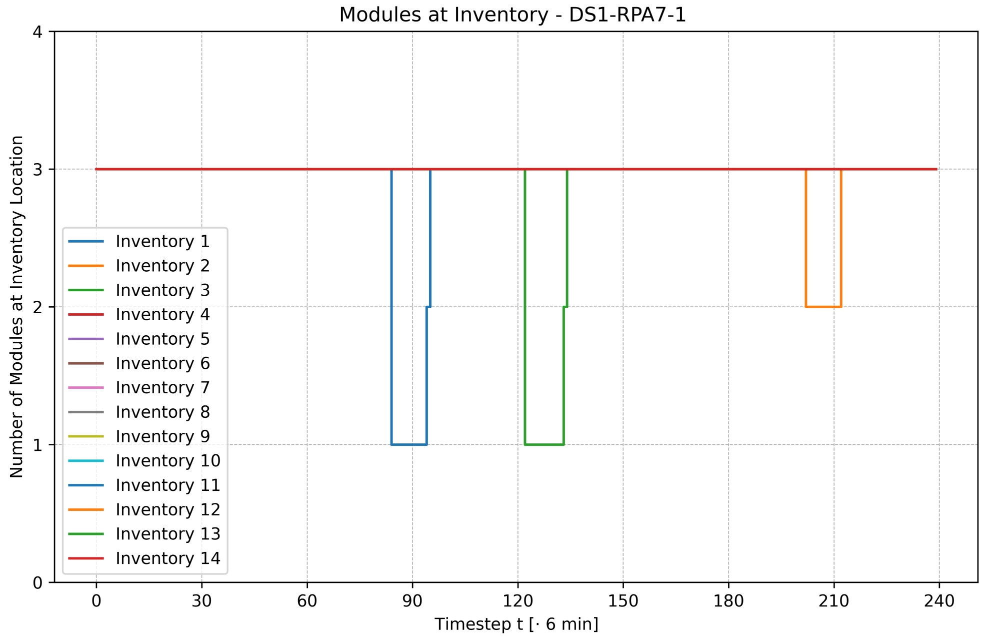

Figure C.15: Inventory area validation RPA7

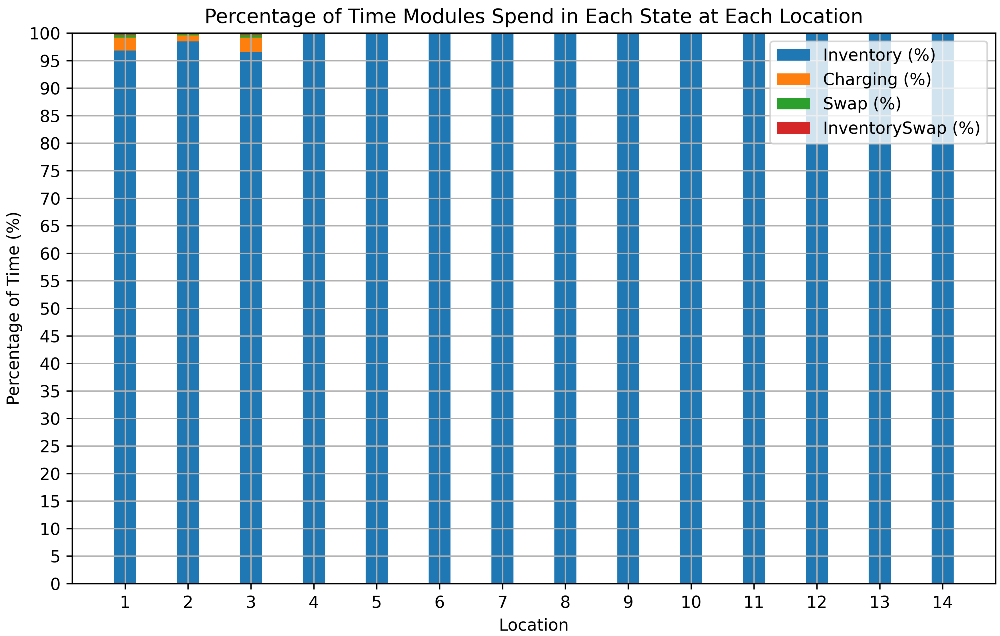

Figure C.16: Percentage of modules for each location in different swapping stations s, validation RPA7

C.3. Validation RPA10

C.3.1. Input

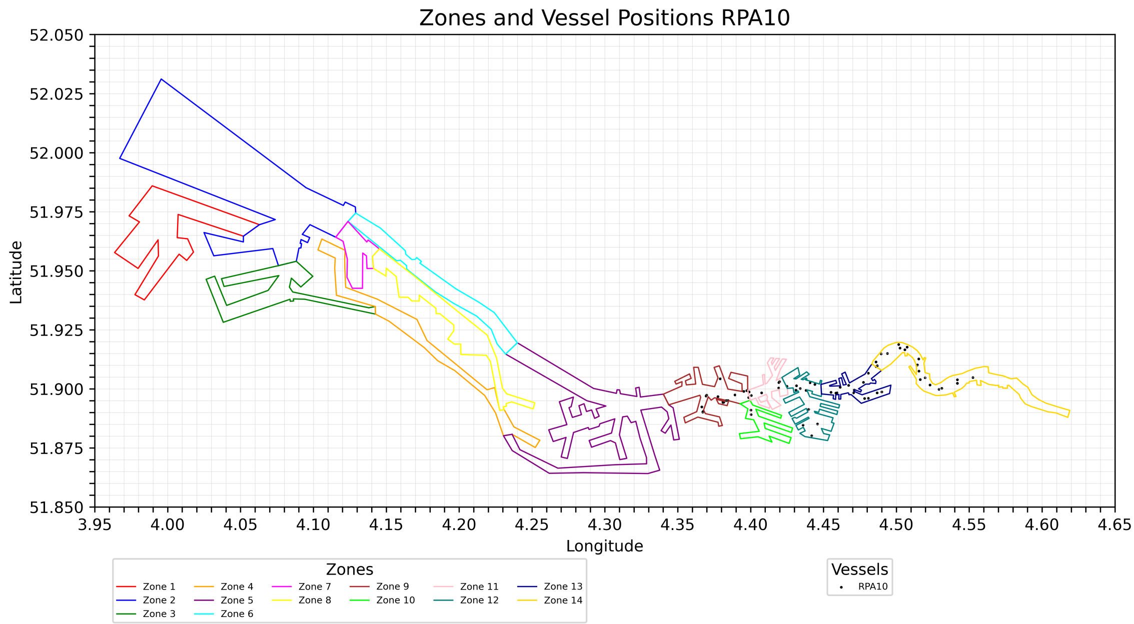

Figure C.17: RPA10 locations (timestep = 6)

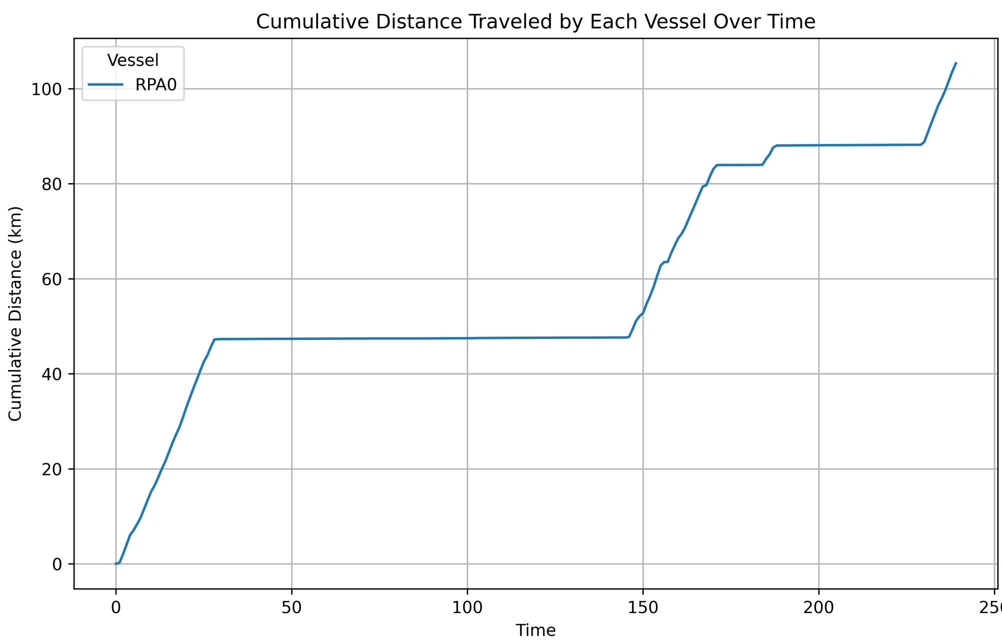

Figure C.18: Power consumption RPA10

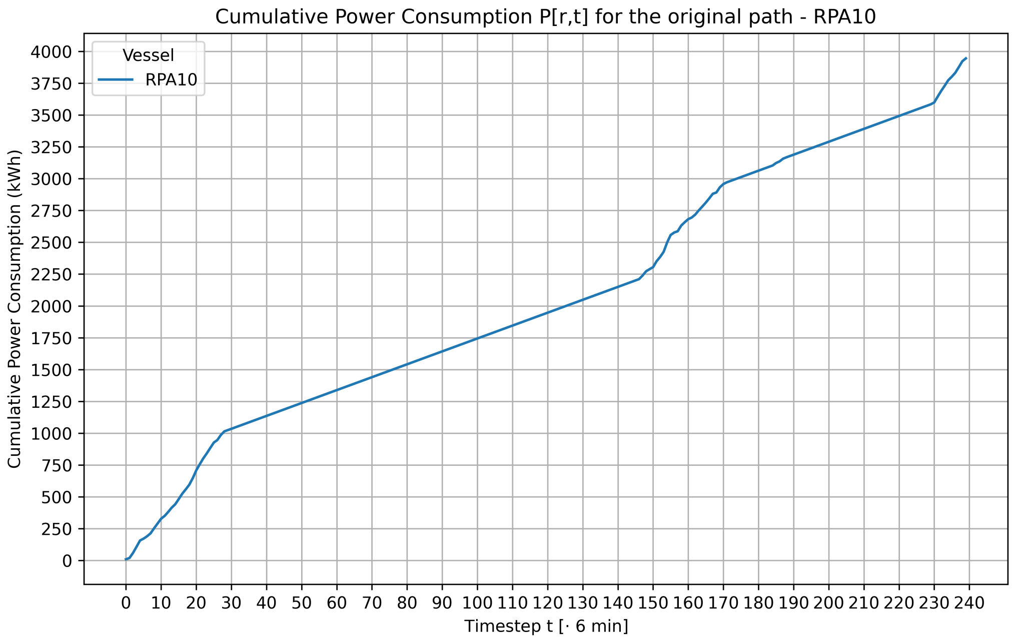

Figure C.19: Cumulative initial power for the RPA10

C.3.2. Results

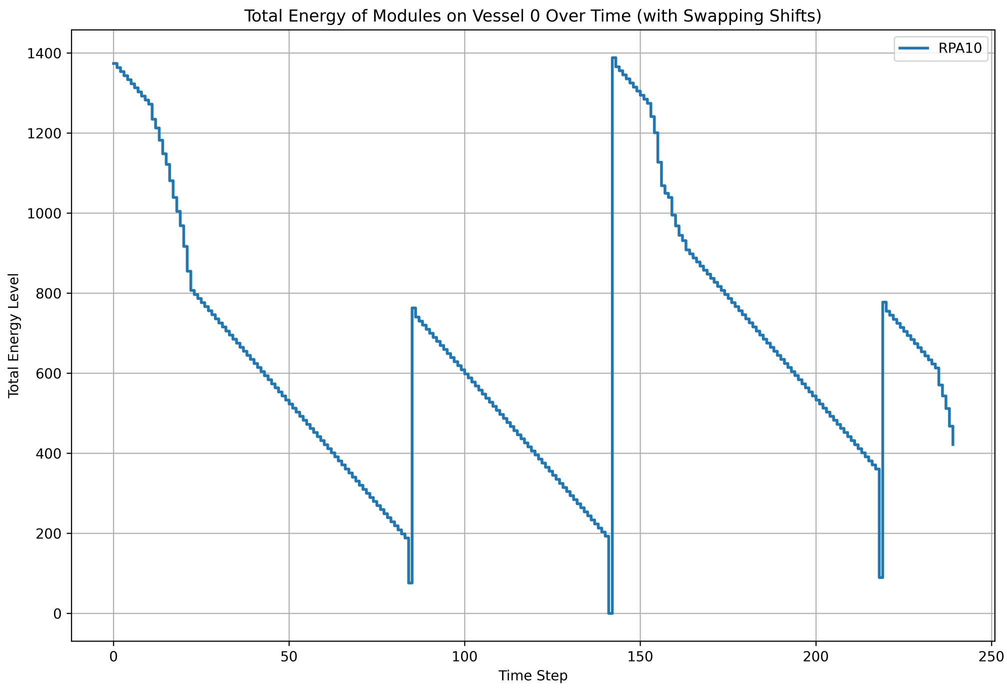

Figure C.20: Power consumption RPA10

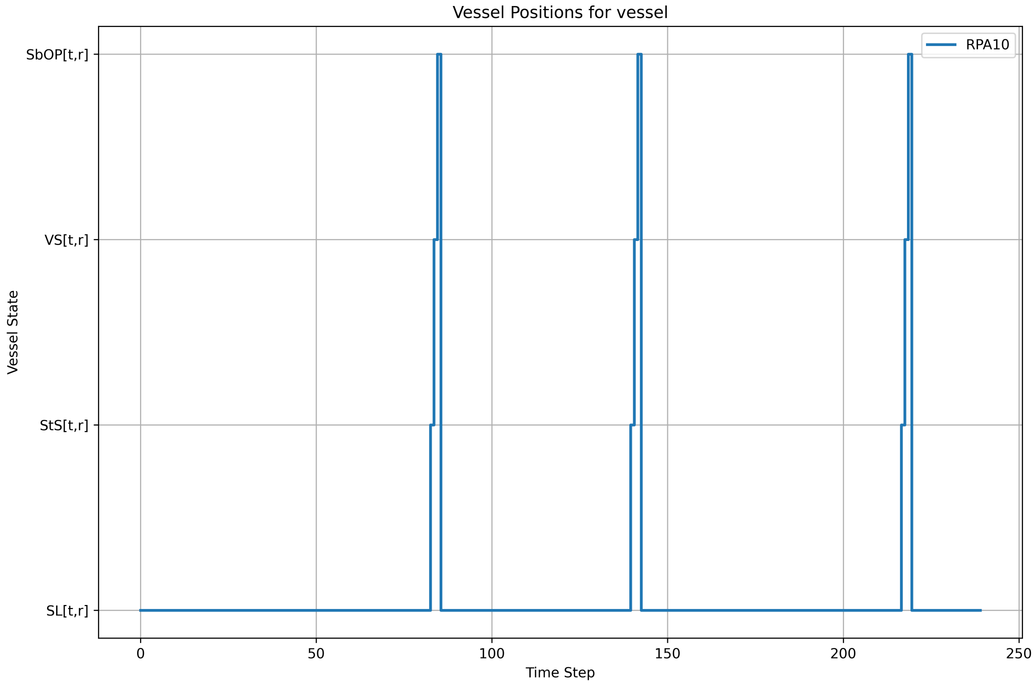

Figure C.21: Swapping states RPA10

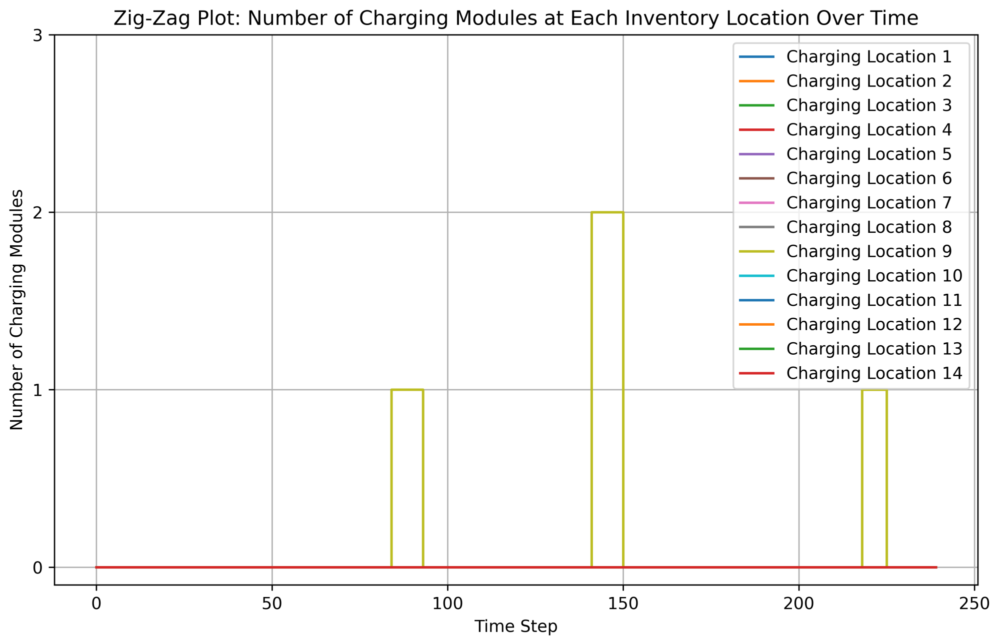

Figure C.22: Charging area for validation RPA10

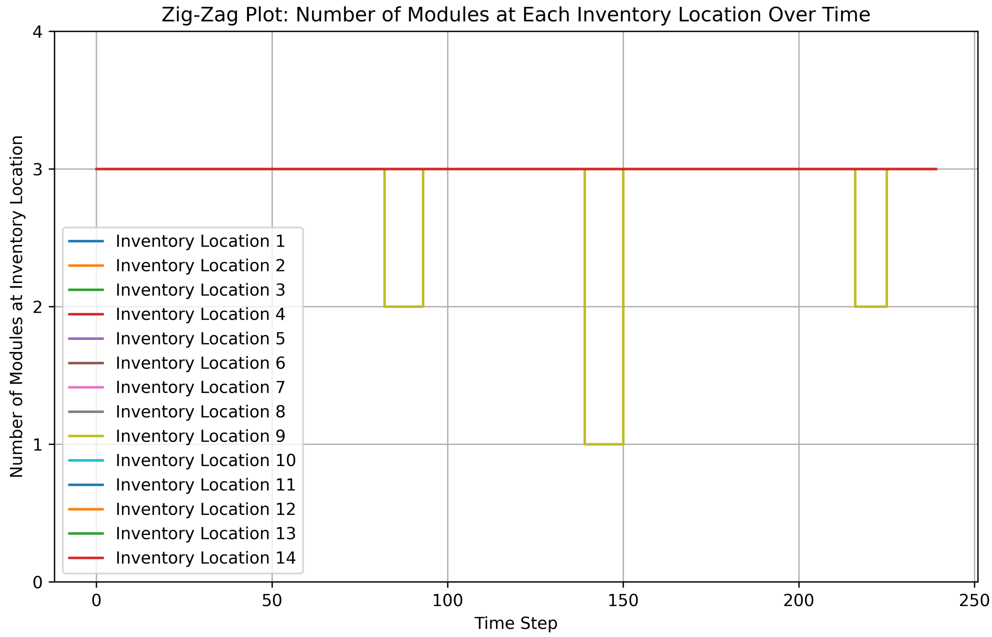

Figure C.23: Inventory area validation RPA10

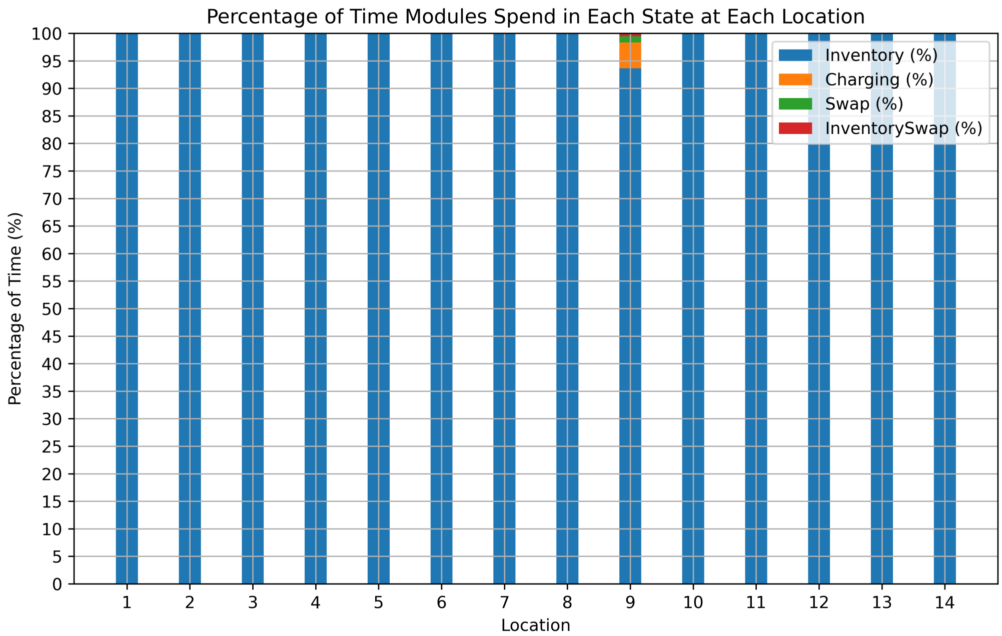

Figure C.24: Percentage of modules for each location in different swapping stations s for RPA10

C.4. Validation RPA13

C.4.1. Input

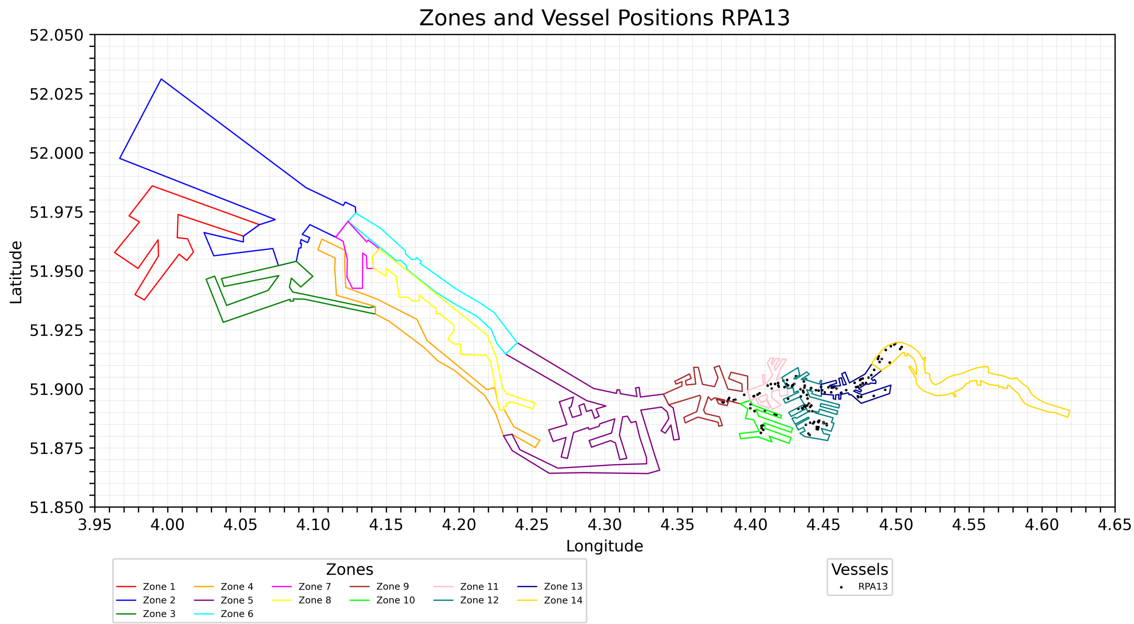

Figure C.25: RPA13 locations (timestep = 6)

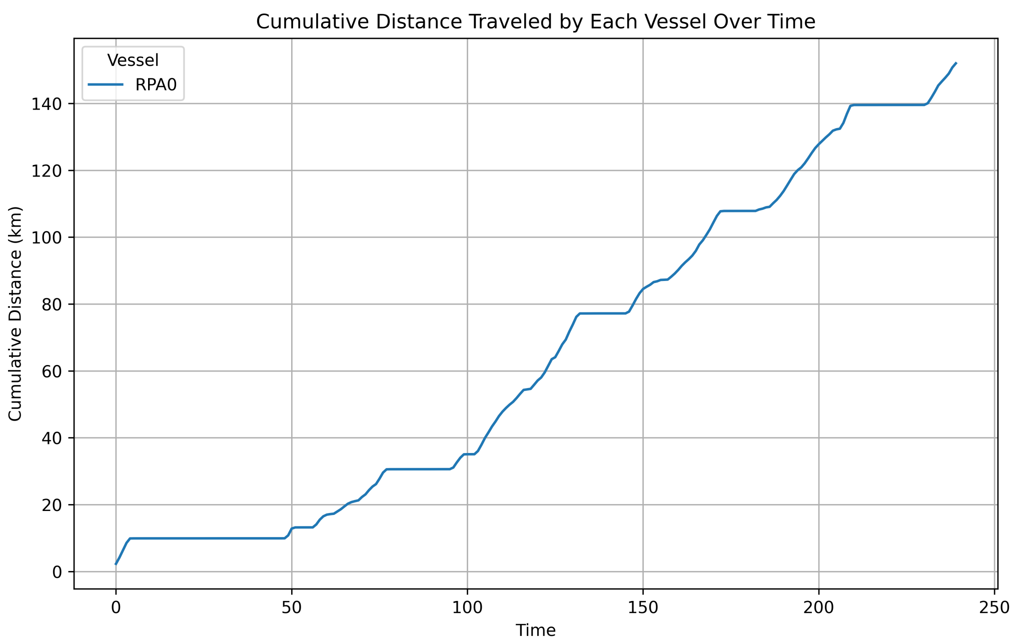

Figure C.26: Cumulative sailed distance for RPA13

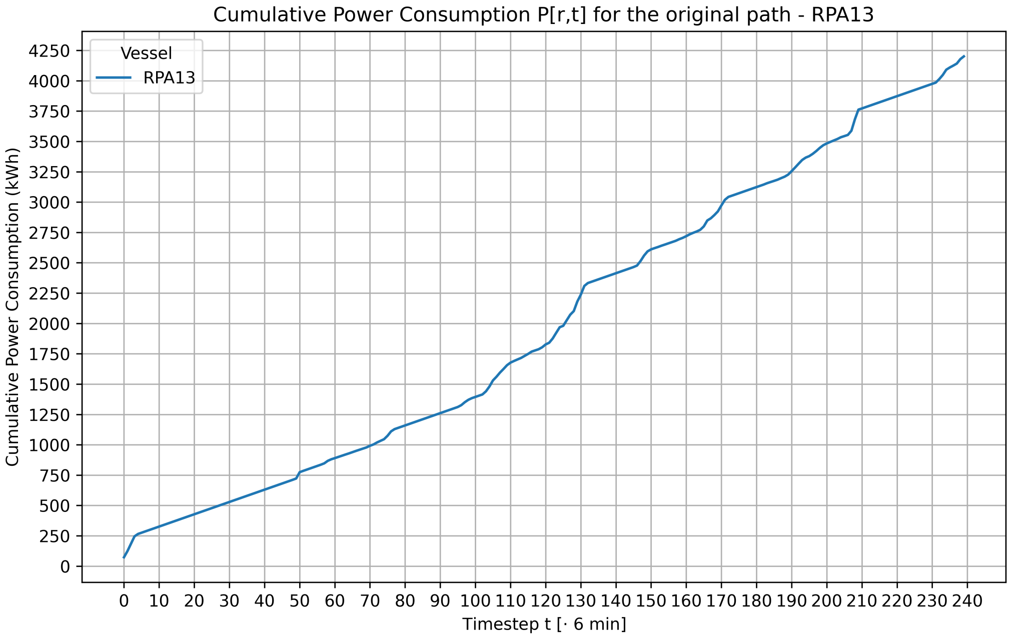

Figure C.27: Cumulative initial power for the RPA13

C.4.2. Results

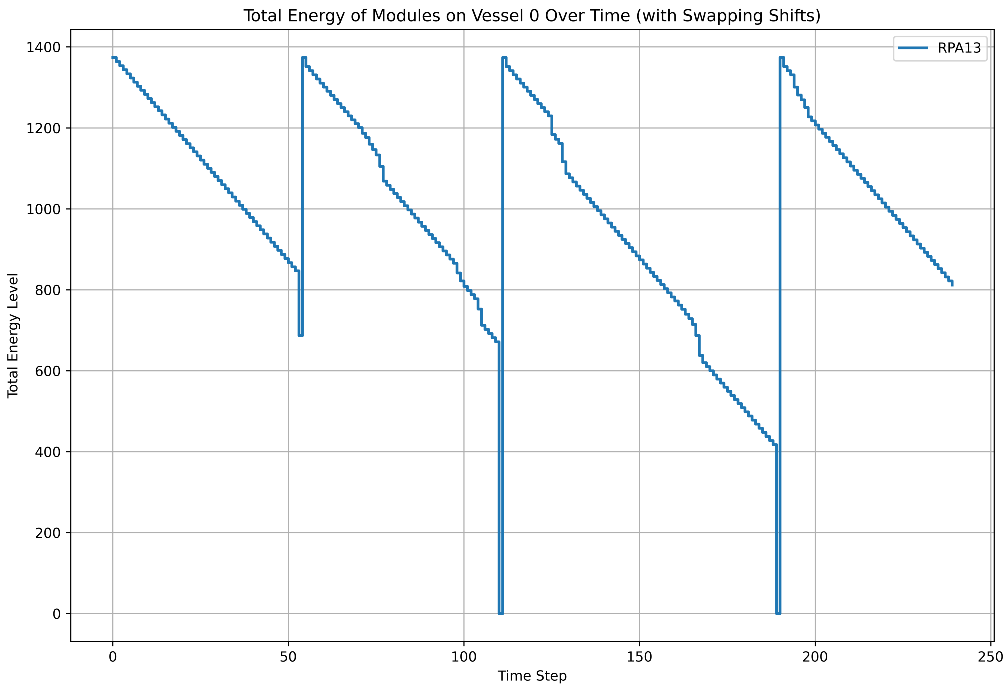

Figure C.28: Power consumption RPA13

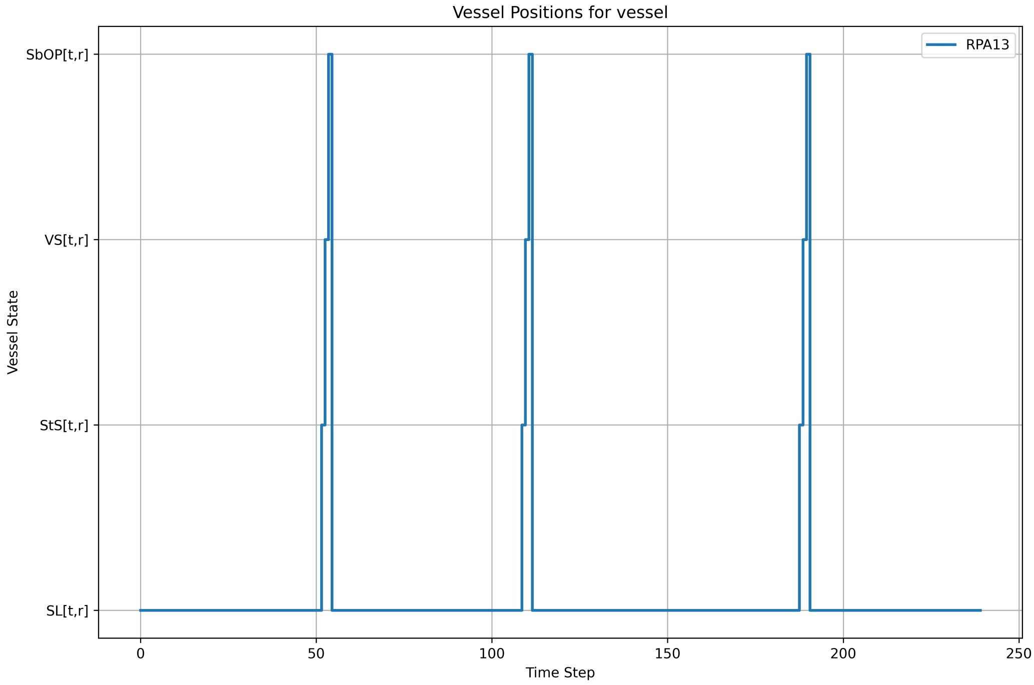

Figure C.29: Swapping states RPA13

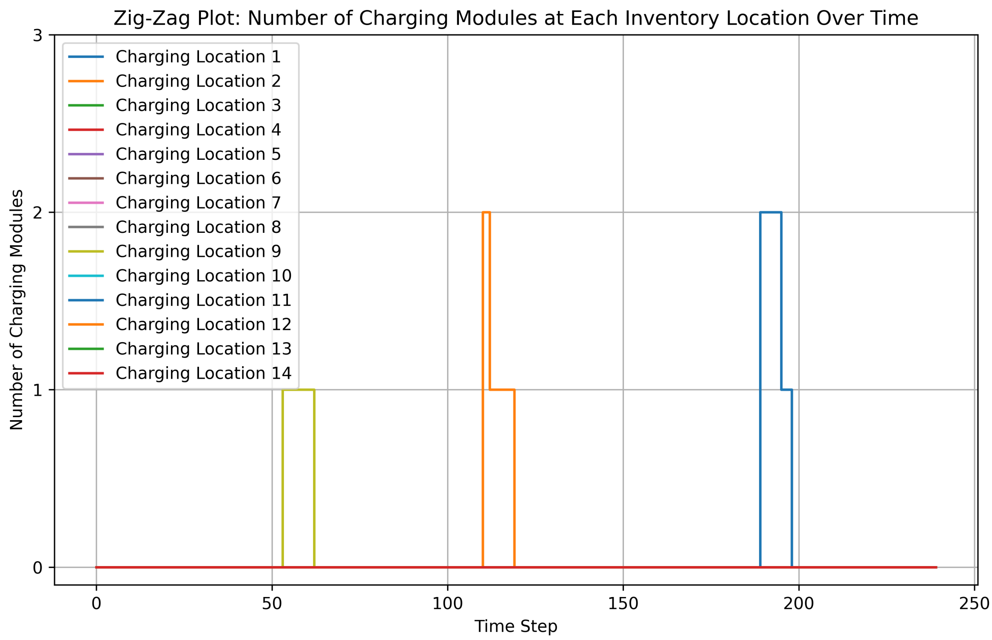

Figure C.30: Charging area for validation RPA13

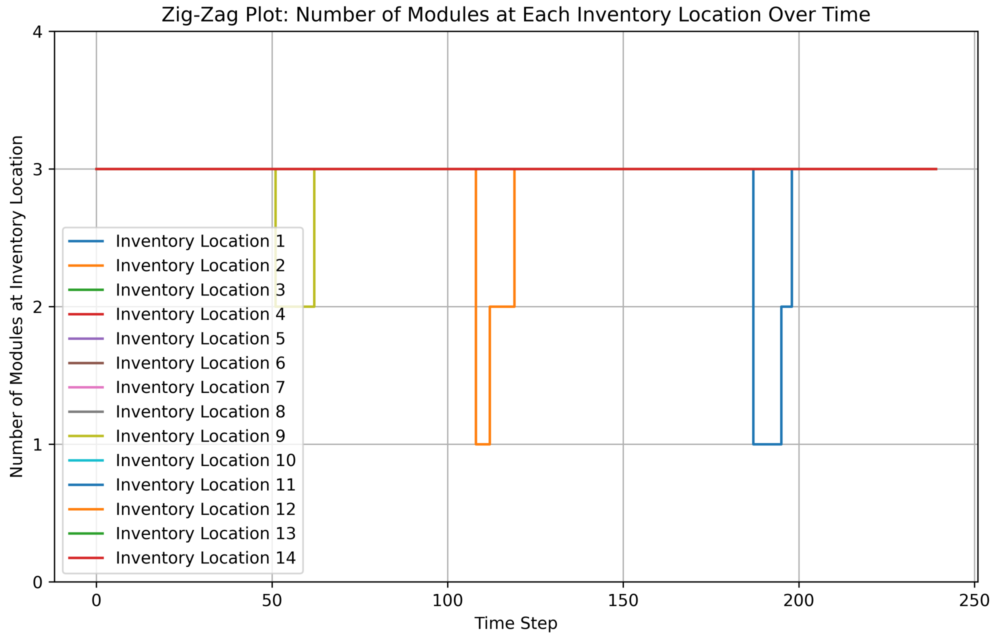

Figure C.31: Inventory area validation RPA13

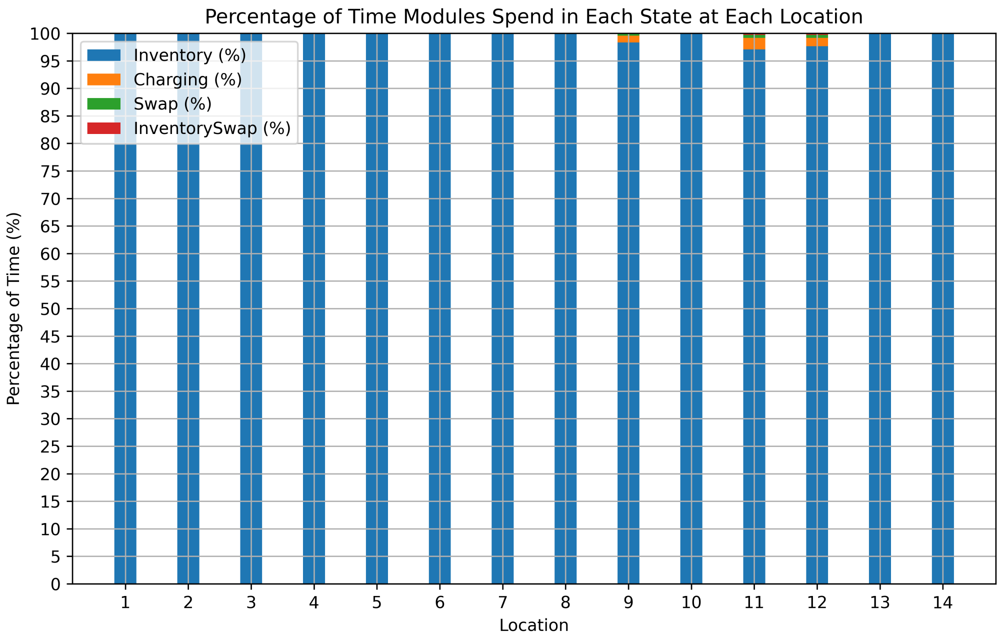

Figure C.32: Percentage of modules for each location in different swapping stations s for RPA13

C.5. Validation RPA15

C.5.1. Input

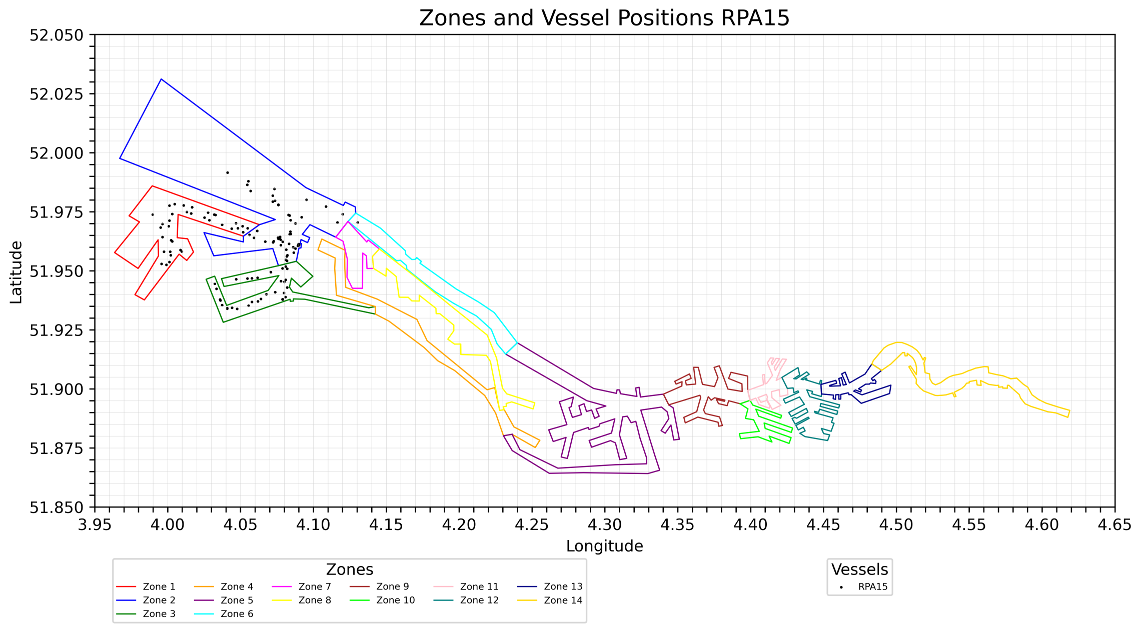

Figure C.33: RPA15 locations (timestep = 6)

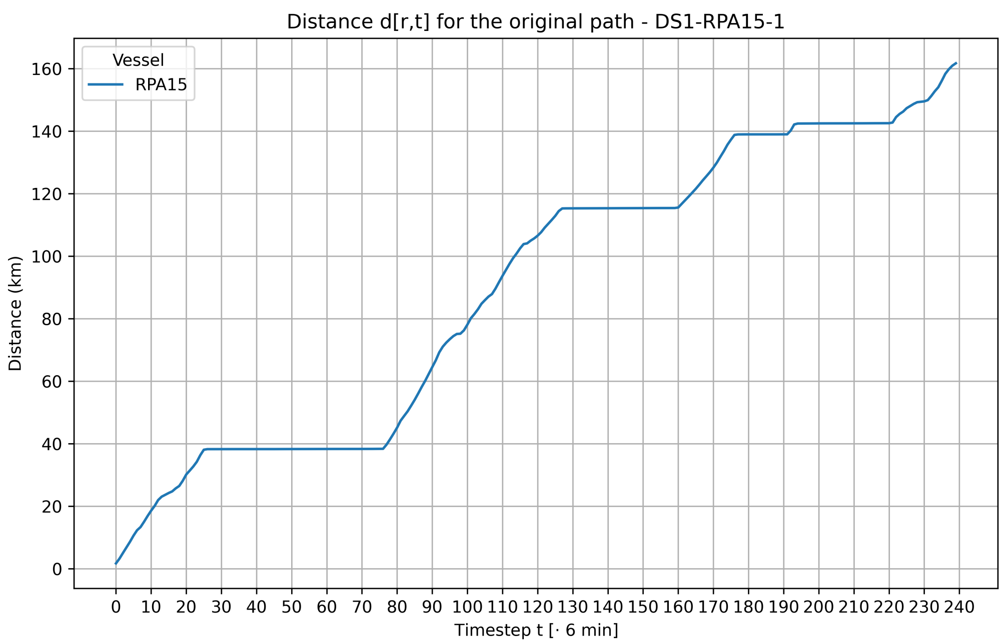

Figure C.34: Cumulative sailed distance for RPA15

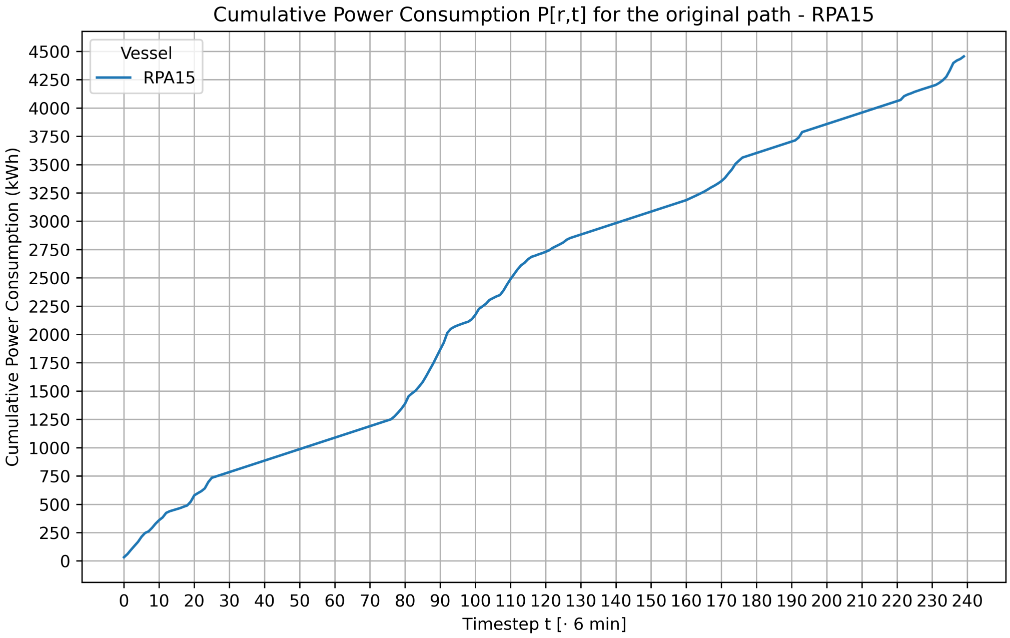

Figure C.35: Cumulative initial power for the RPA15

C.5.2. Results

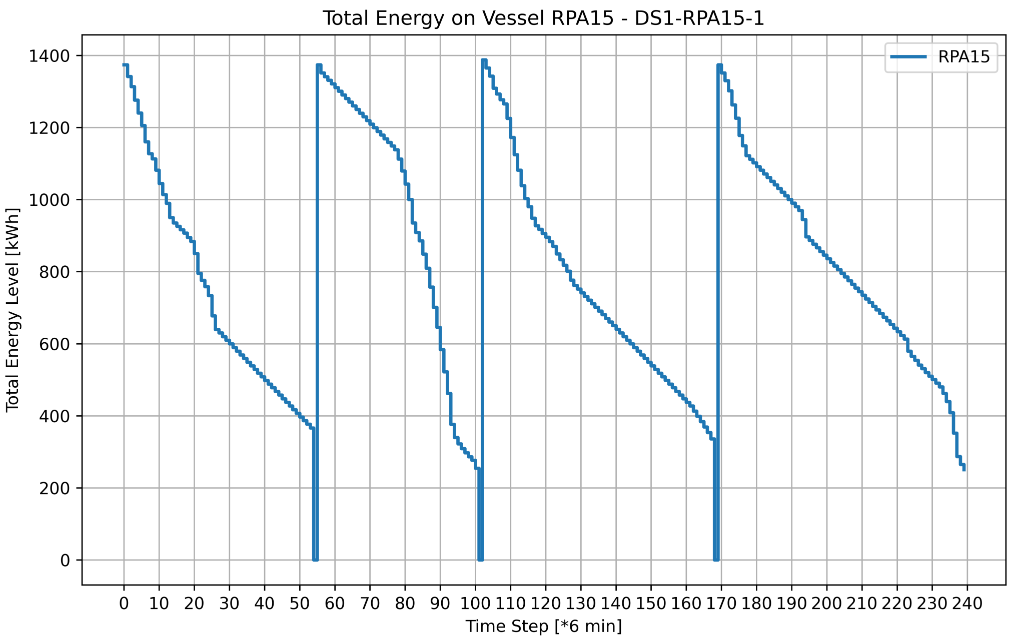

Figure C.36: Power consumption RPA15

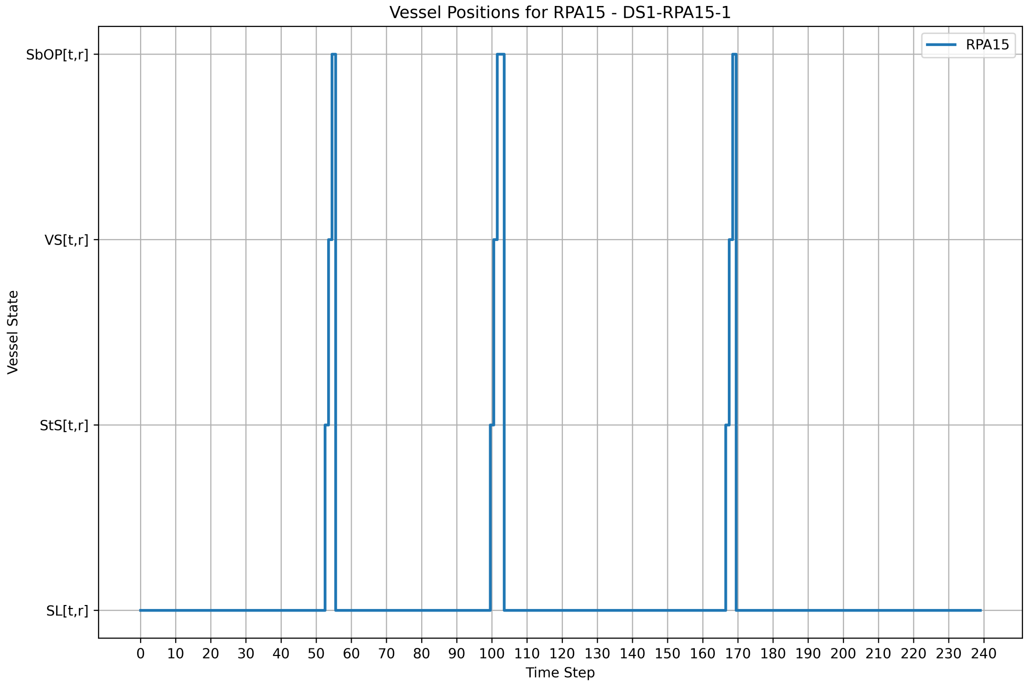

Figure C.37: Swapping states RPA15

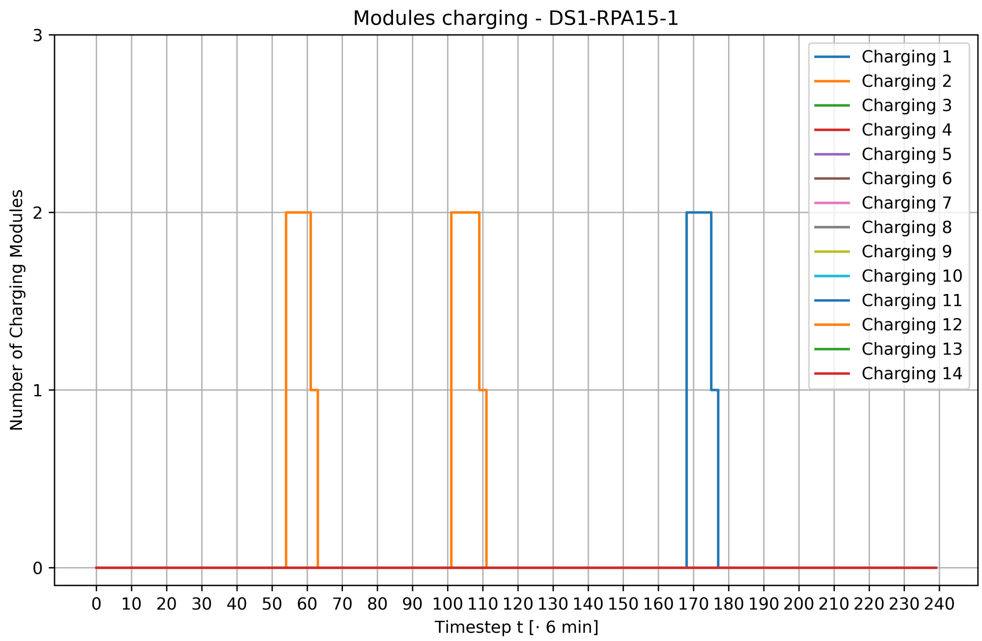

Figure C.38: Charging area for validation RPA15

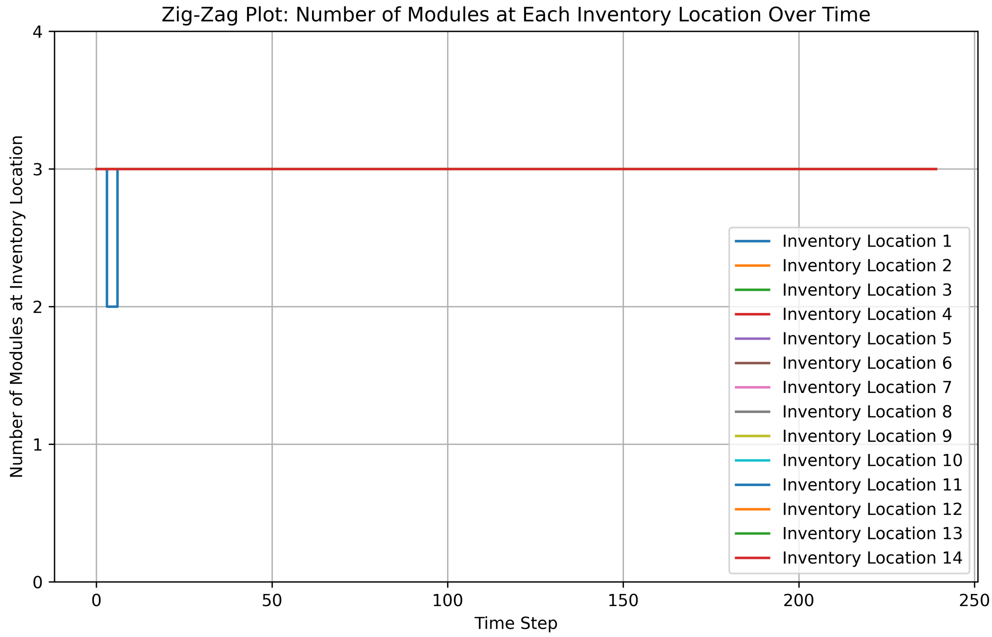

Figure C.39: Inventory area validation RPA15

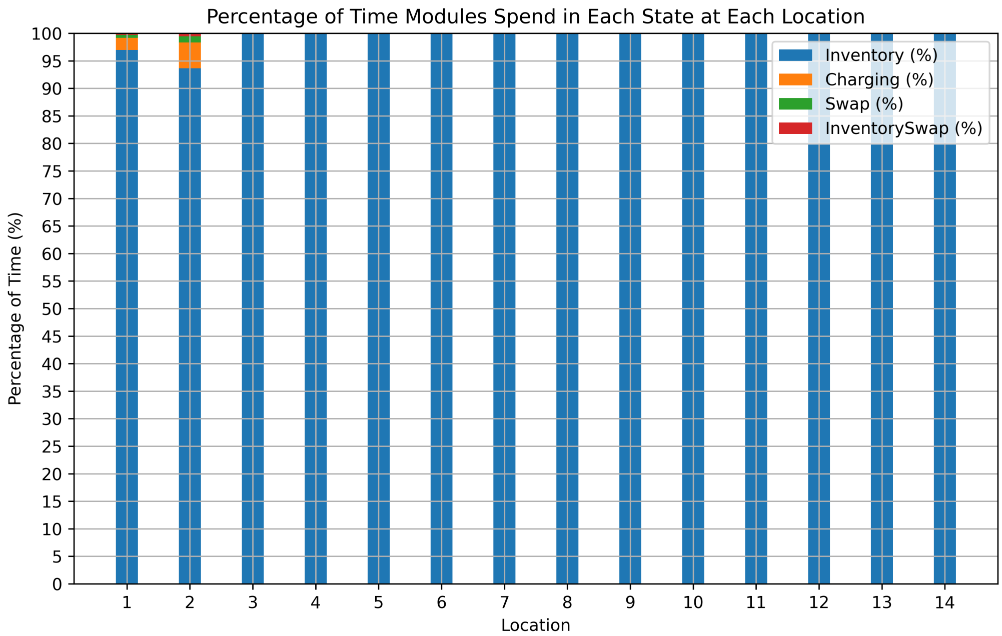

Figure C.40: Percentage of modules for each location in different swapping stations s for RPA10

C.6. Validation RPA16

C.6.1. Input

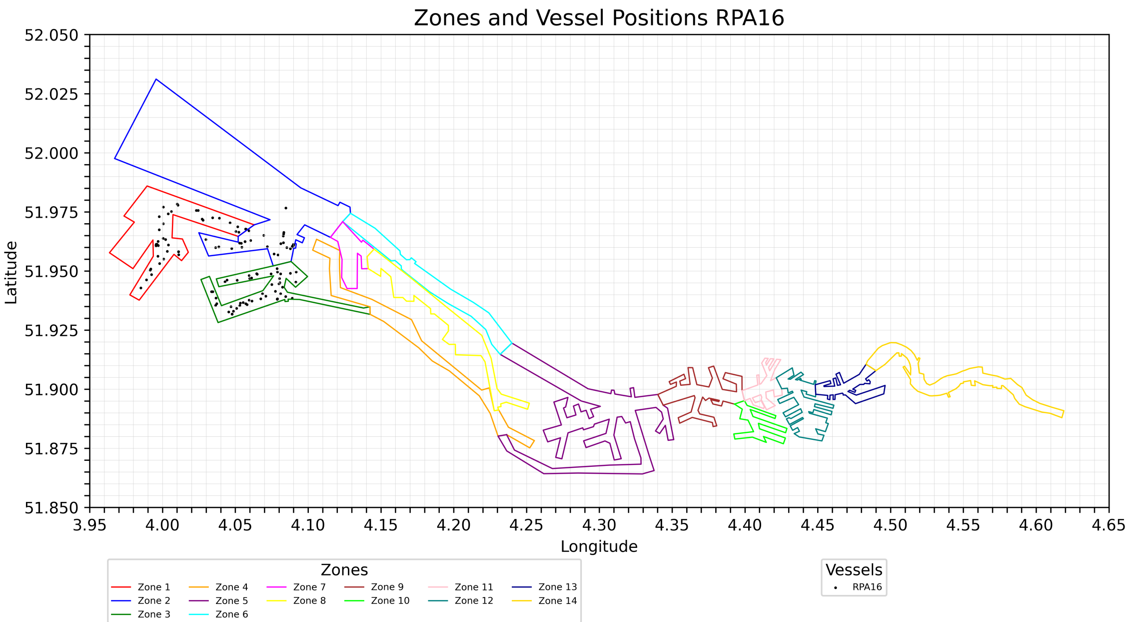

Figure C.41: RPA6 locations (timestep = 6)

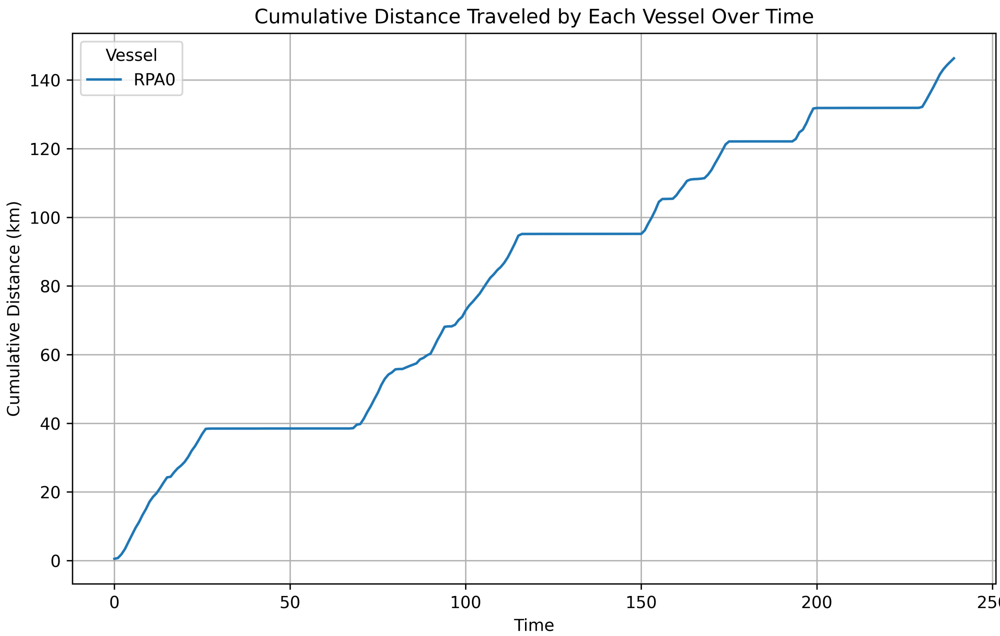

Figure C.42: Cumulative sailed distance for RPA16

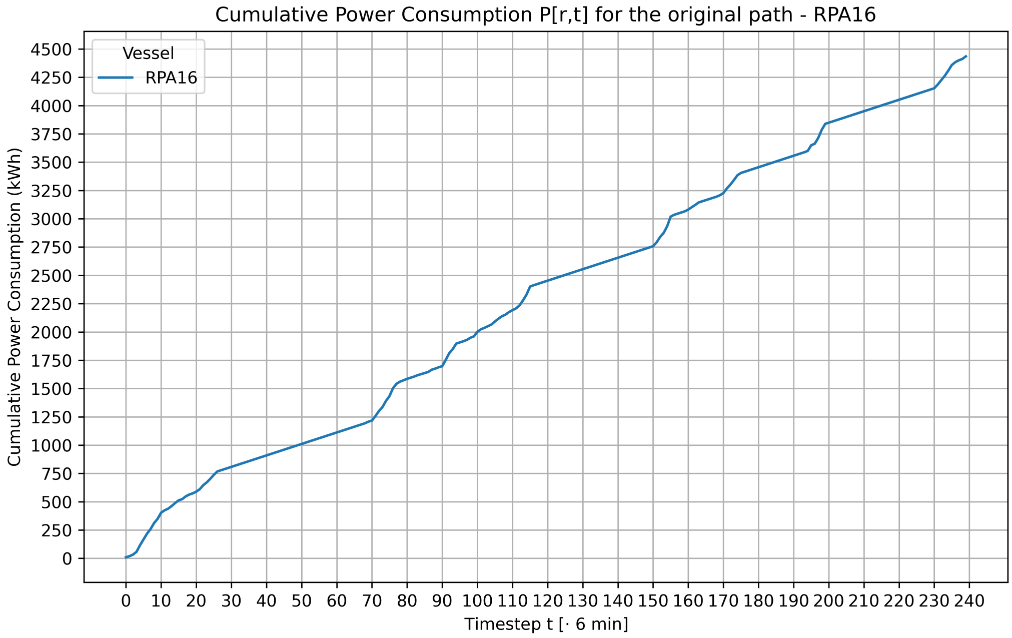

Figure C.43: Cumulative initial power for the RPA16

C.6.2. Results

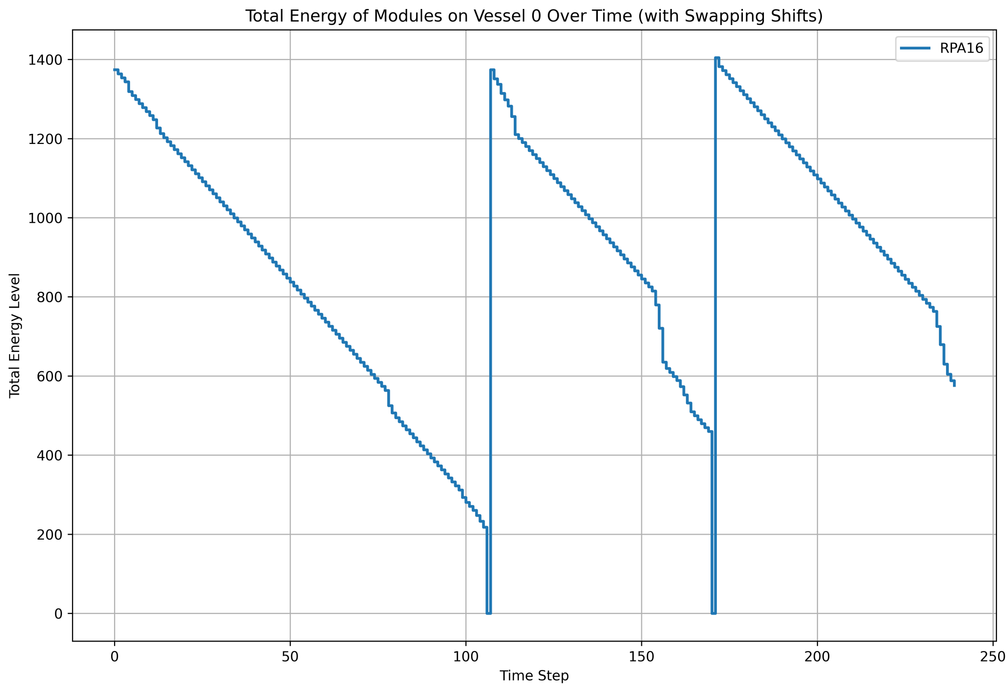

Figure C.44: Power consumption RPA16

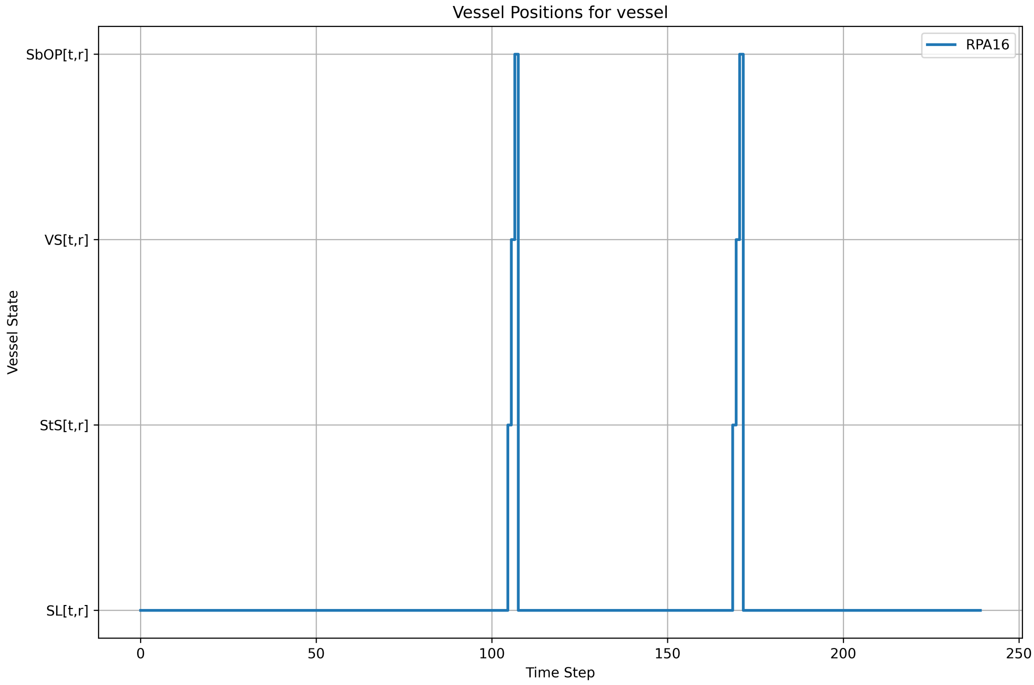

Figure C.45: Swapping states RPA16

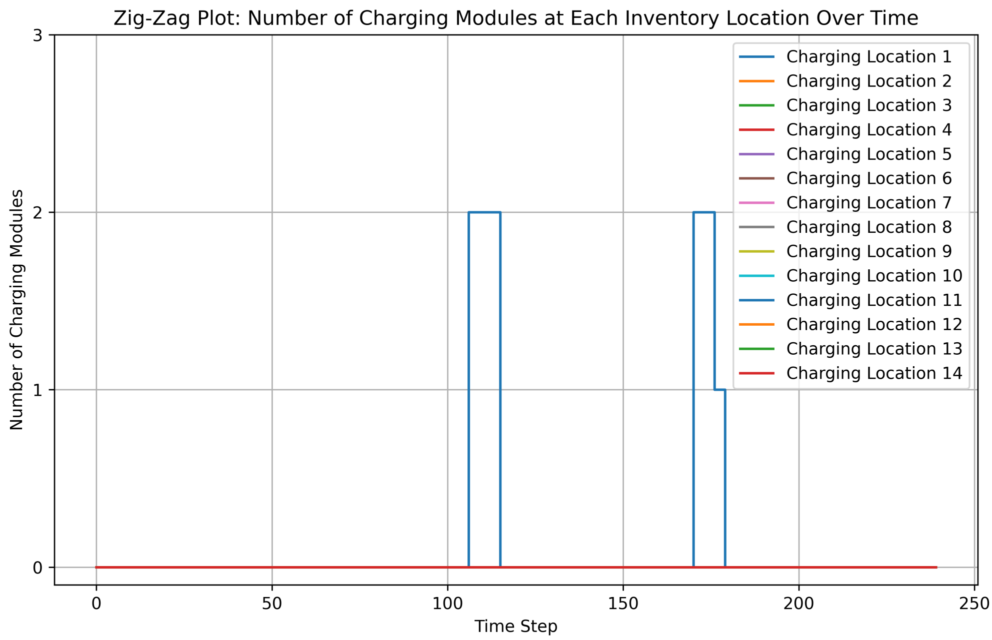

Figure C.46: Charging area for validation RPA16

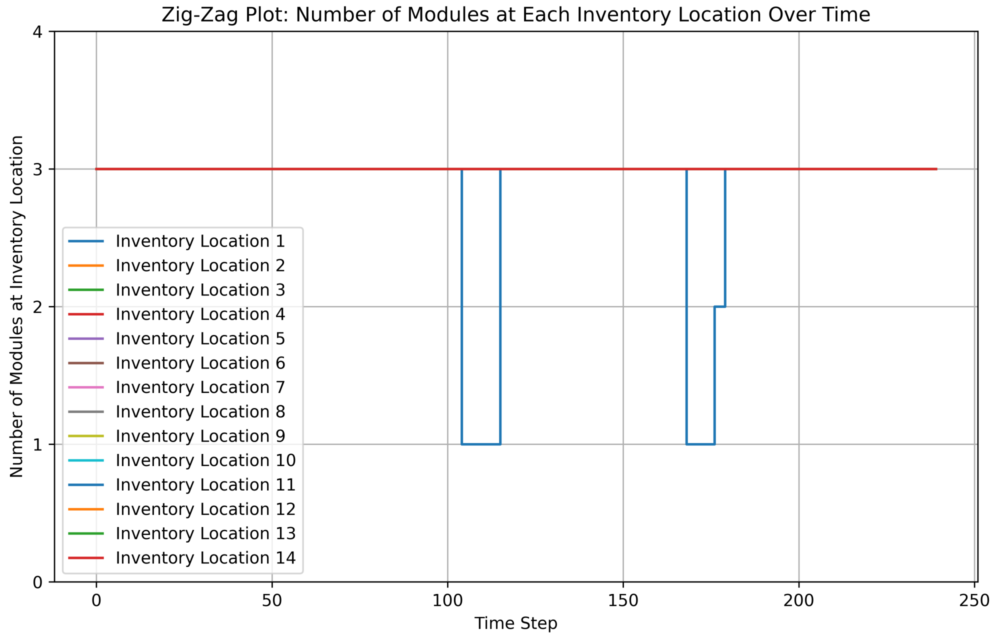

Figure C.47: Inventory area validation RPA16

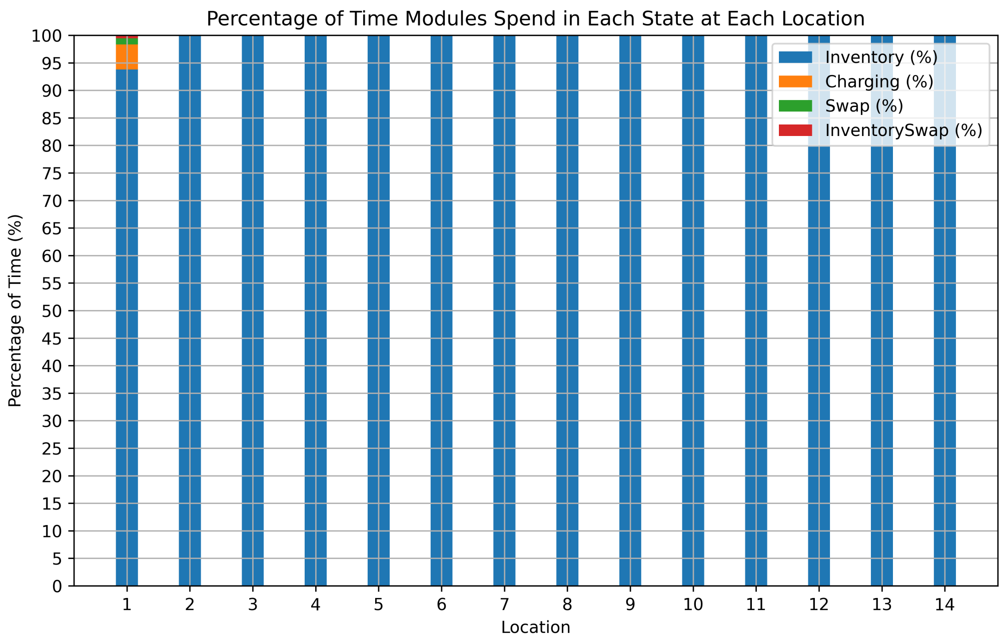

Figure C.48: Percentage of modules for each location in different swapping stations s for RPA16